Evaluation of Heterogeneous Catalysts for Biodiesel Production

Claire MacLeod

A thesis submitted for the degree of Doctor of Philosophy (PhD) at Newcastle University

School of Chemical Engineering and Advanced Materials,
Newcastle University

March 2008

Abstract

Biodiesel is a fuel derived from renewable sources suitable for use in conventional compression-ignition engines. The use of biodiesel is being promoted in many countries through government incentives and targets, and the production of biodiesel is increasing worldwide. As it is derived from renewable feedstocks, lifecycle CO_2 emissions are reduced when petrodiesel usage is displaced by biodiesel usage.

Biodiesel is produced through the transesterification reaction of triglycerides with methanol. Typically, this reaction is carried out at 60 °C, in a batch reactor with an excess of methanol and a homogeneous sodium hydroxide catalyst. The products are biodiesel and glycerol. Following the reaction, the sodium hydroxide must be neutralized and the resulting salt is contained in the glycerol phase, making it difficult to purify the glycerol to pharmaceutical grade to sell as a by-product. Additionally, sodium hydroxide can cause unwanted side-reactions to form soap, through the saponification of triglycerides and the neutralization of free fatty acids present in cheaper feedstocks, resulting in a loss of yield. Therefore, it is desirable to replace sodium hydroxide with a heterogeneous catalyst.

Potential heterogeneous catalysts were evaluated for their activity in the transesterification reaction, and their stability in the reaction environment. Alkali-doped metal oxides and silica-supported guanidines were found to be active, with conversions of >90% reached in 3 hours. This reaction time is feasible for use on an industrial scale. There was a strong correlation between base strength and activity: only catalysts with strong base sites were active. Unfortunately, the catalysts were found to leach and lost activity on repeated use. Thus, in their current form, these catalysts would not be suitable heterogeneous catalysts for biodiesel production because the advantages of using a heterogeneous catalyst are lost if the catalyst leaches. Amberlyst 26, a quaternary ammonium functionalized polystyrene resin was found to be stable, but only 8% conversion was obtained after 3 hours of reaction. This low activity was attributed to internal diffusion limitations.

Acknowledgements

I would like to acknowledge the help, input and support of the following people during my PhD:

- My supervisor, Dr Adam Harvey
- Rob Dixon and Paul Sterling
- Professor Paulo Suarez, University of Brasília and the students and staff of LABCAT and LAPREN, in particular Fernando de Medeiros, Flavia Oliveira and Betania Texeira
- Dr Karen Wilson and Dr Adam Lee at the University of York
- Bob Skelton at the University of Cambridge
- Kath Lidell, Dave Dunbar, Grant Staines and Richard Baron for their help with analytical techniques
- My friends and colleagues at Newcastle, my family and Andy

This work was funded by the EPSRC. The exchange visit to Brasília was funded through the British Council's Researcher Exchange Programme and travel grants for attendance at conferences were funded by the Royal Academy of Engineering and SCI.

Table of Contents

Nomenclature and Abbreviations

Symbols

a_p	particle surface area	m^2/m^3
D	diffusivity	m^2/s
k	rate constant	l/mol/min
k'	rate constant per mole catalyst	$l/mol/min/mol_{cat}$
k_a	rate constant for adsorption	l/mol/s
k_l	solid-liquid mass transfer coefficient	m/s
K	adsorption coefficient	-
K_{dis}	distribution coefficient	-
Q	rate of mass transfer	mol/l/s
R	rate of reaction	mol/l/s
S_{ex}	external surface area	m^2
V	volume	m^3
α	radius of molecule	m
β	radius of pore	m
ε	voidage	-
η	effectiveness factor	-
τ	tortuosity	-
ø	Thiele modulus	-

Subscripts

A	species A
ads	adsorption
b	bulk
e	effective
s	surface
cat	catalyst

Abbreviations

A	alcohol
AAS	atomic absorption spectroscopy
acac	acetylacetonate
BD	biodiesel
BET	Brunauer Emmett Taylor
BJH	Barrett Joyner Halanda
DDBSA	dodecylbenzenesulfonic acid
DG	diglyceride
FAME	fatty acid methyl ester
G	glycerol
GC	gas chromatography
GLYMO	trimethoxysilylpropoxymethyloxirane

HIPE	high internal phase emulsion
HMS	hexagonal mesoporous silica
HPLC	high performance liquid chromatography
IR	infrared
IS	internal standard
M	metal
MG	monoglyceride
MSTFA	N-methyl-N-trimethylsilylfluoroacetamide
NMR	nuclear magnetic resonance
PTSA	p-toluene sulfonic acid
RI	refractive index
RTFO	Renewable Transport Fuels Obligation
TA	tertiary amine
TBD	triazobicyclodecene
TG	triglyceride
TPD	temperature programmed desorption
UV	ultra violet
XRD	x-ray diffraction

1 Introduction

Biodiesel is defined by the European Parliament in Directive 2003/30/EC as 'a methyl-ester produced from vegetable or animal oil, of diesel quality, to be used as biofuel'. Biodiesel is produced by the transesterification reaction between triglycerides and a short chain alcohol. The structure of biodiesel, the fatty acid methyl ester, is shown in figure 1.1. The chain length and degree of unsaturation depends on the feedstock oil or fat used.

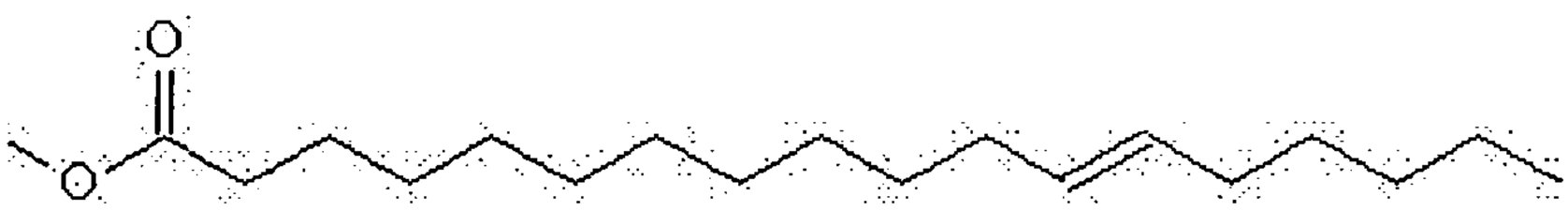

Figure 1.1: structure of biodiesel (fatty acid methyl ester)

The production of biodiesel is a growing industry worldwide; a combination of tax incentives and mandatory targets encourage the growth of the industry. In the UK, we have the Renewable Transport Fuels Obligation, in which distributors must ensure that 5% of all transport fuel sold comes from renewable sources (DFT, 2007). Other countries with significant biodiesel markets are the United States, Brazil and the European Union Member States. The market sizes and incentives/regulations in place in these countries are shown in table 1.1.

Table 1.1: Biodiesel Production in 2006, and regulatory incentive or target in place

Country	Biodiesel Production 2006 (x1000 tonnes)	Incentive/regulations
UK (a)	192	20p/l tax incentive, RTFO
Germany (a)	2662	€0.47/l tax incentive
EU-25 (a)	4890	EU directive: 5.75% target for use of renewable fuels
U.S. (b)	750	$1/gallon tax incentive
Brazil (c)	720	Mandatory 2% blend

(a) EBB, 2007

(b) NBB, 2007

(c) MME, 2007

1.1 Environmental impact

The environmental benefits of biodiesel are its reduced lifecycle greenhouse gas emissions and improved tailpipe emissions, but there are concerns over habitat destruction in order to grow the feedstock crops.

Vegetable oils are renewable resources. As the plants take in CO_2 as they grow, the life-cycle greenhouse gas emissions of biodiesel fuel are lower than those of petro-diesel fuel. However, the plants must be fertilized and harvested, the oil pressed and biodiesel produced by reaction with methanol. All these steps use energy and therefore indirectly emit CO_2, so using biodiesel is not carbon neutral. A comparison of several life cycle analyses of biodiesel fuel found that greenhouse gas emissions were between 22 % and 59% of the emission benchmark of petro-diesel (Frondel and Peters, 2007).

The tailpipe emissions of carbon monoxide, particulates and unburned hydrocarbons are lower for a vehicle running on biodiesel, as shown in table 1.2. This makes biodiesel particularly advantageous for vehicles operating in urban areas. NO_x emissions are increased, although this can be mitigated by changing the timing of the engine.

Table 1.2: Change in tailpipe emission from petro-diesel base line when biodiesel tested in engines

Engine	Fuel used	CO	hydrocarbon	NO_x	particulate matter
1991 DDC series 60[a]	100% biodiesel	-47.5%	-45.2%	+11.6%	-66.7%
Cummins L10E[b]	20% biodiesel	-16.4%	-7.4%	+3.2%	-12.4%
Cummins L10E (retarded timing)[b]	20% biodiesel	-15.7%	-7.4%	-8.0%	-4.8%
Tractor trucks[c]	35% biodiesel	-12%	-11.2%	-0.3%	-25%

a- (Schuhmacher *et. al.*, 2001 a)

b- (Schuhmacher *et. al.*, 2001 b)

c- (Wang *et. al.*, 2000)

Liquid biofuel production requires fertile land, and the rise in the price of basic foodstuffs has been attributed to the increased demand from biofuels (UN, 2007). Capacity of land available for biodiesel production will limit the extent at which it can be substituted for petro-diesel. For example, in the EU, in order to replace 10% of transport fuel with biodiesel, 72% of the current agricultural land will be required (Pearce, 2006). This means that in the EU, vegetable oils and biodiesel will have to be imported from other countries. This results in increased export potential for these countries, but incentivises habitat destruction. Increased oil palm demand has resulted in deforestation in SE Asia (Koh, 2007). Planting and harvesting of energy crops can have a negative impact on greenhouse gas emissions if they replace primary forest (UN, 2007). Use of feedstocks such as used cooking oil and animal tallow does not require any land, and using these oils as a feedstock prevents them being sent to landfill. In the EU, it is estimated that 700 000 to 1 000 000 tonnes of used cooking oil could be collected each year (Kulkarni and Dalai, 2006). This is

equivalent to almost 20% of the current EU-25 biodiesel production capacity. Another alternative feedstock is jatropha oil which is non-edible and grows on marginal land, therefore minimizing the food versus fuel conflict.

Alternative uses of land to produce energy are to grow crops for ligno-cellulosic ethanol production, electricity production or biofuel production by gasification and Fischer-Tropsch synthesis. Yields per hectare are higher in these cases because the whole crop is used, not just the oil containing seed (Frondel and Peters, 2007).

Production of biodiesel is therefore not necessarily environmentally beneficial. While production of biodiesel from waste oils and animal tallow, as well as excess oil production is certainly beneficial, it must be carefully considered whether biodiesel oil grown on former virgin forest land is beneficial or detrimental to society.

1.2 Biodiesel Chemistry

The transesterification reaction from triglyceride to FAME is a series of reversible reactions, shown in equations 1.1 and 1.2. R denotes the fatty acid chain, whose chain length and number of double bond depends on the feedstock used. The most prevalent fatty acid chain in rapeseed oil is oleic acid which has formula $C_{18}H_{35}$ (Ma and Hanna, 1999).

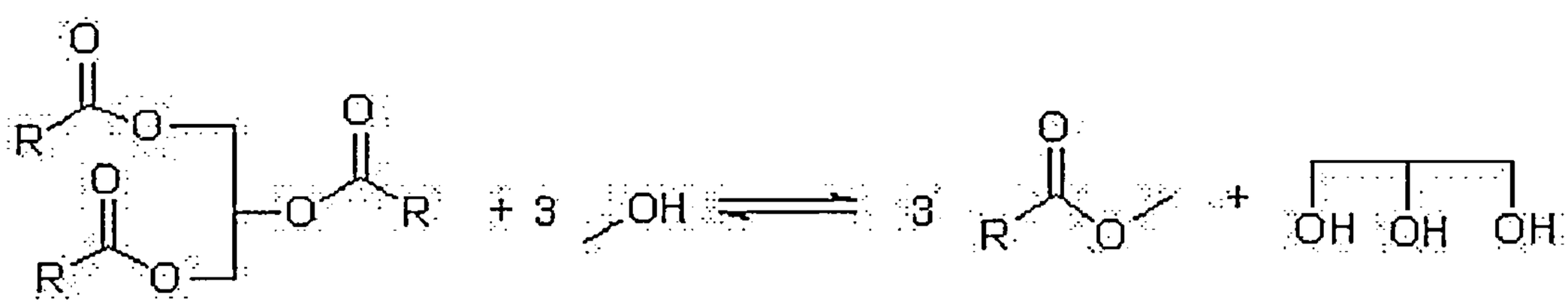

Equation 1.1: overall transesterification reaction

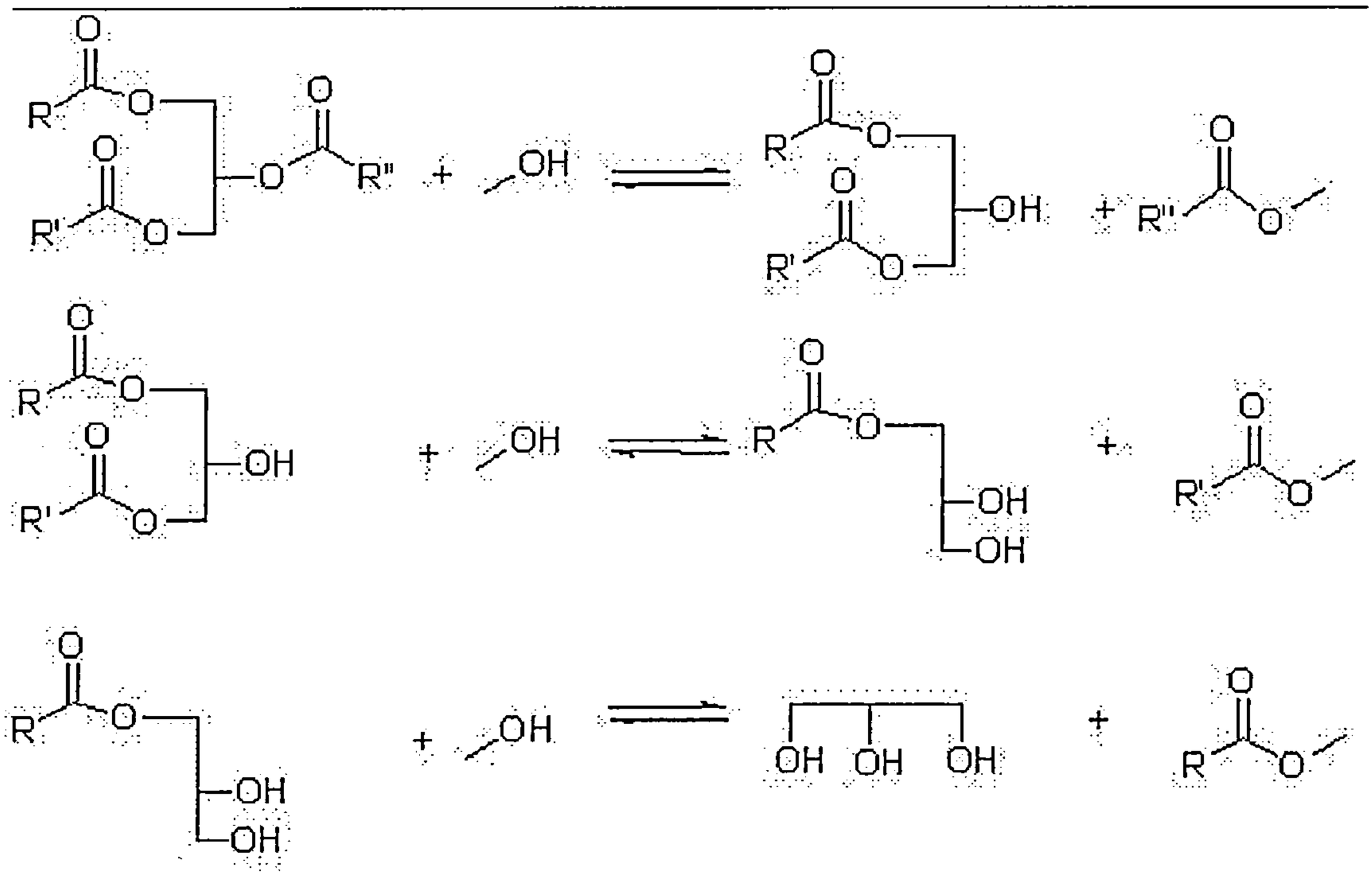

Equation 1.2: step-wise transesterification reactions

The transesterification of triglycerides with methanol can be catalysed by acid, base or enzymatic catalysts (Ma and Hanna, 1999). The reaction can also proceed without a catalyst if supercritical conditions are employed (Demirbas, 2003). In practice, most industrial processes use Na or K hydroxide or methoxide as catalyst (Vicente *et al.*, 2004).

At an industrial scale, the reaction is typically conducted at 60 °C with an excess of methanol. There are often 2 reactors, and an intermediate glycerol separation to push the equilibrium to the product side (Ma and Hanna, 1999). As a guide, the feedstock should have a low content of free fatty acids (< 0.5-1.0 %) and water (< 0.1-0.3 %) to avoid side-reactions (Haas, 2004).

Cheaper feedstocks such as crude oils and used cooking oils have high free fatty acid contents. Processing options for this type of feedstock are to (1) remove the free fatty acids; (2) esterify the free fatty acids with methanol then conduct transesterification or (3) use a

one-stage process with simultaneous esterification and transesterification (Haas, 2004). It is desirable to maximize the yield of biodiesel, so options 2 and 3 are more attractive.

1.3 Advantages of heterogeneous catalyst

The disadvantages of using alkali metal hydroxides or methoxides as the catalyst are twofold: firstly the catalyst is involved in side reactions and secondly the catalyst must be neutralized and the resulting salts removed from the biodiesel and glycerol.

The first side-reaction which can occur is the neutralization of free-fatty acids by the basic catalyst to form the sodium or potassium salt of the free-fatty acid (soap), shown in equation 1.3. The formation of soap reduces the yield of biodiesel produced. Every mole of soap is a mole of biodiesel lost, and the presence of soap hinders phase separation of the glycerol and biodiesel phase, resulting in loss of yield. The feedstock oil is the most expensive part of the process so it is important that yields are maximized. This can be achieved by replacing conventional alkali catalysis with a heterogeneous catalyst.

$$RCOOH + NaOH \leftrightarrow RCOONa + H_2O \qquad [1.3]$$

The alkali catalyst must be neutralized before the excess methanol is removed to prevent the back reaction occurring. This means that not only is the NaOH continually added but also a mineral acid must also be continually added and the resulting neutralization salt disposed of. The salts enter the glycerol phase, and are difficult to remove. They lower the purity of the glycerol and make the raw glycerol phase a less attractive product to sell. As approximately 10% of the output of a biodiesel plant is glycerol, it is important for the economics of the plant that this glycerol can be sold at a good price, so a heterogeneously-catalysed process is desirable, because it will produce cleaner glycerol.

An additional advantage of using a heterogeneous catalyst is that fewer process operations are required for the heterogeneously catalysed process, thus reducing the capital cost of the process. Figure 1.2 is a process flow diagram contrasting the homogeneously and heterogeneously catalysed processes. In the heterogeneously catalysed process all of the

excess methanol can be removed in one stage from the biodiesel/glycerol mixture. This is because the catalyst is retained in the reactor, so upon the removal of methanol the back-reaction will not occur. With a homogeneous catalyst the equilibrium must be kept over to the products side to prevent the back reaction because the catalyst is still present. If the methanol was removed from the biodiesel/glycerol mixture, the back reaction would occur and the content of biodiesel would decrease. Therefore the biodiesel and glycerol must be separated before the methanol is removed.

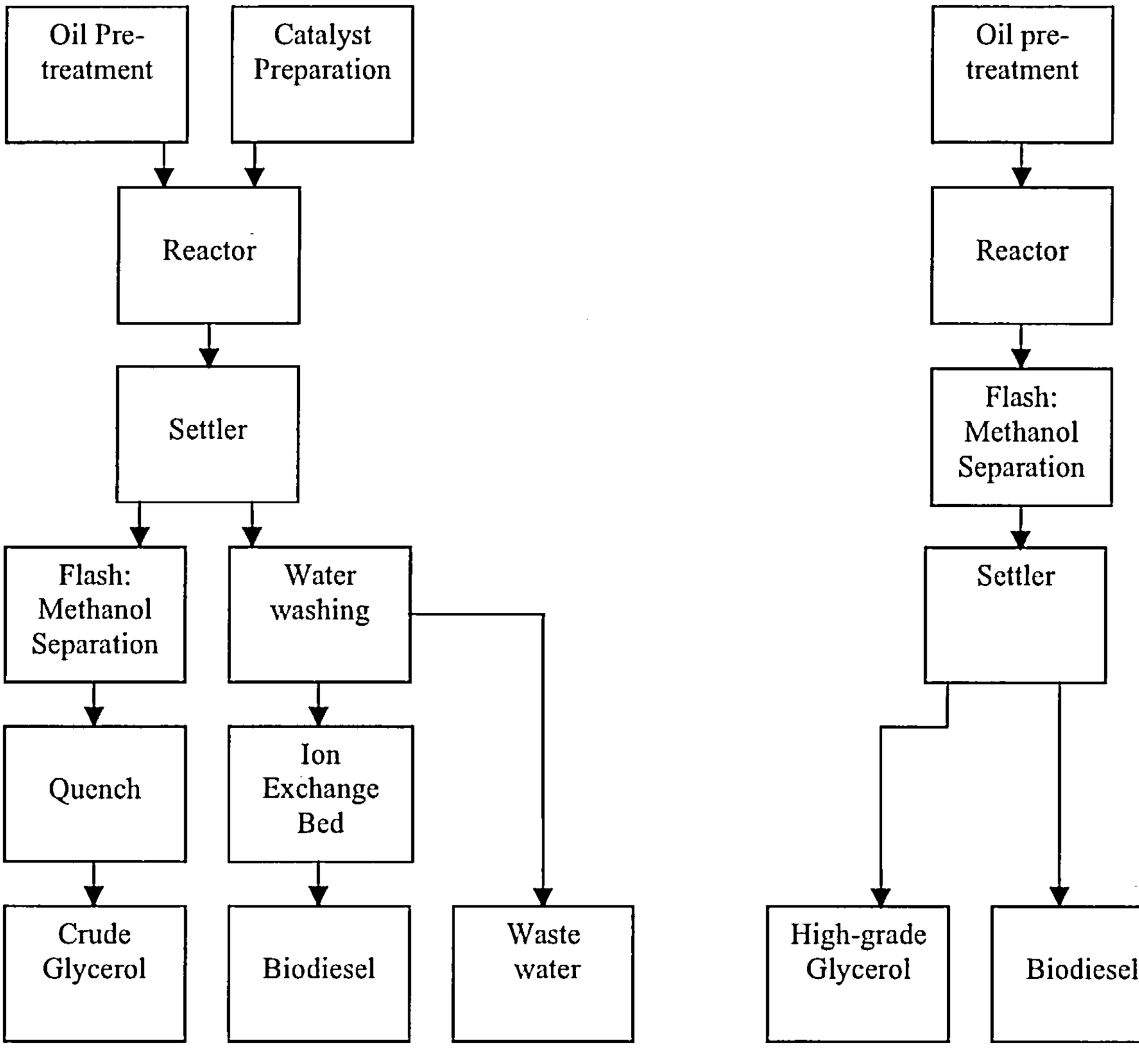

Figure 1.2: schematic flow diagramn of biodiesel process with homogeneous catalyst (left) and heterogeneous catalyst (right)

In some processes where low quality oils with a high free fatty acid content are used, the free fatty acids are esterified first with methanol to make biodiesel. This requires a mineral acid catalyst which must then be neutralised before the base catalysed transesterification takes place. A heterogeneous acid catalyst active for esterification of free fatty acids would eliminate this neutralization step.

Homogeneous catalysts for transesterification reactions are liquid acids or bases, thus we are looking to replace these soluble acids or bases by solid acids or bases. Heterogeneous catalysts in liquid phase reactions will have a mass transfer limitation that is not present in homogeneously catalysed reactions, and as triglycerides are large molecules and the reaction mixture is viscous, we would expect that the reaction time will be greater than in homogeneously catalysed reactions. This means that to achieve the same throughput from a plant the reactor must be larger. Better design of the reactor or catalyst could reduce the mass transfer limitation, for example using an oscillatory flow reactor or large pore material catalyst supports.

The ideal heterogeneous catalyst would be active for both transesterification and free fatty acids esterification, meaning that a one-stage process with simultaneous esterification and transesterification could be designed, allowing complete flexibility of feedstocks. A heterogeneous catalyst active for esterification of free fatty acids is also desirable, because a pre-esterification stage can be used, without requiring neutralization of the acid catalyst. Development of catalysts suitable for dealing with used cooking oil is important, because the biodiesel produced from these feedstocks has no associated environmental concerns.

A successful heterogeneous catalyst for biodiesel production must meet a number of criteria in order to be used industrially. These include:

- Cost: the catalyst should not be prohibitively expensive or difficult to source/manufacture
- Activity: the reaction time should be reasonable for large scale processing at non-extreme conditions
- Lifetime: the catalyst must be stable in methanol and triglycerides/fatty acid esters and mechanically stable

Evaluating the activity of heterogeneous catalysts is straightforward, but evaluation of the stability is more complex. It is very important that the stability is evaluated, because a catalyst must have a long lifetime to be considered for industrial biodiesel production. In this thesis the stability of the catalyst is evaluated by reusing the catalyst, measuring the content of catalytic species in the reaction product and testing the activity of leached species from the catalyst into the methanol. This allows us to see whether the catalysis is wholly heterogeneous, or whether some activity results from the homogeneous species.

2 Literature Review

In this chapter the advantages of replacing a homogeneous catalyst with a heterogeneous catalyst will be discussed, together with strategies for heterogenizing a homogeneous catalyst. Heterogeneous catalysts tested for transesterification of triglycerides with alcohol, esterification of carboxylic acid with alcohols and similar reactions will be reviewed.

2.1 Heterogenizing a homogeneous catalyst

Replacing a homogeneous catalyst by a heterogeneous catalyst has the following advantages (Wilson and Clark, 2000, Corma and Garcia, 2006):

- Ease of separation of the heterogeneous catalyst from reaction product
- Minimization of waste from catalyst separation and disposal
- Facilitating the use of continuous flow processes

For acid and base catalysed reactions, replacing a homogeneous acid or base by a heterogeneous catalyst eliminates the need for the neutralization step and subsequent disposal of neutralization salt. This trend to replace homogeneous catalysts with heterogeneous catalysts is part of the drive towards green chemistry: to minimize waste and eliminate the need for harmful reactants. Many industrial processes now operate with solid acid catalysts (Kiss, 2006 a) but fewer processes operate with solid bases, as solid bases are less prevalent than solid acids (Clacens *et al.*, 2004).

Whereas homogeneous acids and bases have well-defined chemical properties, heterogeneous acid and bases exhibit a variety of sites (Corma and Garcia, 2006). Heterogeneous catalysts can be categorized by the Brønsted or Lewis nature of sites, acid or base strength of sites, number of sites and textural properties of the support.

A homogeneous acid or base catalyst could be replaced by a solid acid or base material, or by acidic or basic species anchored to a support material.

2.1.1 Solid base materials

Materials with basic sites include alkali-metal and alkaline-earth-metal oxides, basic zeolites, supported alkali-metal ions, mixed oxides, oxynitrides and non-oxide materials (Hattori, 1995; Ono, 2003). The basic character of these materials can be identified by adsorption of acidic molecules (e.g. CO_2 temperature programmed desorption), colour change of acid/base indicators and through spectroscopic techniques (Hattori, 1995).

Reactions catalyzed by base catalysts include double bond migration/isomerization, aldol addition/condensation, Michael addition and Knoevenagel condensation (Hattori, 1995). Catalysts found to be active in these reactions could also be active in the transesterification reaction.

Supporting alkali-metal salts on a metal oxide surface forms materials with enhanced basicity. The activity of these catalysts has been well studied for a number of base-catalysed reactions (Hattori, 1995; Ono, 2003). The basic sites are formed on the surface through the decomposition of nitrate or carbonate salts (Yamaguchi *et al.*, 2002). Alternatively, the base strength can be as a result of the substitution of a monovalent cation into the CaO or MgO lattice framework to form a X^+-O^- centre (Ito *et al.*, 1985; Baronetti, 1993). In some cases, both these mechanisms can occur. Li doped into MgO was found to create more base sites than Na-doped MgO and K-doped MgO. This is because Li and Mg have similar ionic radii, so Li-doped MgO exhibits basicity promotion from substitution if Li into the MgO lattice as well as decomposition of the salt on the MgO surface (Diez *et al.*, 2000).

2.1.2 Solid acid materials

Solid acid materials include metal oxides (Al_2O_3, SiO_2), mixed metal oxides, halides of trivalent metals on supports, zeolites and superacids (ZrO_2 and TiO_2 treated with sulfuric acid) (Hagen ,1999).

Zeolites are solid acids that are widely used in industry, but their small pore size makes them unsuitable for liquid phase reactions (Wilson and Clark, 2005).

2.1.3 Silica supported catalysts

Active homogeneous catalysts can be immobilized on silica by covalent anchoring of the catalyst to the silica support (Corma and Garcia, 2006). A variety of species can be immobilized on silica, including sulfonic acid groups, organic bases, Lewis acids such as $AlCl_3$ and $ZnCl_2$ and metal complexes (Corma and Garcia 2006, Brunel *et al.*, 2002).

Mesoporous silicas are a family of porous silicas with high surface areas (reaching 1000 m^2/g) and pores with diameter >2 nm. These mesoporous silicas are synthesized by a micelle templating method. The textural properties of the mesoporous silica depend on the silica source and type of surfactant used (Linssen *et al.*, 2003).

The silicas can be functionalized by a 'one-pot' process or by post-synthesis grafting. 'One-pot' processes are available for the synthesis of amine-functionalized silica (MacQuarrie, 1999) and sulfonic acid functionalized silica (Mbaraka *et al.*, 2003). Many different functional groups can be attached to the silica surface using an alkylsilane linker, as shown in equation 2.1. For example, guanidines can be attached to a silica surface using trimethoxysilylpropoxymethyloxirane as a linker (Subba Rao *et al.*, 1997). This type of catalyst has been used to catalyse Michael additions (Subba Rao *et al.*, 1997), preparation of carbamates (Carloni *et al.*, 2002) and transesterifications (Sercheli *et al.*, 1999; Lakshmi Kantam *et al.*, 2001).

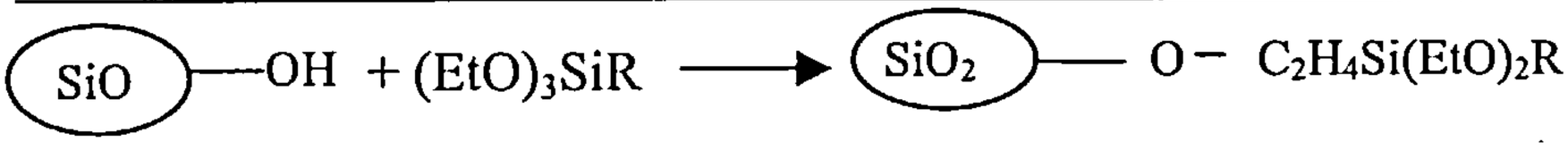

Equation 2.1: anchoring of an alkylsilane group to silica

2.1.4 Polymer supported catalysts

A wide variety of functional groups can be attached to polymeric supports because the reactivity of the pendant group in the polymer (e.g. phenyl group in polystyrene) is similar to the reactivity of the free group. This means classic organic synthesis steps such as chloromethylation and lithiation of the phenyl group can be carried out, and the susbsequent nucleophilic or electrophilic substitution yields a large number of possible functionalities added to polystyrene (Sherrington, 1980 a). Sulfonation of the phenyl groups in polystyrene results in a sulfonic acid functionalized polystyrene as shown in figure 2.2.

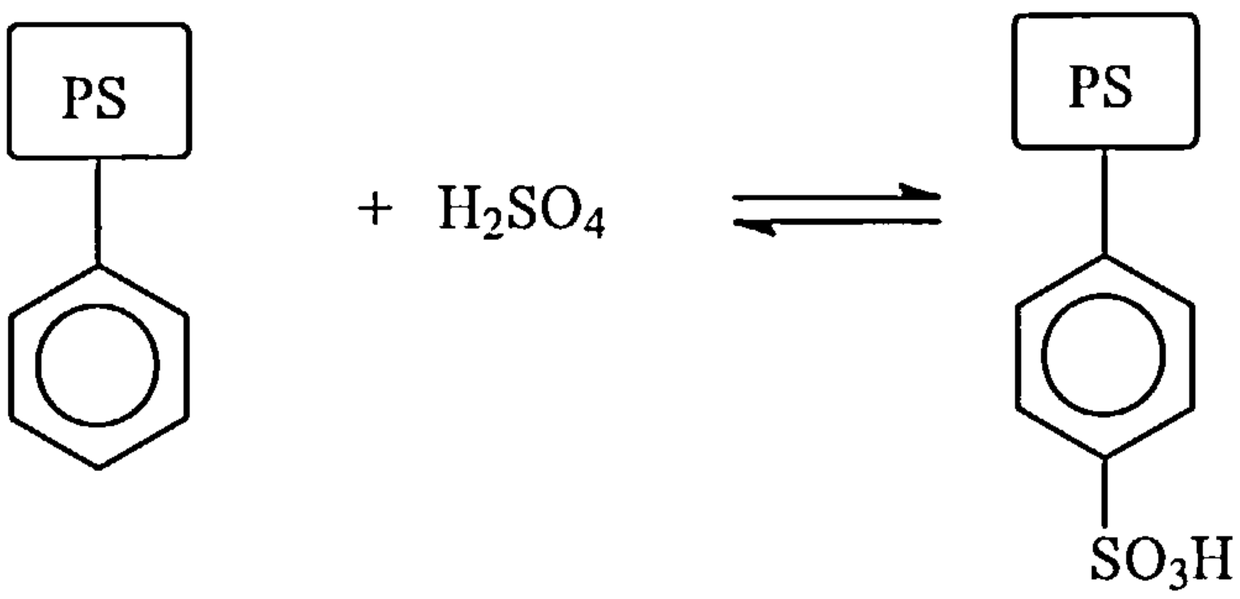

Equation 2.2: Sulfonation of phenyl group in polystyrene (PS)

Polymeric ion exchange resins are a class of polymer supported catalyst that is commercially available. Ion exchange resins can be used for both gas and liquid phase reactions at temperatures up to 125 °C for acid functionalized resins and 60 °C for base functionalized resins (Sherrington, 1980 b). Sulfonic acid functionalized resins are used commercially for the coupling of isobutene with methanol to form MTBE and the condensation of phenol and acetone to form bisphenol-A, among other reactions (Harmer and Sun, 2001).

PolyHIPE is a highly porous macrocellular cross linked styrene-divinylbenzene copolymer, suitable as a catalyst support because its large pore size means that mass transfer limitations can be reduced (Ottens *et al.*, 2000; Cameron *et al.* 1996). PolyHIPE is synthesized by the polymerization of a High Internal Phase Emulsion (HIPE) formed by the dispersal of an organic phase in aqueous solution in the presence of a surfactant. The polymeric material formed has a void volume fraction of >0.9 and pore sizes in the μm range. The PolyHIPE support can then be modified with catalytically active species (Cameron *et al.*, 1996).

2.1.5 Catalysts on magnetic substrates

Magnetite (Fe_3O_4) and other metal ferrites, with general formula (MFe_2O_4), are ferromagnetic and are known catalysts for reactions including the oxidative dehydrogenation of hydrocarbons and decomposition of alcohols (Guin *et al.*, 2005). These materials can be synthesized by the co-precipitation of pre-cursor salts (Martinez-Mera *et al.*, 2007). The magnetization of these ferrites is due to the difference in properties of the sublattices (Rao *et al.*, 2007). Ferrites form a spinel structure or inverse spinel structure; in the case of magnetite, the tetrahedral A sites are occupied by Fe^{3+}, and the octahedral B sites by equal numbers of Fe^{2+} and Fe^{3+} (Yanwa *et al.*, 2006).

Magnetic catalysts are easy to separate from the reaction product by application of an external magnetic field, and this means small particles can be used, without difficulties in filtering out the catalyst (Phan and Jones, 2006). Using small catalyst particles reduces the diffusion limitations present, particularly when a bulky reagent such as triglyceride molecules are involved (Stevens *et al.*, 2005).

Shell-and-core magnetic catalysts can be made by coating the magnetite particles in silica (Phan and Jones, 2006) or polymer (Stevens *et al.*, 2005). The silica or polymer can then be functionalized with the relevant catalytic species.

2.2 Transesterification catalysts for biodiesel production

Transesterification is the process by which an ester is transformed into another through the exchange of the alkoxy moiety, as shown in equation 2.3. Transesterification can be catalysed by acids, bases or enzymes (Otera, 1993).

$$RCOOR_1 + R_2OH \underset{cat}{\longleftrightarrow} RCOOR_2 + R_1OH \qquad [2.3]$$

2.2.1 Homogeneous catalysts for transesterification

2.2.1.1 Basic homogeneous catalysts

The most commonly used catalysts for biodiesel production are alkali-metal hydroxides and methoxides because the reaction is fast and the reaction conditions moderate (Vicente *et. al.,* 2004). In both cases the active species is the methoxide ion. It is formed by the reaction of the hydroxide ion with methanol to form the methoxide and water, as shown in equation 2.4.

$$NaOH + CH_3OH \leftrightarrow NaOCH_3 + H_2O \qquad [2.4]$$

The active catalytic step in the base-catalysed transesterification is the nucleophilic attack of the methoxide ion on the carbonyl carbon. A tetrahedral intermediate is formed, and the original alkoxy group lost to form the methyl ester, and diglyceride. The reaction mechanism is shown in equation 2.5, taken from Schuchardt *et al.* (1997). B represents the basic species, in this reaction the methoxide ion.

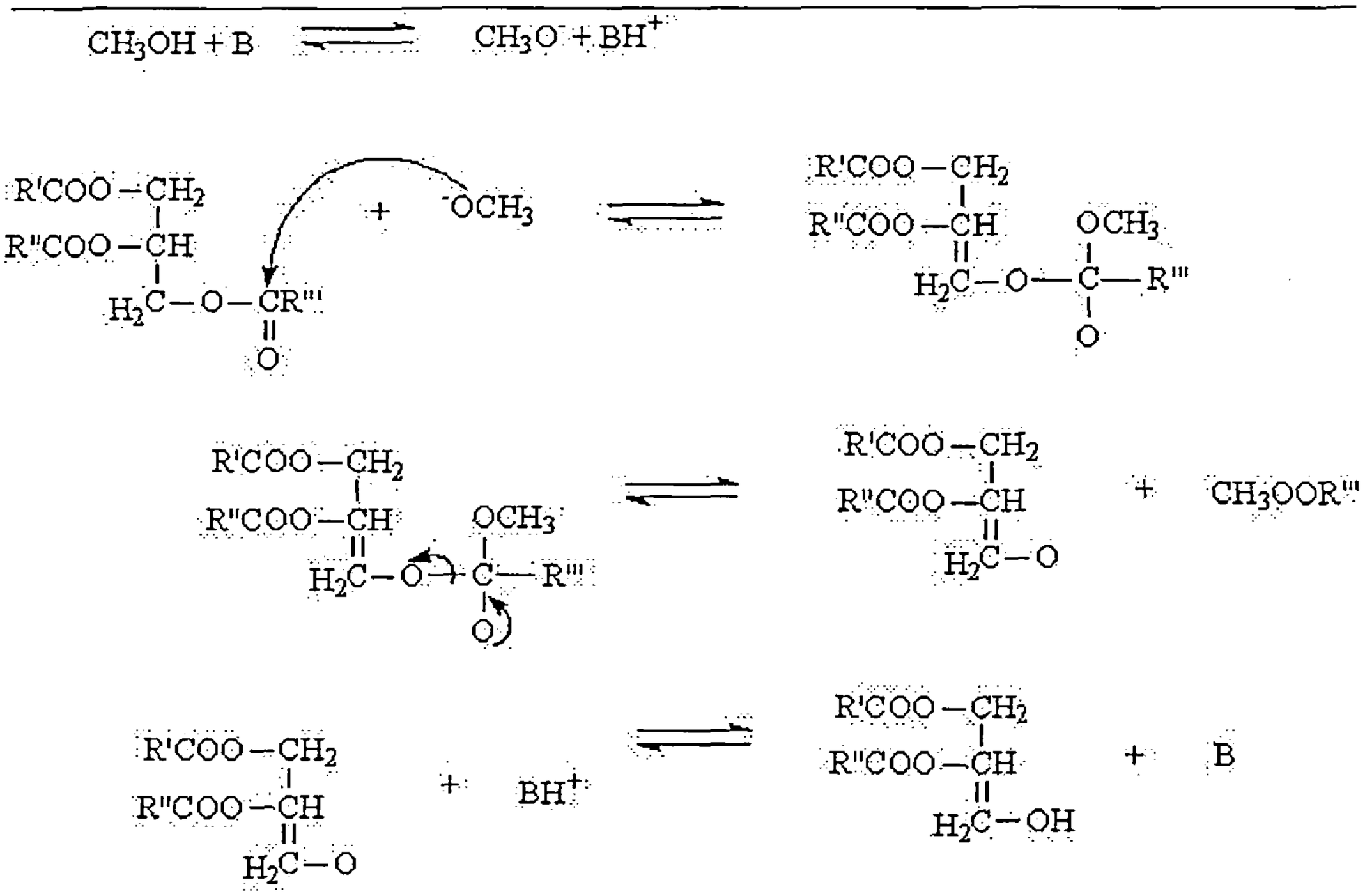

Equation 2.5: reaction mechanism for base catalysed transesterification of triglyceride (Schuchardt *et al.*, 1997)

NaOH is the cheapest of the transesterification catalysts, but NaOMe is preferable, because the saponification of triglycerides (as shown in equation 2.6) does not occur. This is because no water is present from the dissolution of sodium hydroxide in methanol, and saponification requires hydroxide ions. Vicente *et al.* (2004) found that the yield of biodiesel decreased from 98 % to 85 % when sodium hydroxide was used instead of sodium methoxide. This is because some of the triglyceride is saponified and this soap formation causes poorer phase separation and more biodiesel is found in the glycerol layer. The advantage of using KOH or KOMe is that the neutralized salt (usually K_3PO_4) can be used as a potassium fertilizer. The catalyst loading is typically in the region 0.2 -1.5 wt % of the input triglycerides (Ma and Hanna, 1999). Increasing the concentration of the catalyst increases the rate of reaction, but reduces the yield as more triglyceride is saponified, if a hydroxide catalyst is used (Vicente *et al.*,1998).

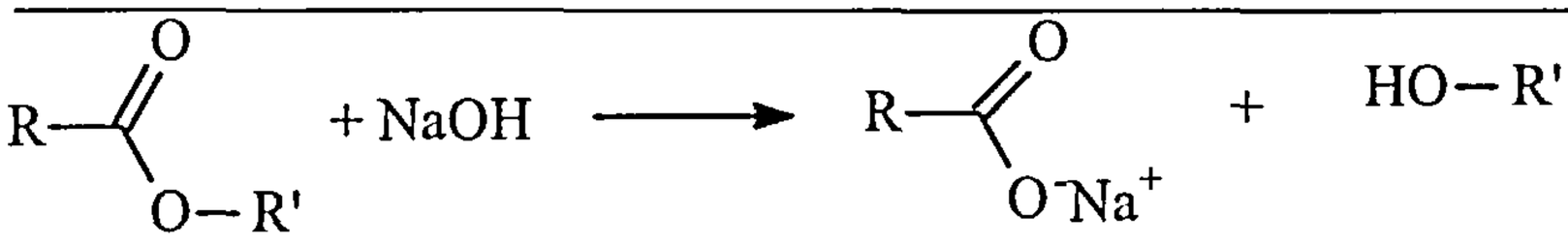

Equation 2.6: Saponification of ester under basic conditions to give soap

The base catalysed transesterification proceeds reasonably quickly with 80% conversion achieved after 1 minute, and the reaction essentially complete after 1 hour. Typical reaction conditions are a temperature of 60 °C and a 6:1 molar ratio of methanol to oil (Ma and Hanna, 1999). The reaction kinetics are 2nd order, with significant mass transfer limitation in the initial stages if the agitation is not vigorous (Vicente *et al.*, 2005, Darnoko and Cheryan, 2000, Noureddini and Zhu, 1997).

Non-ionic bases have been considered as alternative catalysts for the transesterification of vegetable oil. The advantage of using non-ionic bases over NaOH is that no soaps are formed. Guanidines are strong organic bases, which are active for the transesterification of triglycerides. The most basic guanidine tested (triazobicyclodecene, TBD) was found to be almost as active as NaOH (Schuchardt *et al.*, 1997), but guanididnes are more expensive than NaOH.

2.2.1.2 Homogeneous acid catalysts

In general, homogeneous acid catalysts are less active than homogeneous basic catalysts, for example, the rate of reaction using sulfuric acid as a catalyst is 5000 time slower than with NaOH as catalyst (Lotero *et al*, 2005), However, acid catalysts also catalyse the esterification of free fatty acids with methanol to form biodiesel, as shown in equation 2.7, and therefore the possibility of simultaneous esterification and transesterification becomes an option.

$$RCOOH + R'OH \leftrightarrow RCOOR' + H_2O \qquad [2.7]$$

Not all acid catalysts are as slow. When aromatic sulfonic acids were used as catalysts with a molar ratio of 3.6:1 of methanol to oil, 95% conversion was achieved in 50 minutes, a rate one hundred times greater than sulfuric acid (Dittmar *et al.*, 2003). The determining factor

was the solubility of the acid in the organic ester phase. The most soluble and therefore active was 4-dodecylbenzenesulfonic acid, but due to its surfactant properties it would not be suitable for use in a process due to difficulties with the glycerol/biodiesel separation. A compromise between activity and ease of separation was p-toluene sulfonic acid (Dittmar *et. al., 2003).*

Lewis acid materials are known transesterification catalysts. For example organo-tin compounds and titanium tetra-alkoxide catalysts have been used to catalyse different transesterifications (Otera, 1993).

Tin and zinc compounds of the type M(3-hydroxy-2-methyl-4-pyrone)$_2$(H_2O), where M is Sn or Zn, were found to be more active than NaOH and H_2SO_4 catalysts for vegetable oil transesterification under equivalent conditions (Abreu *et. al.*, 2003). Metal acetates and stearates are also active for the transesterification of vegetable oil and the esterification of free fatty acid at 200 °C (Di Serio *et al.*, 2005). The most active, lead stearate, when added at 0.04 % wt, catalysed a 96% conversion of triglycerides and and a 90% conversion of free fatty acids in 3 hours at 200 °C. The activity of this catalyst decreased in the presence of water.

2.2.2 Testing Heterogeneous Catalysts for Transesterification

In most studies on heterogeneous catalysts for transesterification of triglycerides, the activity of the catalyst is correlated with its physico-chemical properties. These properties include acid/base strength, number of acid/base sites and pore size. In addition to testing the activity of the catalysts, the stability of the catalysts should also be tested. However, stability of the catalyst is only tested in a small number of studies.

The stability of a heterogeneous catalyst can be tested by simply reusing the catalyst, but if leaching from the catalyst is slow then simply reusing a catalyst does not prove it is completely stable. The test which proves that a catalyst is stable is known as the hot filtrate test (Sheldon *et al.*, 1998). In this test, the catalyst is removed by filtration from the reaction mixture midway through the reaction and any further reaction progress monitored. For the biodiesel reaction, because of the high viscosity of the reaction mixture, it is simpler to

contact the catalyst with methanol at reaction temperature and then react this methanol with oil and check if the reaction progresses. If no reaction occurs, then the catalysis is heterogeneous. Another method to check the stability of the catalyst is to measure the concentration of the relevant catalytic species in the reaction product.

2.2.3 Heterogeneous Acid Catalysts

Acid catalysts are typically tested at temperatures around 200 °C. At these higher temperatures consideration must be given to reaction occurring without addition of catalyst, e.g. from reactor walls (Suppes *et al.*, 2004) or non-catalytic reaction (Demirbas, 2003). Thermolytic, cracking-type reactions may also occur at these higher temeperatures (Kulkarni and Dalai, 2006). Operating a process at higher temperatures is not a problem for large-scale plants, but would be difficult for smaller, farm-scale plants.

2.2.3.1 Sulfated/tungstated oxides

The activities of sulfated and tungstated zirconia (SO_4/ZrO_2 and WO_3/ZrO_2) were investigated by Lopez *et al.* (2005). Sulfated zirconia was found to have a similar turn over frequency to sulfuric acid; the turnover frequency of tungstated zirconia is lower because its acid strength is lower. Using triacetin as the reactant, with 2 fold excess of methanol, 60 °C and 2 wt% catalyst, 80% conversion was reached with sulfated zirconia and 10% with tungstated zirconia. When the catalysts were reused, the activity was found to decrease, and elemental analysis showed that 8% of the applied tungsten and 20% of the applied sulfur was lost. As tungstated zirconia was considered to be the more stable catalyst, it was investigated in more detail. Tungstated zirconia, with WO_3 loading of 16 wt% was calcined at different temperatures and the effect of calcination on structure and activity assessed (Lopez *et al.*, 2007). The optimum calcination temperature for activity in both the esterification and transesterification reactions was found to be 800 °C, and this temperature corresponded to the WO_3/ZrO_2 material with the maximum surface density of dispersed W atoms. The acidity (as measured by exchange titration) was highest for the material

calcined at 800 °C. Selective poisoning of the Lewis and Brønsted acid sites showed that the Brønsted acid sites were the active sites.

Sulfated zirconia, sulfated tin oxide and tungstated zirconia were used to catalyse the transesterification of soybean oil with a 13-fold excess of methanol at 200 °C to 300 °C (Furuta *et al.*, 2004). After 20 h on stream in a flow reactor, the conversion achieved at 250 °C was 90%, 50% and 15% for tungstated zirconia, sulfated zirconia and sulfated tin oxide respectively. There was a slow decrease in activity with time when the catalyst was used continually on stream for 100 hours. The catalysts were also active for the esterification of octanoic acid with methanol, reaching conversion of 100% at 200 °C after 20 hours. Jitputti *et al.* (2006) used sulfated zirconia to catalyse the transesterification of crude coconut oil and and palm oil with methanol at 200 °C. The activity of the catalyst was high with conversions in excess of 95% reached in 4 hours. However, the catalyst was found to leach, and the activity of the spent catalyst was significantly lower.

Sulfated and tungstated zirconia catalysts appear to be promising for use in biodiesel production, in particular the production of biodiesel from used cooking oil or crude oils where there is a high free fatty acid content, as they are capable of simultaneously catalysing the transesterification of triglycerides and esterification of free fatty acids. However, more work is required to stabilise the catalyst, and also to optimize conditions to bring the residence time required to a reasonable level.

2.2.3.2 Acidic Mixed Oxides

The Esterfip-H process, a heterogeneously catalysed biodiesel production process, operates using a Zn-Al spinel type catalyst in a fixed bed reactor operated at 190-210°C and 40-70 bar (Bournay 2005). The glycerol produced is almost free of metal ions and is >98% pure. This process currently operates at a capacity of 160 000 tonnes per annum and 3 more plants are planned (Axens, 2007).

A study on Sn-Al and Zn-Al mixed oxides showed that these materials were acidic, with Hammett acidity between 4 and 6 (Macedo *et al.*, 2006). The Hammett acidity is measured

by contacting the catalyst with indicators that show a colour change on protonation/deprotonation. The Hammet acidity value of a catalyst is lower than than of the indicator with the lowest pKa which is protonated by the catalyst, but higher than that of the indicator with the highest pKa which is not protonated. Using this method, a value of Hammet acidity is assigned which can be compared with pKa's of liquid acids (Macedo *et al.*, 2006). Sn-Al and Zn-Al mixed oxides had similar catalytic activities in the transesterification of soybean oil, reaching conversions of 80% in 4 hours with a 1.5 fold molar excess of methanol and 5% weight catalyst loading at 67 °C. The catalyst could be reused 4 times without loss in activity, though the catalyst was washed and dried between each use.

The physico-chemical properties of $ZnAl_2O_4$ and Al_2O_3 were compared and related to the activity of these materials in catalysing the ring opening of cyclohexene, a reaction which occurs on strong acid centres (Wrzyszcz *et al.*, 2001). $ZnAl_2O_4$ was found to contain Lewis acid centres, and had a slightly higher total acidity than Al_2O_3. Perhaps more importantly, the proportion of acid sites with high acid strength (ammonia desorption at 773-823 K) was higher for $ZnAl_2O_4$ than Al_2O_3. The activity of Zn-Al mixed oxides in the transesterification of vegetable oil presumably also results from the formation of these strong acid sites.

This type of catalyst has been proven to be effective on an industrial scale, albeit at a higher temperature than the 60°C commonly used. However, the advantages of non-contaminated glycerol compensate for the cost of the extra energy involved.

2.2.3.3 Resins

Amberlyst 15 (a sulfonated polystyrene resin) and Nafion NR-50 (a perfluorinated sulfonic acid resin) were screened for their activity in the transesterification of triacetin with methanol (Lopez *et al.*, 2005). At 60 °C with a 2-fold excess of methanol and 2% wt loading of catalyst a conversion of 70% in 4 hours was reached with Amberlyst 15, and a conversion of 30% in 4 hours with Nafion. The activity of Amberlyst 15 decreased when the catalyst was re-used, with only a slight decrease in S content of the catalyst, so the decrease in activity was attributed to site blocking. The activity of Nafion increased on the first 2 reuses. This is because the resin was able to swell in the methanol. The activity

started to decrease in the 4th cycle of re-use, with no leaching detected, so again was attributed to site blockage.

The low temperature-stability of ion exchange resins may preclude their use as catalysts for the transesterification of triglycerides. Other heterogeneous-acid catalysed vegetable oil transesterifications require temperatures above 180 °C to achieve reasonable conversions, and at these temperatures the ion exchange resins will not be stable.

2.2.3.4 Organo-metallic compounds

Organo-tin compounds, in the form of commercially available catalysts FASCAT® 4100, 4201 and 4350 (Arkema) and LIOCAT® 118 (Miracema Nuodex), were tested for their activity in the transesterification of soybean oil (Ferreira *et al.*, 2007). The reactions were performed at 80 °C, with a 1.3 fold excess of methanol and 0.2 molar % ratio of catalyst. The most active catalyst was dibutyltin dilaurate, with which a conversion of 45% was reached in 10h. However, the solubility of the catalysts was also tested and dibutyltin dilaurate was the most soluble catalyst. The most insoluble catalyst, butylstannoic acid, reached only low conversions at 120 °C. Even though it was the least soluble, the solubility of butylstannoic acid in oil at 100 °C was 0.03 g/ml. Therefore it can be assumed that the mode of action of these catalysts is homogeneous.

Double metal cyanide complexes ($K_2M_3[Fe(CN)_6]_3.xH_2O$) were used in the transesterification of vegetable oil with different alcohols (Sreepasanth *et al.*, 2006). The most active complex was Fe-Zn cyanide: a conversion of 98% was reached in 8 hours at 170 °C with a 5-fold excess of methanol and 3 wt% catalyst. This catalyst could be used 3 times without any loss in activity, and furthermore a hot filtrate test was conducted and no further conversion of oil occurred once the catalyst was removed. No leaching of Fe or Zn into the liquid was observed. Oils with a high free-fatty acid content could be simultaneously transesterified and esterified into biodiesel. There was a correlation between the concentration of Lewis acid sites (coordinatively unsaturated Zn^{2+} ions) and activity. This catalyst appears to be stable and the preparation of the catalyst relatively straightforward, so could be considered for use for biodiesel production. The disadvantages of this catalyts are the high temperature and relatively long reaction time required.

2.2.3.5 Other Acids

Di Serio *et al.* (2007) prepared vanadyl phosphate catalysts ($VOPO_4.2H_2O$) by refluxing V_2O_5 in dilute phosphoric acid, followed by calcination. At 180 °C, a conversion of 78% was reached in 1 hour with 6% catalyst loading and a 9-fold excess of methanol. However, when the catalyst was re-used, the conversion dropped to 30%. This decrease was not due to leaching of vanadium species into methanol, as this was tested for, and a solution of methanol that had been contacted with the VOP catalyst, filtered and reacted with vegetable oil exhibited no catalytic activity. So the catalysis could be defined as heterogeneous. XRD and UV-vis analysis of the catalyst before and after use showed a change in structure and also a change in oxidation state of the vanadium ions on the surface from V^{5+} to V^{3+}. By calcining the used catalyst again at 500 °C the activity of the catalyst was regained, and the oxidation state of the surface V ions returned to V^{5+}. The change in oxidation state of the V ions is thought to be due to the oxidation of methanol, which may have an impact on the process, as the formaldehyde must be separated from the recycled methanol.

Heteropoly acids (HPA) and their salts are materials with a strong acidity. Alkali-exchanged HPAs with large monovalent ions are insoluble in water, and this stability in polar media led to investigation of Cs doped HPA as a catalyst for esterification of palmitic acid and the transesterification of tributyrin (Narasimharao *et al.*, 2007). The most active Cs-exchanged HPA had the formula $Cs_{2.3}H_{0.7}PW_{12}O_{40}$ and reached a conversion of 100% in the esterification of palmitic acid in 6 hours (conditions: 180 °C, 30 fold excess of methanol, 2% catalyst loading by weight of palmitic acid) and 50% conversion in 6 hours in the transesterification of tributyrate (conditions: 180 °C, 10 fold excess of methanol, 2% catalyst loading by weight of tributyrate). Leaching studies showed that the higher Cs content salts were stable to hot methanol reflux, and the catalyst was reused 3 times with only a small drop in activity. Additionally the catalyst was capable of catalysing the 'one-pot' simultaneous esterification and transesterification to form methyl esters.

A similar catalyst was also tested by Chai *et al.* (2006). The activity of this catalyst was high: in 1 hour a conversion of >95% was achieved at 50 °C, a methanol excess of 1.8-fold and 2% molar catalyst. The conversion remained almost stable with the addition of up to

10% free fatty acid because the catalyst was also active for the esterification of the free fatty acids. There was a slow decrease in activity when the catalyst was reused, however the hot leaching test was performed and only 0.4% more conversion was obtained in the 1 hour following removal of catalyst. In 6 runs 5.6 % of the starting material was lost into the liquid phase, which is slight, but would have an impact over time. The reaction time to reach high conversion appears to be too good to be true, even the best homogeneous acid does not reach this high a conversion in the same time (Dittmar *et al.*, 2003).

Heteropoly acid was supported on zirconia, silica, carbon and alumina (Kulkarni *et al.*, 2006). The zirconia-supported heteropoly acid was the most active, with conversion of 60 % reached after 3 hours at 200 °C with a 2-fold excess of methanol and 3 % wt catalyst. The catalyst did not lose activity for transesterification when acid oil was used as a feedstock. There was no decrease in activity on repeated use, and analysis of the metal content of the catalyst before and after use showed a negligible loss of P and W.

Overall, supported or solid heteropoly acids show potential for use is biodiesel production, but the stability must be confirmed first.

Montmorillonite KSF was the most active of several catalysts tested for activity for the transesterification of vegetable oil to biodiesel under microwave heating (Mazzochia *et al.*, 2004). At 170 °C a conversion of 50% was reached in 1 hour with a 3 fold excess of methanol and 10 %wt catalyst. The activity of montmorillonite KSF is due to its strong acid strength, with Hammett acidity =-8.5, acidity stronger than that of concentrated nitric acid. No consideration of the catalyst's stability was presented.

2.2.4 Heterogeneous Base Catalysts

2.2.4.1 Metal oxides

Oxides of group 2 metals are basic and have limited solubility in polar media. These metal oxides, particularly CaO and MgO are cheap and readily available, so if found to be active and stable, would be desirable catalysts for industrial biodiesel production.

CaO has been found to be active at near-ambient temperatures. CaO, BrO and SrO were used as catalysts to transesterify different oils and fats (Hartman, 1956). After 8 hours of reaction >95 % conversion was obtained with CaO as catalyst at reflux temperature with 1.5 % wt catalyst. Around 3% of the triglyceride was saponified. Gryglewicz (1999) found that a conversion of 90% could be obtained in 2.5 hours using CaO as a catalyst at methanol reflux temperature (65 °C) with a 1.5 fold excess of methanol and 1%wt catalyst. The activity of the CaO catalyst was attributed to the formation of CaOMe on the surface of the catalyst.

Nano-crystalline CaO was evaluated for transesterification of various fats and oils at room temperature (Reddy *et al.*, 2006). The reaction was essentially complete after 24h at room temperature with a 25-fold excess of methanol and 1 %wt catalyst when nano-cystalline CaO was used, but, under the same conditions using conventional CaO gave only 2% conversion. The formation of surface bound CaOMe was confirmed by C^{13} NMR. The increased activity of the nano-crystalline CaO was due to higher surface area and smaller crystallite size and thus increased number of catalytically active sites. On reuse of the catalyst, the crystallites agglomerated and the catalyst deactivated.

The activity of CaO was found to be very sensitive to pre-treatment conditions (Lopez-Granados *et al.*, 2007). Surface carbonation and hydration were found to occur rapidly, and significantly reduce the activity. CaO calcined at 973 K is the most active, and a conversion of 90 % was reached in 90 minutes at 60 °C, with a 4-fold excess of methanol and 1 %wt catalyst. When this catalyst was reused, the conversion dropped slightly to ~80 % but remained fairly constant around that value for 8 cycles. However, the activity of leached species was found to be high: a conversion of 60% was reached using methanol which had been contacted with CaO and filtered and thus contained homogeneous species present in the reaction. The solubility of CaO in methanol is low, so it will dissolve or leach relatively slowly into methanol and will be able to be reused several times. Nevertheless, the catalysis is not wholly heterogeneous.

At higher temperatures MgO is also an active catalyst. It is less basic than CaO, but the transesterification reaction can proceed at less basic sites at higher temperatures (Di Serio *et al.*, 2006). MgO prepared by various methods was tested for activity in the transesterification of vegetable oil at 200 °C with a 4-fold excess of methanol and 3.5 wt% catalyst. The MgO produced by the decomposition of $(MgCO_3)_4Mg(OH)_2$ had the strongest basic sites and was the most active, reaching conversions of 95 % in 60 minutes. MgO was also found to be active for the transesterification of glycerol with methyl esters to form monoglycerides (Corma *et al.*, 1998) and the transesterification of ethyl acetate with methanol (Dossin *et al.*, 2005).

CaO and MgO are inexpensive materials, and their activities are relatively high. However, CaO does leach into the reaction mixture, so metal ions would still have to be removed from the biodiesel by water washing, thus the advantage of using a heterogeneous catalyst would be lost. Investigation into the stability of MgO is required before the high temperature MgO-catalysed transesterification is considered.

2.2.4.2 Modified metal oxides

Strongly basic catalysts can be formed by supporting an alkali-metal salt on a support, for example, alumina (Hattori, 1995). The procedure used to prepare such catalysts is that the alkali metal is loaded onto the support from an aqueous pre-cursor salt solution, the resulting solid heat-treated by calcination, then tested in the reaction of either real feedstock oils or shorter-chained triglycerides. The typical variables tested are calcination temperature, alkali metal loading amount and type of pre-cursor salt.

Various basic materials have been prepared by the decomposition of alkali and alkaline-earth salts onto metal oxide supports. Potassium was loaded onto alumina by impregnation of potassium nitrate solution at different loading levels and calcined at temperatures ranging from 673 to 973 K (Xie *et al.*, 2006a). The resulting base strength of these materials, calcined at temperatures higher than 773 K, reached $15.0 < pK_{BH+} < 18.4$. pK_{BH+} is a measure of base strength defined by $pK_{BH+} = -\log_{10}([B][H^+]/[BH^+])$, determined by the colour change of indicators on protonation and deprotonation, as described in section

2.2.3.2. From XRD and IR analyses, together with the basicity measurements, the active sites were identified as surface Al-O-K groups and K_2O. 35 wt% KNO_3 calcined at 773 K had the highest activity and basicity. A conversion of 85% was reached in 8 hours at 65 °C, with a 5 fold excess of methanol and a catalyst loading of 6.5 %. The reuse of this catalyst was not tested, however, the soluble basicities of these catalysts in water were measured, and basicities of up to 0.6 mmol/g catalyst were measured. Although considered small by the authors, this soluble basicity is equivalent to 0.2 wt% NaOH by weight of oil, c.f. the 0.5 -1.5 wt% typically used industrially (Vicente *et al.*, 1998). It appears that the relatively high soluble basicity of this catalyst explains its catalytic activity.

Xie and Li (2006) extended the investigation of alumina-supported potassium to study various K salts supported on alumina. KI, KF, KCl, KBr, K_2CO_3, KNO_3 and KOH were applied by wet impregnation onto alumina. The most active catalyst was KI on alumina. The more basic catalysts were more active and the catalysts with base strength lower than $pK_{BH+}<7$ were not active at all (non-loaded alumina and KCl-alumina). The higher activity of KI-alumina was attributed to its lower thermal stability i.e. more KI decomposed to K_2O. A conversion of 90% was achieved in 8 hours at 65 °C with a 5-fold excess of methanol and 2% wt catalyst. As the origin of basicity and thus activity was thought to be K_2O then the leaching problems for these catalysts are likely to be similar to KNO_3 on alumina. KI was also supported on different materials including ZrO_2, ZnO and zeolites. The zeolite had reduced base strength, and lower activities, with the activities of KI on ZrO_2 and ZnO only slightly lower than KI on alumina. However, a further study on KOH/zeolite optimized the loading of KOH on the zeolite and a conversion of 85% in 8 hours was obtained at 65 °C with a 3.3 fold excess of methanol and 35 wt% catalyst (Xie *et al.*, 2007). This type of catalyst was tested in two successive reaction cycles, and the conversion decreased significantly on the second use, showing that leaching of the KOH from the catalysts was responsible for the catalytic activity.

The activity of KF supported by ZnO was also investigated (Xie and Huang, 2006). KF supported by ZnO was more active than KOH/ZnO and K_2CO_3/ZnO. A conversion of 87% was obtained in 9 hours at 65 °C with a 3.3 fold excess of methanol and 3 wt% catalyst. The loading with the highest activity (15 wt% KF) also showed the highest basicity as

measured by titration. The basic sites were thought to be dispersed KF species on the ZnO surface, as well as surface hydroxyl groups which are present with increased frequency when KF is added to ZnO. The reuse of this catalyst was not tested, nor was the stability of the catalyst.

Alkaline earth metals (Mg, Ca, Sr and Ba) were loaded onto alumina, zirconia and ZnO and screened for activity in the transesterification of soybean oil to biodiesel (Yang and Xie, 2007). The most active catalysts were $Sr(NO_3)_2ZnO$ and $Ba(NO_3)_2ZnO$. These catalysts reached conversions of >90% in 5 hours at 65 °C with a 4 fold excess of methanol and 5 wt% catalyst. Other active catalysts included $Ca(NO_3)_2Al_2O_3$, $Sr(NO_3)_2Al_2O_3$ and $Mg(NO_3)_2ZrO_2$, reaching conversions of 49%, 27 % and 25% respectively. All of these more active catalysts had higher base strengths ($15< pK_{BH+}<18$) than the less active catalysts. It is interesting to note that different alkaline earth metals formed the most active catalyst on each different support, for example Ca on Al_2O_3 forms the most active alumina supported catalyst but $Mg(NO_3)_2ZrO_2$ was the most active zirconia-supported catalyst and $Sr(NO_3)_2ZnO$ the most active ZnO supported catalyst. The origin of the basicity was attributed to the decomposition of the nitrate salt to the oxide. This means that different support-substrate interactions lead to more or less favourable conditions for the decomposition of each salt and thus the different activity of different alkaline earth metal-support oxide combinations. However, on further testing the $Sr(NO_3)_2ZnO$ was found to deactivate when reused, although it could be recovered by treating with a fresh solution of $Sr(NO_3)_2$. It is likely that leaching of the SrO into solution occurred or the active sites were deactivated. It is possible that using a less soluble alkaline earth metal oxide would result in a more stable catalyst.

Alumina was treated with sodium hydroxide and sodium metal to form $Na/NaOH/Al_2O_3$ catalysts (Kim *et al.*, 2004). This type of catalyst has basic sites with strength $pK_{BH+}>37$. $Na/NaOH/Al_2O_3$ was more active than Na/Al_2O_3 and $NaOH/Al_2O_3$, and this catalyst had more strong-base sites (measured by CO_2 TPD). Adding both Na and NaOH caused a greater formation of $NaAlO_2$ on the catalyst and a greater change in binding energy of the O 1s orbital towards a tendency to donate electrons than Na/Al_2O_3 and $NaOH/Al_2O_3$ alone. Therefore, the formation of basic sites was attributed to both the formation of $NaAlO_2$ and

to the dispersal of Na^+ ions in the alumina matrix, increasing the electron pair donating properties of the surface oxygen atom. In 1 hour at 60 °C, with a 2 fold excess of methanol and 1.5 %wt catalyst loading a conversion of 75 % was obtained, increasing to 85% with the addition of n-hexane as a co-solvent and 95% when the molar excess of methanol was increased to 3-fold. The reuse of this catalyst was not tested, nor was the stability of the catalyst.

Alkali metal salts loaded on alumina were compared for their activities in the transesterification of triolein and the double bond isomerization of 2,3-dimethyl-1-butene (Ebiura *et al.*, 2005). The double bond isomerization of 2,3-dimethyl-1-butene is a test reaction to determine the base strength of a catalyst. The most active catalysts for the isomerization (KOH-Al_2O_3 and KNO_3-Al_2O_3), were active for transesterification, but not the most active. The most active catalysts for the transesterification were K_2CO_3- Al_2O_3 and KF- Al_2O_3. It was suggested that as well as a high base strength the catalyst must be able to activate the carbonyl group.

The basicity of alkaline earth oxides can be promoted by doping with alkali metals. The changes in acid-base properties of the oxide depend on both the amount and type of the alkali metal cation (Diez *et al.*, 2000). The origin of the basicity in this case is the formation of O^- centres through the substitution of the M^+ ion into the oxide lattice of the alkaline earth metal (Baronetti *et al.*, 1993). These catalysts are prepared by impregnation of a pre-cursor salt solution onto the metal oxide, followed by drying, but not necessarily calcination.

Watkins *et al.* (2004) tested Li-promoted CaO catalysts for the transesterification of tributyrate with methanol. The tributyrate was chosen as a model substrate to screen catalytic activity. Promoting the CaO with Li by impregnation of $LiNO_3$ solution increased the base strength to $15 > pK_{BH+} > 17.2$, compared with the base strength of CaO alone of $8 > pK_{BH+} > 10$. The catalysts with the highest activity had a Li loading of 1.23 wt%, this loading corresponded to the transition between dispersed Li atoms and Li atoms as bulk $LiNO_3$. Therefore the active site proposed was isolated Li^+ species that react with CaO to form defect sites which then react with water to form surface hydroxyl groups. Li promoted

CaO-catalyst reached 100% conversion for the transesterification of tributyrate after 20 minutes reaction at 60°C with a 120 fold excess of methanol and 0.8% by weight catalyst loading. Under the same conditions, the CaO catalysed reaction reached only 2.5% conversion. It was reported that only a slight reduction in activity occurred when the catalyst was reused, and, as pure $LiNO_3$ was inactive, it was considered that homogeneous Li^+ species had no activity.

Meher *et al.* (2006) tested Li, Na and K doped CaO catalysts for the transesterification of karanja oil. Li-CaO was found to be slightly more active than Na-CaO and K-CaO, when the alkali metals were doped at equal weight onto the support. CO_2-TPD showed that the base strength of Li-CaO was higher than that of Na-CaO and K-CaO. It was thought that increasing the size of the alkali metal cation decreased the basicity. A conversion of 82% was reached in 4 hours at 65 °C with a 4 fold excess of methanol and 2 % wt catalyst. This conversion was reduced to 80% for Na-CaO and 75% for K-CaO. The high conversion was maintained at free fatty acid levels up to 6% with Li-CaO catalyst, while under the same conditions the conversion using KOH catalyst dropped to less than 20% as the free fatty acid concentration was increased. Unfortunately, no tests of leaching or reuse were included in the paper.

The stability of this type of catalyst must be tested. Although the reaction time required for high conversions are short, it is unlikely that this class of catalyst is suitable for heterogeneously catalysed biodiesel production because none of these catalysts have been proven to be stable.

2.2.4.3 Hydrotalcites

Hydrotalcites are layered double hydroxides with the general formula $M_x^{2+}M_y^{3+}(OH)_{2(x+y)}A^{n-}.mH_2O$ (Corma *et al.*, 2005).

Mg-Al hydrotalcites with tunable base strength were prepared by an alkali-free co-precipitation route (Cantrell *et al.*, 2005). The activity of the hydrotalcites in the transesterification of tributyrate with methanol increased with increasing Mg content; this increase in activity is mirrored by the increase in base strength as measured by Hammett

indicators. After 3 hours a conversion of 70 % was reached at 60 °C with a 10 fold excess of methanol and 0.3 %wt catalyst. There was no discussion on the stability of these catalysts, although the use of the alkali-free precipitation route eliminates any alkali-metal cations being present in the calcined catalyst, which can contribute to the apparent activity of the catalyst.

Li-Al hydrotalcites were characterized and evaluated for use in the transesterification of soybean oil with methanol (Schumaker *et al.*, 2007). The Li-Al hydrotalcites were found to be more active than Mg-Al hydrotalcites prepared by similar methods. 53% methyl esters were formed after 1 hour reaction at 65 °C with a 5 fold excess of methanol and 1 wt% of catalyst, whereas under the same conditions the Mg-Al hydrotalcite reached 3 % conversion. The leaching of lithium was quantified, and it was found that 3.6% of the lithium present in the catalyst leached out into solution. There was also a small decrease in activity when the catalyst was reused. When the hot filtrate test was carried out the reaction did continue, but slowly. It remains unclear whether the leaching of the lithium is slow enough to consider use of this catalyst as a heterogeneous catalyst.

Mg-Al hydrotalcites were prepared with different Mg:Al ratios and at different calcination temperatures (Xie *et al.*, 2006 b). The most active hydrotalcite had a Mg:Al ratio of 3, and was calcined at 773 K. Above 773 K the non-active spinel phase starts to be formed, reducing the catalysts' activity. In the transesterification of soybean oil, a conversion of 65% was reached in 9 hours at 65 °C with a 5 fold excess of methanol and 7.5 wt % catalyst. No studies were conducted on the reuse of this catalyst, however the soluble basicity (i.e. basic species in solution measured by titration with acid) in water of the catalyst was measured and was found to be 0.48 mmol/g. This soluble basicity is equivalent to 0.1 %wt NaOH, approximately one tenth of the level of homogeneous catalyst added industrially.

The catalytic activity of Mg-Al hydrotalcite was compared to that of MgO for transesterification of vegetable oil at 100-200 °C (Di Serio *et al.*, 2006). Using Mg-Al hydrotalcite, conversion of >95 % could be obtained in 60 minutes at 200 °C with a 4 fold excess of methanol and 3.5 % wt catalyst. At higher temperatures (200 °C), there was little

difference in the conversions achieved by hydrotalcite and MgO (all 80-95%), but as the temperature was reduced to 100 °C the hydrotalcite was significantly more active than the MgO catalysts. It was concluded that stronger base sites are active when the transesterification reaction is conducted at 100 °C, but when the temperature is increased above this, basic sites with medium strength also become active, so materials such as MgO become catalytically active. The hydrotalcite catalyst maintained its activity when 10 000 ppm water was added to the reaction mixture. However, no data on the reuse of the catalyst was presented.

Hydrotalcites, particularly when used at high temperatures are sufficiently active that the reaction time required for high conversion is reasonably practical for industrial use. However, data on stability is required.

2.2.4.4 Anionic Resin

Ion exchange resins functionalized with quaternary ammonium groups were teseted for the transesterification of triacetin (Liu *et al.*, 2007) and triolein (Shibasaki-Kitakawa, 2007). Amberlyst 26 was found to be active for the transesterification of triacetin with methanol, reaching a conversion of 60% in 4 hours at 60 °C with a 2 fold excess of methanol and 0.8% wt catalyst. Amberlyst 26 was stable under these conditions with only a small loss in activity and negligible activity of the catalyst leachate. Silica functionalized with the same quaternary ammonium group was not stable. For the transesterification of triolein with ethanol, the anionic resin with the smallest particle size was found to be the most active. After 3 hours a conversion of 80% was reached at 50 °C with a 3 fold excess of methanol and 40 %wt catalyst. This is a very high level of catalyst loading, and as such it is particularly important to demonstrate that the catalyst is stable. Reuse of the catalyst showed a drop in activity, attributed to leaching of hydroxyl ions from the resin. Treating the catalyst with NaOH solution after washing off organic contaminants recovered the catalyst's activity, but treating the catalyst with NaOH after each cycle is impractical in an industrial process.

2.2.4.5 Solid organic bases

Guanidines are basic organic molecules that can be used in place of alkali metal oxides or hydroxides (Gelbard and Vielfaure-Joly, 2001). When used in the homogeneous phase as catalysts for biodiesel production, no emulsions or soap are formed (Schuchardt *et al.*, 1997). Guanidines can be supported on polystyrene or silica to form heterogeneous catalysts.

Tricyclohexylguanidine (TCG) and triazobicyclodecene (TBD) were attached to polystyrene and mesoporous silica (Sercheli *et al.*, 1999). TBD is the more basic species, so was more active in the homogeneous phase and when supported on polystyrene and silica. The polystyrene-supported TBD and TCG were slightly more active than silica supported TBD and TCG. These catalysts reached conversions in the range 85-95% (except TCG-silica, conversion 65 %) in 5 hours at 70 °C, with a 2 fold molar excess of methanol and 5 mol% catalyst. Reuse of the catalysts resulted in a decrease in activity, and also a loss of the guanidines from the support.

The heterogenization of guanidines onto different substituted polystyrenes was investigated by Schuchardt *et al.* (1996). Guanidines were attached to polystyrene through substitution on a chloromethyl group or via a bromohexyl spacer arm. The supported guanidines had lower activities than their homogeneous counterparts, but conversions in excess of 90% were achieved in 6 hours with supported TBD at 70 °C with a 2 fold excess of methanol and 5 mol% catalyst. However, there was a significant decrease in activity when the catalysts were reused due to leaching of the guandines or reaction of the guanidines with the unsubstituted bromo-hexyl groups. An attempt to improve the stability of polystyrene supported guanidines was to reduce the guanidine loading by reducing the loading of chloromethyl groups (Jerome *et al.*, 2004). Hot filtrate tests showed that no reaction occurred in the absence of the catalyst, and there was only a slight decrease in activity when the catalyst was reused.

Biguanides are more basic than guanidines, and were supported on polystyrene to be tested as catalyst for the production of biodiesel (Gelbard and Vielfaure –Joly, 2001). Polystyrene supported biguanides performed better in terms of initial activity (90 % conversion in 30 minutes, at 70 °C, with 2 fold excess methanol and 6 mol% catalyst), and also in reusability than polystyrene supported guanidines, but the activity began to fall after the 10^{th} cycle of use, and at this point the amount of N on the catalysts began to drop. This drop in N content was attributed to the cleavage of the biguanide units by methanolysis.

The metal salts of amino acids are basic materials that are insoluble in methanol, glycerol and fatty acid esters (Peter *et al.*, 2002). Zn-arginate was found to be the most active of the tested catalysts, reaching a conversion of 70% in 3 hours at 75 °C with a 2 fold excess of methanol. Increasing the temperature to 150 °C resulted in a conversion approaching 100% being reached in 3 hours. No Zn was detected in the reaction mixture so this catalyst could be considered stable.

Organic bases in the homogeneous phase are desirable catalysts because soaps are not formed. As these chemicals are expensive, they must be recovered for the process to be economic. Thus, supporting guanidines on solid supports seems a sensible route to follow. Polystyrene-supported guanidines and biguanides are catalytically active, but are unlikely to be stable enough to justify their high cost. Zn-arginate is also catalytically active and should be studied further because it is chemically stable to leaching in methanol.

2.3 Esterification catalysts for biodiesel production

Free fatty acids are present in cheaper feedstocks such as animal tallow and used cooking oil. Free fatty acids can be esterified with methanol to form biodiesel. The esterification reaction can take place before the transesterification reaction as a pre-treatment stage, in which case any homogeneous catalyst must be neutralized or an acid catalyst could be used to catalyse the esterification and transesterification reactions simultaneously.

2.3.1 Homogeneous

The catalyst generally employed in industry for esterification is sulfuric acid, although other Brønsted and Lewis acids are active for esterification. Titanium and tin compounds are active for esterification and also have activity in transesterification reactions (Hoydonckx *et al.*, 2004).

2.3.2 Heterogeneous

Several heterogeneous catalysts were compared for their activity in the esterification of acetic acid with butanol (Peters *et al.*, 2006). The most active were the acidic ion exchange resins Smopex 101 and Amberlyst 15, followed by sulfated zirconia. Zeolites had a low activity due to internal diffusion limitations in the small pores. Kiss *et al.* (2006) evaluated commercially available solid catalysts for the esterification of dodecanoic aicd with 2-ethylhexanol at 130 °C. Amberlyst 15, Nafion and sulfated zirconia were found to have similar activities, reaching conversions of approximately 60% in 1 hour at 130 °C, but Amberlyst 15 and Nafion were found to be thermally unstable at this temperature (Kiss *et al.*, 2006)..

An acidic ion exchange resin has been evaluated as a catalyst for the esterification of free fatty acids in the presence of triglycerides in a batch and continuous process (Tesser *et al.*, 2005; Santacesaria *et al.*, 2007). Reaction conditions required to convert 80% of the oleic acid are 1 hour at 100 °C with an 8 fold excess of methanol and 1.6 wt% catalyst. The starting free-fatty acid content of the oil was 56%. The low maximum operating temperature of acidic ion exchange resins may make other catalysts more attractive because the reaction time is reduced at higher temperatures.

The activity of organosulfonic acid functionalized mesoporous silica was found to increase with acid strength and pore size (Mbaraka *et al.*, 2003). The most active heterogeneous catalyst, SBA-15 with pore size 50Å and functionalized with phenyl-sulfonic acid was found to be more active than Nafion and Amberlyst 15 in the esterification of palmitic acid

in the presence of triglycerides at 85 °C. Further investigation (Mbaraka *et al.*, 2006) showed that the activity of acid-functionalized mesoporous silica remained constant on repeated use, however when beef tallow was used as reactant, the activity decreased on repeated use. This loss in activity is attributed to blocking of the active sites by carbonaceous material. Purification of the beef tallow allowed the catalyst to be reused without drop in activity.

Kiss *et al.* (2006b) showed that sulfated zirconia catalysed an 80% conversion of dodecanoic acid after 20 minutes at 140 °C with a 3 fold excess of methanol and 3 wt% catalyst. However, it has been shown that sulfated zirconia leaches into methanol and triglycerides and tungstated zirconia is more stable (Lopez *et al.*, 2007). Tungstated zirconia is also active for the esterification of palmitic acid (Ramu *et al.*, 2004).

Heteropoly acids can be supported on a number of supports to give a heterogeneous catalyst. Heteropoly acids were supported on zirconia and mesoporous silica and evaluated as catalysts for the esterification of fatty acids (Juan *et al.*, 2007; Kulkarni *et al.*, 2006). Both catalysts were found to be active, but only heteropoly acid on zirconia was found to be stable. Using the heteropoly acid on zirconia, catalyst conversions of 80% were reached in 3 hours at 200 °C with a 9 fold excess of methanol and 3 %wt catalyst.

2.4 Summary

It is difficult to find an active heterogeneous catalyst that is stable in this system. Although many studies of different catalysts have been carried out, only a small number present data on the stability of the catalysts, and of those, few have been found to be stable. These considerations apply to both transesterification and esterification. The advantages of using a heterogeneous catalyst are lost, or greatly reduced, if the catalyst leaches.

A number of different base catalysts have been found to be active at ambient temperature, however it is unlikely that any of these catalyst are stable. Zn-arginate and the ion exchange resin functionalized with the quarternary ammonium group (Amberlyst 26) appear to be stable, and these catalysts should be investigated further. If the reaction temperature is

increased then hydrotalcites become active, and could be practical catalysts if they are found to be chemically stable at these temperatures.

Several solid acid catalysts are active for both transesterification and esterification. A process of simultaneous esterification of free fatty acids and transesterification of triglycerides is desirable because lower quality, cheaper feedstocks can be used. A high temperature process is required, for both reactions to proceeed at an appreciable rate.

Some solid acid catalysts which could be studied further are:

- supported heteropoly acids or heteropoly acid salts
- double metal cyanide complexes
- sulfonic acid-functionalized silica
- Sn-Al and Zn-Al mixed oxides

These catalysts have been shown to be relatively stable to leaching in methanol, and have been shown to be active for transesterification or esterification. The first two catalysts in the list are active for both transesterification and esterification, however as they are all acid catalysts they all could be active for both reactions. However, the reaction time required is quite long, above 8 hours, so would have to be shortened if these catalysts were to be used at an industrial scale.

3 Materials and Methods

For all of the catalysts tested the same general procedure was followed. Firstly, catalysts to be tested were identified from screening of a number of candidates or from the literature. A residence time of 3 hours was chosen as the standard reaction time, because this time would be the largest residence time still practical on an industrial scale. The catalysts' physico-chemical properties, such as surface area and acid/base strength were analysed. The catalysts were then tested in a 200 ml batch reactor. At this stage the stability of the catalysts was also tested. Finally, modifications were made to the catalysts in an attempt to improve the activity and stability.

3.1 Analytical methods to determine conversion to biodiesel

The standard method for quality control of biodiesel is gas chromatography, however this method is time-consuming and for this reaction, off-line. Enzymatic glycerol determination and refractive index measurements were compared with gas chromatography for accuracy and speed of analysis.

3.1.1 Enzymatic glycerol determination

An enzymatic glycerol test kit (R-Biopharm) was used to determine both free glycerol in a reaction mixture and bound glycerol (in glycerides) in the biodiesel layer. This enzymatic method has been used to determine free glycerol in biodiesel samples for quality control of the finished product (Bailer and de Heuber, 1991). Determining the free and bound glycerol content gives two different measures of conversion, which can be compared to mutually validate each other. For the free glycerol analysis, 40mg samples of the reaction mixture were quenched with 1ml of 0.1M HCl, then 1 ml distilled water and 2ml petroleum ether were added, the sample tube shaken and the upper, organic layer extracted. The aqueous extract was then diluted to 10ml. A 0.1ml sample was then taken, added to an aqueous

solution of adenosine-5-triphosphate (ATP) and NADH (1ml) then a solution of glycerokinase suspension (0.01 ml), to form L-glycerol-3-phosphate and adenosine-5-diphosphate (ADP). A solution of phosphoenolpyruvate, pyruvate kinase and L-lactate dehydrogenase (0.01ml) is then added to convert the ADP back to ATP and forming pyruvate. The pyruvate reacts with the NADH to form NAD^+. The amount of NADH oxidized to NAD^+ is proportional to the amount of glycerol in the sample. The concentration of NADH is determined by absorbance of light at 340 nm.

The bound glycerol (i.e. that present in mono-, di- and tri-glycerides) first had to be released by saponification before analysis could be carried out. 500mg samples of the biodiesel layer were saponified with 0.5 g KOH in 2.5 ml of diethylene glycol at 130 °C for 1 hour. Once cooled, the samples were acidified with 0.7 ml concentrated HCl and diluted with 1 ml of water. Petroleum ether was added to separate organic and aqueous phases. The aqueous extract was then prepared as before for enzymatic analysis.

3.1.2 Refractive index

The refractive index was measured initially in a bench top Abbé refractometer with temperature-controlled water bath, and later, using a 4 decimal point digital refractometer (Refracto, Mettler). To assess the change in refractive index with conversion, mixtures of oil, biodiesel, methanol and glycerol in proportions representative of 0 %, 20 %, 40 %, 60 %, 80 % and 100 % conversion were mixed thoroughly and the refractive index measured at 25 °C. These mixtures were then spiked with additional methanol and glycerol to assess the effect on refractive index of these components. The refractive index of the reaction mixture was also measured at 33 °C to investigate the temperature dependence of the refractive index.

3.1.3 Gas Chromatography – Glyceride method

The reaction product was analysed by gas chromatography using the method of EN 14105 with modifications to the calibration samples to account for the higher glyceride contents to

be measured. Two internal standards were used to quantify the peak sizes. The internal standard solutions were ~ 6 mg/ml 1,2,4-butanetriol in pyridine (IS1) and ~ 15 mg/ml tricaprin in pyridine (IS2). An approximately 100 mg sample was accurately weighed into a 12 ml vial. To this, 80 µl of IS1 and 100 µl of IS2 were added. 100 µl of MSTFA (N-methyl-N-trimethylsilylfluoroacetamide) was then added to silylate the OH bonds, increasing the volatility of the sample. The vial was sealed, shaken and left for 15 minutes at room temperature. 8 ml of heptane was then added. The injection volume for the analysis was 0.5 µl. A Unicam ProGC fitted with a DB-1ht column (Agilent) with dimensions 0.32 mm x 15 m x 0.10 µm was used. The injector temperature was 350 °C, detector 370 °C and split flow 1:20 with helium used as a carrier gas. The temperature programme used was as follows:

- hold at 50 °C for 1 minute
- ramp 15 °C/min up to 180 °C
- ramp 7 °C/min up to 230 °C
- ramp 10 °C/min up to 370 °C
- hold at 370 °C for 5 minutes

Calibration curves were constructed using glycerol, monoglyceride (monoolein, monostearin and monopalmitin), diglyceride (diolein), triglyceride (triolein) and biodiesel (methyl heptadecanoate) stock solutions. Calibrations were in the range 0-50 % for triglyceride and biodiesel and in the range 0-2 % for mono- and diglyceride.

3.1.4 Gas chromatography – Ester method

An alternative gas chromatography method was also available, which gave the ester content of a sample. In this method, 0.0625g of the sample and 1.25 g of a stock solution of methyl heptadecanoate in heptane were weighed accurately into a vial. The injection volume was 0.1 µl. The ratio of internal standard (methyl heptadecanoate) to ester peak area was calibrated with samples of biodiesel with known weight in the range 0 – 100% wt methyl oleate. The GC used was a HP 5100, with a Varian CP wax column with dimensions 0.32

mm i.d. and 30 m length. The carrier gas was helium at a flowrate of 2 ml/min and the column temperature was maintained at 220 °C.

3.2 Acid catalysts

Catalysts were chosen for this study based on potential catalysts identified in the literature review: Amberlyst A36, A46 and XE781; Montmorillonite KSF and sulfonated polyHIPE. Amberlyst A36, A46 and XE781 are sulfonic acid funtionalized polystyrene resins, montmorillonite KSF is clay impregnated with sulfuric acid and sulfonated polyhipe is a sulfonic acid functionalized polystyrene material.The structure of sulfonic acid functionalized polystyrene is shown in Figure 3.1.

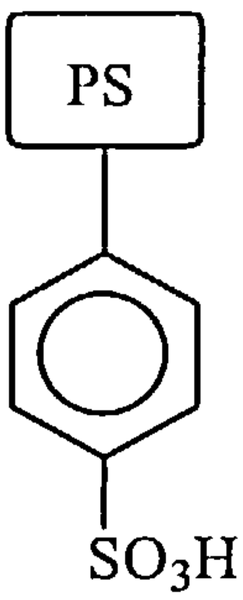

Figure 3.1: structure of sulfonic acid functionalized polystyrene

3.2.1 Supplied materials

Montmorillonite KSF was obtained from Sigma-Aldrich. Amberlyst A36, A46 and XE 781 were obtained as a gift from Rohm and Haas. A sulfonated polyHIPE was obtained as a gift from Professor Galip Akay, School of Chemical Engineering and Advanced Materials, Newcastle University. This PolyHIPE, from Prof. Akay (denoted PolyHIPE GA), was manufactured according to the method in Akay *et al.* (2004).

Oleic acid (technical grade) was purchased from Sigma-Aldrich and reagent grade methanol and ethanol were used.

3.2.2 PolyHIPE catalyst manufacture

To investigate the effects of pore size distribution and functional group on the activity of sulfonated polyHIPE catalysts, polyHIPE monoliths were manufactured and functionalized with the aim of producing monoliths with varying pore diameter distributions, which could then be functionalized with various functional groups. These polyHIPE supports are deonted polyHIPE 1-4.

For the polyHIPE manufacture, p-toluene sulfonic acid and dodecylbenzenesulfonic acid and SPAN 80 (sorbitan monooleate) were purchased from Sigma-Aldrich, and styrene, divinylbenzene, THF, concentrated sulphuric acid and petroleum ether of reagent grade were used.

The styrene/divinylbenzene polyHIPE monoliths were synthesized using the method of Cameron *et al.* (1996). The polyHIPE monoliths had 90% pore volume, with varying cross-linker and surfactant content and were prepared with and without addition of a water miscible porogen (THF). These parameters were varied to change the pore size distribution. An example composition for a 90% pore volume, 5 % cross-linker density monolith is 22.5 ml styrene, 2.5 ml divinylbenzene and 5g Span 80. These reagents were placed in a 300 ml polyethylene bottle. 1g $K_2S_2O_8$ and 1.5 g of NaCl were dissolved in 225 ml of distilled water. The aqueous phase was then added drop-wise to the organic phase under constant stirring with an overhead stirrer at 500 rpm. Once a homogeneous emulsion was obtained, the bottle was sealed then heated to 60 °C for 48 hours to polymerise the emulsion. The monolith was then cut out from the bottle and washed in water, petroleum ether and methanol, then dried.

The polymer monoliths were then functionalised using sulphuric acid, p-toluenesulfonic acid (PTSA) or dodecylbenzenesulfonic acid (DDBSA). To functionalise 5g of polyHIPE, 10 ml of concentrated sulphuric acid, or 15 ml of a solution of 57g PTSA in 100ml cyclohexane, or 24 ml of a solution of 138g DDBSA in 100 ml cyclohexane was added and heated to 50 °C for 72 hours. The functionalised polymer was then washed with petroleum

ether and dried at 50 °C. Once functionalized with sulfuric acid, the tested catalyst (on support polyHIPE 2) was denoted polyHIPE (CM).

3.2.3 Characterization

The acid strengths of the catalysts were determined using Hammett indicators (4-nitroanaline, pKa = +1.1 and dicinnamolacetone, pKa = -3.0) dissolved in a non-polar solvent (cyclohexane). The surface area of the catalyst was determined by nitrogen adsorption/desorption in a Micromeritics Pulse Chemisorb 2700. Samples were first degassed at 373 K under flowing argon, then adsorption and desorption of N_2 measured.

The acid capacity of the catalysts was determined by exchanging H^+ ions for Na^+ by immersing the catalysts in a 0.5 M NaCl solution for 3 hours. After equilibration, the concentration of dissolved H^+ ions was determined by titration against NaOH. This figure was compared to tests simulating the reaction environment, where the catalyst (0.1 g) was contacted with methanol (10 ml). In these tests, the total acidity was measured by titration of NaOH against the catalyst in methanol; the soluble acidity by contacting the catalyst with methanol for 1 hour then filtering and titrating against the methanol filtrate; and the residual acidity by titration against the filtered catalyst in a fresh aliquot of methanol.

The pore size distributions of the polyHIPEs were obtained by image analysis of an SEM micrograph.

3.2.4 Small-scale Screening

The standard esterification test was carried out in a 2ml vial, placed in a shaker situated inside an incubator maintained at 60 °C. A 3:1 molar ratio of methanol to oleic acid was used, with 0.1g catalyst and the conversion measured after 3 hours by titrating the remaining acid against 0.1 M NaOH to the endpoint of phenolphthalein indicator.

Screening for activity for transesterification was conducted in a 200 ml stainless steel autoclave, at 220 °C for 3 hours. A 6:1 molar ratio of methanol to vegetable oil was used with 5 g of catalyst.

3.2.5 Optimization of reaction conditions

Catalysts which were active for the esterification reaction were then screened under different reaction conditions to identify the conditions to maximize conversion. In order to screen activity of catalysts across a number of different variables, a 2 level factorial design was generated using StatEase Design Expert software. The variables were: agitation, temperature, time, mass ratio of methanol and amount of catalyst. 2 centre-point experiments were conducted for each catalyst. The high, low and centre-point for each variable are shown in Table 3.1. The resulting 18 experiments were conducted in the 2 ml vials in the shaker inside the incubator for Amberlyst A46, montmorrilonite and polyHIPE (GA).

Table 3.1: Design space for factorial design of experiments

Variable	High	Low	Mid-point
Agitation	600 rpm	0 rpm	300 rpm
Temperature	80 °C	40 °C	60 °C
Time	5 hours	1 hour	3 hours
Molar ratio	12:1	6:1	9:1
Mass of catalyst	0.15 g	0.05g	0.1g

3.3 Alkali-doped metal oxides

A series of alkali-doped metal oxide were prepared, and the effects of changing alkali metal, support materials and preparation method on the catalysts' activity for the transesterification of rapeseed oil to FAME were investigated. The stability of these catalysts under reaction conditions was analysed.

3.3.1 Catalyst preparation

CaO (reagent grade, Fisher Scientific), MgO (reagent grade, light, Fisher Scientific), γ-Al_2O_3 (reagent grade, Merck) were used as received. The alkali metal sources were reagent grade $LiNO_3$, $NaNO_3$, KNO_3 and LiOH.

The incipient wetness method, also known as dry impregnation, was used to prepare the catalysts. The alkali metal salts, weighed to give an alkali metal loading of 5 %wt on the support were dissolved in a set volume of distilled water, and added to the metal oxide to form a paste. This paste was then dried in an oven at 110°C for 3 hours, then calcined in a furnace at 600 °C. The catalysts were then stored in closed vials.

3.3.2 Initial screening

Initial screening for activity was carried out in a 2ml sealed vial in a IKA mini-shaker set to 600 rpm (Re_m=64) inside an incubator kept at a constant 60 °C. This set-up was sufficient to screen catalysts, even though the degree of agitation was significantly less than that recommended for a batch reactor (Re_m>3000, Noureddini and Zhu, 1997). 0.1g of catalyst and 2 ml of a 6:1 molar ratio mixture of methanol to oil were added to the vial and reacted for 3 hours. After this time the refractive index of the final product was measured and the product analysed for glyceride content by GC.

3.3.3 Catalyst characterization

The surface areas of the catalysts were measured by nitrogen adsorption/desorption Micromeritics Pulse Chemisorb 2700. The samples were degassed at 373 K under flowing argon, then the adsorption and desorption of N_2 was measured.

The base strength was determined using Hammett indicators dissolved in methanol following the method of Watkins *et al.* (2004). The base strength of a material will be higher than that of the indicator with the highest pK_{BH+} that changes colour on contact with

the materials, but lower than the indicator with the lowest pK_{BH+} that does not change colour on contact with the material. The indicators used were: neutral red pK_{BH+} = 6.8; phenolphthalein pK_{BH+} = 8.2; nile blue pK_{BH+} = 10.1, trapaeolein –O pK_{BH+} =11; 2,4 dinitroaniline pK_{BH+} =15 and 4-chloro-2-nitro-aniline pK_{BH+} =17.2. For example, if a solution of nile blue changed colour from blue to pink when in contact with a material, but trapaeolein indicator solution contacted with the same material did not change colour from yellow to orange the base strength of the material is $10.1 < pK_{BH+} < 11$. Approximately 5mg of each indicator was dissolved in 50 ml of methanol; methanol was chosen as a solvent because it is representative of the reaction conditions. Then a small amount of the catalyst (~25mg) was shaken with 1 ml of the indicator solution and left to equilibrate for 2 hours. The colour change was then recorded.

X-ray diffraction (XRD) was used to determine which phases were present in the catalysts. A Phillips PA2000 diffractometer captured the diffraction pattern using Cu Kα and a 2θ range of 3-80 ° and a scan speed of 3 °/min, and the phases were then matched to the pattern using the International Centre of Diffraction Data (ICDD) database.

3.3.4 Batch reaction

Catalysts that were found to be active at the initial screening stage were then evaluated in a batch reactor. 2 g of catalyst, 165 ml oil and 40 ml methanol (1:6 molar ratio) were added to the 200 ml capacity glass jacketed reactor, heated by a heater/circulator to 60°C, and agitated by a magnetic stirrer. Samples were taken periodically and analysed by GC for glyceride content.

3.3.5 Tests of leaching and reusability

The reusability of the catalyst was first evaluated by 5 cycles of use in the 2ml vial shaker (section 3.3.2). The liquid phase was removed after each reaction (reaction time 3 hours) and new reactants added. The product of each reaction was analysed by GC for glyceride content.

The reusability of selected catalysts was then tested in the batch reactor, where 165 ml of oil, 40 ml methanol and 2 g of catalyst were reacted for 1 hour. The catalyst was then filtered out from the reaction mixture, and reused with fresh reactants. The conversion with each cycle of use of the catalyst was determined by GC for glyceride content.

According to Sheldon *et al.* (1998) a heterogeneous catalyst in the liquid phase will fall into 3 categories:

1. The metal leaches but does not form an active homogeneous catalyst
2. The metal leaches to form an active homogeneous catalyst
3. The metal does not leach and the observed catalysis is truly heterogeneous in nature

Simply testing a catalyst's reusability by repeated use indicates the catalysis is heterogeneous, but does not eliminate a homogeneous effect as the leaching could be slow. After performing a reuse test the catalyst could still be in categories 1, 2 or 3. The recommended test to determine whether a catalyst is truly heterogeneous is to 'filter the catalyst at reaction temperature before completion of the reaction and testing the filtrate for activity' (Sheldon *et al.*, 1998). Since the biodiesel reaction mixture is too viscous to filter easily, this test was not performed, however an adapted version was performed. Methanol is the substantially more polar of the 2 reactants so it was assumed that the majority of the leaching would occur into the methanol rather than into vegetable oil. Therefore contacting the methanol with the catalyst, filtering out the catalyst and then testing the filtrate's activity would quantify how significant the homogeneous contribution is. This method was used in other studies of catalysis for biodiesel production (Di Serio *et al.*, 2007; Liu *et al.*, 2007). In this test 0.1g of catalyst was contacted with 2 ml methanol in a vial at 60 °C for 3 hours. 0.4 ml of this methanol was then reacted with 1.6 ml of oil in a vial at 60 °C for 3 hours. The reaction product was then analysed by GC. This test could be considered to test the homogeneity of the catalyst at more extreme conditions than those encountered during the reaction, so may overestimate the homogeneous contribution. However, it is better that the homogeneous contribution is overestimated rather than underestimated when a catalyst is being considered for industrial use, as any leaching will significantly shorten the

catalyst's lifetime. If, however, a catalyst passes this test, then it can be expected to be stable in the real reaction.

The concentration of leached metals in the reaction product was measured by atomic absorption spectroscopy (AAS) (Li, Mg, Ca) and flame photometry (Na, K). The reaction product was filtered and then diluted 10:1 with methanol before being analysed. The atomic absorption spectrometer used was a Unicam AAS 929, and the flame photometer a Jenway pfp7. Both instruments were calibrated against solutions of metal nitrates in water with 4 different concentrations in the range 5 mg/l to 20 mg/l. In flame photometry the Na or K present in the sample is ionized by the flame (burning natural gas), and absorbs energy from the flame. Light is then emitted with the characteristic wavelength of the element, and the intensity of the light is proportional to the concentration of the element in the sample. A photocell then converts the measured emitted light intensity into a voltage which is then related to conentrstion through the calibration chart. In atomic absorption spectroscopy, an acetylene flame is used to atomize the sample. Light is passed through the flame from a hollow cathode lamp of the element being analysed for. The emitted light has wavelengths corresponding to the emission spectrum of the relevant element. This light is then absorbed by the atoms in the flame to promote electrons to a higher energy level, reducing the energy of the light detected at the other side of the flame. This loss is energy is related to the concentration of the element and related to the concentration of the element through the calibration curve.

The soluble basicity of each catalyst was measured by contacting the catalyst with methanol for 1 hour, filtering, then titrating the liquid against 0.1 M HCl. Two indicators were used: the first, phenolphthalein, to give the concentration of strong, soluble basicity, and the second, bromophenol blue, to give the concentration of weak, soluble basicity, which could indicate the presence of carbonates. Titration of a carbonate with acid gives two end points, the first at pH=7 (phenolphthalein endpoint) and the second at pH=4 (bromophenol blue endpoint). Therefore the titre to the phenolphthalein endpoint (equation 3.1) gives the total soluble basicity from the alkali metal oxide and carbonate, and the bromophenol blue endpoint (equation 3.2) gives the concentration of HCO_3^- and therefore the concentration of dissolved carbonate present.

$$X_2CO_3 + HCl \leftrightarrow XHCO_3 + XCl \qquad [3.1]$$

$$XHCO_3 + HCl \leftrightarrow CO_2 + H_2O + XCl \qquad [3.2]$$

Reactions were performed at low levels of LiOH dissolved in methanol, representative of the measured Li levels in the reaction mixture, and higher levels, up to an equivalent Li (and thus hydroxide) concentration to the standard 1% by weight of oil NaOH typically used (Vicente *et al.*, 1998).

3.3.6 Alternative catalysts and preparation methods

To determine whether the stability of Li-MgO could be improved by changing the preparation method, the calcination temperature was varied from 500 °C to 900 °C. Additionally, the preparation was changed to that of Diez *et al.* (2006). LiOH was used instead of $LiNO_3$ as the alkali metal source and the catalyst calcined at 500 °C for 24 hours. It was claimed by Diez *et al.* (2006) that this basic catalyst was active for the aldol condensation of citral with acetone but stable in water.

KF-alumina and Mg-Zr mixed oxides were identified from the literature as potential catalysts. KF-alumina was obtained from Sigma Aldrich, and Mg-Zr mixed oxide was manufactured according to the method of Aramandia et al. (2004). $MgNO_3$ and $ZrOCl_2$ were co-precipitated using ammonia as the precipitating agent. The powder was washed thoroughly in distilled water, then calcined at 600 °C.

The activities of these catalysts were tested in the batch reactor. The stability was assessed by measuring the soluble basicity in the case of KF/alumina and LiOH/MgO. For the Li-MgO catalysts calcined at different temperatures the concentrations of leached Li and Mg were measured by AAS.

3.4 Organic base anchored on silica support

As an alternative to metal oxide based catalysts, solid-supported organic bases were evaluated. Triazobicycloguanidine was covalently anchored to silica supports and tested for activity and stability. Trimethylamine functionalised silica was also tested for its activity and stability.

3.4.1 Catalyst preparation

Silica supports of various pore sizes were obtained from commercial sources: Davisil grade 636 and grade 646 (Sigma Aldrich) with pore sizes 60 Å and 150 Å respectively. A silica support was synthesized from tetraethoxysilane (TEOS) to produce a silica support with 22 Å pore size.

The mesoporous silica was manufactured using dodecylamine as the surfactant, giving an HMS-type silica (Linssen *et al.*, 2005). TEOS (16g) was added to a solution of 53g of water, 41g of ethanol and 5g of dodecylamine. The mixture was stirred for 24 hours, the solid removed by filtration, then washed in ethanol to remove the template. The pore size obtained by this method should be 22 Å (Mbaraka *et al.*, 2003).

The TBD-functionalised catalysts were functionalised by the method of Subba Rao *et al.* (1995) because the guanidine base is covalently coupled to the inorganic silica support in this method, as shown in equation 3.1. The guanidine is attached via an inorganic-organic linker (GLYMO) to the silica support.

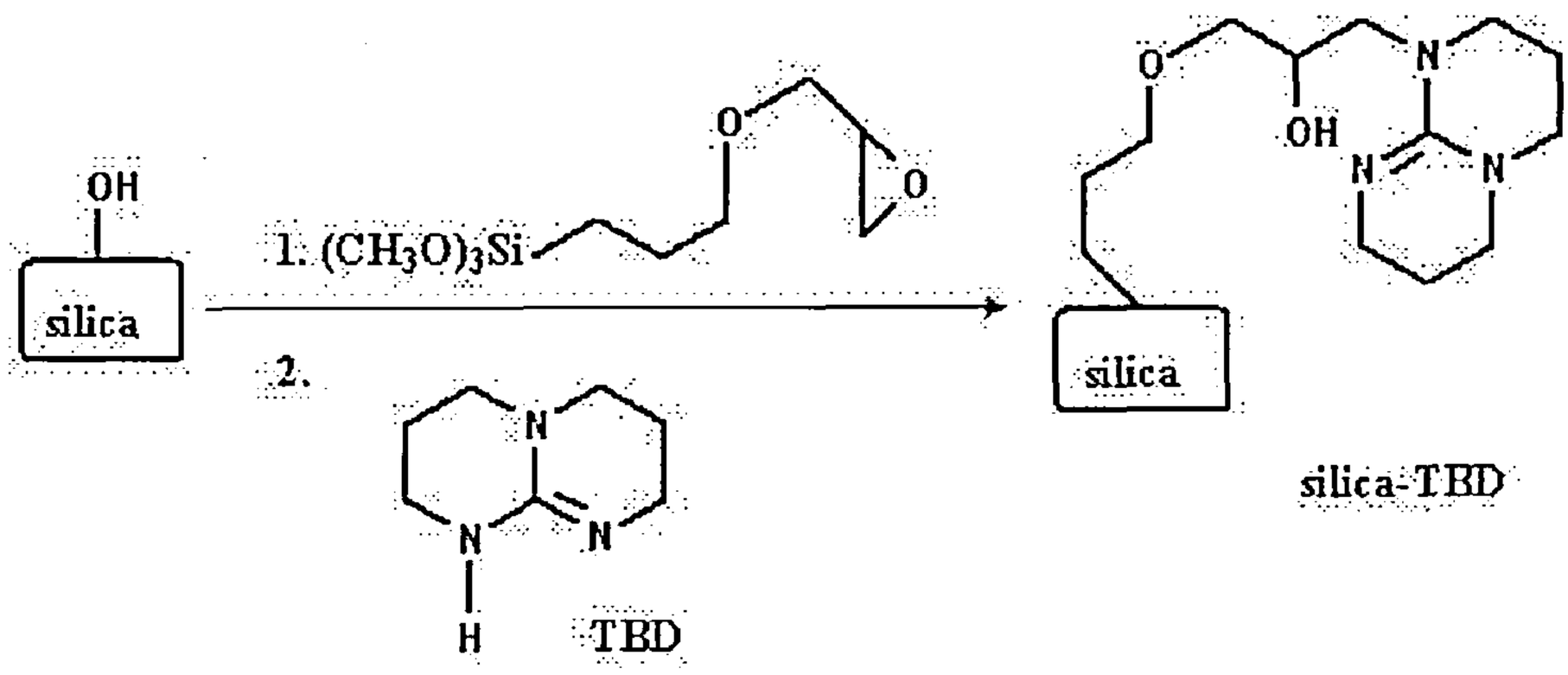

Equation 3.1 – reaction scheme and structure of TBD-silica catalyst

This method is easier to conduct than the more usual route involving substitution of a chloro- or bromo-propyl group. The resulting catalyst has been found to be active and stable for Michael additions and Knoevenagel condensations, which are base catalysed. The silica (3g) was reacted with 1g of trimethoxysilylpropoxymethyloxirane (GLYMO) in refluxing toluene for 8 hours. The glycidylated silica is then reacted with 1g of triazabicyclodec-5-ene (TBD) in toluene at room temperature for 10h. Excess TBD was then removed by washing in dichloromethane.

The trimethylamine-functionalised catalyst was synthesised in a one pot method (Mdoe et al., 1998). 10g of dodecylamine was dissolved in 100 g of water and 100 g of ethanol, to which was added 37.5 g of TEOS and 4 g of triethoxysilylpropyl(trimethyl)amine. The structure of the trimethylamine-funcitonalised catalyst is shown in figure 3.2. The mixture was stirred for 24 h before removal of the template by washing in refluxing ethanol.

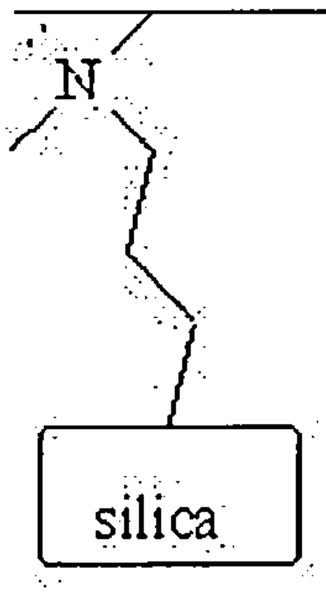

Figure 3.2: structure of trimethylamine functionalised silica

3.4.2 Catalyst characterization

The surface area and average pore size of the catalysts were measured using the Barrett-Joyner-Halenda (BJH) method in a Quantochrome NOVA 2200. The BJH method was chosen because it is more suitable than the Braunauer-Emmett-Teller (BET) method for mesoporous materials, as the BET surface area often overestimates the true surface area for mesoporous materials (Quantochrome, 1998). The catalysts were degassed under flowing nitrogen at 80 °C for 5 hours, then the adsorption of nitrogen at 77 K and subsequent desorption at room temperature measured. The volume of gas is recorded at each applied pressure, and the BJH method used ot relate this data to surface area and pore size.

The nitrogen content and thus degree of functionalisation was measured by CHN elemental analysis in a Carlo Erba Elemental Analyser 1106. Infra-red spectra of the functional groups on the catalyst surface were recorded using a Bruker Vertex 80 spectrometer with DRIFTS attachment. The sample powder was mixed with KBr powder and then spread onto a metal sample holder to form a flat surface and the wavenumber scanned from 100 to 4000 cm^{-1}. A background scan of the sample holder was taken before the samples and this spectra was subtracted from that of the sample. 16 scane were taken and averaged to give the reported spectra.

3.4.3 Catalyst testing

The catalysts were tested for activity in the batch reactor as in section 3.5. The activity of the leachate and reusability of the catalyst were also tested. Additionally, leaching of the TBD into methanol was analysed by infrared (IR) spectroscopy by identification of a characteristic peak at 1640 cm^{-1}, the C=N bond (Fessenden and Fessenden, 1984). Spectra were recorded on a ReactIR 2 spectrometer. The catalysts were contacted with methanol for 3 hours at 60 °C, filtered and the methanol analysed by IR. In order to determine if the tertiary amine leached into the reaction mixture, CHN analysis on the reaction product was performed because the N-H and O-H IR absorbances occur at the same wavenumber.

The silica-supported catalysts were found to be covered in a 'gel-like' substance after the reaction. The gel material was analysed by mass spectrometry to determine which components were present. In an attempt to remove the 'gel' layer, the catalyst were washed in butanol, as this was the solvent used to remove a layer of glycerol from an enzyme support in Dossat *et al.* (1999).

3.5 Basic ion exchange resin

Amberlyst A26 is a macroreticular ion exchange resin functionalized with a strongly basic quaternary ammonium group. The A26 resin was washed thoroughly with methanol before use as it contains a large amount of water in its as received form (Liu *et al.*, 2007). This catalyst was then tested for activity and stability. A batch reaction was carried out using 5.0 g of the catalyst with 165ml oil and 40 ml methanol. The reusability was tested by filtering out the catalysts and using it again with fresh reactants. 5.0 g of catalyst was contacted with 40ml of methanol at 60 °C, filtered and the methanol reacted with 165ml oil to determine if there was a homogeneous contribution to the activity.

3.6 Magnetic catalysts

3.6.1 Catalyst preparation

Fe_3O_4, $CoFe_2O_4$ and $SnFe_2O_4$ were prepared by the co-precipitation method to produce a solution of magnetic nano-particles. These solutions were then dried to produce the solid catalyst. The reagents and conditions of preparation are shown in Table 3.2. 5ml of concentrated HCl was added to the M^{2+} and Fe^{3+} solutions to aid dissolution, and dissolved oxygen was removed from all solutions by bubbling nitrogen through for 30 minutes. After precipitation the catalysts were washed with distilled water until pH 7 was reached, then the catalyst was dried in an oven overnight.

Table 3.2: Reagents and conditions for manufacture of MFe_2O_4 catalysts

Catalyst	M^{2+} solution	Fe^{3+} solution	Precipatation agent	Precipitation temperature
Fe_3O_4	$FeSO_4.7H_2O$ (6.25 g in 250ml water)	$FeCl_3.6H_2O$ (12.16 g in 250ml water)	NaOH (75g in 1250 ml water)	60 °C
$CoFe_2O_4$	$CoCl_2.6H_2O$ (5.92g in 250 ml water)	$FeCl_3.6H_2O$ (13.52 g in 250ml water)	NaOH (30g in 250 ml water)	100 °C
$SnFe_2O_4$	$SnCl_2.2H_2O$ (5.52g in 250 ml water)	$FeCl_3.6H_2O$ (13.52 g in 250ml water)	NaOH (30g in 250 ml water)	100 °C

Shell and core magnetic catalysts were manufactured by coating magnetite particles in tin compounds. To prepare tin carbonate coated magnetite, a solution of 3g $SnCl_2.2H_2O$ in 250 ml water was added to a beaker containing 8g of Na_2CO_3 in 250 ml of water and the magnetite particles. On mixing the 2 solutions, $SnCO_3$ was formed by precipitation. The precipitate was then dried in an oven at 200 °C overnight. $Sn(acac)_2$ (acetylacetonate) was prepared by the precipitation of $SnCl_2.2H_2O$ solution with a solution containg NaOH and acetylacetone. The $Sn(acac)_2$ was dissolved in acetylacetone, then placed in a rotavap with

the magnetite particles. Once the solvent was driven off, the resulting solid was heated to 200 °C to decompose the acac species to form SnO.

3.6.2 Batch reaction

Reactions with magnetic catalysts were carried out in a 3 necked round bottomed flask, agitated by an overhead stirrer and immersed in an oil bath. A 6:1 molar ratio of methanol to oil and catalyst loading of 1% by weight of oil were used. Reactions were carried out at methanol reflux temperature (67 °C) for 6 h with samples periodically withdrawn through a septum.

3.6.3 Analysis of reaction product

Conversion from triglyceride to diglyceride, monoglyceride and biodiesel was measured by liquid chromatography in a Shimadzu Prominence HPLC with UV detector. The solvents were methanol and a 5:4 propanol-hexane mixture. 100 µl of the reaction mixture was added to 2ml of a 5:4 propanol to hexane mixture, and an injection volume of 10 µl used.

3.7 Kinetic fitting and modelling

3.7.1 Homogenous Second Order Kinetics

The mass-time profiles were fitted to a second-order rate models to determine the apparent rate constants. The sequential reaction scheme is shown in Figure 3.2, and the form of the 2^{nd} order rate equations in equations 3.3-3.6. A second order model was chosen as a first step towards describing the kinetics because the homogeneous reaction is 2^{nd} order (Noureddini and Zhu ,1997; Vicente *et al.*, 2005).

The following abbreviations are used in the equations that describe the reaction kinetics: TG – triglyceride; DG – diglyceride; MG – monoglyceride; G – glycerol; BD – biodiesel (FAME); A – methanol. The apparent rate constant, k, depends on the concentration of

catalyst in the system and can be represented as k=k'[cat]. This relationship was used to compare systems with different concentration of catalysts.

$$TG + A \underset{k_2}{\overset{k_1}{\leftrightarrow}} DG + BD$$

$$DG + A \underset{k_4}{\overset{k_3}{\leftrightarrow}} MG + BD$$

$$MG + A \underset{k_6}{\overset{k_5}{\leftrightarrow}} G + BD$$

Figure 3.2 – reaction scheme for sequential transesterification of triglycerides to methyl esters

$$\frac{d[TG]}{dt} = -k_1[TG][A] + k_2[DG][BD] \quad [3.3]$$

$$\frac{d[DG]}{dt} = -k_2[DG][BD] - k_3[DG][A] + k_4[MG][BD] \quad [3.4]$$

$$\frac{d[MG]}{dt} = -k_4[MG][BD] - k_5[MG][A] + k_6[G][BD] \quad [3.5]$$

$$\frac{d[BD]}{dt} = k_1[TG][A] + k_3[DG][A] + k_5[MG][A] - k_2[DG][BD] - k_4[MG][BD] - k_6[G][BD] \quad [3.6]$$

The equations were differentiated numerically using equations of the form in equation 3.7 to produce the modelled concentration-time profile. The full set of equations are presented in appendix 3.

$$[TG]_t = [TG]_{t-1} - k_1[TG]_{t-1}[Me]_{t-1} + k_2[DG]_{t-1}[BD]_{t-1} \quad [3.7]$$

The rate constants were fitted by minimising the squared error between the modelled data and the measured data.

3.7.2 Eley-Rideal and Langmuir-Hinshelwood Kinetics

Eley-Rideal and Langmuir-Hinshelwood kinetics were fitted to the batch reaction data for Li-CaO.

Eley-Rideal kinetics involves the adsorption of one reactant, in this case the alcohol, which is then attacked by the other reactant from the liquid phase. This is shown schematically in Figure 3.3. Eley-Rideal kinetics were found to be the best representation of the kinetics for the transesterification of ethyl acetate with methanol over a MgO catalyst (Dossin et al., 2006).

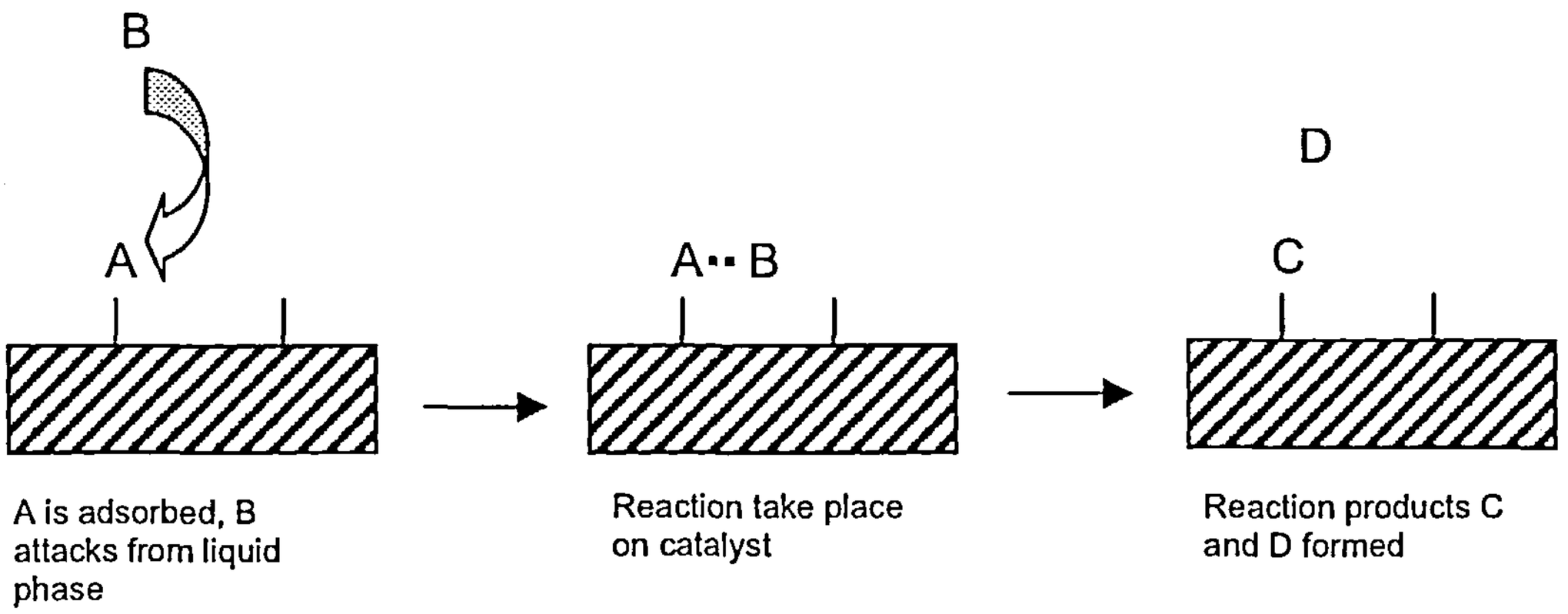

Figure 3.3: schematic representation of Eley-Rideal mechanism for A+B ↔C+D

The reaction scheme for transesterification of triglycerides over a solid base catalyst following Eley-Rideal kinetics is shown in equations 3.8 to 3.11. The full set of equations are presented in appendix 4.

$$\frac{d[TG]}{dt} = -k_1[TG]\theta_A + k_2\theta_{DG}[BD] \quad [3.8]$$

$$\frac{d[DG]}{dt} = k_1[TG]\theta_A - k_2\theta_{DG}[BD] - k_3[DG]\theta_A + k_4\theta_{MG}[BD] \quad [3.9]$$

$$\frac{d[MG]}{dt} = k_3[DG]\theta_A - k_4\theta_{MG}[BD] - k_5[MG]\theta_A + k_6\theta_G[BD] \quad [3.10]$$

$$\frac{d[BD]}{dt} = k_1[TG]\theta_A + k_3[DG]\theta_A + k_5[MG]\theta_A - k_2\theta_{DG}[BD] - k_4\theta_{MG}[BD] - k_6\theta_G[BD] \quad [3.11]$$

The concentration of bulk species is in square brackets, and surface coverage of adsorbed species by θ_i. The partial glycerides have both alcohol and ester functionality, so for the back reaction, it was assumed that the partial glycerides are adsorbed and their alcohol functionality reacts with the ester functionality of the biodiesel. The value of adsorption coefficient, K=3 l/mol at 40 °C, was taken from Dossin et al. (2006) for methanol adsorbing onto MgO. The value of the adsorption coeffcient was calculated from experimental data for the transesterification of ethyl acetate with methanol. This coefficient was assumed to be constant for all species. This assumption is likely to be incorrect because the components involved vary widely in size and polarity, thus we can expect there to be significant error in this value. It was considered that only the more polar component would adsorb onto the active sites. This approach would not be valid for an acid catalyst where the catalytic step is on the triglyceride molecule (Schuchardt *et al.*, 1997).

The relationship between the adsorbed and bulk species is given in equation 3.12

$$\theta_A = \frac{K_A[A]}{(1+K_A[A]+K_{DG}[DG]+K_{MG}[MG]+K_G[G])} \quad [3.12]$$

Equation 3.12 is derived through use of the Langmuir isotherm. The Langmuir isotherm relates the adsorption and desorption of a species form the surface as shown in equation 3.13 (Augustine, 1996). Equation 3.13 applies for all species being adsorbed. Rearranging for θ_i, defining $K_i=k_a/k_a'$ and adding the exprerssion together gives the number of free sites, shown in equation 3.14. Rearranging equation 3.13 to give the surface coverage of A, θ_A, gives equation 3.12.

$$k_A[A](1-\sum\theta_i) = k_A'\theta_A \quad [3.13]$$

$$1-\sum\theta_i = \frac{1}{1+K_A[A]+K_B[B]+K_C[C]} \quad [3.14]$$

Langmuir-Hinshelwood kinetics requires the adsorption of both reactants onto adjacent sites on the catalyst surface. The reaction takes place on the catalyst surface and both

products then desorb. This mechanism has been proven to take place for numerous reactions including oxidation of CO on Pt catalysts, methanol synthesis on ZnO catalyst and hydrogenation of ethylene on Cu catalysts (Hagen,1999).

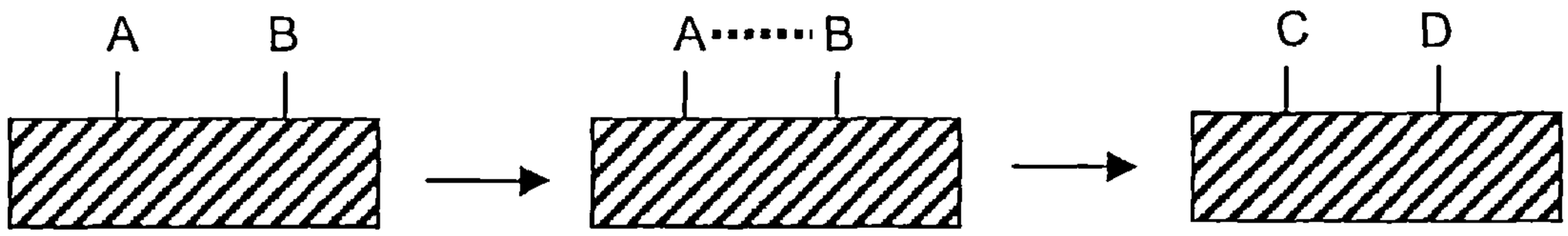

Figure 3.4: schematic representation of Langmuir-Hinshelwood mechanism for A+B ↔C+D

The reaction scheme for the transesterification of triglycerides following Langmuir – Hinshelwood kinetics is shown in equations 3.15 to 3.17. The concentration of species in the bulk phase are shown in square brackets, and θ_i represents the surface coverage of adsorbed species i and the rate constants are k=k'[cat]. The relationship between bulk and adsorbed species is as in Eley-Rideal kinetics. The full set of equations is presented in appendix 5.

$$\frac{d[TG]}{dt} = -k_1\theta_{TG}\theta_A + k_2\theta_{DG}\theta_{BD} \quad [3.15]$$

$$\frac{d[DG]}{dt} = k_1\theta_{TG}\theta_A - k_2\theta_{DG}\theta_{BD} - k_3\theta_{DG}\theta_A + k_4\theta_{MG}\theta_{BD} \quad [3.16]$$

$$\frac{d[MG]}{dt} = k_3\theta_{DG}\theta_A - k_4\theta_{MG}\theta_{BD} - k_5\theta_{MG}\theta_A + k_6\theta_G\theta_{BD} \quad [3.17]$$

$$\frac{d[BD]}{dt} = k_1\theta_{TG}\theta_A + k_3\theta_{DG}\theta_A + k_5\theta_{MG}\theta_A - k_2\theta_{DG}\theta_{BD} - k_4\theta_{MG}\theta_{BD} - k_6\theta_G\theta_{BD} \quad [3.18]$$

The squared error was compared for homogeneous 2nd order, Eley-Rideal and Langmuir-Hinshelwood kinetics to evaluate which model is the best representation of the reaction.

3.7.3 Eley-Rideal Kinetics: Effect of changing Adsorption coefficient

It was assumed that the adsorption coefficient of all species was equal to that of methanol adsorbing on MgO, K=3 l/mol (Dossin et al.,2006). It is unlikely that the adsorption

coefficient of all the species will be the same, it might be expected that glycerol would adsorb more strongly onto the active sites because it is very polar. The adsorption coefficients of glycerol and partial glycerides were varied to determine its effect on the reaction profile.

3.7.4 External Mass Transfer

The rate determining step in heterogeneous catalysis can be transport from bulk solution to the catalyst particle, transport within the particle to the active sites or the reaction itself, as shown in Figure 3.5.

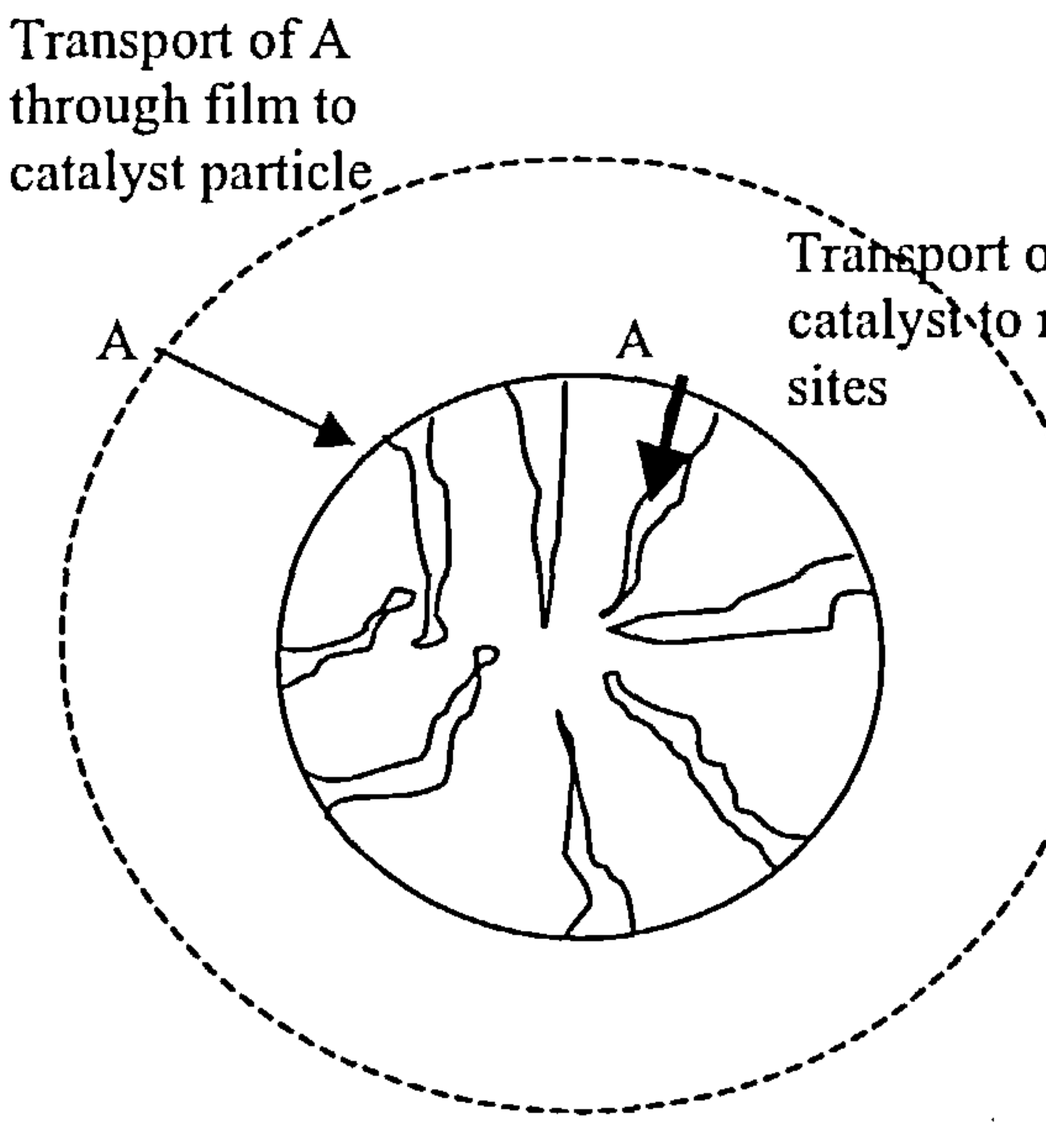

Figure 3.5: transport processes involved in a heterogensously catalysed reaction

To determine if external mass transfer would be rate limiting for the transesterification of triglycerides, the rate of reaction at different conversions was compared to the rate of mass transport to the catalyst particle (calculations shown in appendix 6). The fluid through which the triglyceride must travel was thought to change depending on the extent of conversion and this is shown in
Table 3.3. The polarity of glycerol means that it is likely it will coat the polar catalyst surface. Similarly it was assumed that the more polar methanol would surround the catalyst particle. At times midway through the reaction, the reaction mixture is one-phase, so the properties of this phase were assumed to be the same as the properties of biodiesel. The

diffusivities were calculated using the Wilke-Chang equation (Sinnott, 1999). The Wilke-Chang equation is shown in equation 3.19 where D is the diffusion coefficient, μ the viscosity, φ the association factor for the solvent (for methanol 1.9), V_m the molar volume of the solute at boiling point, M the molecular mass of the solvent and T the temperature.

$$D = \frac{1.173x10^{-13}(\phi M)^{0.5}T}{\mu V_m^{0.6}} \qquad [3.19]$$

Table 3.3: properties of fluid through which triglyceride must diffuse to reach catalyst particle

Extent of conversion	Fluid surrounding particle	Diffusivity of fluid (m^2/s)
0%	Methanol	$5x10^{-10}$
50%	Biodiesel	$3x10^{-11}$
90 %	Glycerol	$3x10^{-13}$

The rate of mass transport was calculated from $Q=k_l a_p(C_{A,b}-C_{A,s})$, where Q is the molar flux in mol/l/s, k_l the mass transfer coefficient in m/s and $C_{A,b}$ the concentration in bulk and $C_{A,s}$ the concentration on the solid surface and a_p is the particle surface area in m^2/m^3. The mass transfer coefficient was estimated based on a Sherwood number of 2. A Sherwood number of 2 represents a stagnant environment, and a pseudo-stagnant environment can exist in viscous reactions (Moo-Young and Blanch, 1989). This was the method used to calculate mass transfer rates in a solid catalysed slurry-type reactor (Kumbhar and Yadav, 1989).

3.7.5 Calculation of the Effectiveness Factor

The fitted rate constants were then used to calculate the effectiveness factor of the catalysts. The effectiveness factor is defined as the ratio of observed rate of reaction and the rate of reaction without any internal diffusion limitation. The effectiveness factor, η, is calculated from the Thiele modulus ø, using the relationship in equation 3.20.

$$\eta = \frac{\tanh\phi}{\phi} \qquad [3.20]$$

The generalised Thiele modulus is shown in equation 3.21, where V is the volume of the reactor, S_{ex} the external surface area of the catalyst particles, k the rate contstant, C_s the concentration at the catalyst particle surface and D_e the effective diffusivity.

$$\phi = \frac{V}{S_{ex}} \sqrt{\frac{(n+1)k\ C_s^{n-1}}{2D_e}} \qquad [3.21]$$

Using the fitted rate constants and diffusivity values, the effect of particle size on effectiveness factor could be evaluated.

The effective diffusivity, D_e, can be calculated from the relation with pore size as described in equation 3.22, where ε is the voidage of the catalyst, τ is the tortuosity, α is the radius of the molecule and β is the radius of the pore (Jonker et al., 1998). This allowed the effect of pore size on effectivenss factor to be investigated.

$$D_e = D \times \frac{\varepsilon}{\tau} \times 10^{\frac{-\alpha}{\beta}} \qquad [3.22]$$

3.8 Cost estimation

The process model of Haas *et al.* (2006) was used to estimate the capital cost of a biodiesel plant with capacity of 10 million gallons of biodiesel per year where the plant operates with different solid catalysts, and the costs compared to the standard NaOH catalysed process. In the cases where there is no leaching, the number of process steps is reduced. The steps relating to NaOH dissolution, biodiesel water washing, methanol-water separation and glycerol-water separation are removed. The costs of the reactor at a different capacity or pressure rating to that in the process model of Haas et al. (2006) were estimated using the cost factors in Sinnott (1999).

Data from manufacturers and standard texts was used to compare the operating costs (energy consumption, reagent costs and disposal costs) per litre of biodiesel for the different solid catalysts.

The scenarios for the solid catalyst are:

1 - ideal heterogeneous catalyst. The catalyst does not leach, does not lose activity and requires the same residence time for full conversion as NaOMe (1 h)

2 - heterogeneous catalyst, with increased reaction time. The catalyst does not leach, does not lose activity but requires a residence time of 3 h, three times larger than that for NaOMe

3 - heterogeneous catalyst, but higher reaction temperature required. Similar to Esterfip-H process. The catalyst does not leach and does not lose activity.

4 - LiCaO cal type heterogeneous catalyst. The catalyst leaches, and can only catalyse 3 cycles in batch operation. Dissolved metals must be removed from biodiesel.

5 - NaOMe catalysed reaction – standard process.

4 Results and Discussion

4.1 Analysis Methods

In this section the three different analytical methods are evaluated with regard to accuracy and speed of analysis.

4.1.1 Enzymatic Glycerol Determination

The free glycerol content of the reaction mixture and the bound glycerol content of the biodiesel layer were measured using the procedure described in section 3.1.1. The reproducibility and accuracy of the free glycerol analysis was found to be unacceptably low. Table 4.1 shows the results obtained when the conversion of a finished reaction mixture (conversion ~100%) was measured by the free and bound glycerol enzymatic method.

Table 4.1: conversion measured by bound and free glycerol technique

Sample	Conversion measured by free glycerol technique (%)	Conversion measured by bound glycerol technique (%)
1	104	96
2	90	95
3	81	96
4	106	95
5	-	95
6	-	95

The extent of conversion measured by the bound glycerol technique was 95 ± 2% where the 2% error is due to systematic errors from the liquid handling (pipetting and dilution) involved in the sample work-up. However the random error in the free glycerol results is ±

6%, calculated from the standard error in the results. The reproducibility of this technique was tested further by comparing the results from 2 parallel reactions and the variation in results was unacceptably high. The concentration of a standardized glycerol solution was measured accurately, but when a mixture of 50 % standard and 50 % experimental sample was measured, the recovery of the glycerol standard was only 73%. The poor recovery of the internal standard means that a substance in the reaction mixture is interfering with the performance of the assay. Although the bound glycerol technique gave repeatable results, it was time-consuming and laborious. Neither of these techniques was therefore a substitute for GC analysis.

4.1.2 Refractive index

The refractive index of vegetable oil at 25 °C is 1.471 compared with 1.453 for biodiesel. Figure 4.1 shows that there is a linear relationship with good correlation between conversion and refractive index, when the refractive indices of non-reacting mixtures of compositions of triglyceride, biodiesel, methanol and glycerol representing 0 to 100% conversion in 20% steps were measured. Therefore, refractive index is a useful analysis technique to give approximate but real-time information about conversion.

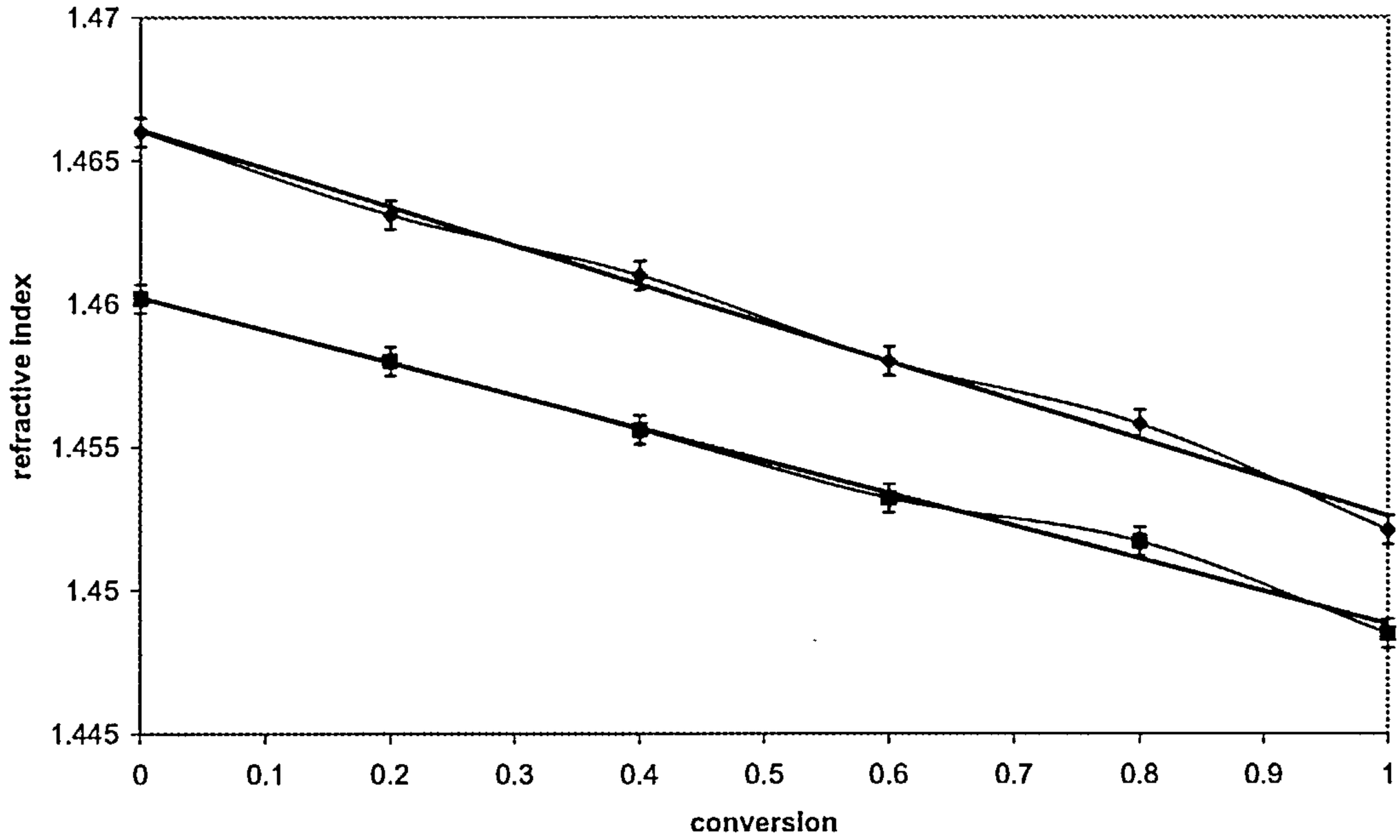

Figure 4.1 : refractive index against conversion for non-reacting mixtures at 20 °C (diamonds) and 33 °C (squares). Correlation coefficient was >0.99 in both cases

However the decrease in refractive index is not just caused by conversion to methyl esters, but also by increasing temperature as shown in Figure 4.1, increasing amounts of methanol and formation of soaps. Refractive index cannot, therefore, be used as the sole method of analysis. It can, however, be used to get a quick and approximate measure of conversion provided the following conditions are met:

- the temperature is kept constant throughout (or is known, and a calibration between refractive index and temperature is used).
- the conversion and refractive index of the reaction mixture at t=0 are known.
- the conversion and refractive index of the reaction mixture of the final samples are known.

This technique is online, so there is no delay during sample work-up and the analysis time is very short. Measuring conversion by refractive index is a good way to test different quenching methods, because the conversion can be measured during the reaction and after quenching. To quench the homogeneously catalysed reaction, an acid must be added to neutralize the alkali. Monitoring the refractive index showed that the reaction could not

progress in the presence of glacial acetic acid, demonstrating that acetic acid is a good quenching agent. As glacial acetic acid contains no water, there is no phase separation, which makes sampling difficult, as is the case with dilute HCl and water.

The online measure of conversion enables investigation of the effect of agitation intensity on reaction rate. Figure 4.2 shows the reaction profile when the mixture was stirred at different stirring rates.

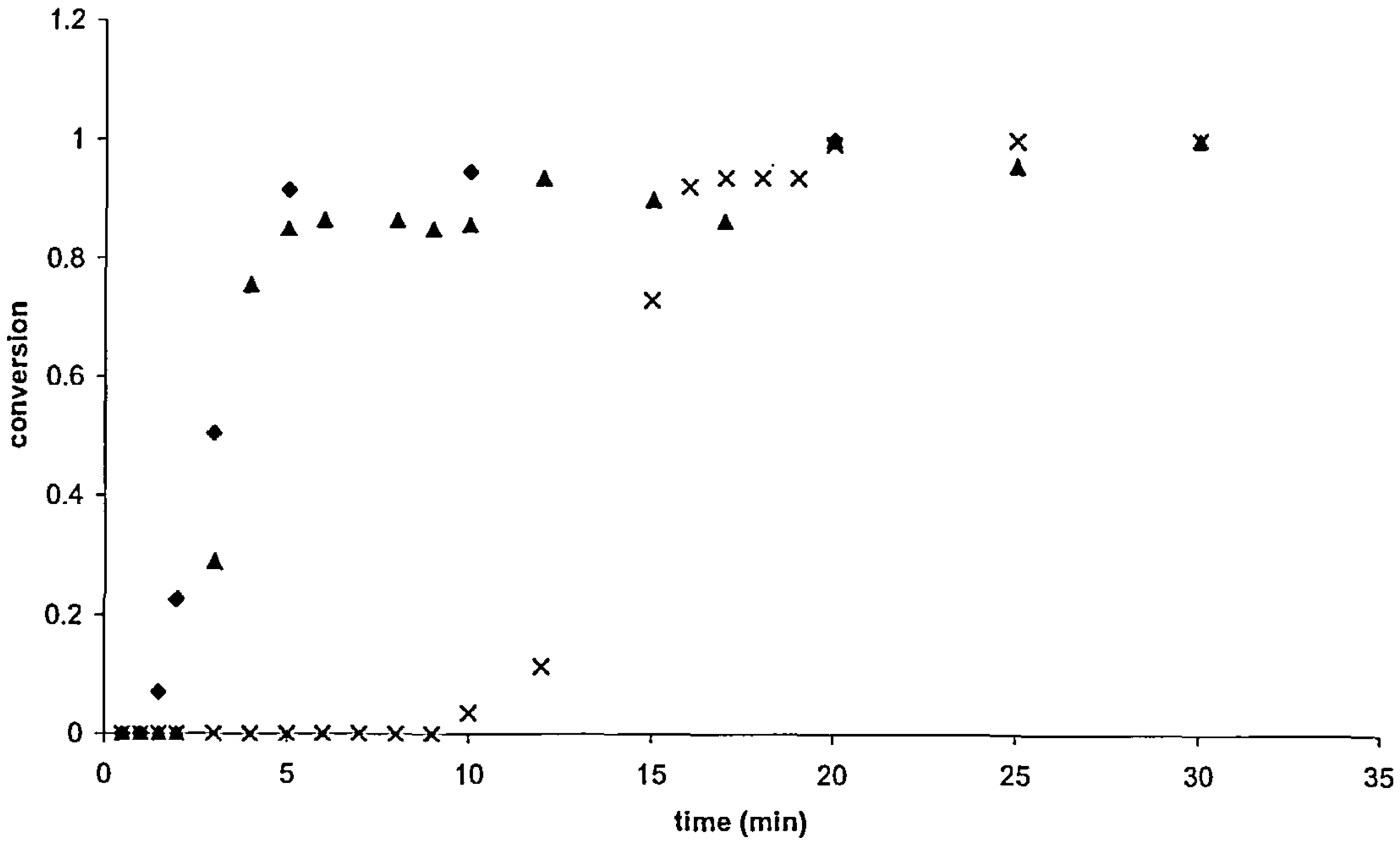

Figure 4.2: Effect of agitation on reaction rate – reaction profiles for vessels stirred at 1000 rpm/ Re_m= 2150 (diamonds), 700rpm/Re_m= 1500 (triangles) and 500 rpm/ Re_m=1080 (crosses). Reaction conditions T=25 °C, catalyst 1% NaOH by weight of oil, 6:1 molar ratio of methanol to oil.

As the intensity of agitation decreases, the "induction time" increases. The rate of the reaction, after this time, is similar across the 3 different agitation speeds. This same effect was noted by Noureddini and Zhu (1997), who divided the reaction profile into 2 zones:

- Induction: the reaction rate is slow. Mass transfer controlled.
- Fast reaction: process is reaction controlled.

At the transition between stage 1 and 2, the mixture becomes single phase. This is due to the formation of mono- and di-glycerides which are surfactants and of methyl esters, which act as a co-solvent. Once this 1-phase mixture is formed, the inter-phase mass transfer

limitation is removed and the reaction rate dramatically increases. In order to isolate the kinetics from mass transfer effects the agitation should be vigorous, with Re_m (the Reynolds number of mixing) greater than 1500, because at this stirring rate in Figure 4.2, the "induction time" is very small, so the mass transfer limitation is only slight.

Figure 4.3 shows the reaction progress followed by ester GC and refractive index. The agreement between the 2 methods is good in the initial stages of the reaction, however, as the reaction nears completion, the refractive index does not continue to decrease. This means the use of refractive index for reaction monitoring is limited to catalyst screening, and will only give a semi-quantitative answer as to whether a catalyst is active. There is not enough sensitivity at high conversions to compare different catalysts and different reaction conditions.

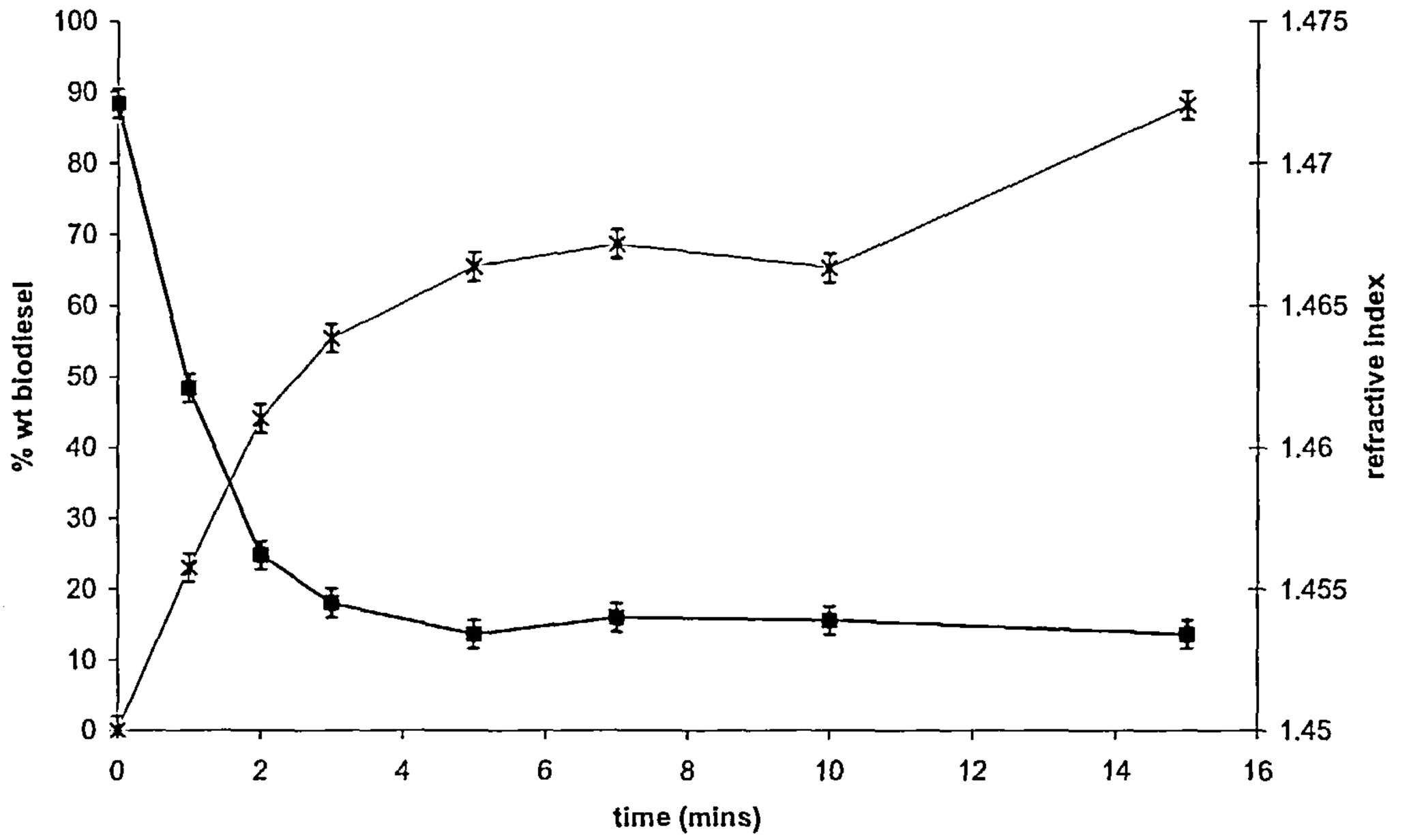

Figure 4.3: Reaction progress analysed by ester GC (x, left axis) and refractive index (■, right axis). Reaction at 20 °C, 6:1 ratio methanol to oil, 1.2 %wt by oil NaOMe catalyst.

4.1.3 Gas Chromatography

Figure 4.4 and Figure 4.5 show typical traces produced by the ester GC and glyceride GC respectively. More information is obtained from the glyceride GC, because the triglyceride, diglyceride and monoglyceride contents are quantified, whereas the ester GC only gives the ester content. However, the sample work-up with the ester GC is easier and analysis time shorter. The glyceride GC would be required for industrial quality control, and as a method of obtaining the concentrations of the partial glycerides, which are required to determine the full kinetics of the reaction, but for catalyst screening, the ester GC is more suitable.

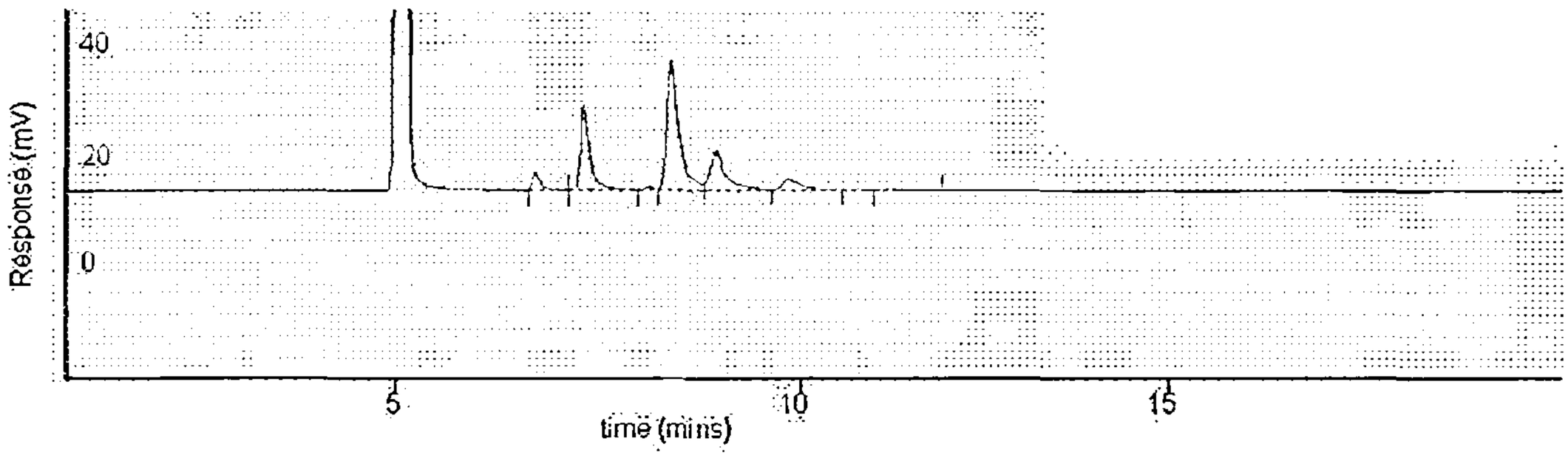

Figure 4.4: GC trace from ester GC (1st peak solvent, 2nd peak methyl palmate, 3rd peak methyl heptadecanoate, 4th peak methyl stearate, 5th peak methyl oleate, 6th peak methyl linoleate)

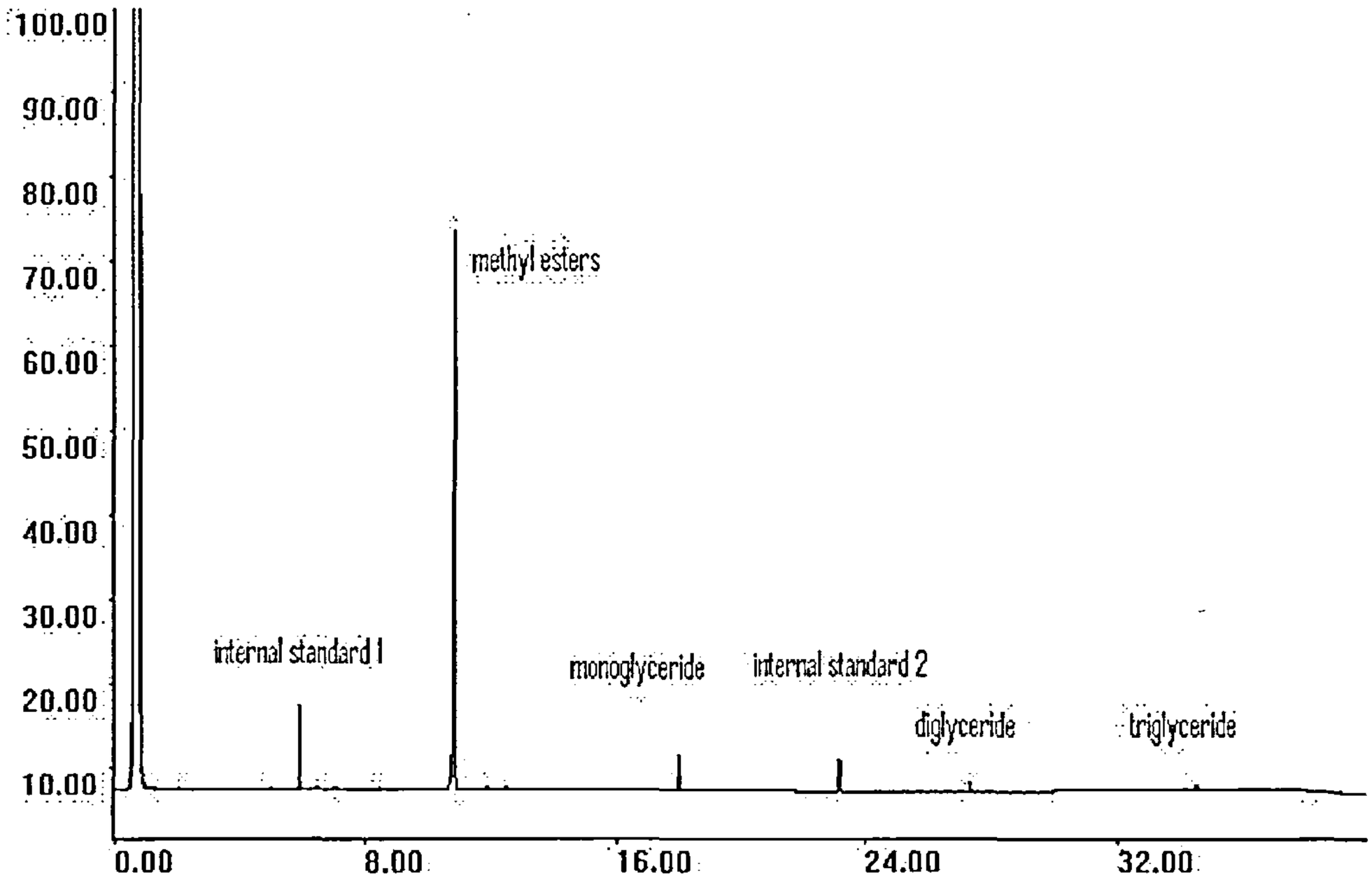

Figure 4.5: GC trace from glyceride GC

The calibration curve for triglyceride content, and diglyceride and monoglyceride content are shown in Figure 4.6, 4.7 and 4.8.

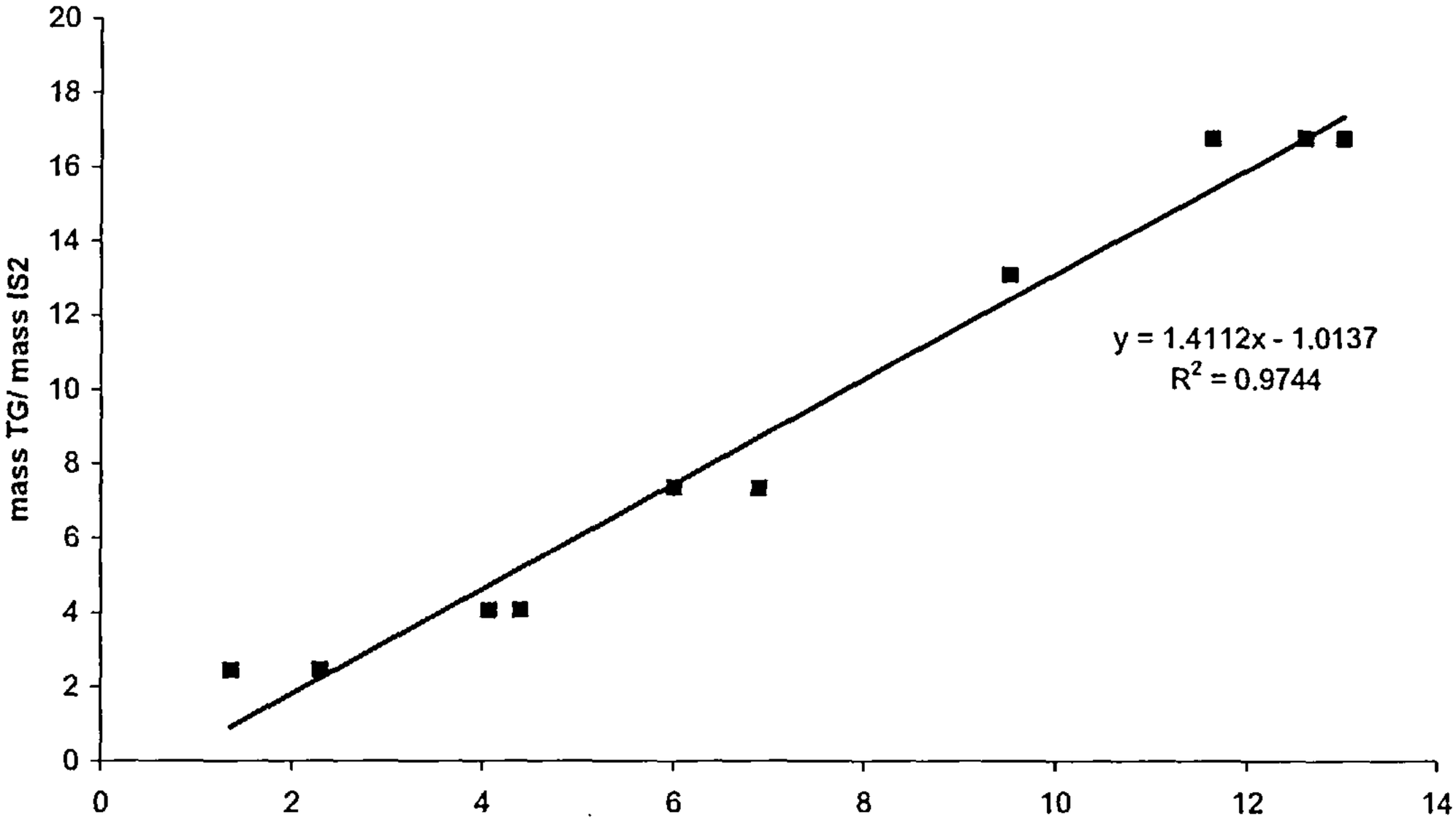

Figure 4.6: calibration curve for triglyceride content, range 0-30% mass. Measured points by analysis of a known quantity of triglyceride standard ■, linear line of best fit __.

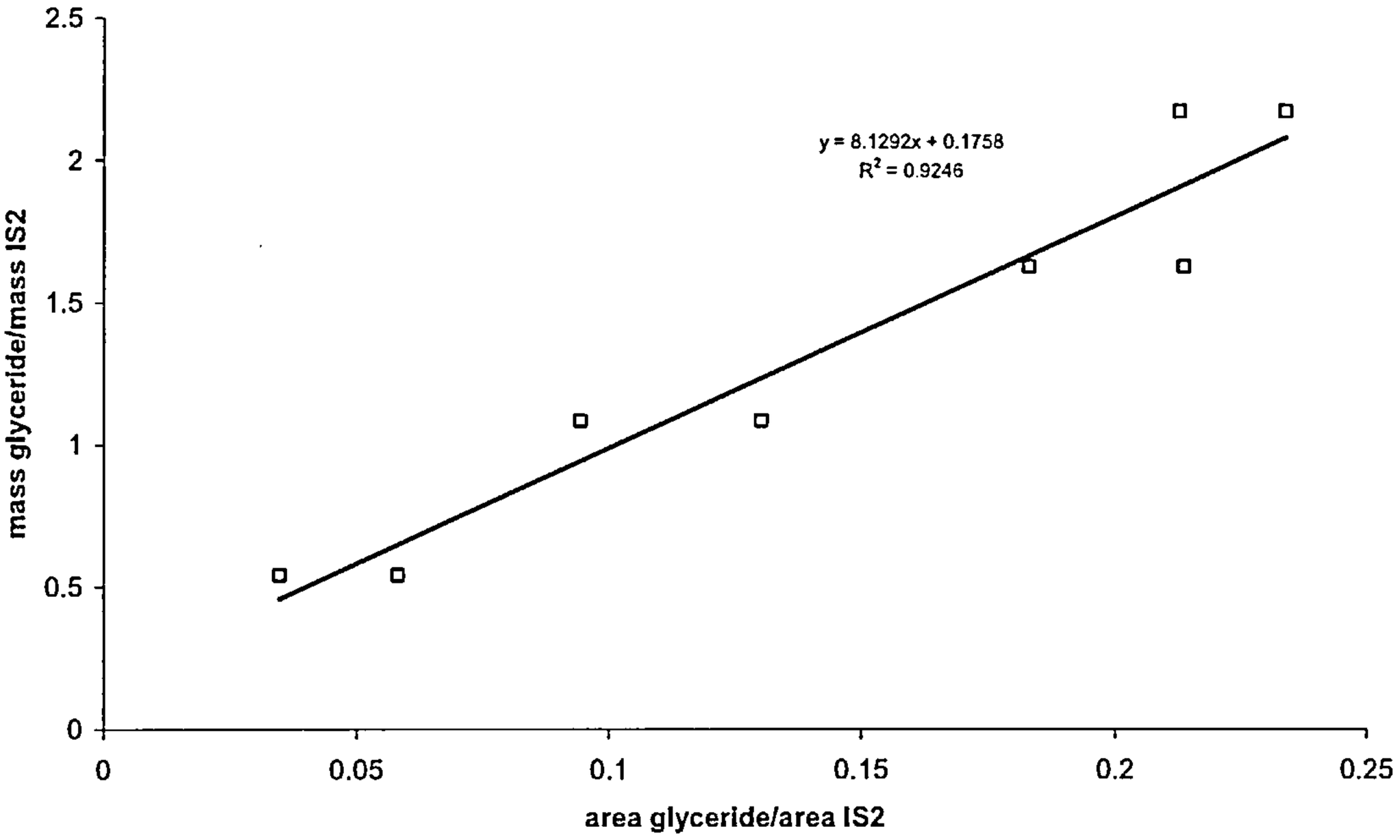

Figure 4.7: calibration curve for diglyceride content, range 0-3% mass. Measured points by analysis of a known quantity of diglyceride standard □, linear line of best fit __.

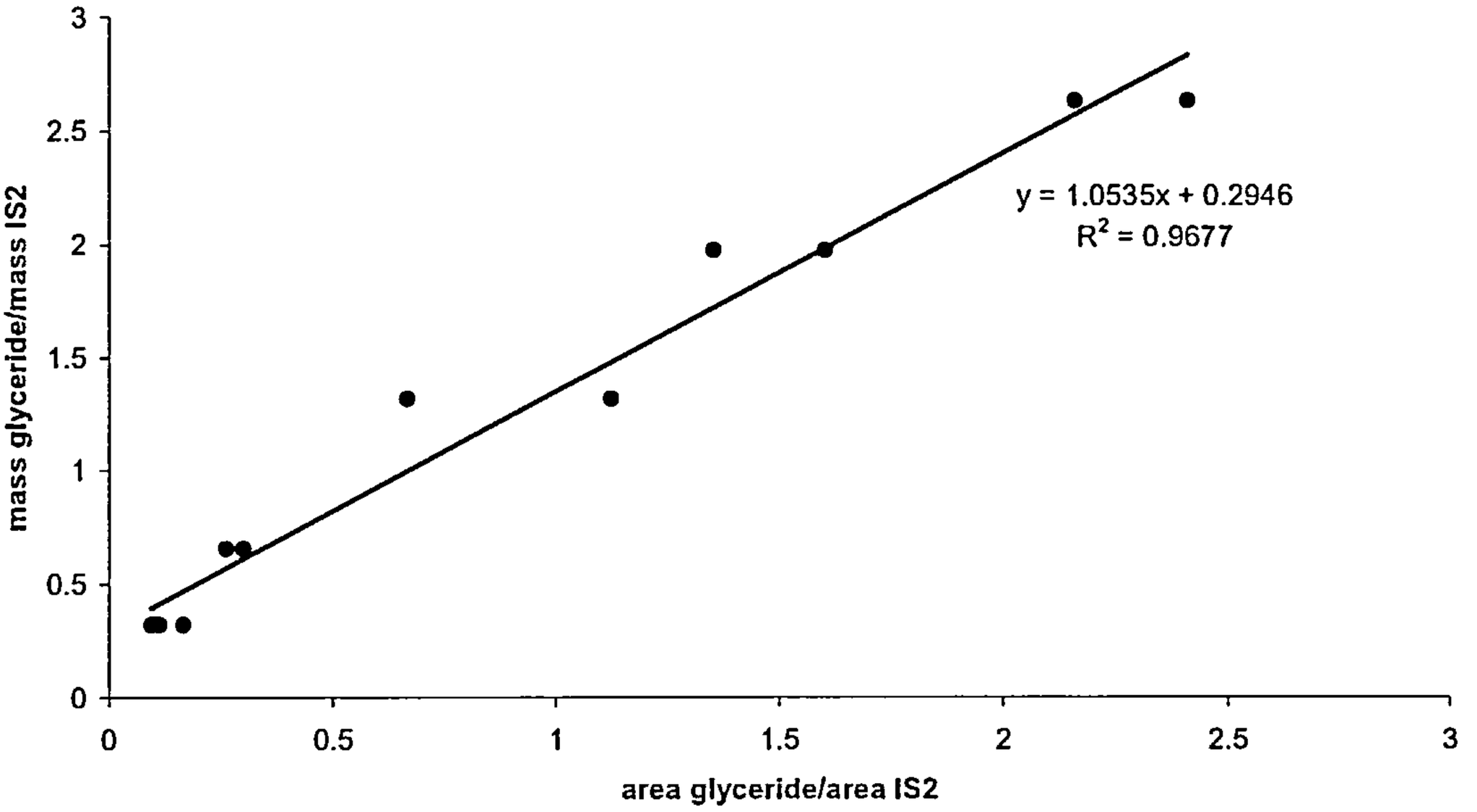

Figure 4.8: calibration curve for monoglyceride content, range 0-4 % mass, measured points by analysis of a known quantity of monoglyceride standard •, linear best fit line__.

The R^2 values for triglyceride and monoglyceride are inside the specifications of BS 14105, but for diglyceride the R^2 value is lower than the 0.95 specified in BS 14105. The random errors in the results for each measured component are shown in table 4.3.

Table 4.2: Random error in results quantified by repeated analysis of the same sample

Species	Error (% mass)
Triglyceride	± 5 %
Diglyceride	± 0.5 %
Monoglyceride	± 1 %
Biodiesel	± 2 %

The results for large percentage triglyceride samples were found to be unreliable by the glyceride method, so samples where the conversion was low were analysed by the ester GC method. The errors are relatively high in the glyceride method because the technique was being used outside the specifications of the method. The method was designed for quality control of commercial biodiesel samples, to ensure the EN 14214 standard was met and the maximum percentage triglyceride content suitable for analysis by this method is 0.4 % (BSi, 2003). In addition, the GC was not set-up correctly for the analysis. For the analysis of triglycerides it is more suitable to operate with direct on-column injection, rather than split injection, so that no sample discrimination occurs (Christie, 1990). Sample discrimination is when high boiling components are not volatilized and are swept away with the split flow gas, instead of entering the column. Unfortunately an on-column injector was not available.

4.2 Acidic catalysts

Acidic catalysts were screened for their activity in the esterification of free fatty acids and for the high-temperature transesterification of triglycerides, with the aim of finding a catalyst active for both reactions.

4.2.1 Screening and characterization

The results of the initial screening of the acid catalysts are shown in Table 4.3. PolyHIPE (GA) was the most active catalyst, followed by polyHIPE (CM), then montmorillonite KSF, and Amberlyst 46. The conversions are not high. The most active, polyHIPE, reached 50% conversion after 3 hours. This is similar to the conversion reached by H_2SO_4 as a catalyst after 1 hour reaction (at equivalent H^+ concentration to that of Amberlyst 46). As Amberlyst 46 was the most active of the Amberlyst resins tested, only Amberlyst 46 was studied further.

Table 4.3: Conversion for the esterification of oleic acid with methanol, 1:3 molar ratio, 60 °C, 5 % mass catalyst.

Catalyst	Conversion
blank (no catalyst)	0 ± 3 %
Amberlyst XE 781	2 ± 3 %
Amberlyst 46	25 ± 3 %
Amberlyst 36	16 ± 3 %
montmorillonite KSF	28 ± 3 %
polyHIPE (GA, CM)	49 ± 3 %, 31 ± 3 %
sulphuric acid (at equivalent acid level to Amberlyst 46)	49 ± 3 %

The factors affecting activity of a solid acid catalyst for esterification are listed below (Peters *et al.*, 2006, Mbaraka *et al.*, 2003):

- Strength of acid sites
- Number/density of acid sites
- Pore size
- Environment surrounding acid site i.e. hydrophobicity

The physico-chemical properties of Amberlyst 46, montmorillonite KSF and polyHIPE are shown in table 4.5. The surface area of the polyHIPE catalyst is low. This is because the pore size is very large (μm range) compared to the other catalysts, thus reducing the surface area. The surface area of montmorillonite is also low but the surface area of Amberlyst 46 is relatively high. Montmorillonite has the strongest acid sites, and an intermediate acid capacity amongst this set. PolyHIPE has the highest acid capacity, with Amberlyst 46 having the lowest acid capacity.

Table 4.4: Surface area and acid strength of acid catalysts

Catalyst	Surface area (m^2/g)	Approximate Pore size	Particle diameter	Acid strength	Acid capacity (mequiv/g)
Amberlyst 46	30	240 Å (a)	0.4-1.1 mm (a)	-3.0<pKa<1.1	0.6
montmorrilonite KSF	3	3.5 Å (b)	<75 μm	pKa<-3.0	1.8
PolyHIPE	3)	μm range (c)	0.5-5mm (d)	-3.0<pKa<1.1	5.2 (GA), 0.5 (CM)

(a) data from Rohm and Haas

(b) Binitha *et al.*, 2006

(c) SEM images (figure 4.15)

(d) from digital image

It has been shown that intra-particle diffusion limits the reaction rate for esterification of free fatty acids (Mbaraka *et al.,* 2003, Bondioli, 2004). Montmorillonite has small pores, but the particle size is very small, thus we would expect most of the reaction will take place on the external surface. The pores in Amberlyst 46 are reasonably large (240 Å), and the polymer will swell in contact with methanol (Shibasaki-Kitikawa *et al.*, 2007), thereby increasing the pore size further. The particle size of the polyHIPE is quite large, but as the structure is open, the intra-particle diffusion limitation should be lower.

Unfortunately the physico-chemical properties of these catalysts could not be varied independently. PolyHIPE has the highest activity, probably because of the increased number of acid sites, and because the large pores means that all of the sites are accessible. The activities of montmorillonite and Amberlyst 46 are similar. Montmorillonite has stronger acid sites and a higher number of acid sites but the small pore size means only some are accessible, whereas on Amberlyst 46 the acid strength is lower and the number of sites lower, but all sites are accessible.

PolyHIPE (GA), Amberlyst 46 and montmorillonite KSF did not exhibit any significant activity for the transesterification of triglycerides to methyl esters when tested at 60 °C and at 180 °C.

4.2.2 Reusability of the catalysts

Figure 4.9 shows that Amberlyst 46 and montmorillonite KSF could be reused successfully for 5 cycles. PolyHIPE (GA) showed a decrease in activity from 55% conversion to 35% conversion with repeated use (as shown in Figure 4.9). The conversion obtained using Amberlyst 46 improves slightly on repeated use, this could be due to swelling of the polymer, increasing accessibility of the acid sites (Lopez *et al.*, 2005).

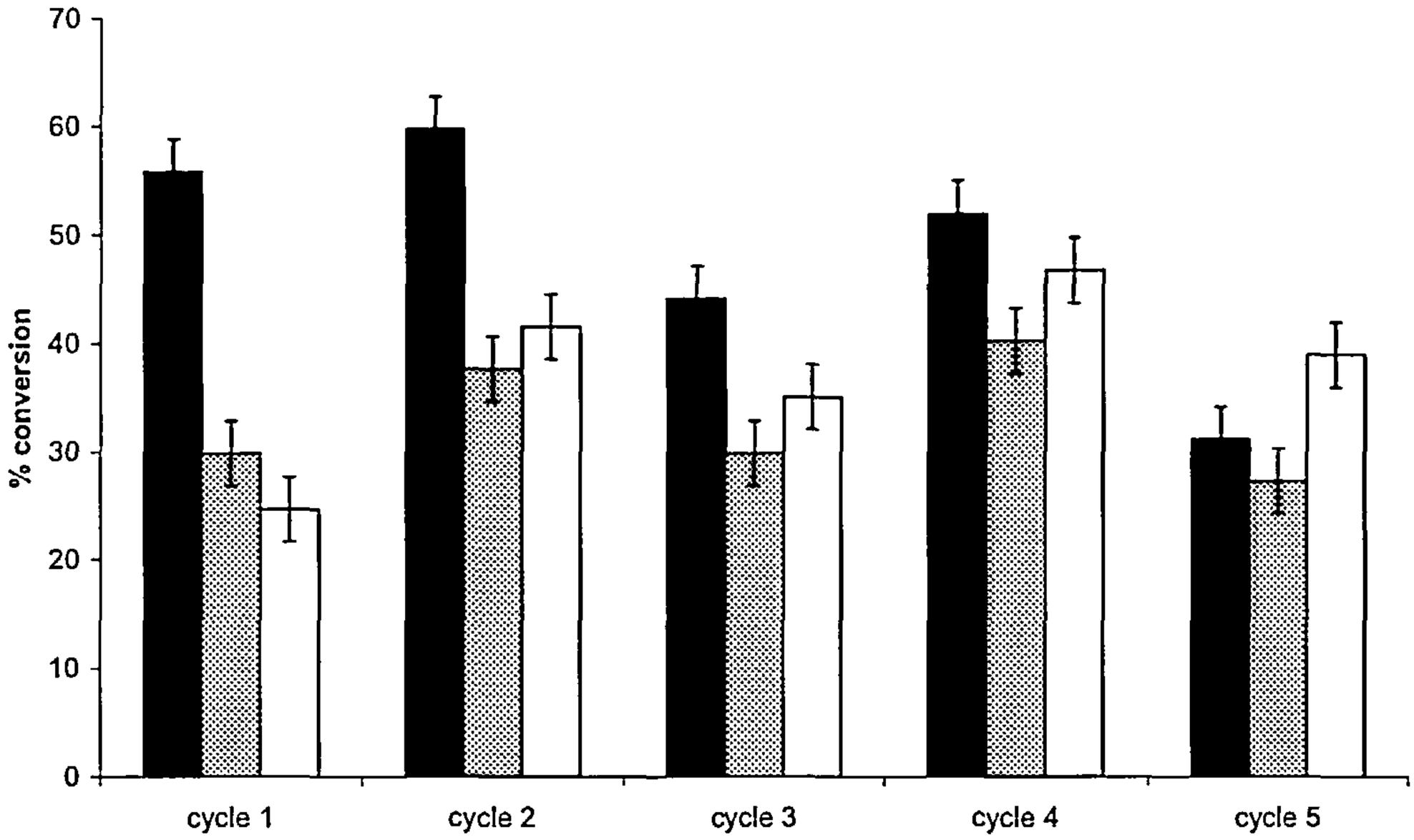

Figure 4.9: Reusability of catalyst quantified by using the same catalyst (Polyhipe GA – black, montmorillonite-grey, Amberlyst 46 –white) for 5 consecutive reactions (T=60 °C, molar ratio oleic acid to methanol 1:3, agitation at 600rpm)

However, if the leaching is slow, simply testing if the catalyst can be reused does not show whether the catalyst is stable. The soluble acidity of the catalysts when they were contacted with methanol at 60 °C for 3 hours is shown in table 4.6. The soluble acidity from the polyHIPE catalysts is high. Up to 40% is lost on contact with hot methanol. This explains why the activity started to decrease when the polyHIPE catalyst was reused. Soluble acidity was still detected for a polyHIPE sample (polyHIPE CM) even after thorough washing in a Soxhlet extractor. This means that it is not just the more labile acid groups leaching to leave the more strongly bonded acid groups as a stable acid catalyst, but that all acid groups can leach. The soluble acidity from the montmorillonite catalyst is also high, with over half of the acid sites present leaching into hot methanol. However, the catalyst maintains its activity for 5 cycles of use, so leaching in the reaction mixture must be slower. Amberlyst 46 has a low soluble acidity, so this catalyst can be considered to be stable under the conditions studied.

Table 4.5: Soluble acidity of acid catalysts

Catalyst	Soluble acidity in MeOH (mmole H^+/g)	% initial acid lost
PolyHIPE+ sulphuric acid (CM) (after Soxhlet)	0.2	40 %
PolyHIPE (G. Akay)	2.3	44 %
Amberlyst 46	0.04	6 %
montmorillonite	1.0	55 %

PolyHIPE will not be a suitable catalyst for the esterification of free fatty acid because it is not stable, so will only have a short life-time in the reactor. Additionally most of the advantages of a heterogeneous catalyst result from there being no acid present when the pre-treated oil exits the reactor and thus the neutralization step and its resulting salts can be eliminated. This would not be the case with if PolyHIPE was the catalyst. Montmorillonite appears to be stable in terms of activity, but some leaching should be expected, thus a neutralization step is likely to be required, and, again, the advantage of using a heterogeneous catalyst is lost. Amberlyst 46 is stable, and therefore would be a suitable catalyst for the esterification of free fatty acid. The conditions should be optimized to increase the conversion.

Other catalysts active for the esterification of free fatty acids are heteropoly acids and sulfonic acid functionalized mesoporous silica, as described in section 2.3. These catalysts may be better options because they can be used at higher temperatures, reducing the reaction time, and these catalysts have been shown to be stable to leaching in methanol.

4.2.3 Varying the reaction conditions

After identifying some active catalysts, the next stage was to change the reaction conditions to increase the conversion. Table 4.7 shows the conversion when the molar ratio of methanol to oleic acid was doubled from 3:1 to 6:1. The conversions reached under these conditions are higher than when a 3:1 molar ratio is used (except in the case of Amberlyst 46).

Table 4.6: Conversions with increased excess of methanol. Oleic acid : methanol ratio 1:6, 60 °C, 3 hours

Catalyst	Conversion
Amberlyst 46	24 ± 3 %
montmorillonite KSF	51 ± 3 %
polyHIPE (GA, CM)	66% ± 3, 38 ± 3 %

Figure 4.10 shows the effect of changing the intensity of agitation on the conversion. There is very little change in conversion with agitation. This implies that external mass transfer is not the rate controlling step: it is either reaction at the surface or internal mass transfer.

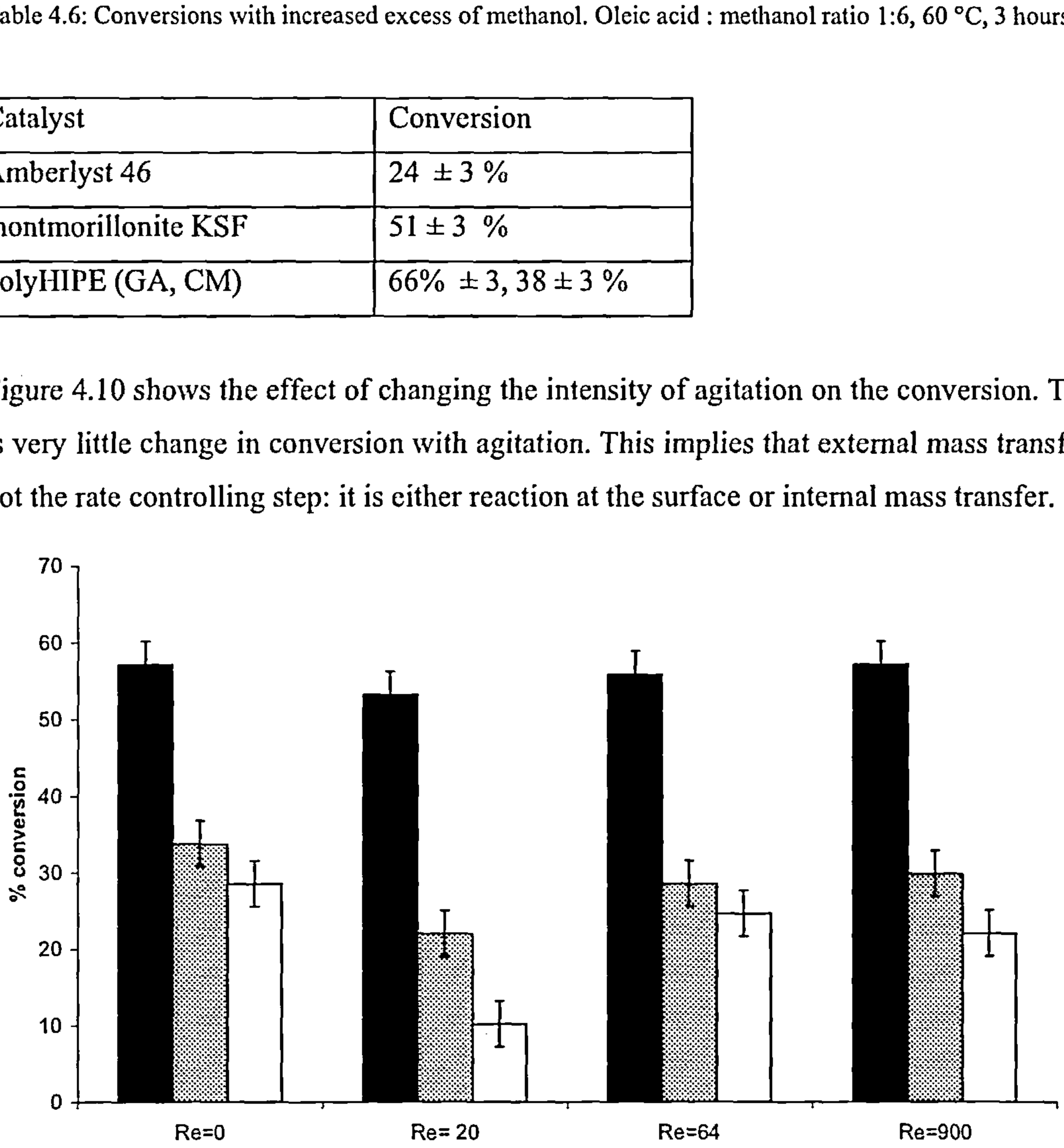

Figure 4.10: Effect of agitation on conversion of oleic acid at a oleic acid:methanol ratio of 1:3, at 60 °C, reaction time 3 hours. Black – polyHIPE (GA) , grey-montmorillonite, white – Amberlyst 46

Results from the experimental design also showed that increasing agitation intensity did not increase conversion, as this factor was found to be insignificant. Although there was an increase in conversion with increasing catalyst loading, this effect was less significant than the noise from random error in the system. As would be expected, the highest conversions occurred at longer times and high temperatures, with less than 5% probability that the effects shown resulted from noise. Increasing the molar ratio increased the conversion in all cases, however the influence of molar ratio was only observed to be statistically significant in the case of montmorillonite KSF. For polyHIPE, there was a statistically significant interaction between molar ratio and temperature.

Figure 4.11 shows the conditions required for 80% conversion after 5 hours of reaction with polyHIPE as catalyst. Temperatures above 65 °C are required with a lower molar ratio of methanol to oleic acid, but increasing the molar ratio means that the temperature required is decreased. The maximum conversion attained was 89 %. The curved line shows that there is an interaction between molar ratio and temperature. The interaction is more clearly seen in Figure 4.12.

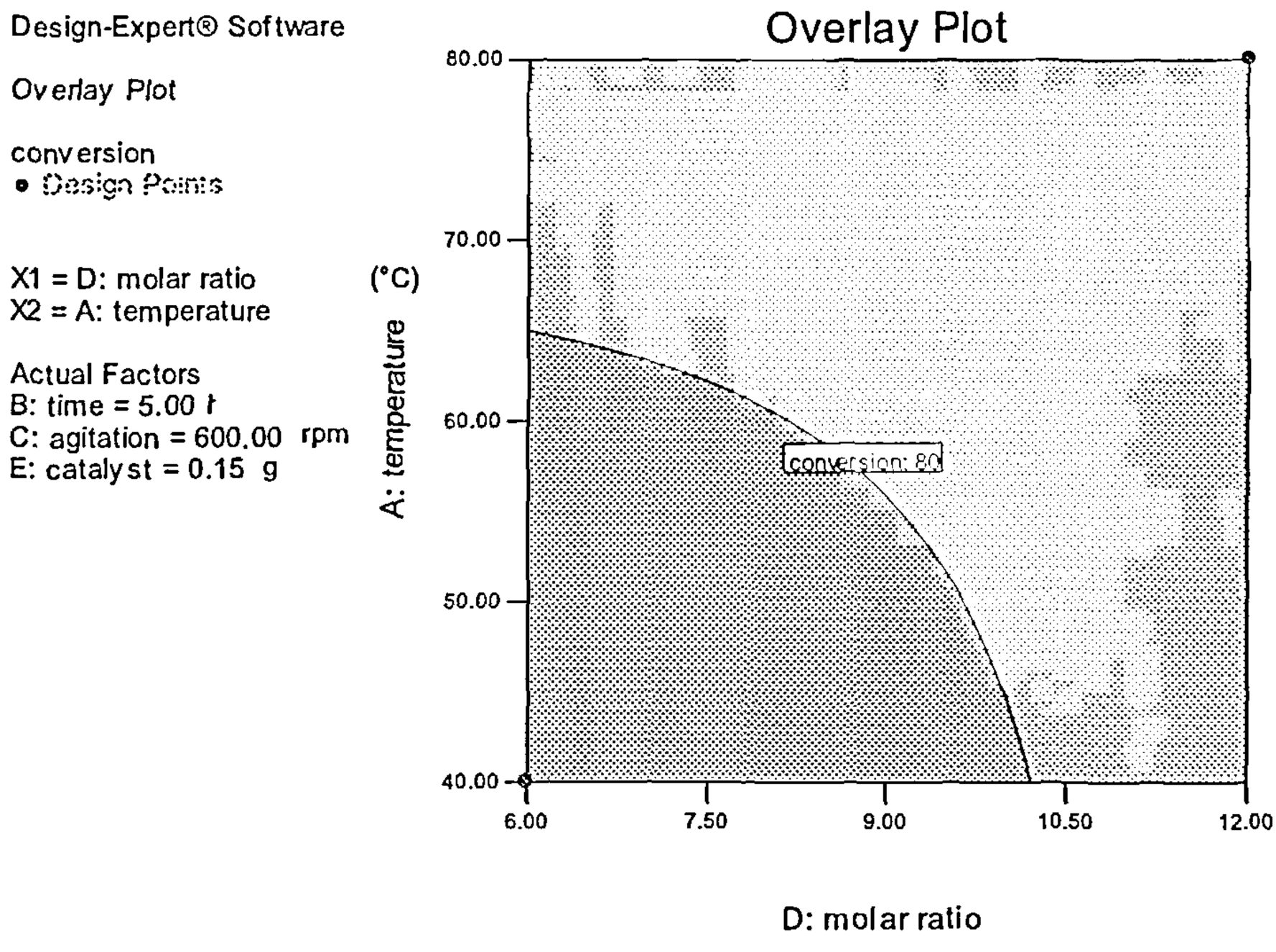

Figure 4.11: Plot from experimental design showing conditions where conversion is greater than 80% (light grey area) for PolyHIPE (GA). Plot is for t=5 hours.

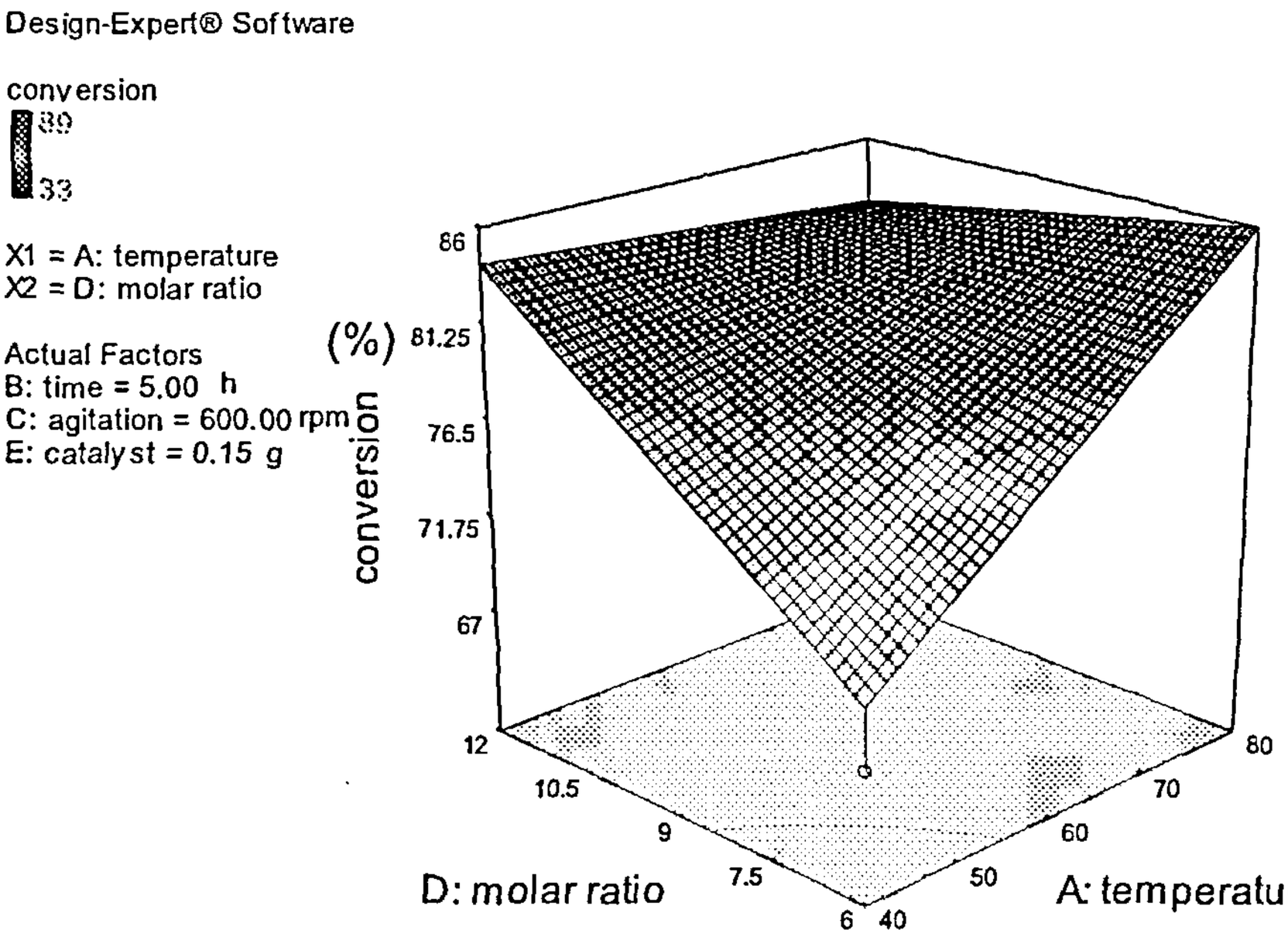

Figure 4.12 : Graph of dependence of conversion on molar ratio and temperature for the esterification of oleic acid and methanol.

Figure 4.13 shows the conditions required to reach 70% conversion using montmorillonite KSF after 5 hours of reaction, again a relatively high temperature and molar ratio of methanol are required. The maximum conversion obtained was 83 %

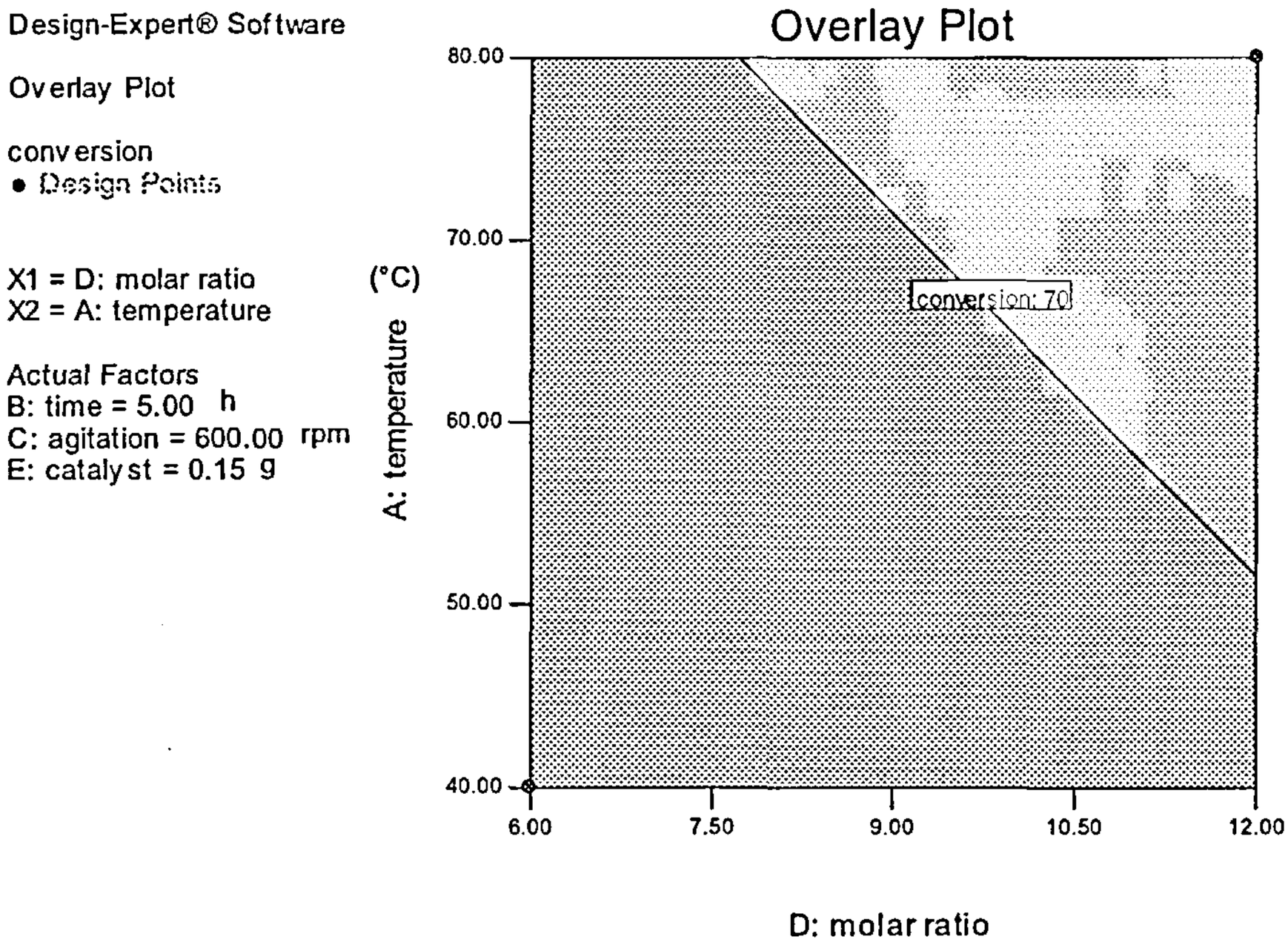

Figure 4.13: Plot from experimental design showing conditions where conversion is greater than 70% (light grey area) for montmorillonite KSF. Plot is for t=5 hours.

Figure 4.14 shows the conditions required to reach 60% conversion using Amberlyst 46 after 5 hours of reaction. The maximum conversion obtained was 72%.

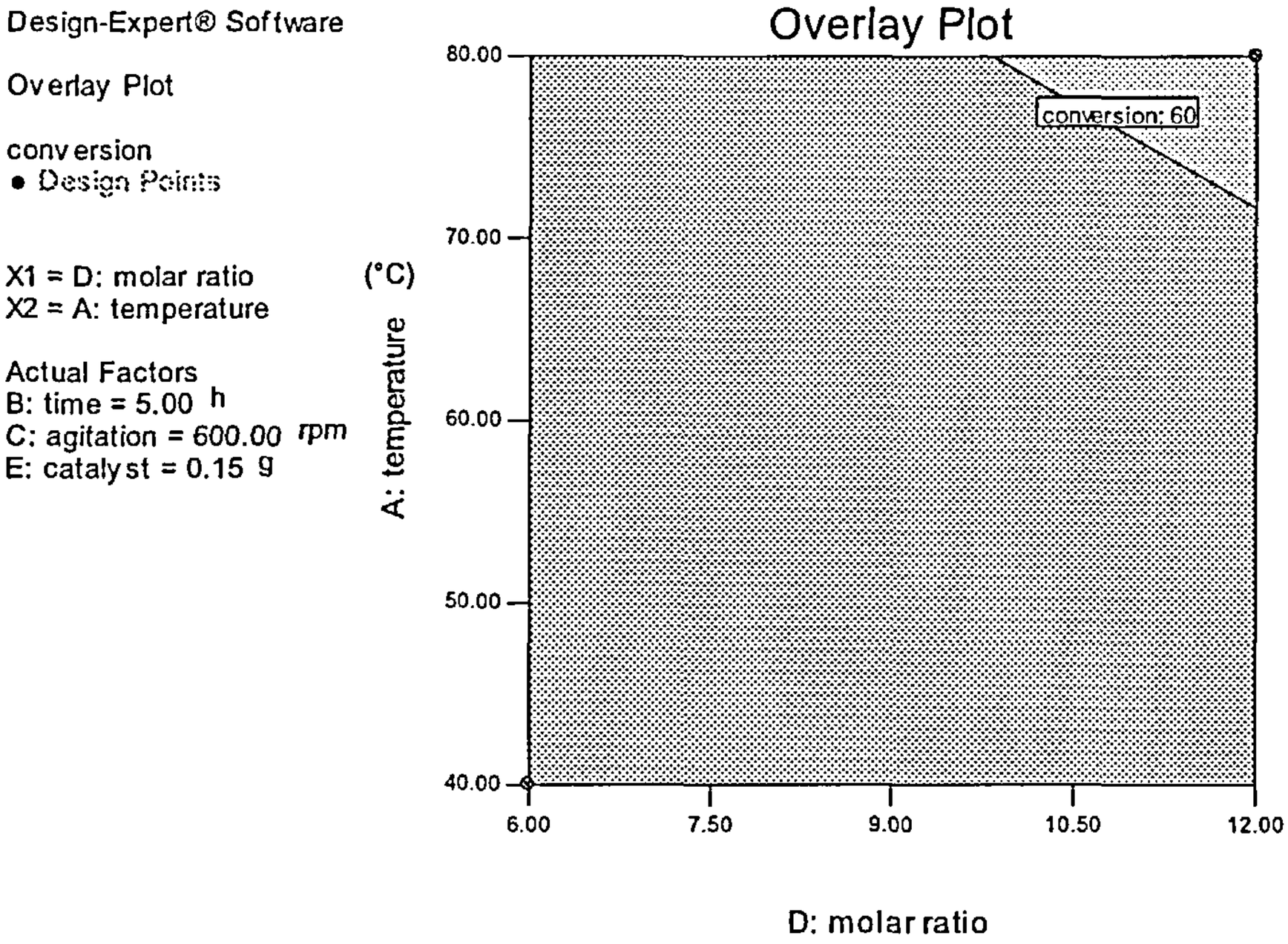

Figure 4.14: Plot from experimental design showing conditions where conversion is greater than 60% (light grey area) for Amberlyst 46. Plot is for t=5 hours.

The results from the experimental design do not generate any new insights, but it is a convenient way to display the most practical areas of the parameter field in which to operate.

As Amberlyst 46 is the only catalyst tested that does not suffer from significant leaching, this criteria would make it the best candidate. It is also readily available (unlike polyHIPE) and as it comes in the form of beads, which are much easier to separate from the reaction mixture than montmorillonite. However, esterification using Amberlyst 46 is not rapid, and in 5 hours, conversions of 72% are reached at 80 °C with a large molar excess of methanol. Reaching a conversion of 90 %, especially when in the presence of triglycerides would

require a prohibitively long residence time, and the adverse economic impact of the resulting large reactor, versus using a homogeneous catalyst and neutralization would be significant.

4.2.4 PolyHIPE manufacture, functionalization and characterization

The pore size distributions of the in-house manufactured polyHIPEs are shown in figure 4.15 and Table 4.7. PolyHIPE 1 (Figure 4.16) was the "standard" 5% crosslinker density polymer, polyHIPE 2 (Figure 4.17) had increased crosslinker content (15%), and increased surfactant content. PolyHIPE 3 (Figure 4.18) and polyHIPE 4 (Figure 4.19) had THF added to the aqueous phase in order to increase the pore size (1 ml and 3 ml respectively). The increase in pore size with addition of THF was negligible (see table 4.8); the only significant morphological change observed was the cell and pore structure of polyHIPE 2. The pores and cells on polyHIPE 2 are marked on the micrograph on Figure 4.19. In order to study the effects of pore size on activity, a wider range of pore sizes would be required, so only the activity of different acid functionalities on support 2 was tested. One method to achieve a wider range of pore sizes would be to use an oil-soluble initiator like AIBN, and make polyHIPEs with 0-100% divinylbenzene (Williams *et al.*, 1990).

Table 4.7: Mean pore size and standard deviation of pore size of manufactured polyHIPEs

Support	Mean diameter of pores (μm)	Standard deviation (μm)
1	14.9	4.1
2	15.3	3.5
3	13.6	6.8
4	16.9	7.3

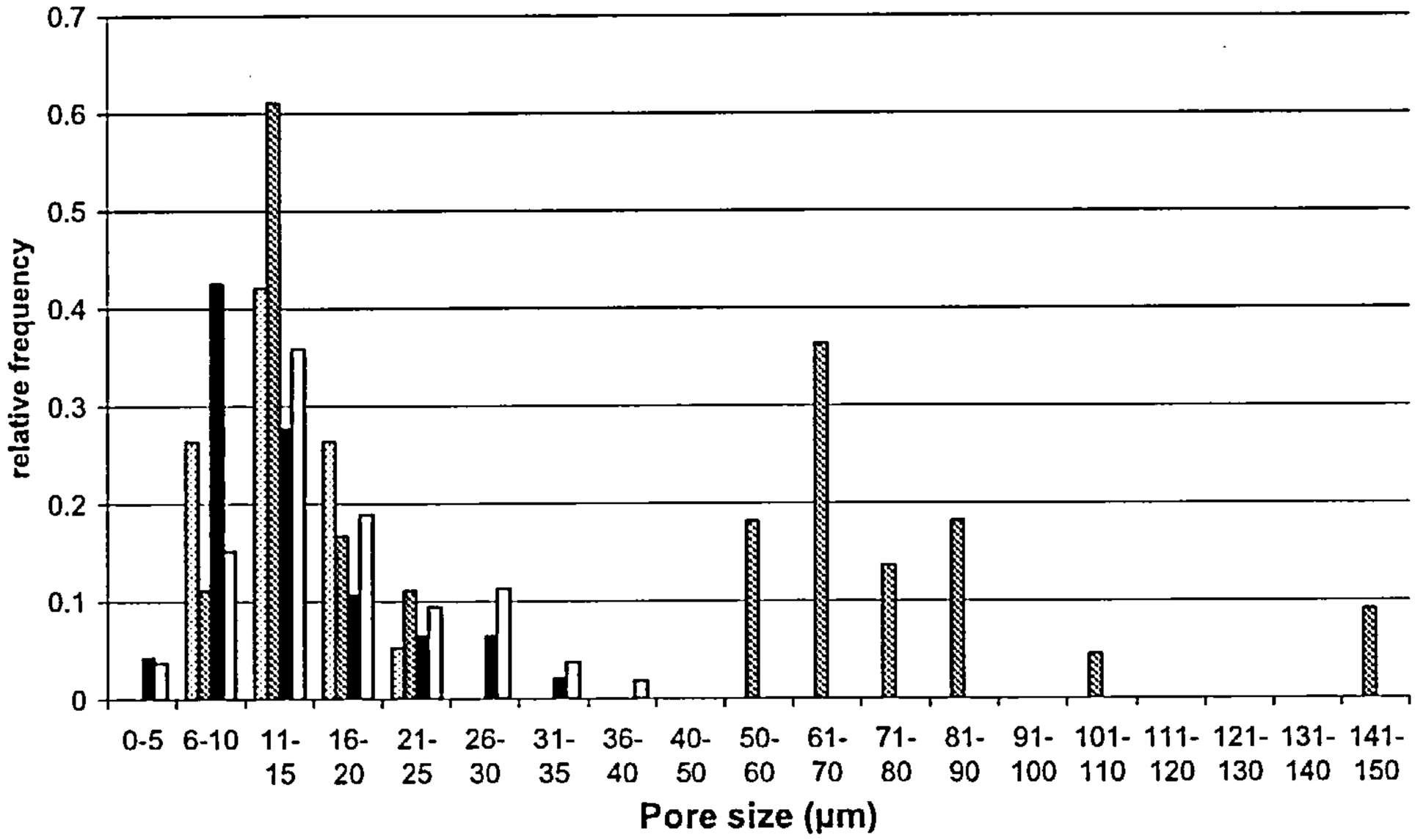

Figure 4.15: Pore size distribution of pores and cells in polyHIPE (CM) as determined from SEM micrographs. Light grey bars -sample 1, dark grey bars - sample 2, black bars - sample 3, white bars – sample 4.

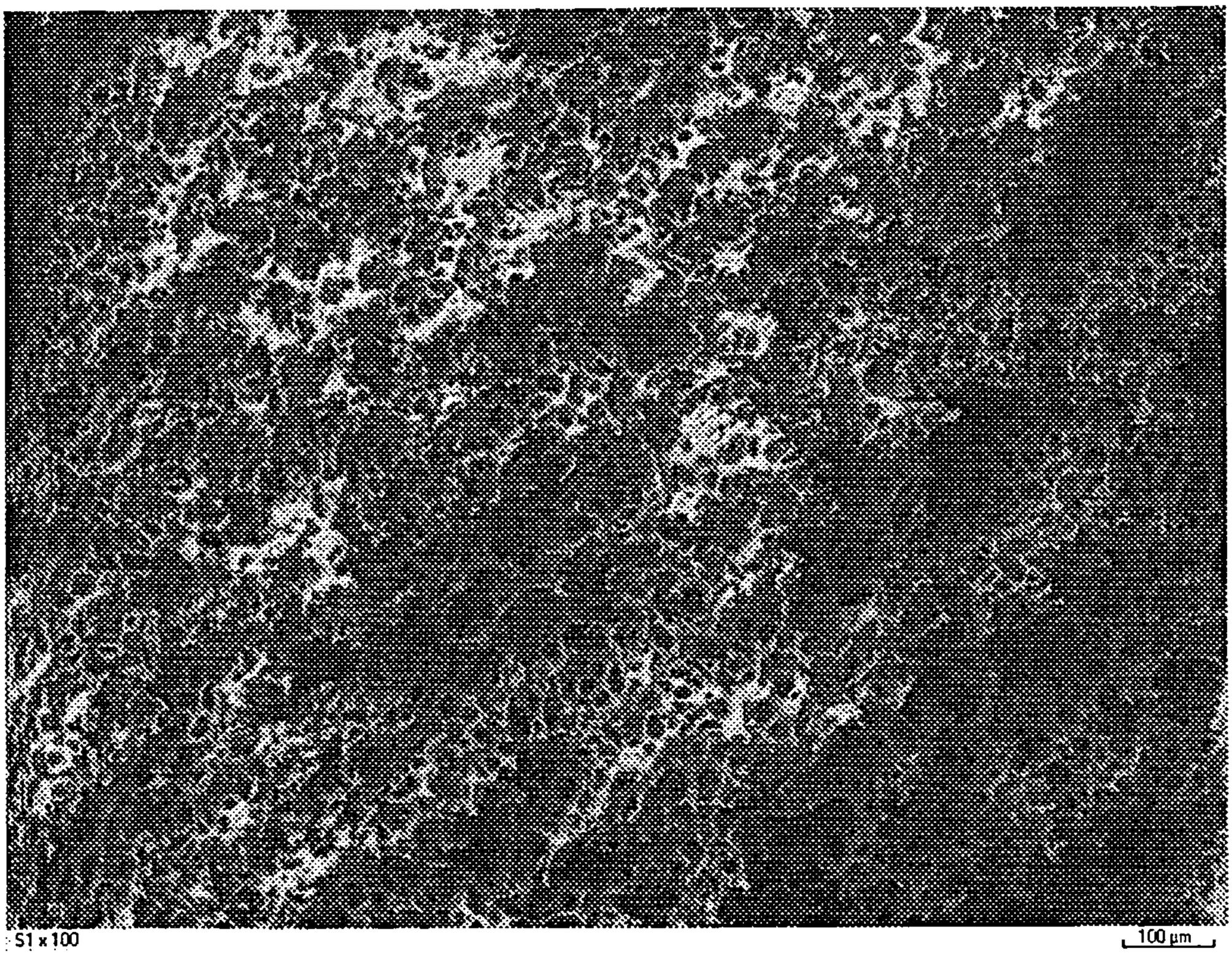

Figure 4.16: SEM micrograph at 100x magnification of polyHIPE 1

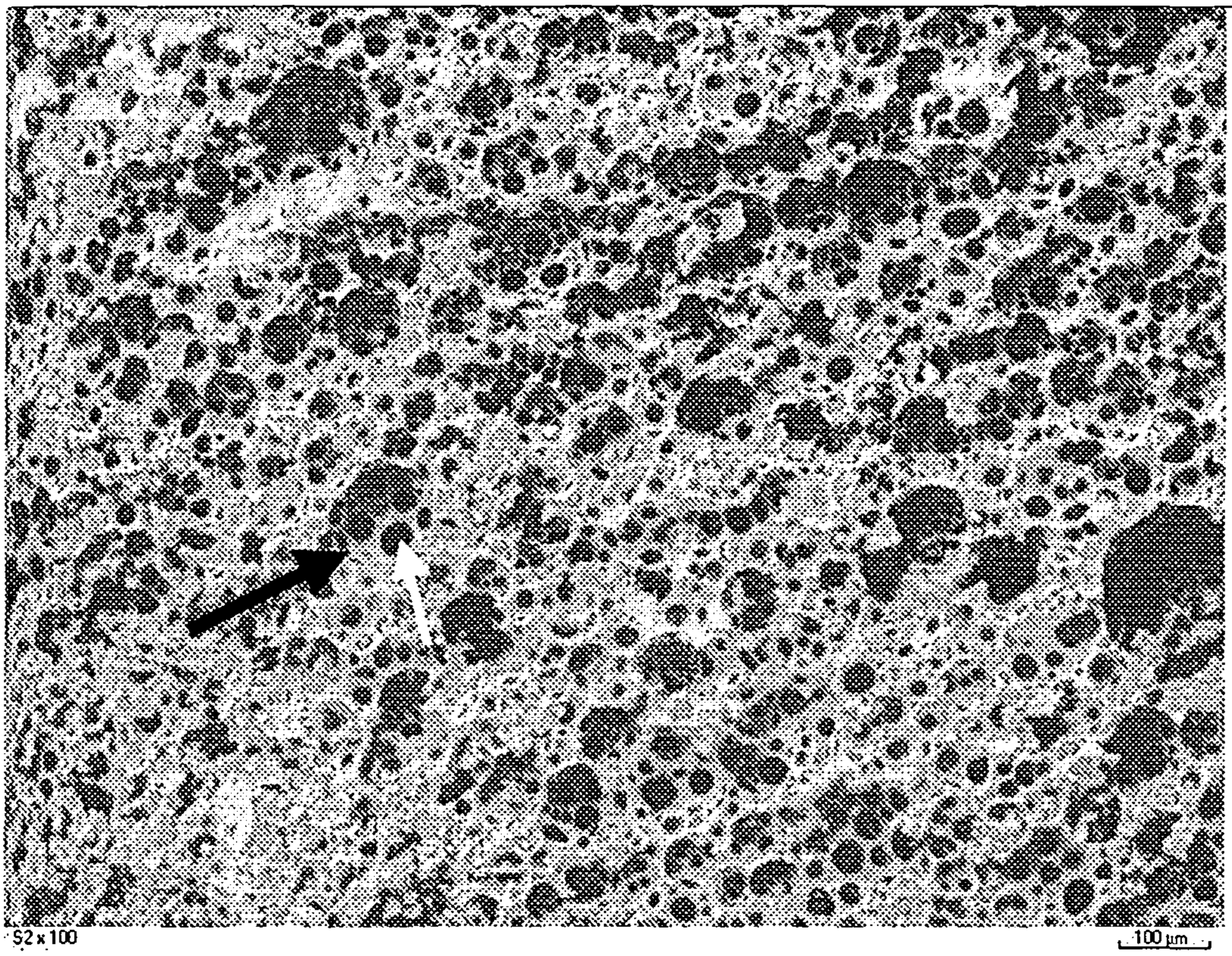

Figure 4.17: SEM micrograph at 100x magnification of PolyHIPE 2. Cell marked with black arrow, pore marked with white arrow.

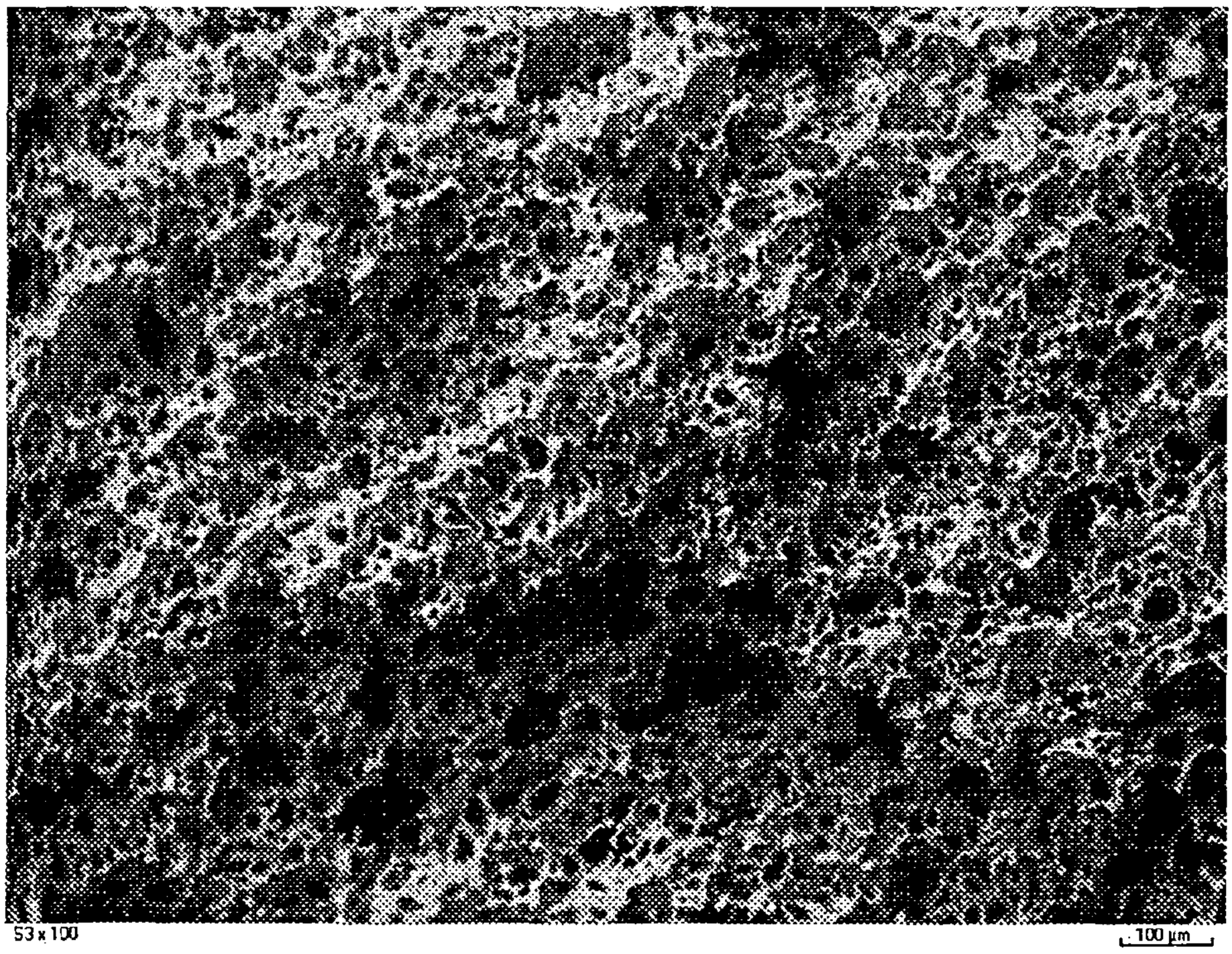

Figure 4.18: SEM micrograph at 100x magnification of polyHIPE 3

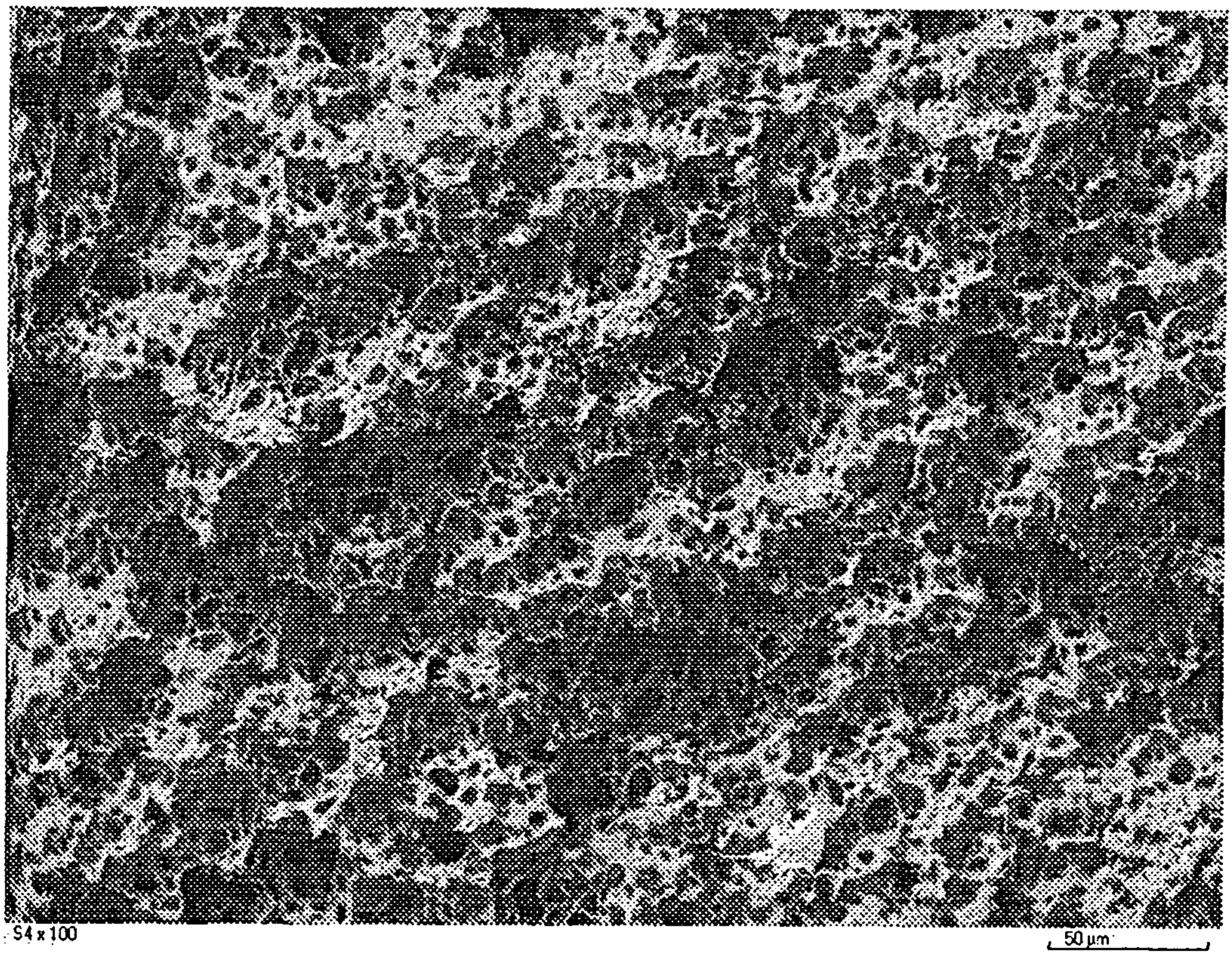

Figure 4.19: SEM micrograph at 100x magnification of polyHIPE 4

The acid capacity and soluble acidity of the functionalized polyHIPEs are given in table 4.9.

Table 4.8: Acid capacity and soluble acidity of PolyHIPEs functionalized with different acid groups

Catalyst	Acid capacity (mequiv/g)	Soluble acidity (mequiv/g)
polyHIPE+ sulphuric acid	0.5	0.2
polyHIPE + PTSA	1.2	1.2
polyHIPE + DDBSA	1.7	1.7

The soluble acidity is large, therefore a significant number of the acid groups leach from the support into the solution. This is confirmed by the high conversion achieved on initial use of these catalysts (complete conversion after 3 hours) and reduced conversion on second use. It is likely that the sulfonic acids groups will leach from the support into the methanol, i.e. that the catalysis is principally homogeneous. The sulfonation reaction is reversible, and the sulfonic group can be easily removed from the benzene ring (Fessenden and Fessenden, 1982). However, it is unclear whether the sulfonic acid groups leached as a result of cleaving of the C-S bond or whether they were not covalently attached. PTSA and DDBSA functionalized polyHIPE lose 100% of their acidity on the first use, so we can assume that the acid groups were simply adsorbed and not covalently bonded to the support. Sulfuric acid functionalized polyHIPE loses only 40% of the acid initially present, so we can assume that at least some of the acid groups are covalently bonded to the support. However, as the reaction is reversible, as discussed earlier, this does not mean that the catalyst is necessarily stable. Possibly, a better functionalization method could be used, for example propionic anhydride and sulphuric acid (Thaler, 1983) but this catalyst would only be stable if the reverse sulfonation reaction does not occur.

PolyHIPEs were manufactured with a narrow range of pore size distributions; all supports had mean pore sizes in the 13-17 μm range. Functionalizing with sulphuric acid, p-toluenesulfonic acid and dodecylbenzensulfonic acids did not give stable sulfonated polystyrenes – because the sulfonic acid groups leached from the support into the methanol. Therefore these catalysts would not be practical for industrial use.

4.2.5 Summary: Acid Catalysts

A solid acid catalyst for esterification of free fatty acids would be desirable to eliminate the neutralization stage required when free fatty acids are pre-esterified. Even more desirable would be a catalyst capable of both transesterification and esterification. However none of the tested catalysts showed any activity for transesterification, and the esterification reaction was slow. Sulfonated PolyHIPE and montmorillonite KSF leached significantly into solution, so these catalysts would not eliminate the neutralization stage and would also lose activity over time. Therefore these catalysts are unlikely to be practical. Amberlyst 46 is more stable, but has a lower activity. At the optimum conditions identified a conversion

of 72% in 5 hours was reached. There is perhaps scope to increase temperature further to increase the reaction rate, but whether a high-temperature, larger reactor with solid catalyst is more economical than a smaller, lower-temperature reactor plus neutralization stage and homogeneous catalyst must be assessed.

4.3 Alkali doped metal oxides

In this section Li, Na and K were doped onto MgO, CaO and Al_2O_3. These catalysts were dried at 110 °C and then calcined at 600 °C to allow the effect of pre-treatment temperature to be investigated. The catalysts were characterized using base strength indicators and X-ray diffraction. After screening for activity, the catalysts were tested in batch reaction to obtain kinetic data. The stability, and thus re-usability of the catalyst were also quantified.

This information allowed the origin of the high base strength and activity of these catalysts to be discussed, as well as the mechanism for the reduction in activity after use. Some alternative options to these catalysts were tested and the feasibility of use considered.

4.3.1 Initial screening and characterization

The surface areas of the CaO-supported catalysts (~10 m^2/g) and MgO-supported catalyst (~20 m^2/g) were low while the Al_2O_3 supported catalyst had higher surface areas (~70 m^2/g). Calcining the CaO- and MgO- supported catalysts significantly reduced the surface areas, to 1-2 m^2/g. Compared to commercially-used catalysts these surface areas are very low, but unlike a gas phase reaction where gases can easily diffuse into the interior of the catalyst particle, the microporous internal surface area would not be accessed by the large triglyceride molecules. Triglycerides would only be able to diffuse into the pores of a mesoporous material.

The base strengths of the catalyst are shown in Table 4.9, together with the conversion from the initial screening runs. All of the alkali-doped CaO catalysts have base strengths $pK_{BH+}>11$, which is higher than the base strength of CaO alone ($8.2<pK_{BH+}<10.1$). This increased base strength occurs with all alkali metals, regardless of whether the catalyst is calcined or just dried. All of the alkali-doped CaO catalysts are active, reaching conversions >85% in 3 hours.

Of the MgO-supported catalysts, only calcined Li-MgO exhibits base strength $pK_{BH+}>11$, and is the only one of the MgO supported catalysts to be active, again reaching a conversion >90% in 3 hours.

The Al_2O_3-supported catalysts have much lower base strengths and although this increases with calcination, the base strength is still too low for the catalysts to be active.

Table 4.9: Base strength and conversion from initial screening run (60 °C, 3 hours) of screened catalysts

Catalyst	Base strength (pK_{BH+})	Conversion (%)
Li-CaO	$11< pK_{BH+}<15$	85%
Na-CaO	$11< pK_{BH+}<15$	98%
K-CaO	$11< pK_{BH+}<15$	90%
Li-CaO (calcined)	$11< pK_{BH+}<15$	99%
Na-CaO (calcined)	$11< pK_{BH+}<15$	100 %
K-CaO (calcined)	$11< pK_{BH+}<15$	100 %
Li-MgO	$8.2< pK_{BH+}<10.1$	5 %
Na-MgO	$10.1< pK_{BH+}<11$	4 %
K-MgO	$10.1< pK_{BH+}<11$	4 %
Li-MgO (calcined)	$11< pK_{BH+}<15$	100 %
Na-MgO (calcined)	$10.1< pK_{BH+}<11$	7 %
K-MgO (calcined)	$10.1< pK_{BH+}<11$	4 %
Li-Al_2O_3	<8.2	8 %
Na- Al_2O_3	<8.2	3 %
K- Al_2O_3	<8.2	6 %
Li- Al_2O_3 (calcined)	$10.1< pK_{BH+}<11$	5 %
Na- Al_2O_3 (calcined)	$10.1< pK_{BH+}<11$	6 %
K- Al_2O_3 (calcined)	$10.1< pK_{BH+}<11$	5 %

Catalysts with a higher base strength are active for the transesterification reaction. These were alkali-doped CaO catalysts and Li-doped MgO after calcination. After 3 hours reaction, conversions in excess of 85% were achieved. There is no effect on activity when changing the alkali-metal dopant on CaO, and the catalyst did not require calcination at 600

°C to be active. Alkali-doped Al_2O_3 catalyst were not active, despite a prior study showing they had some activity (Xie *et al.*, 2006a), probably because the alkali loading level was lower in this study (5%) than in Xie's study (15-45%). The loading level of 5% was chosen because it was shown that increasing the loading reduced the activity of Li-CaO catalysts because a bulk layer of $LiNO_3$ was formed at higher loadings, rather than the dispersed Li^+ ions, which were thought to form the active sites (Watkins *et al.*, 2004). It is more likely that with a higher alkali loading level, the activity will result from the leaching of the alkali metal.

The nucleophilic attack of the methoxide ion on the carbonyl carbon on the ester is thought to be the mechanism for base catalysed transesterification (Schuchardt *et al.*1997), the base strength of the catalyst should be high, so that this pathway can occur. Other studies have noted an increase in activity with increasing base strength (Suppes *et al.*, 2004, Kim *et al.*, 2004).

4.3.2 Characterization by XRD

As the most promising candidates, Li-MgO and Li-CaO catalysts were analysed by XRD after drying at 110 °C and calcination at 600 °C. The phases were identified by matching the peaks on the XRD trace with known diffraction patterns in the ICDD database, these assignments and reference peaks are shown in appendix 1.

Table 4.10 – phases identified by XRD for Li catalysts, diffractograms shown in appendix 1

Catalyst	Li phases present	Mg phases present	Ca phases present
LiMgO	Li_2CO_3	MgO, $Mg(OH)_2$	
LiMgO (calcined)	Li_2CO_3, LiOH, $LiOH.H_2O$	MgO	
LiCaO	$LiNO_3.(H_2O)_3$		$Ca(OH_2)$, $CaCO_3$
LiCaO (calcined)	Li_2CO_3		$Ca(OH_2)$, CaO

From the XRD results shown in Table 4.10 the source of the basicity and thus activity in the Li-MgO (calcined) catalyst can be clearly identified as the formation of the LiOH and $LiOH.H_2O$ phase from the source nitrate salt. Further analysis of LiMgO catalysts showed that when the calcination temperature was 500 °C a LiOH phase was not formed, and the catalyst was not active. Similarly, when the alkali dopant was K at a calcination temperature of 600 °C a KOH phase was not formed, and this catalyst was not active. Therefore the formation of a hydroxide phase through the decomposition of the nitrate is the source of the activity.

The Li-CaO catalysts show a change in structure on calcination in both the Li phase and Ca phase. When the catalyst is dried at 110 °C only, the lithium phase remains as $LiNO_3$, but, on calcination, Li_2CO_3 is formed. The dried catalyst contains $CaCO_3$ and $Ca(OH)_2$, whereas the calcined catalyst contains CaO and $Ca(OH)_2$. The source of the carbonate is probably atmospheric CO_2. With the change in structure and phases present, it would be expected that there would be a change in activity, and the Li-CaO (calcined) is more active as shown in section 4.3.3. For LiCaO, there are no strong base species, such as LiOH, or Li_2O formed and this makes identification of the active species more difficult.

The phases detected here are similar to those found in a study of alkali-doped calcium oxide for oxidative coupling of methane (Baronetti *et al.*, 1993). The preparation method was slightly different, in that the alkali pre-cursor salts were hydroxides, and a higher calcination temperature of 750 °C was used. The Ca phases present in that catalyst were $CaCO_3$, CaO and $Ca(OH)_2$, with the lithium present as Li_2CO_3. Similarly, for a Na-CaO catalyst $Ca(OH)_2$, $CaCO_3$, Na_2CO_3 and $NaCa(CO_3)_2$ were present; and for a K-CaO catalyst $Ca(OH)_2$, $CaCO_3$, K_2O and $KCa(CO_3)_2$ were present .

4.3.3 Batch tests

The % mass of triglycerides, diglycerides, monoglycerides and biodiesel versus reaction time for the tested catalysts are shown in figures 4.20-4.27.

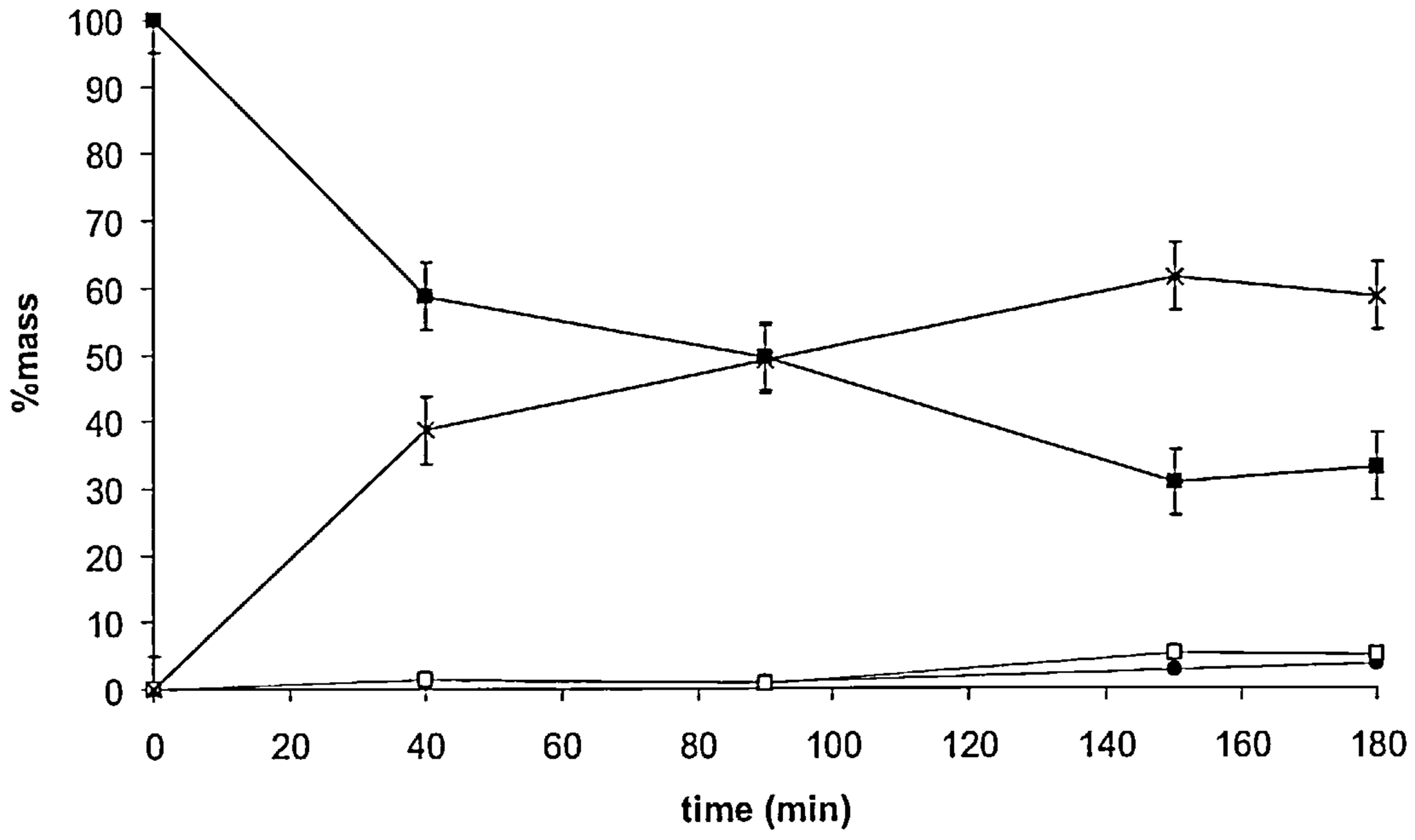

Figure 4.20: CaO-catalysed reaction, 60 °C, 6:1 molar ratio oil to methanol, 2 g catalyst. Triglycerides ■, diglycerides □, monoglycerides •, biodiesel x.

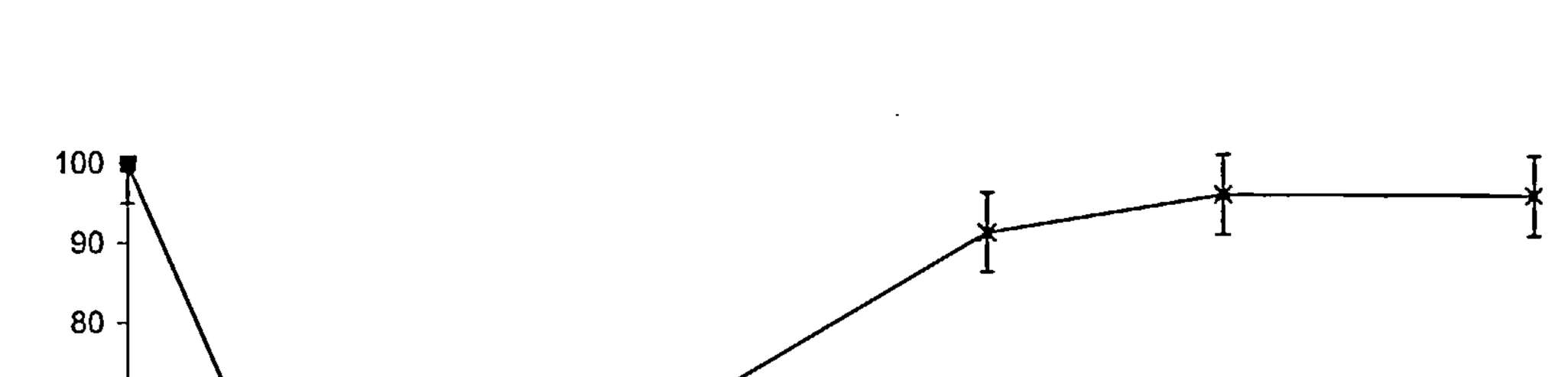

Figure 4.21: LiCaO-catalysed reaction, 60 °C, 6:1 molar ratio oil to methanol, 2 g catalyst. Triglycerides ■, diglycerides □, monoglycerides •, biodiesel x.

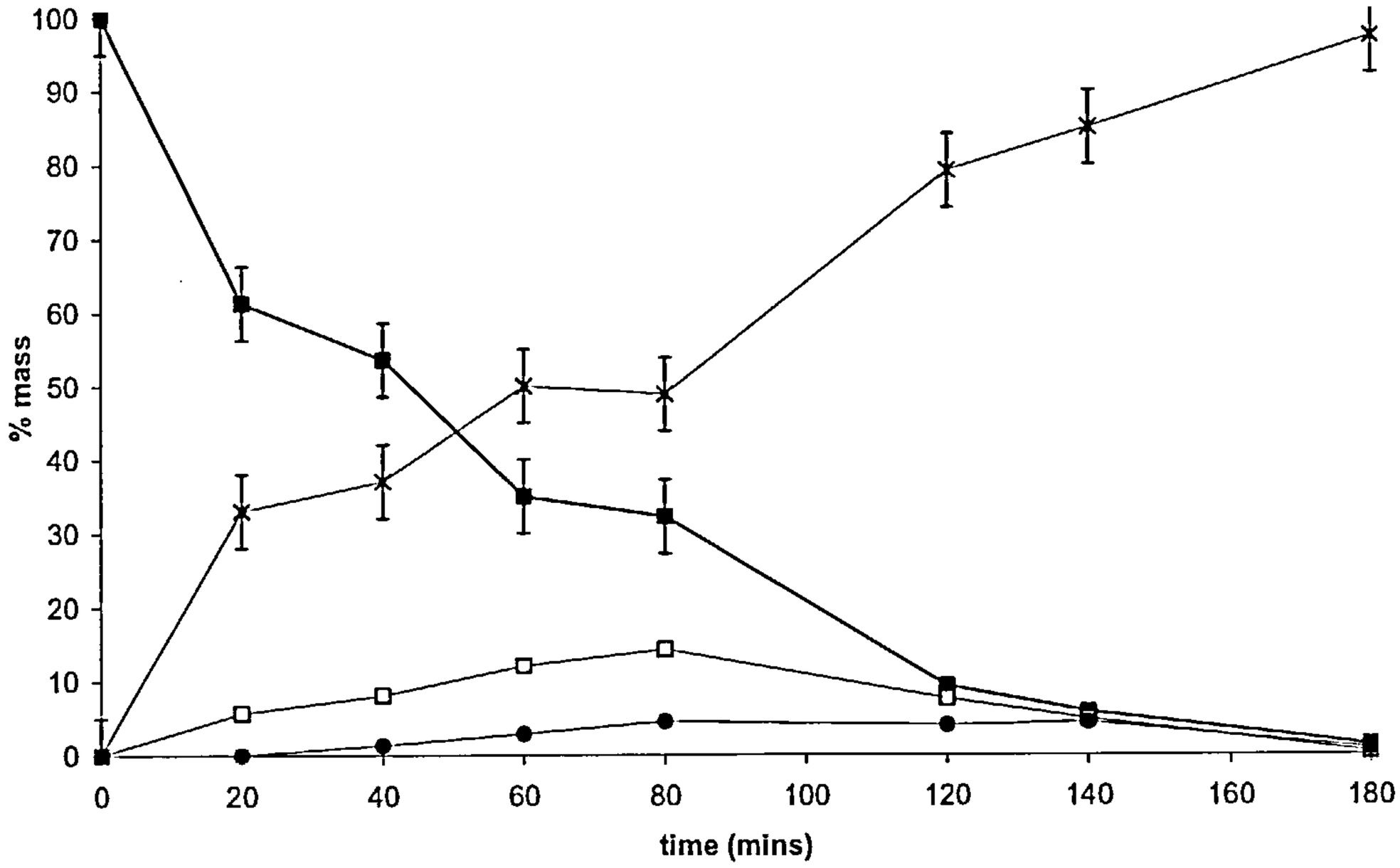

Figure 4.22: NaCaO-catalysed reaction, 60 °C, 6:1 molar ratio oil to methanol, 2 g catalyst. Triglycerides ■, diglycerides □, monoglycerides ●, biodiesel x.

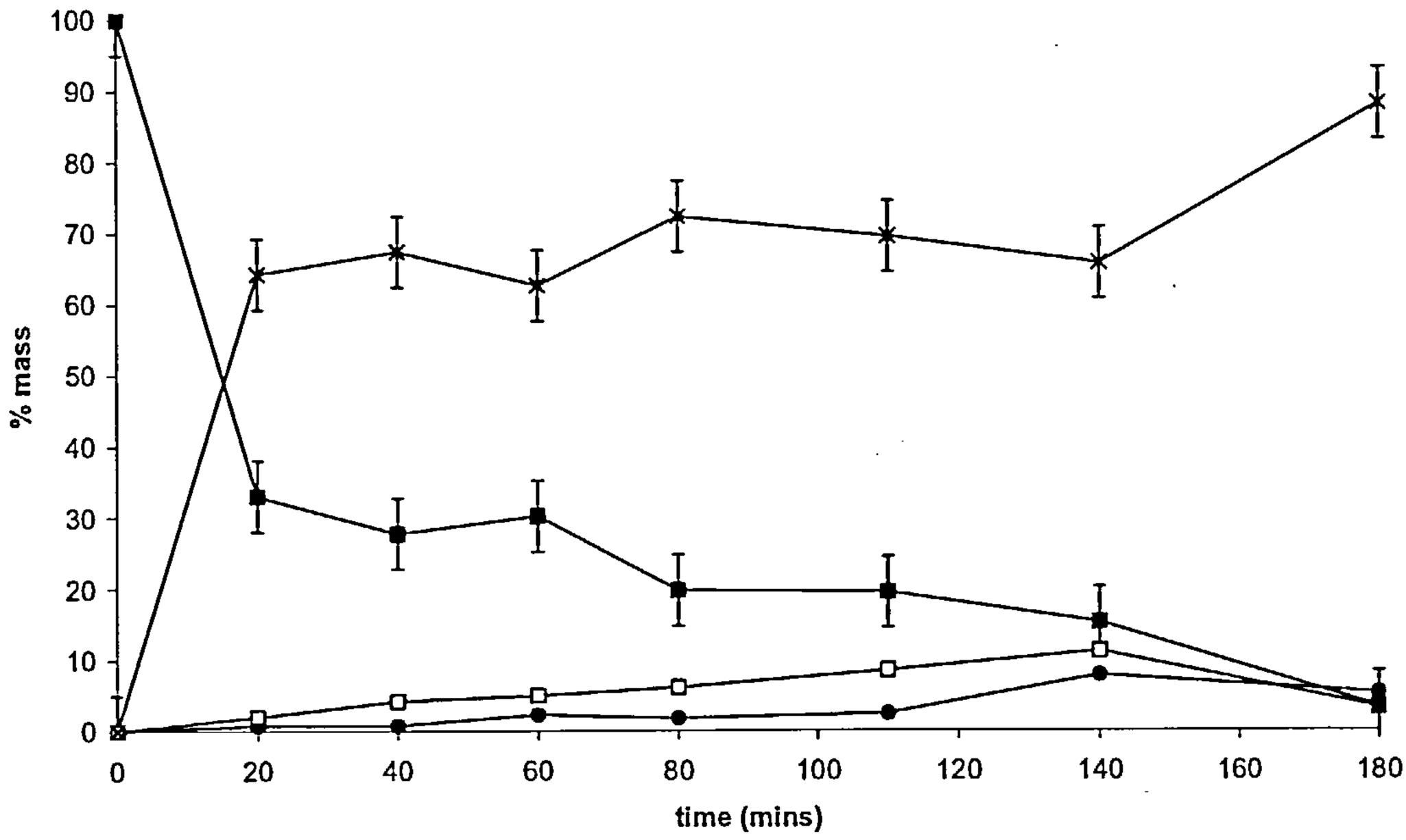

Figure 4.23: KCaO-catalysed reaction, 60 °C, 6:1 molar ratio oil to methanol, 2 g catalyst. Triglycerides ■, diglycerides □, monoglycerides ●, biodiesel x.

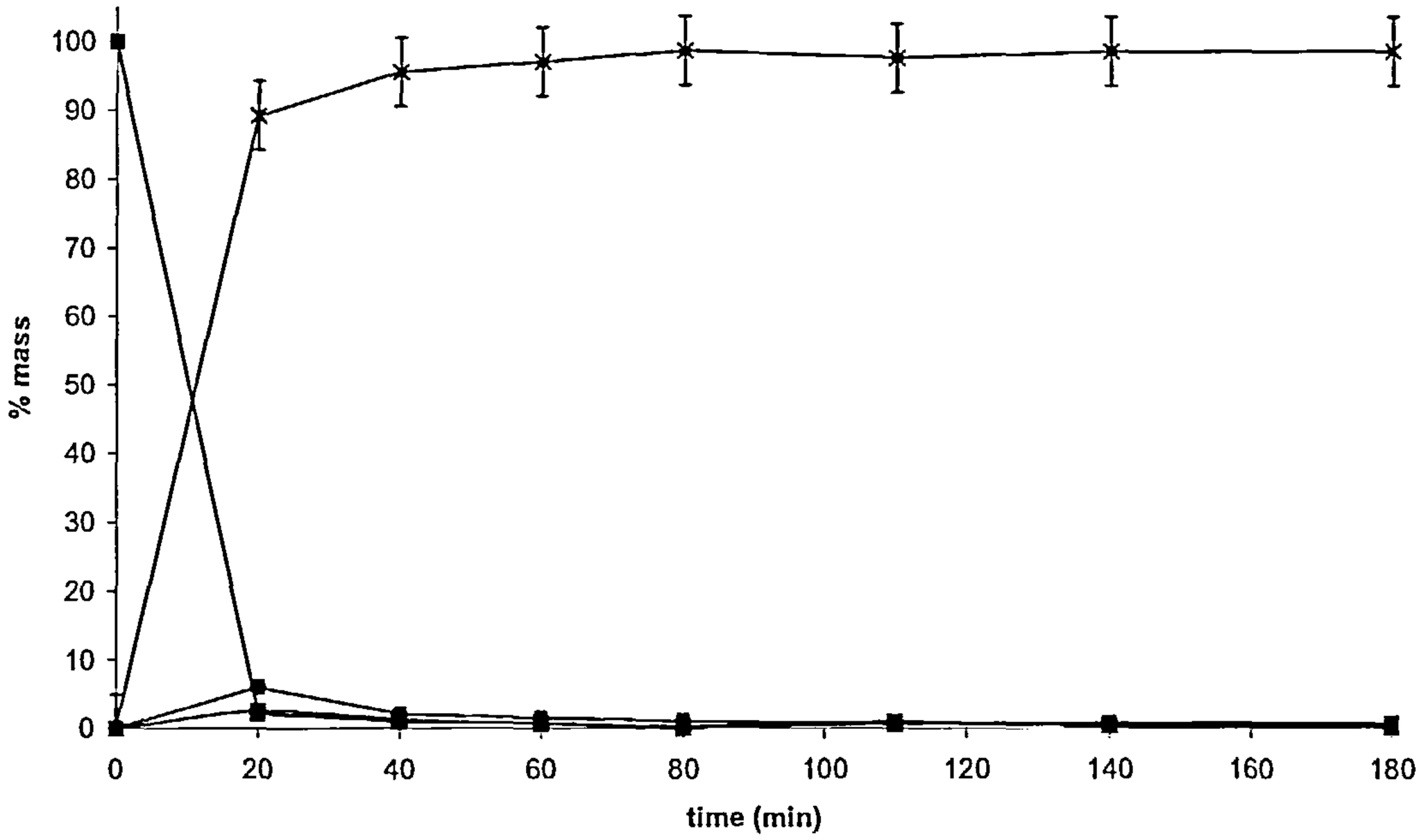

Figure 4.24: LiCaO(calcined)-catalysed reaction, 60 °C, 6:1 molar ratio oil to methanol, 2 g catalyst. Triglycerides ■, diglycerides □, monoglycerides •, biodiesel x.

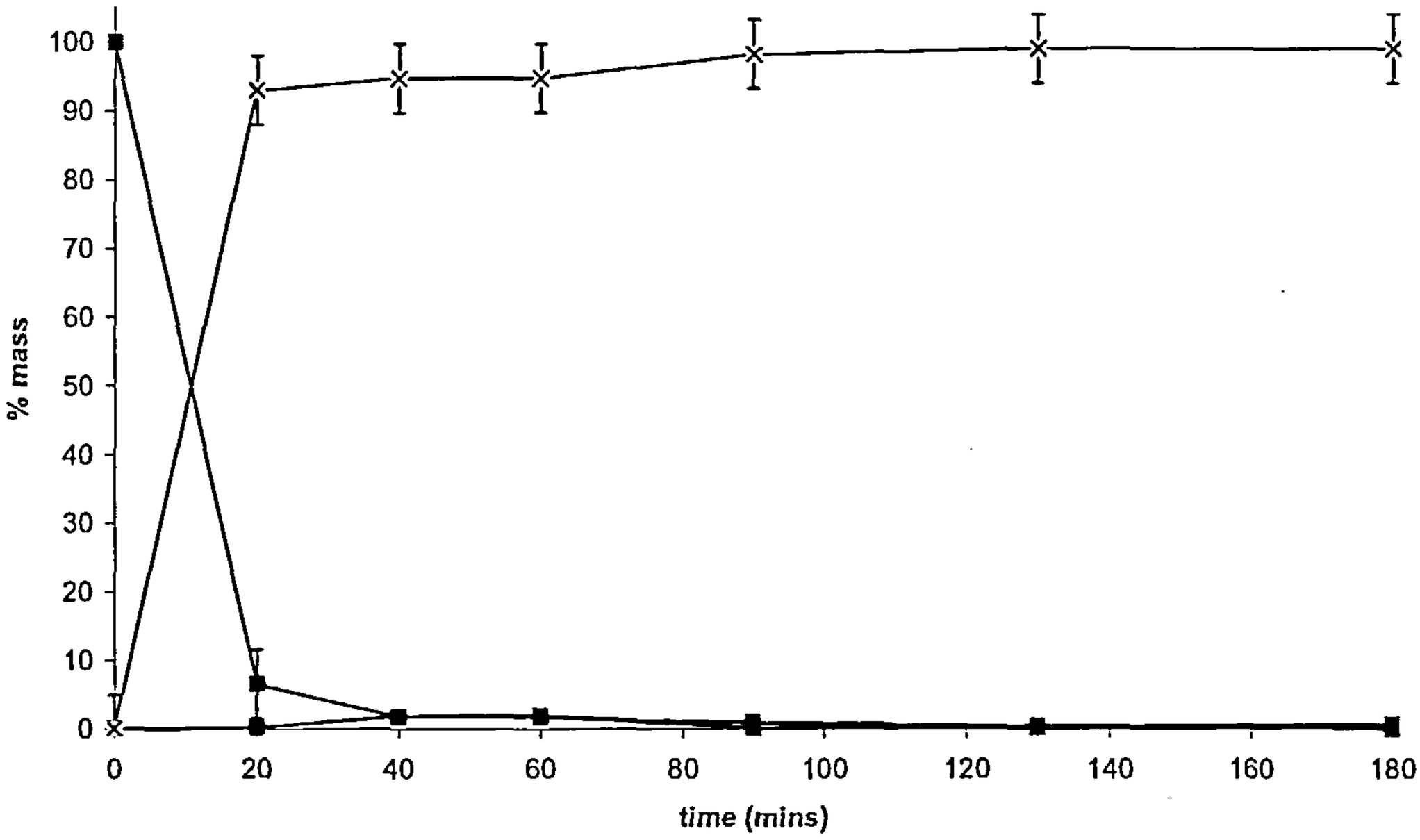

Figure 4.25: NaCaO(calcined)-catalysed reaction, 60 °C, 6:1 molar ratio oil to methanol, 2 g catalyst. Triglycerides ■, diglycerides □, monoglycerides •, biodiesel x.

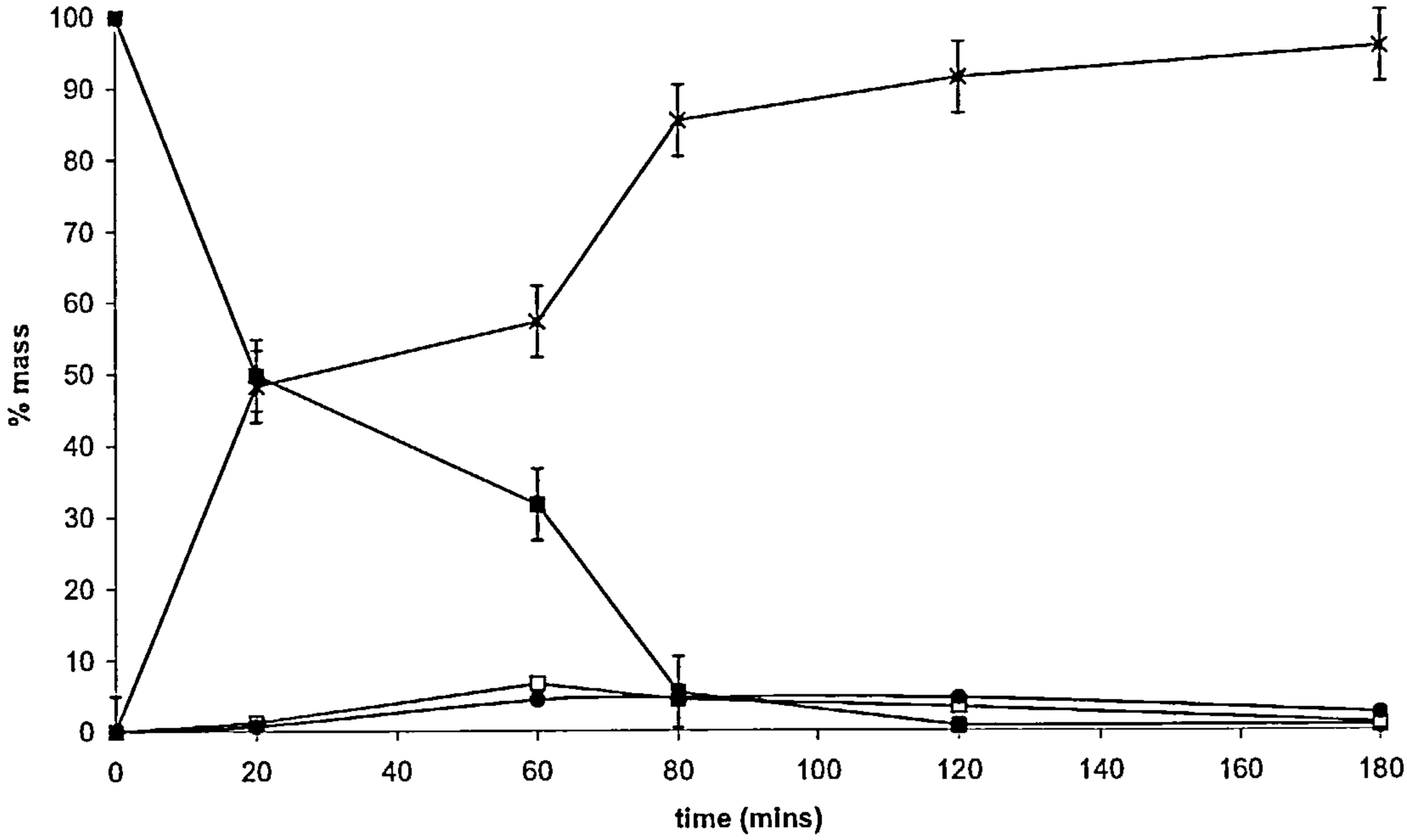

Figure 4.26: KCaO(calcined)-catalysed reaction, 60 °C, 6:1 molar ratio oil to methanol, 2 g catalyst. Triglycerides ■, diglycerides □, monoglycerides •, biodiesel x.

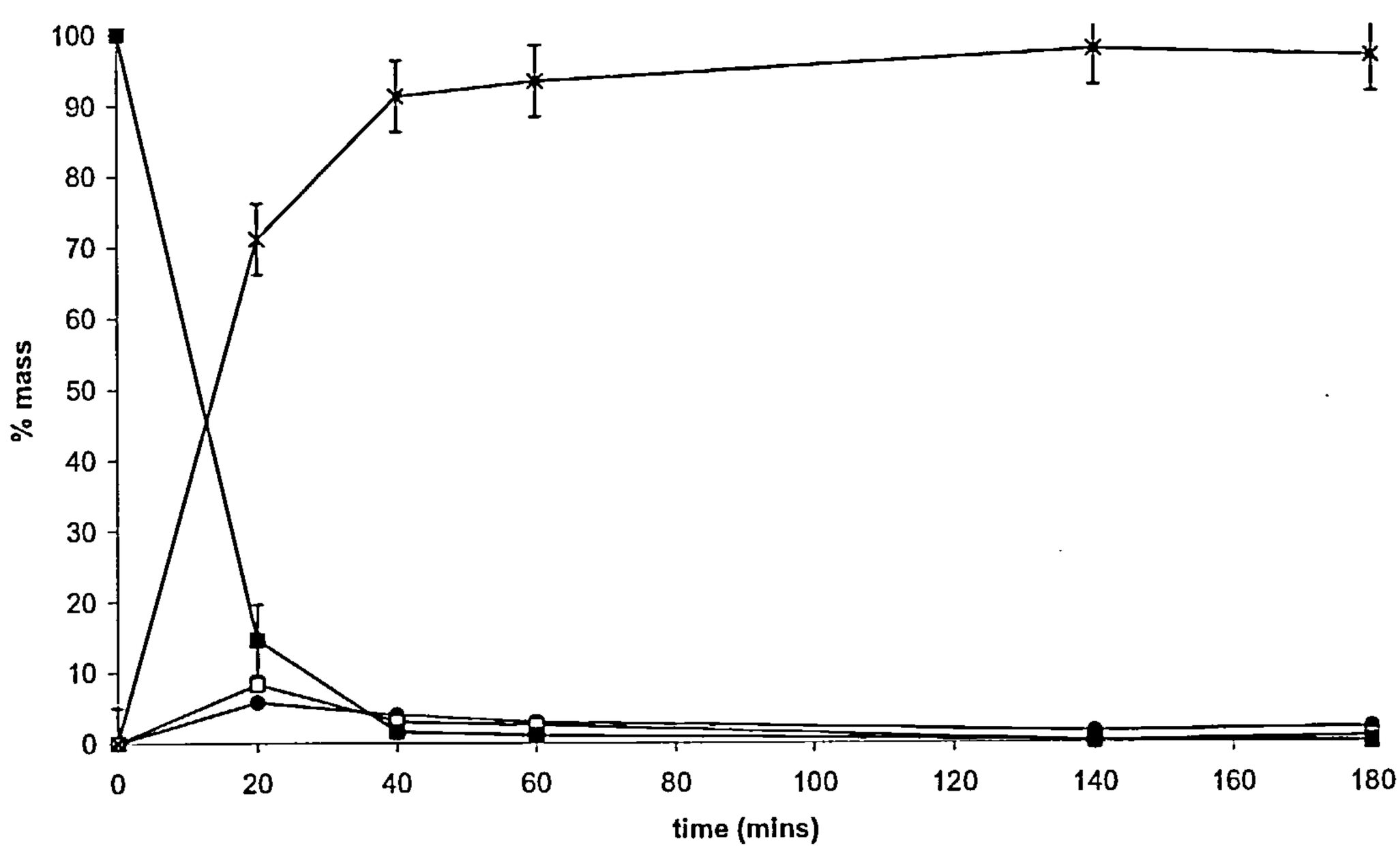

Figure 4.27: Li-MgO-(calcined)-catalysed reaction, 60 °C, 6:1 molar ratio oil to methanol, 2 g catalyst. Triglycerides ■, diglycerides □, monoglycerides •, biodiesel x.

The reaction profiles are similar to those when homogeneous catalysts such as NaOH are used, with an initial rise in partial glyceride concentrations, which then decreases as the reaction continues (Freedman *et al.*, 1986). However, the heterogeneously-catalysed reactions tend to have higher levels of partial glycerides which persist throughout the reaction. One reason for the relatively high partial glyceride levels could be that the glycerol formed coats the catalyst forming a mass transfer barrier (Bondioli, 2004; Dossat *et al.*, 1999). This means the reaction will be slower than expected at high conversions. Relatively low levels of triglycerides (less than 5%) remain after 3 hours, so these catalysts exhibit good activities compared to other catalyst in the literature.

Some comparable examples are:

- Li-CaO with a lower Li loading of 1.25 wt % , but under similar conditions required 8 hours to reach 80% biodiesel content (Meher *et al.*, 2006). The catalyst in that case was prepared by wet impregnation as opposed to dry impregnation in this study, and the oil feedstock used was karanja oil.
- A Na/NaOH/γ-Al_2O_3 catalyst required 6 hours to reach 80% biodiesel content under similar reaction conditions (Kim *et al.*, 2004).
- Nanocrystalline CaO tested at a 1:9 oil methanol ratio gave 85% conversion after 24 hours at room temperature (Reddy *et al.*, 2006)..
- CaO at a 4.5:1 molar ratio methanol to oil achieved 90% conversion after 2.5 hours at methanol reflux temperature (Gryglewicz, 1999)
- K_2CO_3 on alumina, with a 25:1 molar ratio of methanol to oil, and THF co-colvent gave >90% conversion after 1 hour at 60 °C (Ebiura *et al.*, 2002)

Of these alternative catalysts reported in the literature, only the CaO catalyst (Gryglewicz, 1999) appears to have a comparable activity to the alkali-doped metal oxide catalysts tested here. The conditions used for the reaction with K_2CO_3-alumina as catalyst are more conducive to high conversions, so cannot be directly compared. The conditions used with the alkali-doped metal oxide catalysts are realistic for industrial use, and the reaction time required not prohibitively long.

Although CaO does not have such a high base strength, it is active. The activity of CaO is thought to arise from the formation of $Ca(OMe)_2$ on the surface of the catalyst, as $Ca(OMe)_2$ is a known active catalyst. (Gryglewicz, 1999). A comparison of the triglyceride levels in the reaction with different catalyst is shown in Figure 4.28. The most active catalysts are LiCaO calcined, LiMgO calcined and NaCaO calcined. In general the calcined catalysts were more active. All of the catalysts are more active than CaO alone (figure 3.20). The Li-doped catalysts are more active than Na- or K- doped. This is the same result as in Meher *et al.* (2006) for transesterification of karanja oil using Li-CaO, Na-CaO and K-CaO catalysts.

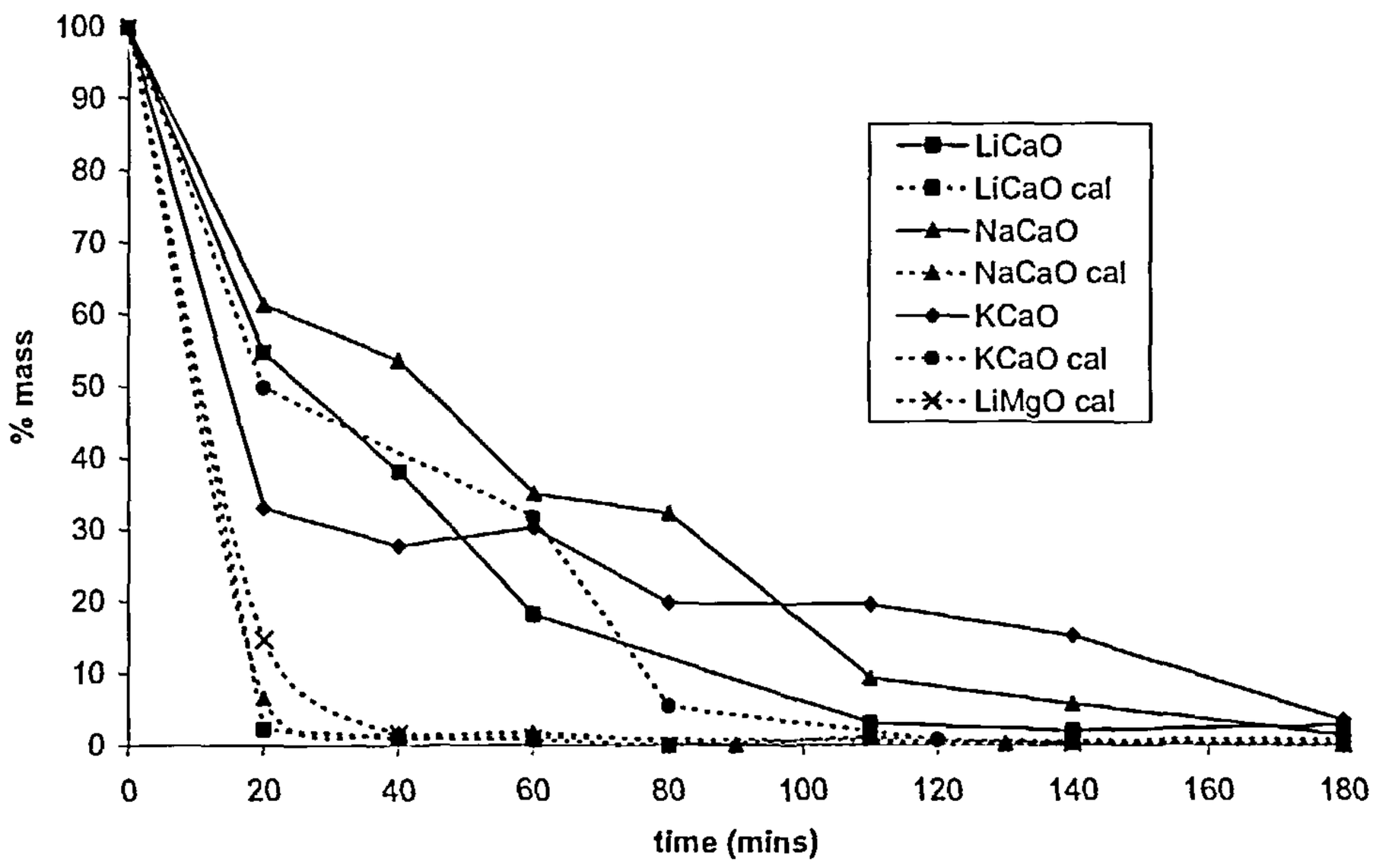

Figure 4.28: Comparison of triglyceride mass % for reaction catalysed with different catalysts at 60 °C with a 6:1 molar ratio of methanol to oil

As the alkali metals were doped at equal weight onto the support, it would be expected that lower molecular weight species with the higher number of moles and, it can be inferred, a higher number of active sites, would be the most active. Correcting the rate constants so that the active site concentration of all the catalysts is the same as that of KCaO and KCaO (calcined) i.e. dividing the rate constant for the Li doped catalysts by a factor of 5.8 (molar mass of potassium/molar mass of Li), gives the result shown in Figure 4.29. The corrected order of activity is NaCaO(calcined) >LiCaO(calcined) >KCaOand KCaO(calcined)

>LiMgO(calcined) >NaCaO >LiCaO. This figure was produced from fitted rate constants, so the incongruous profile for KCaO is as a result of the data fitting. It appears that for the non-calcined samples base strength is important, as the most active is KCaO, the alkali metal with the strongest base strength. For calcined catalysts, there is no clear trend. The activities of NaCaO (calcined) and LiCaO (calcined) are very similar.

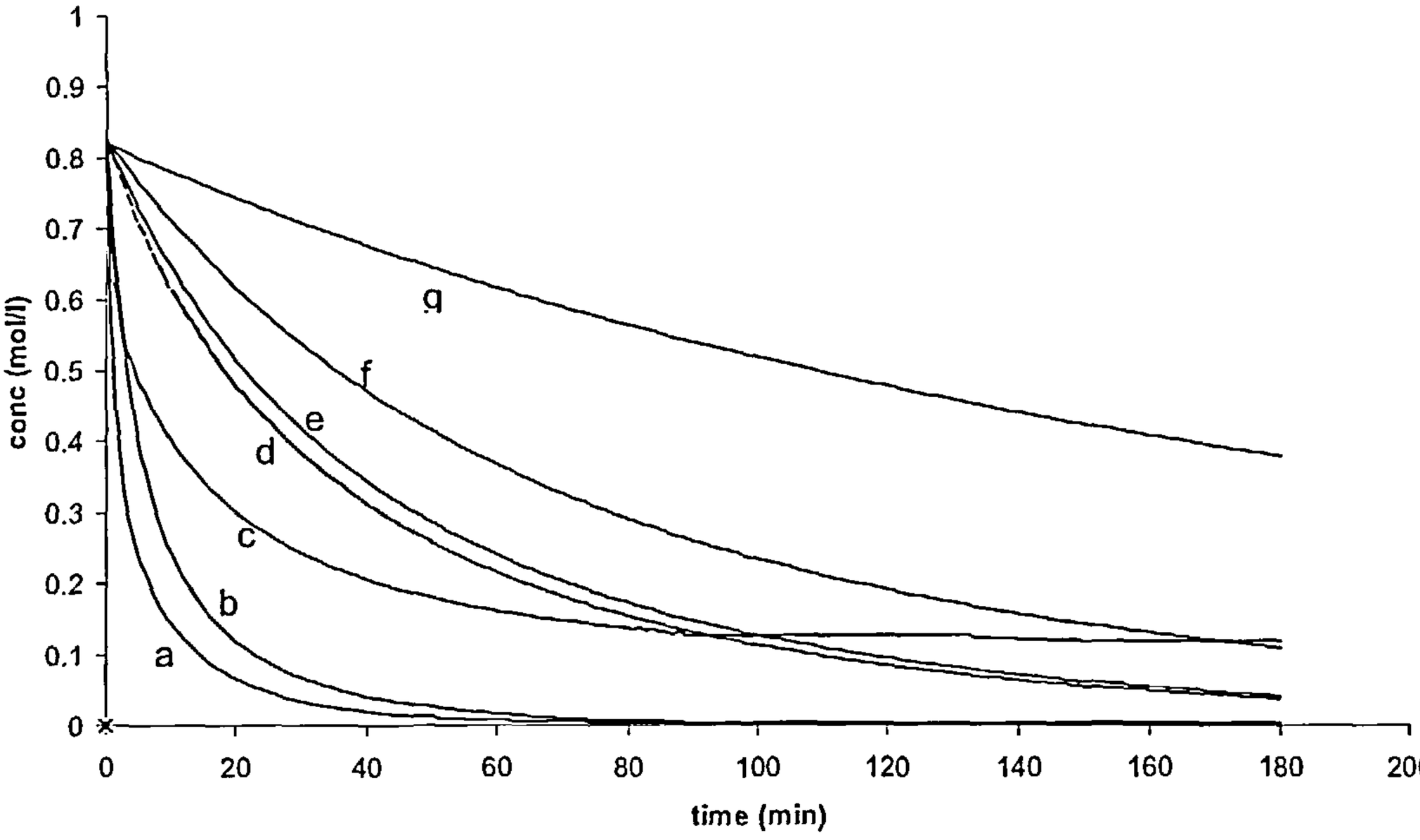

Figure 4.29: Comparison of activities of alkali-doped metal oxides at equivalent alkali metal concentration (from fitted rate constant data). a – NaCaO (calcined), b – LiCaO (calcined), c – KCaO, d –KCaO (calcined), e – LiMgO (calcined), f – NaCaO, g – LiCaO.

The glycerides remaining after 3 hours reaction are shown in Table 4.11. The triglyceride standard is met by Li-MgO (calcined), LiCaO (calcined) and NaCaO (calcined) after 3 hours. The standard for monoglycerides is met by LiCaO (calcined) and NaCaO (calcined) and only NaCaO (calcined) meets the standard for diglycerides. The reaction was not optimized at this stage and it is possible that using a 2 stage process would lead to the standard for remaining glycerides being met.

Table 4.11: remaining glycerides after 3 hours reaction at 60 °C, 6:1 molar ratio methanol to oil, compared with EU standard EN14214

Catalyst	monoglyceride (% mass)	diglyceride (% mass)	triglyceride (% mass)
Li-CaO	5.2	5.0	3.3
Li-CaO (calcined)	0.7	0.7	0.2
Na-CaO	2.9	2.5	1.6
Na-CaO (calcined)	0.7	0.2	0.1
K-CaO	5.3	3.2	3.4
K-CaO (calcined)	2.5	1.1	0.7
Li-MgO (calcined)	2.2	0.9	0.1
EU standard EN14214	0.8	0.2	0.2

4.3.4 Discussion of the origin of basicity and activity

The inactive alumina supported catalysts had a lower base strength than the other catalysts. This lower base strength is not predicted by the literature, where examples of alumina supported alkali metal salt catalysts with high base strength exist (Hattori, 1995). The alumina catalysts in this study must either have too low a loading, be from the wrong pre-cursor salt or pre-treated at the wrong temperatures. The cause will be discussed in the following sections.

Yamaguchi *et al.* (2002) studied the dispersion of nitrates or carbonates of alkali metals onto alumina to form a solid base catalyst for the isomerization of cis-butene and the effect of pre-treatment temperature, alkali-metal loading and salt precursor. The origin of the basicity is thought to be the decomposition of the metal nitrate or carbonate to form an oxygen anion. Nitrate and carbonates were both found to form active catalysts. The highest rate for the isomerization of cis-butene, a test reaction for base catalysis, was found at pre-

treatment temperatures of 500-600 °C, at the same range used in this study. When the effect of alkali metal loading was tested at loadings equivalent to the 5 wt% used in this study, the rate was extremely low, and the maximum rate occurred at around 26 wt%. This implies then that the method used to manufacture the catalysts was applicable, but the loading used was too low.

Xie *et al.* (2006a) evaluated KNO_3 on alumina for the transesterification of vegetable oil and methanol, and found the highest activity to be at 35wt % KNO_3. However, the soluble basicity was also measured and although the authors found it acceptable, it will be shown later in this study that that level of base in solution was sufficient to catalyse the reaction. Therefore, it would be expected that increasing the alkali metal level on the alumina would result in an active catalyst, but this line of investigation was not pursued because the catalyst would not be stable.

The XRD analysis shows that $LiNO_3$ on MgO decomposes to Li_2O when calcined at 600 °C (Table 4.10). The identification of a bulk phase by XRD implies that the activity is not due to a dispersed phase. This Li_2O phase is the origin of the basicity of the Li-MgO (calcined) catalyst. Na and K nitrates do not decompose to the corresponding oxide because the decomposition of the nitrates at 600 °C is only partial (shown in equation 4.1), leaving the nitrite salt and releasing oxygen (Freeman, 1956a; Freeman 1956 b). In comparison $LiNO_3$ decomposes fully to Li_2O at around 600 °C (Chang *et al.*, 2001).

$$2XNO_3 \rightarrow 2XNO_2 + O_2 \qquad [4.1]$$

The origin of basicity in all these cases is the same: the decomposition of alkali metal salts. For the catalysts studied, the alumina catalysts require a higher loading of alkali metal salt in order to be basic and thus active, and the MgO supported Na and K require a higher calcination temperature. Only $LiNO_3$ on MgO decomposes to the oxide to form a basic and active catalyst.

It is known that changing the support material changes the behaviour of the supported salt. For example KNO_3 on silica is not active (Yamaguchi *et al.*, 2002). Therefore it can be expected that changing the support material will result in a change in activity and a change in the mechanism by which the catalytic sites are formed.

Changing the support material to CaO causes a significant change in the mechanism of basicity and activity formation. CaO as a support has a higher catalytic activity, in that $LiNO_3$, $NaNO_3$ and KNO_3 salts dispersed on the surface, without heat treatment, form an active catalyst with enhanced basicity, whereas on MgO or alumina neither activity nor basicity occurs. This could be due to better matching between the size of the Ca^{2+} ion relative to the other cations allowing akali metal cations to substitute into the CaO lattice, the higher basicity of CaO or the interaction between CaO and nitrate salts. Similarly when the CaO catalysts are calcined, the use of all 3 alkali metal dopants lead to catalytic activity, implying that it is not simply a decomposition to the oxide or hydroxide, but an interaction between the alkali-metal dopant and CaO lattice.

According to Watkins *et al.*, (2004), $LiNO_3$ adsorption on CaO forms dispersed Li^+ species. These Li^+ species promote hydration of CaO defect sites to generate hydroxyl groups (Watkins *et al.*, 2004). This mechanism would allow all 3 alkali metal cations to form an active catalyst. In this study, $LiNO_3$ crystalline domains were formed as shown by XRD (Table 4.10), possibly because the loading was too high, but it can be expected that the defect sites were also formed. After calcination, the Li phase is present as Li_2CO_3 (Table 4.10), but it seems reasonable to suspect that a similar mechanism occurs where some of the alkali metal is dispersed at defect sites in the CaO and thus forms surface hydroxyl groups. Calcination of the alkali-doped CaO catalysts increases their activity. The calcined CaO catalysts exist as CaO whereas the non-calcined CaO catalysts actually exist as $CaCO_3$ (shown in Table 4.10, XRD results). The presence of CaO allows CaOMe to be formed on the catalyst surface and thus increases the catalysts' activities (Gryglewicz, 1999).

Previous studies have shown that the base strength of NaCaO and KCaO catalysts were less than that of a LiCaO catalyst. This is because the increasing size of the metal cation renders substitution into the CaO matrix and formation of an oxygen defect site increasingly

difficult (Meher *et al.*, 2006). However a slight increase in the activity for isomerization of 4,4-dimethylpent-1-ene (a reaction catalysed by a strongly basic catalyst) was observed from Li-CaO to Na-CaO to K-CaO (Matsuhashi *et al.*, 2000). The basicity of group 1 metals increases down the group but the metal ions become too big to substitute easily for Ca ions. For transesterification, NaCaO (calcined) is the most active, which suggests there is a trade-off between base strength and ion size, to form the most active catalyst.

4.3.5 Tests of leaching and reuse

The results of the repeated use of catalysts in the small scale reactors (Table 4.12) and larger scale batch reactor (Figure 4.30) are shown below.

Table 4.12: Reuse of catalysts – comparison of triglyceride levels (mass %) after 1 cycle and 5 cycles of reaction in small scale apparatus 0.1 g catalyst to 1.6 ml oil.

Catalyst	1st cycle	5th cycle
Li-MgO (calcined)	1.4 %	1.9 %
Li-CaO	< 0.1 %	< 0.1 %
Li-CaO (calcined)	0.3 %	0.8 %
Na-CaO	1.4 %	0.2 %
Na-CaO (calcined)	< 0.1 %	0.5 %
K-CaO	< 0.1 %	0.3 %
K-CaO (calcined)	< 0.1 %	< 0.1 %

From the reuse experiments in the small scale apparatus it appears that the catalysts can be reused satisfactorily. However when Li-CaO (calcined) was tested six times in the standard batch reactor (2 g catalyst to 165 ml oil) the conversion decreases slowly after 1 cycle, then rapidly after the 5^{th} cycle. Although some of this loss in activity can be attributed to a small degree of loss of catalyst material in recycling the catalyst, most of the loss in activity is either due to leaching or to the blocking of active sites by the coating of the catalyst particles in glycerol. This decrease in conversion with repeated use was also observed for

Li-MgO (calcined) and Li-CaO catalysts. As the decline in activity with repeated use is only apparent in the larger scale apparatus, it is likely the loss in activity is due to leaching. This is because the small-scale apparatus has a higher ratio of catalyst to oil, so proportionally more active species remain after 5 cycles of reaction, thus the activity is preserved. If the loss of activity was due to glycerol coating, it would be expected that the larger scale apparatus, with its higher degree of agitation would be able to 'wash off' the glycerol more effectively and therefore the activity would be preserved in the larger-scale reactor rather than the small scale apparatus.

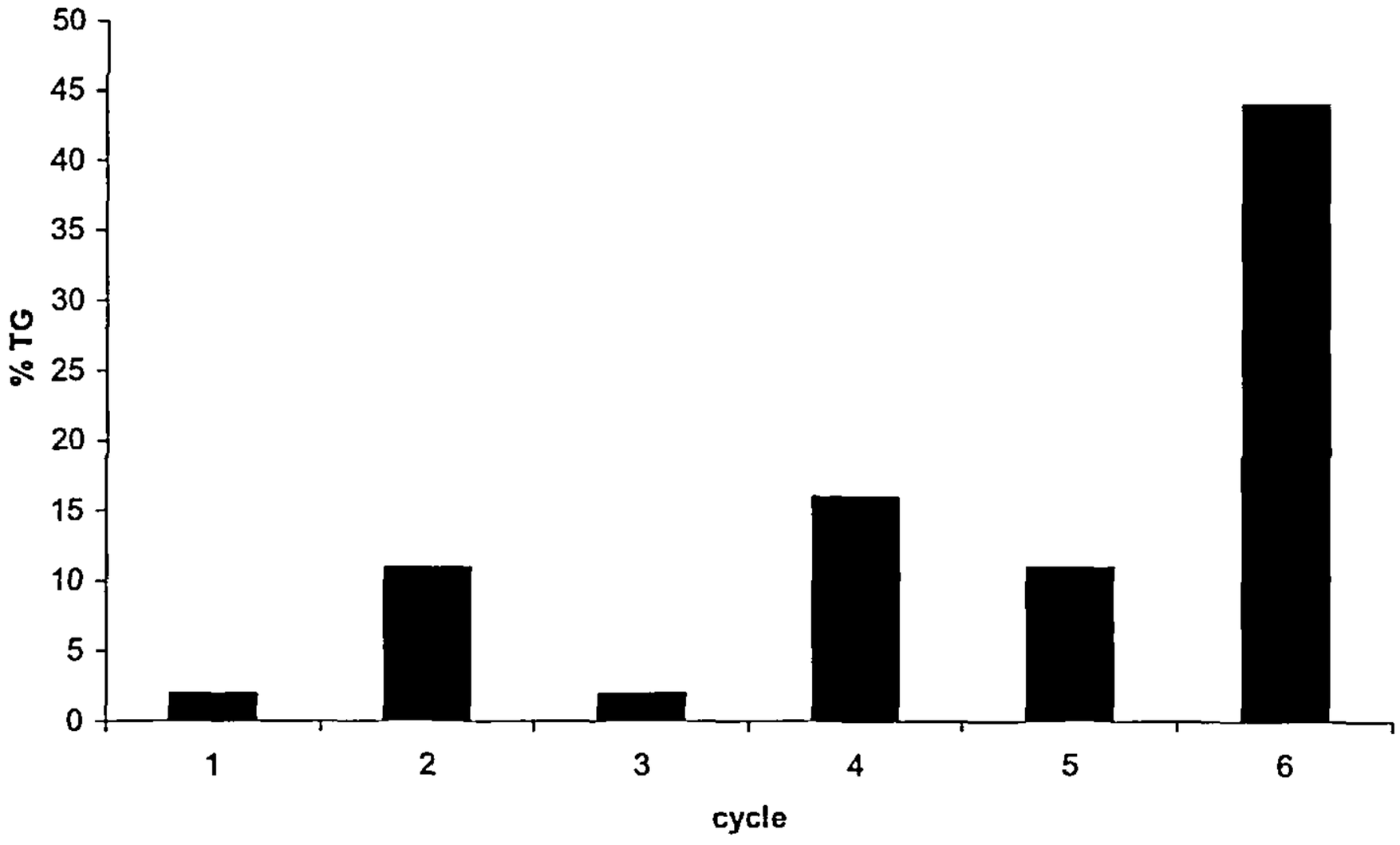

Figure 4.30: triglyceride remaining after 1hour reaction with LiCaO (calcined) as catalyst, 60 °C, 6:1 molar ratio methanol to oil

Since there is a reduction in conversion with reuse, there may be detectable metal in the biodiesel formed. If there is no metal leaching into the biodiesel then the decrease in activity would be due to a surface coating effect or deactivation (without leaching) of active sites. The metal levels in the reaction mixture were quantified by AAS and flame photometry by comparison of the detector response with the response seen for known concentration of each metal. Experimental details are given in section 3.3.5. Table 4.13 shows the alkali metal levels in the reaction mixture, and although the levels may seem low, they are significant. The 98 ppm of Li present in the reaction mixture for LiMgO, for

example, corresponds to 20% of the initial mass of Li added. The levels of Mg and Ca in the reaction mixture were also analysed. The level of Mg was approximately 30 ppm, the levels of Ca were much higher at 200-600 ppm. The calcined catalysts had higher Ca concentrations than the uncalcined catalysts. The concentration of Ca leached into biodiesel was approximately the same as the Ca leached from the catalyst into methanol at 60 °C. This means that we can assume that leaching into methanol is reasonably representative of leaching into the biodiesel reaction mixture. The solubility of CaO in methanol has been quoted as 0.035 % and MgO in methanol 0.13 % (Gryglewicz, 1999). This result would then be expected to be followed by a higher level of Mg in the leachate than Ca, but this was not the case. 600 ppm of Ca in methanol is roughly equivalent to a solubility of 0.08 % which is higher than the value quoted. The higher level of Ca in the leachate from the calcined catalysts could be due to the formation of $Ca(OMe)_2$ from the reaction between CaO and methanol. $Ca(OMe)_2$ is more souble in methanol than CaO and $CaCO_3$ (Gryglewicz, 2000).

Table 4.13: Residual alkali metal levels in reaction mixture as measured by flame photometry and atomic absorption spectrometry.

Catalyst	Tested metal	Concentration (ppm)
Li-MgO (calcined)	Li	98
Li-CaO	Li	22
Li-CaO (calcined)	Li	18
Na-CaO	Na	78
Na-CaO (calcined)	Na	52
K-CaO	K	36
K-CaO (calcined)	K	32

To determine whether the detected levels of Li in the reaction mixture were catalytic, 2 homogeneously catalysed reactions were run (shown in Figure 4.31). Levels of LiOH at a concentration equal to 10ppm Li were catalytically active, and levels of LiOH corresponding to 100ppm Li reached 50 % conversion to biodiesel in 30 minutes. 100ppm Li is equivalent to the Li level measured in the reaction mixture when the reaction was

catalysed by LiMgO (calcined). The 'standard' 0.5 % NaOH by weight of oil homogeneous catalysis for biodiesel production (Vicente *et al.*, 1998) corresponds to a Li level of 1000ppm. The concentration of dissolved LiOH is not responsible for all of the catalytic activity of Li doped CaO or MgO, but forms at least part of it.

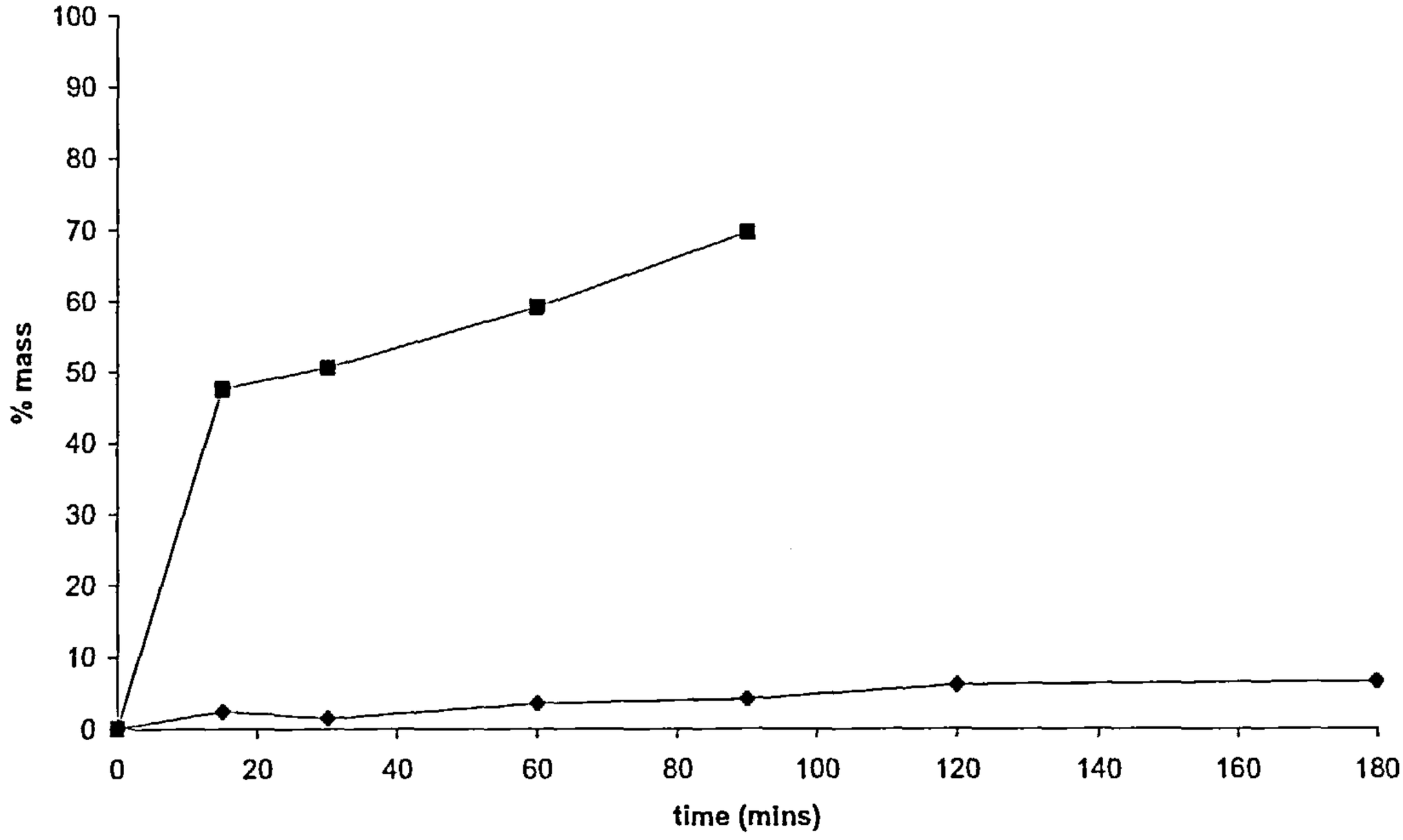

Figure 4.31: Biodiesel formed with LiOH homogeneous catalysis at 60 °C, 6:1 molar ratio methanol to oil. ■ 100 ppm Li, ♦ 10 ppm Li

Table 4.14 shows the conversion to biodiesel obtained by testing the catalyst leachate. In all cases some biodiesel was formed, showing that at least some of the activity is homogeneous.

Table 4.14: %mass biodiesel formed by reaction of oil with the catalyst leachate. Reaction conditions were 3 hours at 60 °C with a 6:1 molar ratio methanol to oil

Catalyst	% mass biodiesel formed
Li-MgO cal	26
Li-CaO	44
Li-CaO cal	54
Na-CaO	15
Na-CaO cal	29

K-CaO	3
K-CaO cal	14

As the activity of the alkali-doped metal oxide catalyst appears to result partly from the homogeneous metal ions in solution, the catalyst should then dissolve in methanol to make a basic solution, the concentration of which can then be measured. In Table 4.15 the soluble basicity as measured by titration of an acid solution against the catalyst filtrate is presented for Li catalysts. The double end-point titration was used to determine the concentration of dissolved carbonates in addition to strong bases.

Table 4.15 Table of soluble basicity

Catalyst	cycle 1 strong base (mmol/g)	cycle 1 carbonates (mmol/g)	cycle 2 strong base (mmol/g)	cycle 2 carbonates (mmol/g)	cycle 3 strong base (mmol/g)	cycle 3 carbonates (mmol/g)
LiCaO	0.47	0.07	0.07	0.01	0.02	0.05
LiCaO cal	1.0	0.37	0.5	0.18	0.36	0.08
LiMgO	1.0	0.12	0.05	0.10	0	0.05

There is significant soluble basicity present, 1 mmol/g catalyst corresponds to 0.5 g NaOH per litre of biodiesel at the tested conditions, around 10% of the recommended 0.5 wt % of oil level used industrially to produce biodiesel (Vicente *et al.*, 2002). The soluble basicity drops with each cycle of contact with methanol, in the case of LiMgO there is no soluble basicity remaining on the 3rd use. This reduction in basicity mirrors the reduction in activity and adds more evidence to the hypothesis that the activity is due to soluble basicity. When the LiMgO catalyst which had been contacted with methanol until no soluble base remained was tested as a catalyst, no biodiesel was formed, thus no heterogeneous activity remained.

The soluble basicity (in water) of potassium loaded onto alumina was found to be in the region 0.4 -0.6 mmol/g when the catalyst was calcined at 773 K for potassium levels in the range 15-45% KNO_3 on alumina, and increased with calcination temperature reaching 0.9 mmol/g at 873 K and 1.2 mmol/g at 923 K for 35% KNO_3 (Xie *et al.*, 2006a). The levels found in the potassium on alumina study were assumed by the authors to be small enough for the catalyst to be considered stable. However, under the reaction conditions used by Xie *et al.* (6.5 %wt catalyst) a 1 mmol/g soluble basicity dissolved from the catalyst is equivalent to 2.5 g NaOH/kg oil, which is 50% of the recommended 0.5% NaOH by weight of oil used industrially to produce biodiesel (Vicente *et al.*,1998). 1 mmol/g catalyst is also equivalent to 70 ppm of Li under the reaction conditions used in this study (1.3 %wt catalyst) which has been shown the be catalytic (Figure 4.31).

The concentration of carbonates is lower than the concentration of strong base, and the decay is not as rapid. XRD analysis showed that carbonates were present on the surface of the catalysts. To determine whether the surface carbonates were catalytic, 2 g of solid lithium carbonate was screened for activity. It was not found to be active, producing only trace amounts of biodiesel. It appears that carbonates do not cause the activity of these catalysts.

Table 4.17 compares the triglyceride content after 20 minutes to the amount of soluble basicity under simulated reaction conditions. The higher the soluble basicity, in general, the lower the level of triglycerides. The soluble basicity of LiMgO appears lower than that expected from its activity, probably because no soluble basicity results from the support, unlike the CaO-supported catalysts.

Table 4.16: comparison of triglyceride content after 20 minutes to amount of soluble basicity

catalyst	soluble basicity (mmol from 2 g catalyst in 40 ml methanol)	TG content at 20 minutes (% mass)
LiCaO	0.47	55
LiCao cal	1.7	3
LiMgO	1	15
NaCaO	0.63	60

NaCaO cal	3	7
KCaO	1.58	32
KCaO cal	1.58	50

4.3.6 Catalyst characterization after use

XRD analyses were performed on catalysts after they had been contacted with methanol 5 times. The phases detected before and after contact with methanol are presented in Table 4.17. The diffraction patterns and peak assignments are shown in appendix 1.

Table 4.17 : phases detected by XRD before and after contact with methanol

Catalyst	Li phases present	Mg phases present	Ca phases present
LiCaO	$LiNO_3.(H_2O)_3$		$Ca(OH)_2$, $CaCO_3$ (calcite)
LiCaO after	-		$Ca(OH)_2$, $CaCO_3$ (calcite and vaterite)
LiCaO (calcined)	Li_2CO_3		CaO, $Ca(OH)_2$
LiCaO (calcined) after	Li_2CO_3		$Ca(OH)_2$, $CaCO_3$ (calcite and vaterite)
LiMgO (calcined)	LiOH, $LiOH.H_2O$, Li_2CO_3	MgO	
LiMgO (calcined) after	Li_2CO_3	MgO	

The Li-MgO (calcined) catalyst clearly loses its basic sites due to the loss of LiOH and $LiOH.H_2O$ phases. The Li-CaO catalyst also loses all its detectable Li phases after contact with methanol. The Li-CaO (calcined) does not completely lose the Li phase, but $CaCO_3$ is

formed after the reaction. The formation of the $CaCO_3$ correlates with the decrease in activity.

4.3.7 Summary of heterogeneous versus homogeneous

The alkali-doped metal catalysts cannot be reused without a decrease in activity. Additionally, metal was found to leach from the catalyst into the reaction mixture, and this leached material was found to be active. The levels of base species were measured by titration and found to be approximately 10% of the typical amount of NaOH added as a homogeneous catalyst. The catalyst with the highest soluble basicity, NaCaO (calcined) was the most active. From this, it can be concluded that the alkali-doped metal oxide catalyst act as a source of alkali metal ions which then act as a homogeneous catalyst. Although it is unlikely that all of the catalysis is homogeneous in origin, it appears that a substantial amount is and therefore this class of catalyst will not be suitable for a heterogeneously catalysed process, unless the labile species can be stabilized.

4.3.8 Changing calcination temperature

The temperature at which the catalysts were calcined was varied to determine if there were any changes to the catalytic activity or the stability.

As long as the calcination temperature was greater than 600 °C, there was no significant change in the activity of the Li-MgO catalyst. Increasing the calcination temperature did not decrease the amount of Li leached as shown in table 4.19. As the Li still leaches, this implies that the catalysis will still be mainly homogeneous so no stabilization is achieved on increasing the calcination temperature above 600 °C.

Table 4.18: Li levels in reaction mixture measured by AAS, when LiMgO (calcined) catalyst calcined at different temperatures

Calcination temperature (°C)	Li level in reaction mixture (ppm)

600	90
700	75
800	80
900	80

4.3.9 KF alumina

KF on alumina is a commercially available solid base catalyst that has been applied to a number of organic reactions, including Michael additions and Knoevenagel condensations. It is thought that the basicity arises from either F^- ions dispersed on the surface or the formation of KOH on the alumina surface (Hattori, 1995).

KF on alumina was found to have a base strength of $pK_{BH+}>11$, and in the initial screening test, was found to be active. Reaction in the batch reactor resulted in 95% conversion of the triglycerides after 20 minutes, an activity comparable to that of calcined LiMgO. However, KF on alumina also exhibited a soluble basicity of 1.2 mmol/g catalyst (again this is comparable to LiMgO), dropping to zero after 3 cycles. Thus KF on alumina although active, is not stable to leaching, so is not practical.

4.3.10 Li-MgO with alternative preparation method

Li-doped MgO was manufactured according to the method of Diez *et al.* (2006). This catalyst had been demonstrated to be active for the liquid phase aldol condensation without lithium leaching into the water-containing liquid. Thus, it was thought this catalyst could be more stable. 0.5 wt% Li in the form of aqueous LiOH was added to MgO by incipient wetness impregnation, then dried. The sample was then calcined at 500 °C for 18 hours. The activity of this catalyst was less than that of the 5% LiMgO catalyst, with 240 minutes of reaction required to reach a triglyceride level of 15 wt %. The soluble basicity was measured at 0.14 mmol/g, less than that of LiCaO. However, as the initial loading of Li was lower, the loss of strong base, if assumed to result from Li only, corresponded to 40% of

the Li initially present. The strong basicity dropped to zero after 3 cycles. Again, it is clear that this catalyst is not stable and therefore not practical. It is unclear why this catalyst was found to be stable by Diez *et al.*. The only change in the preparation method was that Diez *et al.* used continuously flowing nitrogen for the calcination, whereas in this study the catalyst was calcined in air. Calcination in air may lead to carbonates, but carbonates are less soluble than hydroxides so this does not explain why leaching was detected.

4.3.11 Mg-Zr mixed oxide

The basicity of Mg-Zr mixed oxide was found to be $8.2<pK_{BH+}<10.1$, so it has a low base strength. As expected from this low base strength, there was only a trace of biodiesel formed after 3 hours reaction at 60 °C. This catalyst could be evaluated for catalytic activity at higher temperatures.

4.4 Functionalized silica

To heterogenize a homogeneous catalyst, the 'ultimate' immobilization method is to covalently attach the homogeneous catalyst to an insoluble support (Corma and Garcia, 2006). Hence, triazobicyclodecene and a tertiary amine group were covalently attached to silica supports and the resulting materials evaluated for activity and stability in the transesterification reaction.

4.4.1 Characterization

All of the functionalized silica catalysts have high surface areas, as shown in Table 4.19. The measured pore size of the functionalized Davisil catalysts has significantly decreased from their initial values: from 60 Å to 33 Å, and from 150 Å to 66 Å. This same effect was observed by Subba Rao *et al.* (1997). The narrowing of the pores is due to the functionalization of the support with bulky groups. The HMS type silicas have similar pore sizes to their expected pore size value (22 Å, Mbaraka *et al.*, 2003).

Table 4.19: surface area and mean pore diameter of functionalized silica catalysts, calculated from nitrogen desorption using BJH method. Adsorption desorption isotherms shown in appendix 2.

Catalyst	Surface area	Mean pore diameter
HMS-TBD	162 m^2/g	19 Å
Davisil (60Å pore size)-TBD	292 m^2/g	33 Å
Davisil (150Å pore size)-TBD	200 m^2/g	66 Å
HMS-TA	326 m^2/g	20 Å

Figure 4.32 shows IR spectra of the TBD-functionalized catalysts. All catalysts show similar spectra with peaks at around 3500 cm^{-1}, 3000 cm^{-1}, 1600 cm^{-1} and a large peak at 1100 cm^{-1}. The peak at 3500 cm^{-1} is a combined function of the N-H and O-H stretch

(Fessenden and Fessenden, 1982), at 3000 cm^{-1} the C-H stretch (Fessenden and Fessenden, 1982), at 1600 cm^{-1} the C=N stretch and N-H bend (Fessenden and Fessenden, 1982), and at 1100 cm^{-1} the C-N and C-C stretches (Fessenden and Fessenden, 1982). Figure 4.33 shows the IR spectrum of the tertiary amine functionalized silica. There is a smaller peak at 1600 cm^{-1} as it represents only the N-H bend as there is no C=N functionality on the amine.

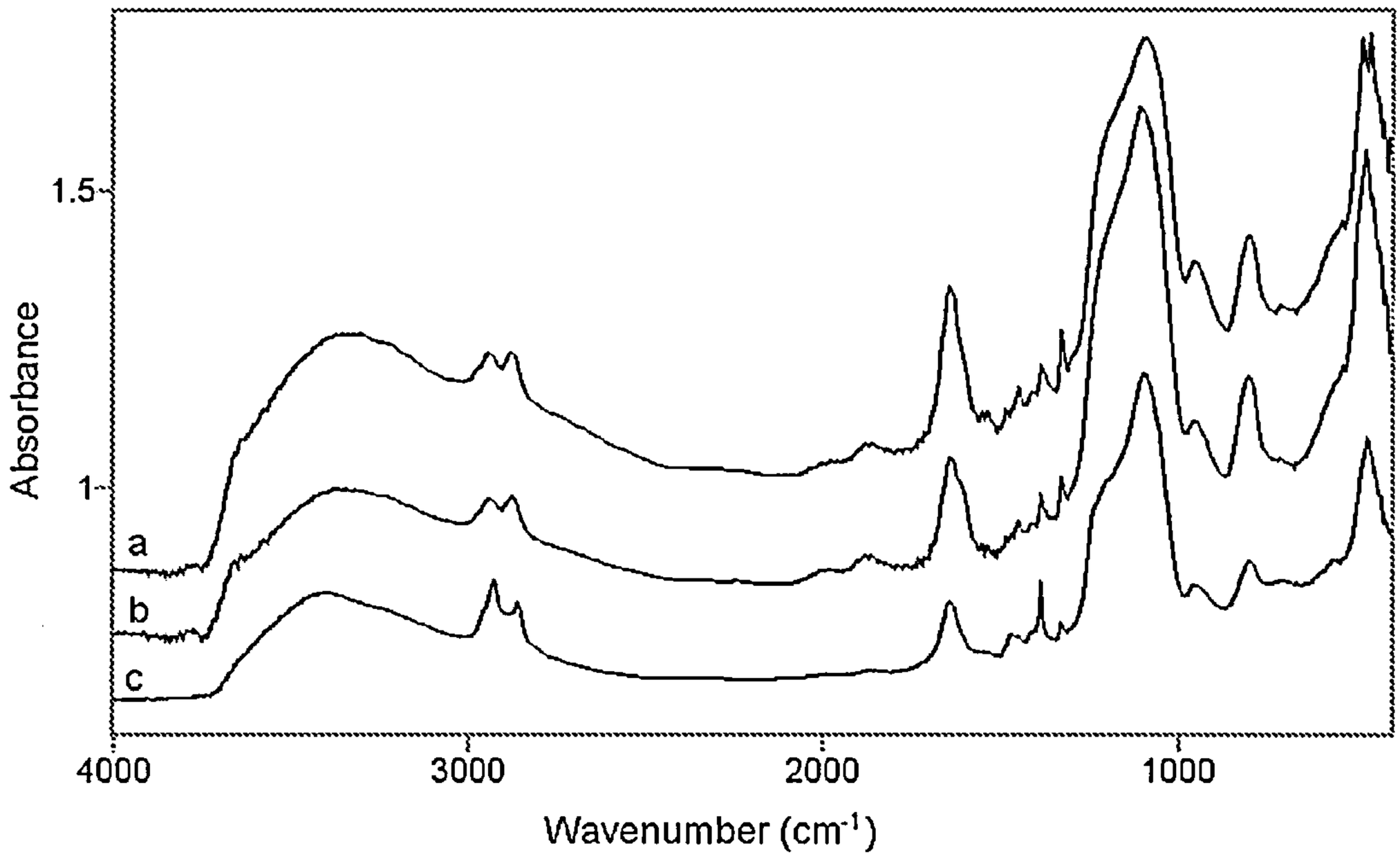

Figure 4.32: IR spectra of functionalized silica catalysts, a - HMS-TBD, b - Davisil (60Å pore size)- TBD, c - Davisil (150Å pore size)- TBD

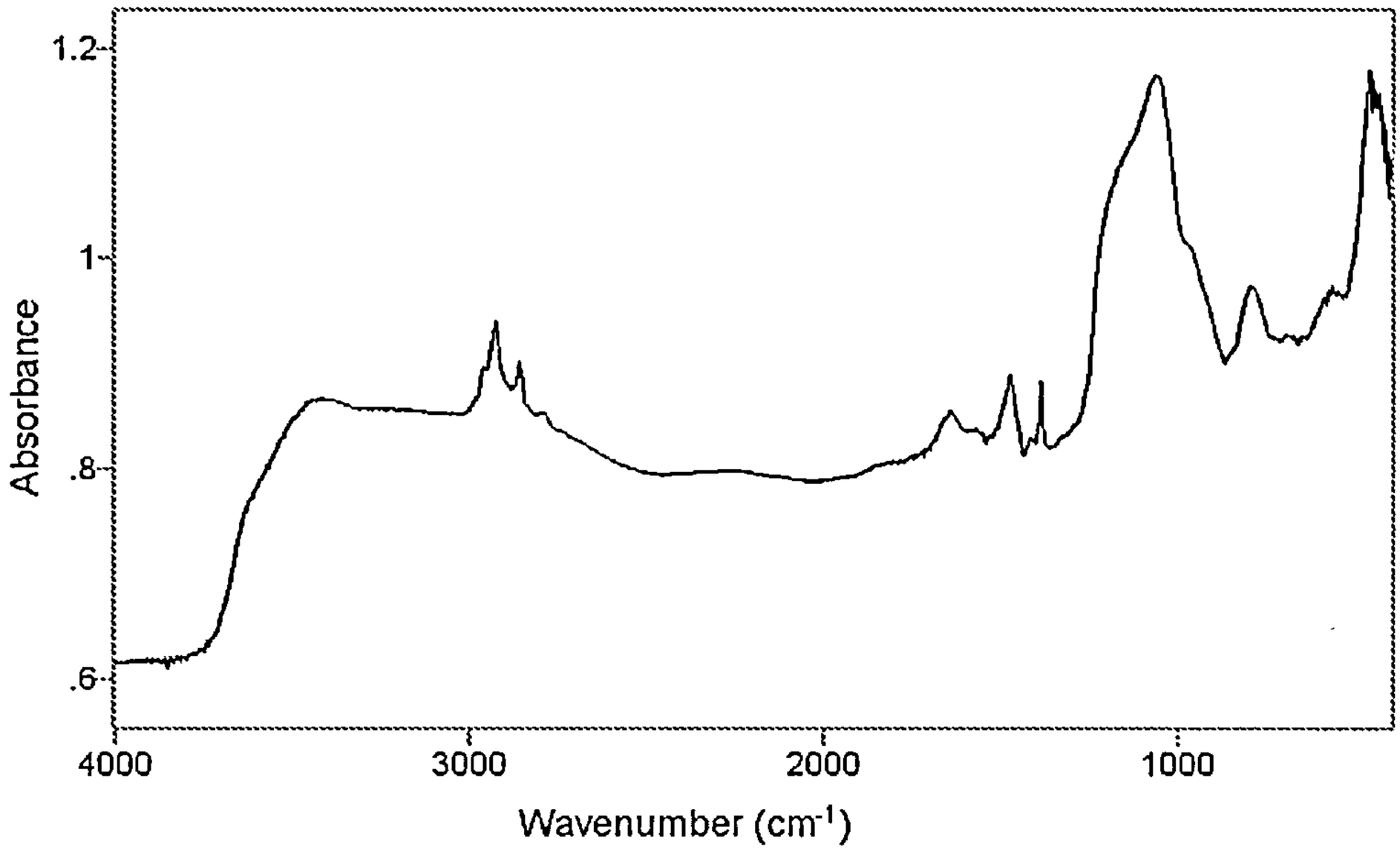

Figure 4.33: IR spectra of HMS-TA

The N content and functional group loading of the silica-supported catalysts is shown in table 4.21. The functional group loading of these catalysts is similar to that used in other studies. The functional group loading of silica supported TBD catalysts found in the literature is in the range 0.35 mmol/g – 0.58 mmol/g (Subba Rao, 1997; Sercheli 1999; Kantam and Sreekanth, 2001). The functional group loading of the silica-supported tertiary amine is higher than the silica-supported TBD because it was produced by a one-pot method, which results in a catalyst with higher functional group loading but not all of the functional groups are on the surface of the catalyst (MacQuarrie, 1999, Mdoe *et al.*,1998).

Table 4.20 – N content of functionalized silica catalysts

Catalyst	N content (%)	Functional group loading by CHN analysis (mmol/g)
HMS-TBD	2.9 %	0.7
Davisil (60Å pore size)- TBD	2.4 %	0.6
Davisil (150Å pore size)-TBD	1.8%	0.4
HMS-TA	3.5%	2.5

4.4.2 Batch reaction profiles

The reaction profiles when the silica-supported TBD catalysts were tested in the batch reactor are shown in figure 4.34, Figure 4.35 and Figure 4.36. HMS-TBD is the most active, followed by Davisil (60 Å pore size)-TBD then Davisil (150 Å pore size)-TBD. There are two competing effects on activity: functional group loading and pore size. Increasing the pore size should increase the activity of the catalyst, because of increased access of the bulky triglyceride molecule to the active sites (Linssen *et al.*, 2003; Corma and Garcia, 2006)). The increase in activity with pore size is seen in other studies on esterification or transesterification of large molecules (Mbaraka *et al.*, 2003, Suppes *et al.*, 2004) However, this is not the effect seen here, as the smallest pore size catalyst has the highest activity. Instead it is likely that the higher functional group loading of HMS-TBD is responsible for its increased activity. Another explanation could be that the increased

particle surface area (because the particle diameter is smaller) of HMS-TBD is responsible for its increased activity, as we can expect that (and it is shown in section 4.7.5) diffusion of triglycerides into the pores is slow.

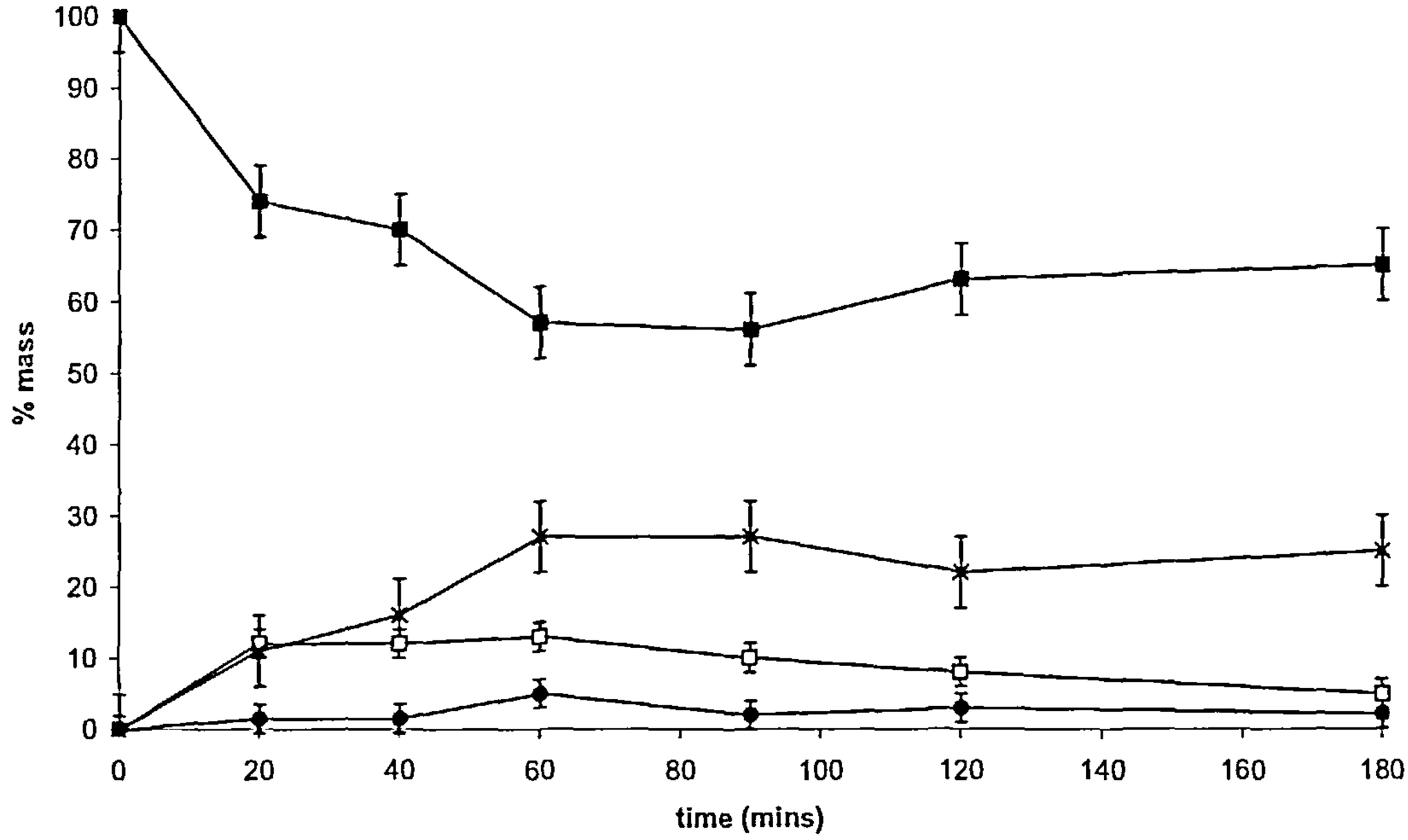

Figure 4.34: HMS-TBD catalysed reaction, 60 °C, 6:1 molar ratio methanol to oil, 2 g catalyst. Triglycerides ■, diglycerides □, monoglycerides ●, biodiesel x.

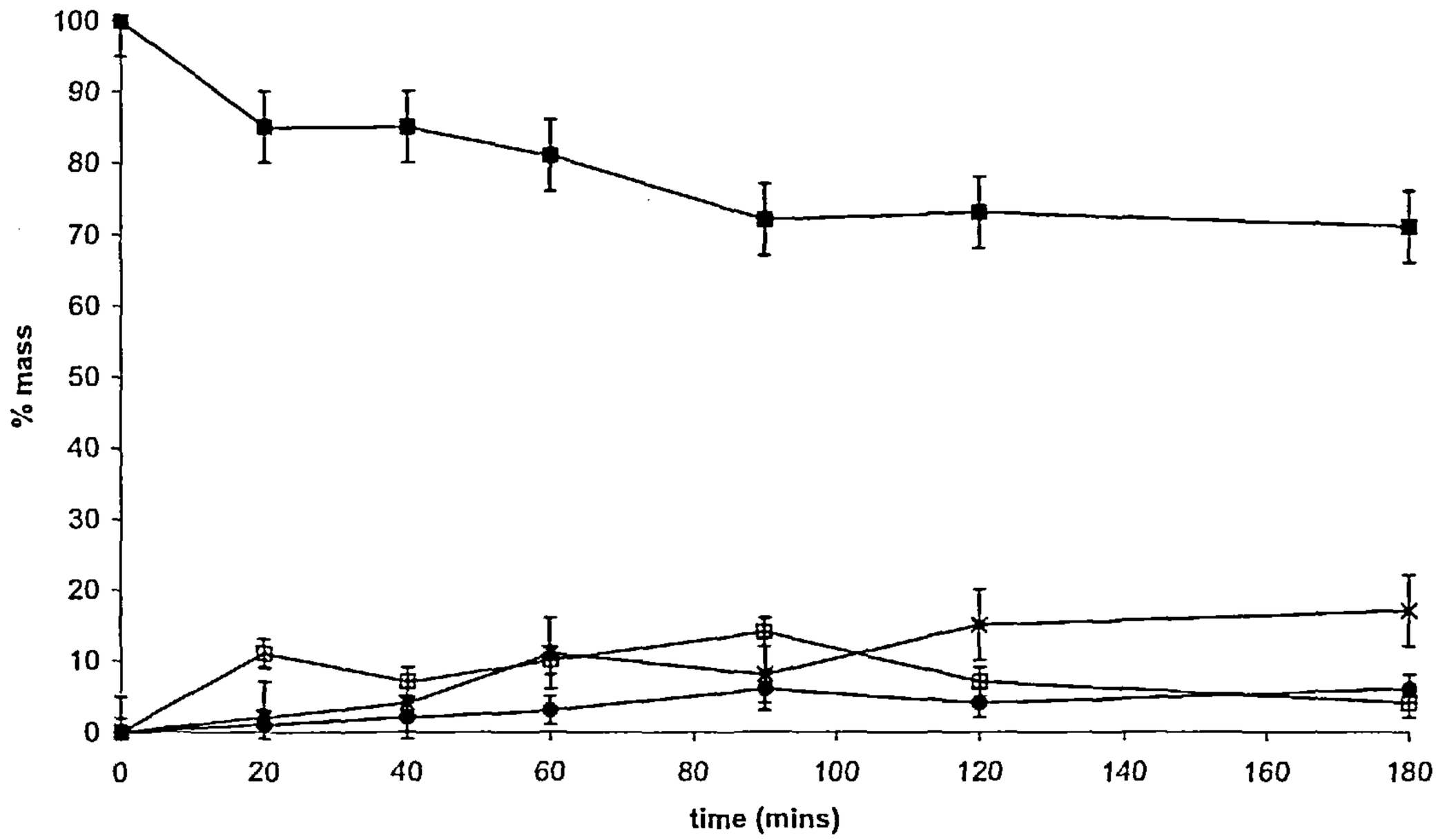

Figure 4.35: Davisil (60 Å pore size)-TBD catalysed reaction, 60 °C, 6:1 molar ratio methanol to oil, 2 g catalyst. Triglycerides ■, diglycerides □, monoglycerides ●, biodiesel x.

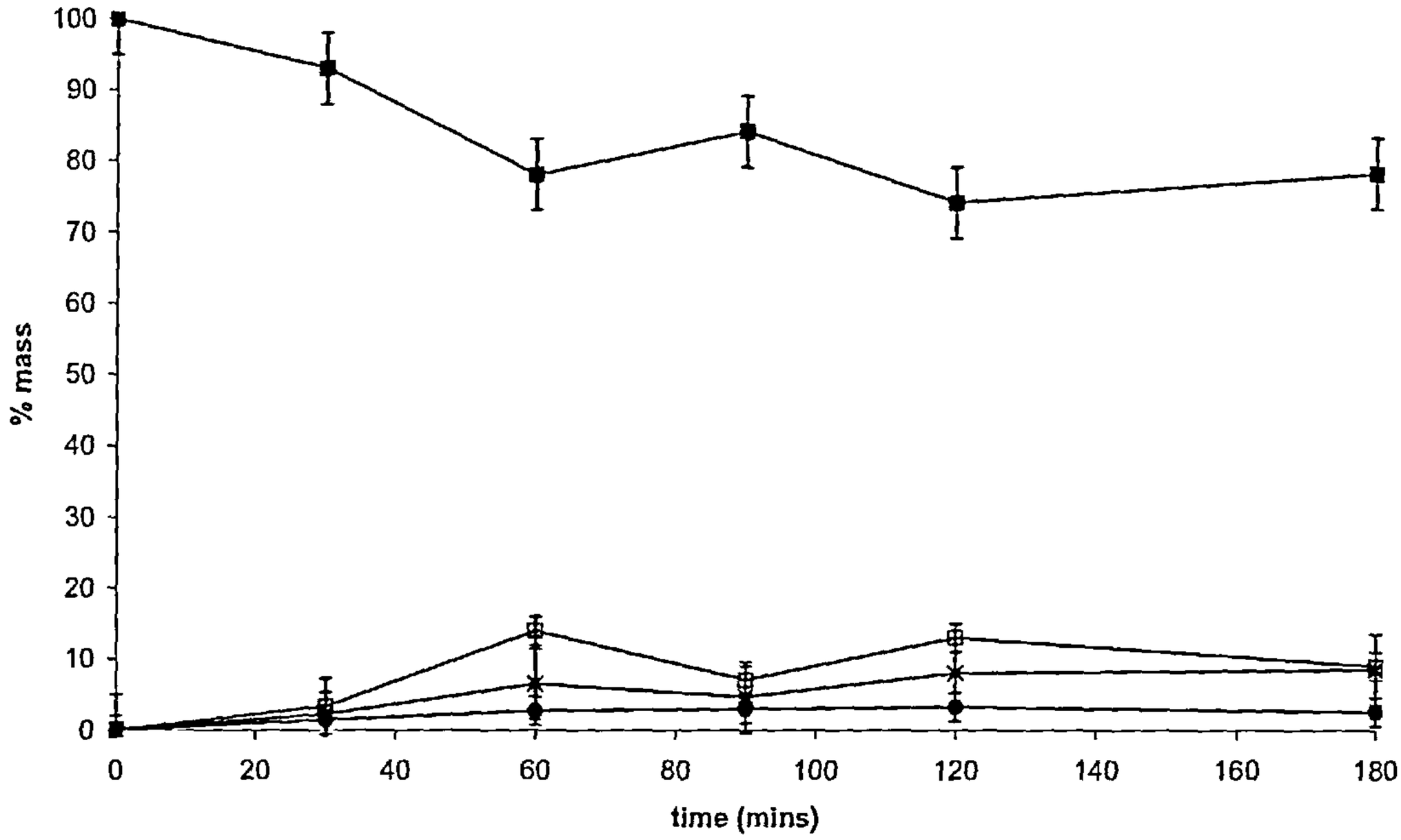

Figure 4.36: Davisil (150 Å pore size)-TBD catalysed reaction, 60 °C, 6:1 molar ratio methanol to oil, 2 g catalyst. Triglycerides ■, diglycerides □, monoglycerides •, biodiesel x.

The conversion to biodiesel attained by each of the catalysts is presented in Table 4.21. The activity of the catalysts is quite low, as only a small amount of biodiesel is produced in 3 hours under tested conditions.

Table 4.21: final biodiesel level after 3 hours reaction at 60 °C, 6:1 molar ratio of methanol to oil and 2g of catalyst.

Catalyst	Final biodiesel level (mass %)
HMS-TBD	28 ± 5%
Davisil (60 Å pore size)-TBD	17 ± 5%
Davisil (150 Å pore size)-TBD	9 ± 5 %

There have been a number of studies on the use of supported TBD-type catalysts for the transesterification of vegetable oil with methanol, and also for the transesterification of fatty acid esters with glycerol to produce monoglycerides. TBD was covalently anchored to MCM silica (a mesoporous silica) using the surface glycidylation route (that of Subba Rao

et al., 1997). At a 7:1 Molar ratio methanol to oil, 70 °C and 5% molar catalyst concentration a conversion of 65% was achieved in 3 hours (Sercheli *et al.*, 1999). The higher conversion attained with the MCM-TBD could be because the catalyst loading used was higher in Sercheli's study than in this work (5 molar % catalyst versus 1 molar %). However, it may not be economically viable to use such a large amount of catalyst in the bulk production of biodiesel, especially if the lifetime of the catalyst is not long.

In order to compare the activity of HMS-TBD with the examples from the literature the catalyst loading was increased by a factor of 5 to a loading of 5 molar %. The result is shown in Figure 4.37: the conversion obtained in 3 hours is around 80%, which is in good agreement with the value in the literature.

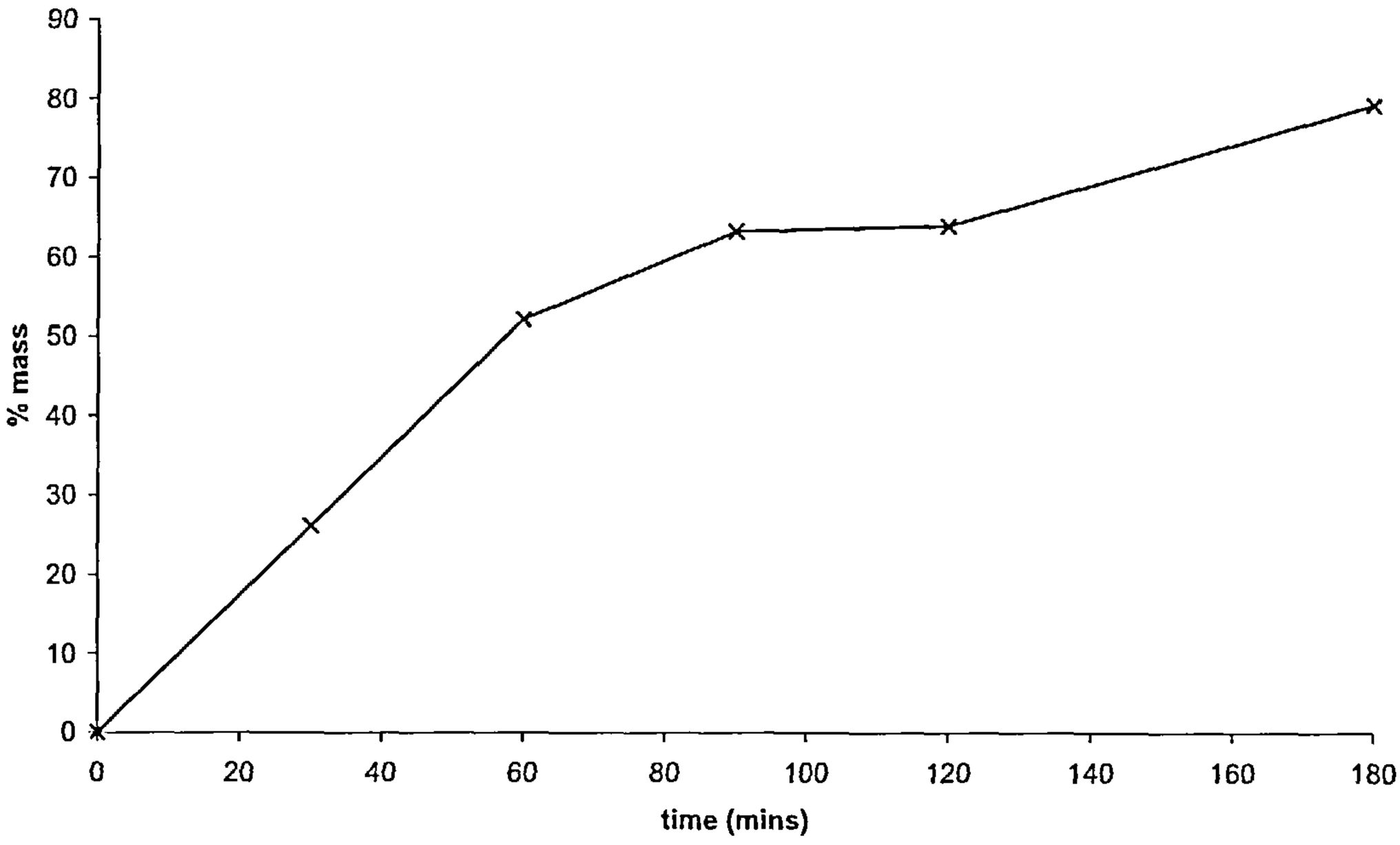

Figure 4.37: HMS-TBD catalysed reaction, 60 °C, 6:1 molar ratio methanol to oil, 5 mol% catalyst. Biodiesel x.

4.4.3 Homogeneously catalysed reaction

In order to assess the effect of the support on the activity of TBD, its activity was assessed as a purely homogeneous catalyst. The reaction profiles for 0.1 g (0.5 molar %) and 1 g (5 molar %) are shown in Figure 4.38. The conversion reached with 0.1g of TBD was very

low. 14 wt % biodiesel was formed in 3 hours. As expected, when the amount of TBD was increased to 1g the reaction was very rapid, with >90% biodiesel formed in 15 minutes.

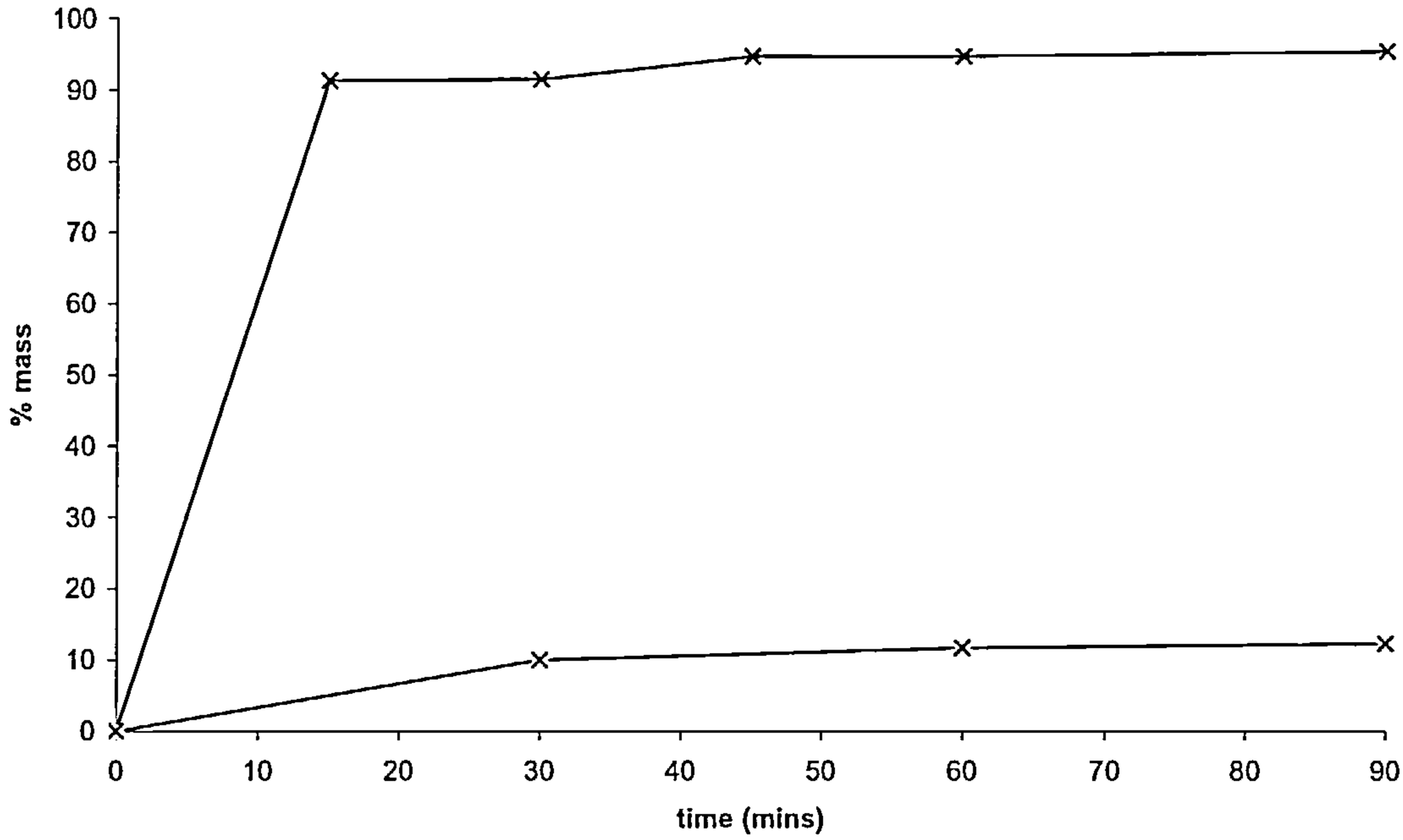

Figure 4.38: Biodiesel formation in homogeneous TBD catalysed reaction, 1g TBD (upper line), 100 mg TBD (lower line), 6:1 molar ratio of methanol to oil, 60 °C.

4.4.4 Re-use and stability

Silica-TBD is a catalyst which is relatively difficult and costly to make, as 3 consecutive process steps are involved (glycidylation, functionalization and washing). Therefore it must have a long lifetime in order for it to be considered for industrial use, this is especially the case when the catalyst loading required for the reaction to reach high conversion is very high. The results of reusing the catalyst and the leachate activity test (section 3.3.5) are shown in Table 4.22.

Table 4.22: results of reuse of silica –TBD catalysts and leachate activity tests

catalyst	Reuse test - % biodiesel formed when catalyst reused	Leachate activity test - % biodiesel formed
HMS-TBD	1%	4%
Davisil (60 Å pore size)-TBD	<1%	2%
Davisil (150 Å pore size)-TBD	<1%	1%

When the catalysts were reused there is almost no conversion. This could be due to leaching of the active components or a covering of the catalyst by a viscous material, preventing access to the active sites. After the reaction, the catalyst did appear to be covered in an orange 'gel'. In order to remove this layer, the recovered catalyst was washed in first methanol, and then isopropyl alcohol. The catalyst was then reused, but the conversion remained at <1%.

The conversion in the leachate activity test is low. However, the conversion attained when using the catalyst itself was also quite low (Table 4.21) so the conversion achieved in the leachate activity test is significant in comparison. It can be expected that some of the catalytic activity seen is due to homogeneous activity of leached species. To further investigate the leaching, an IR spectrum of methanol that the catalyst had been in contact with and an IR spectrum of the final reaction mixture were taken (see figures 4.39-4.43). The absorbance at 1650 cm^{-1} is the characteristic absorbance of the C=N stretch (Fessenden and Fessenden, 1982). In each of the samples tested there is a peak at around 1650 cm^{-1}. This means that the TBD leaches from the silica into methanol, and also from the silica into the reaction mixture

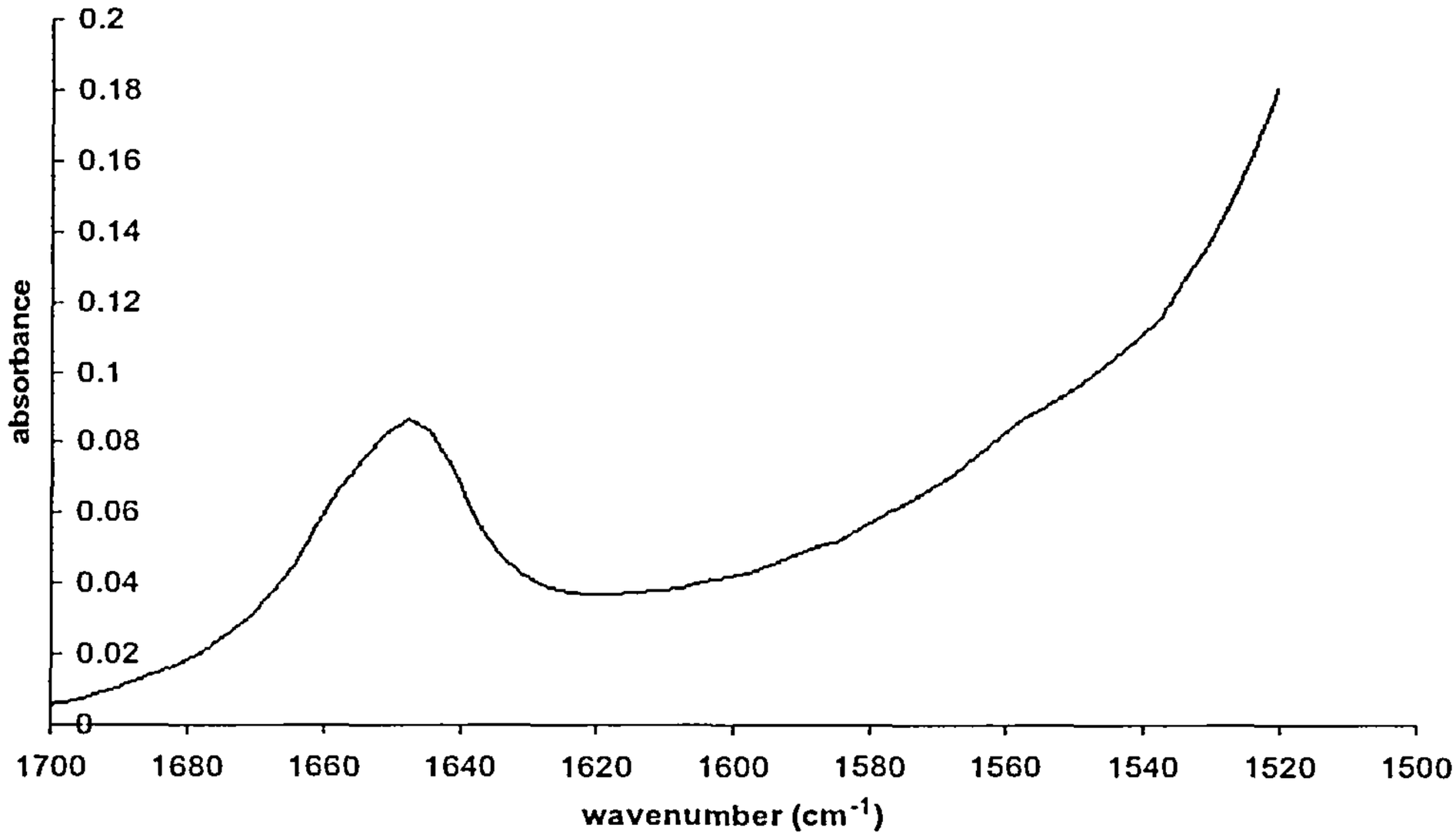

Figure 4.39: IR spectrum of TBD dissolved in methanol

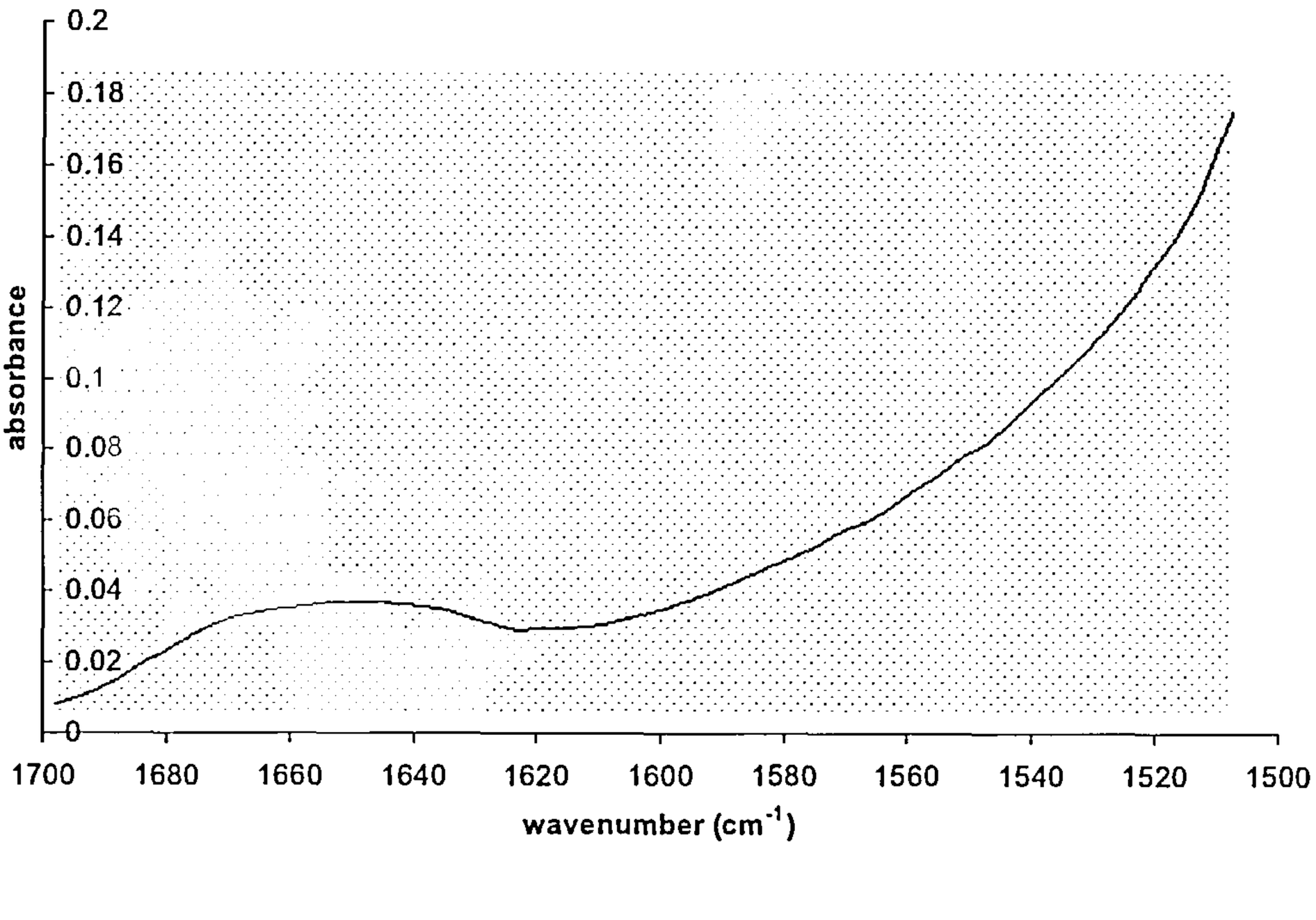

Figure 4.40: IR spectrum of methanol contacted with HMS-TBD

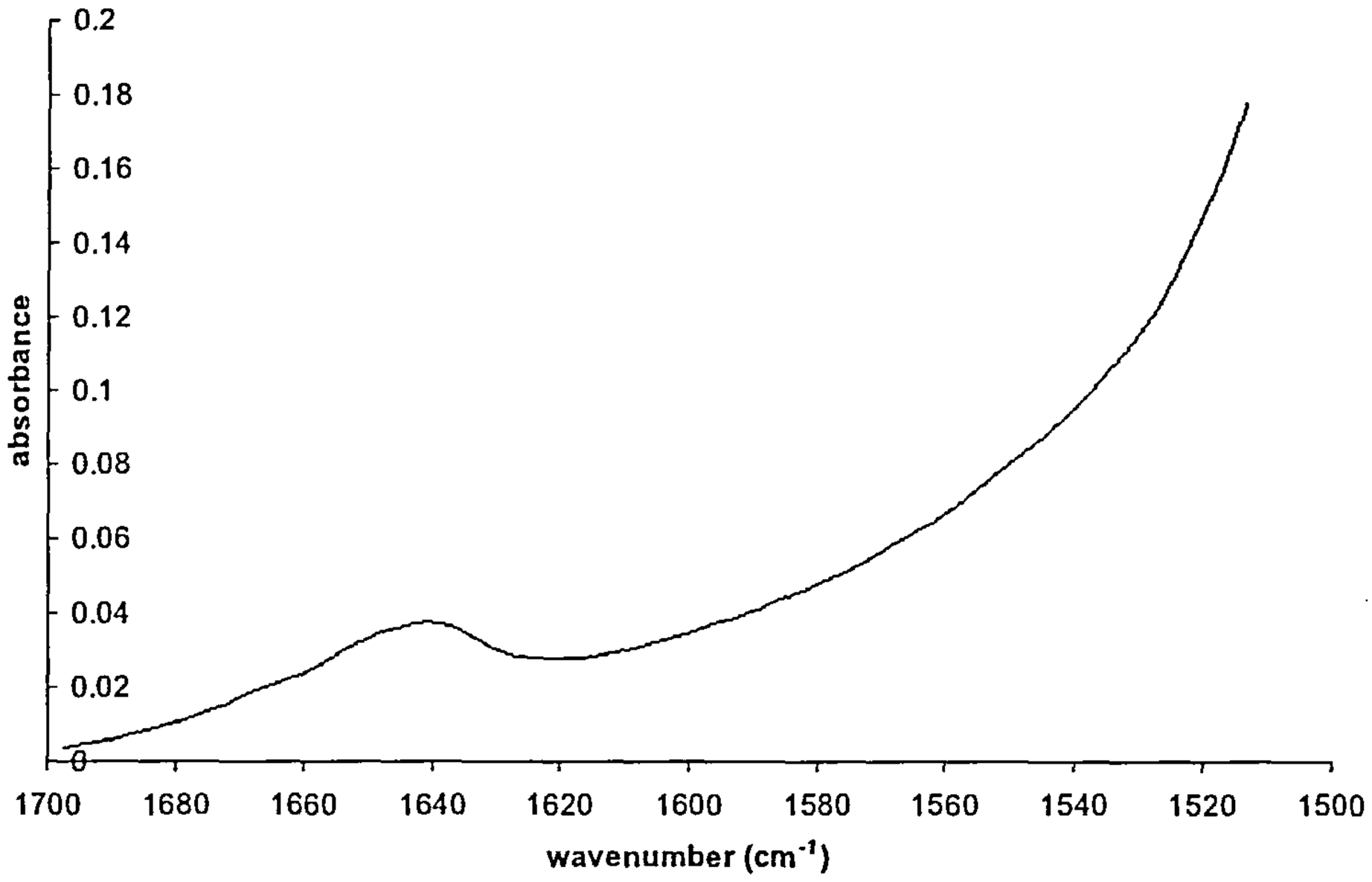

Figure 4.41: IR spectrum of methanol contacted with Davisil (60 Å pore size)-TBD

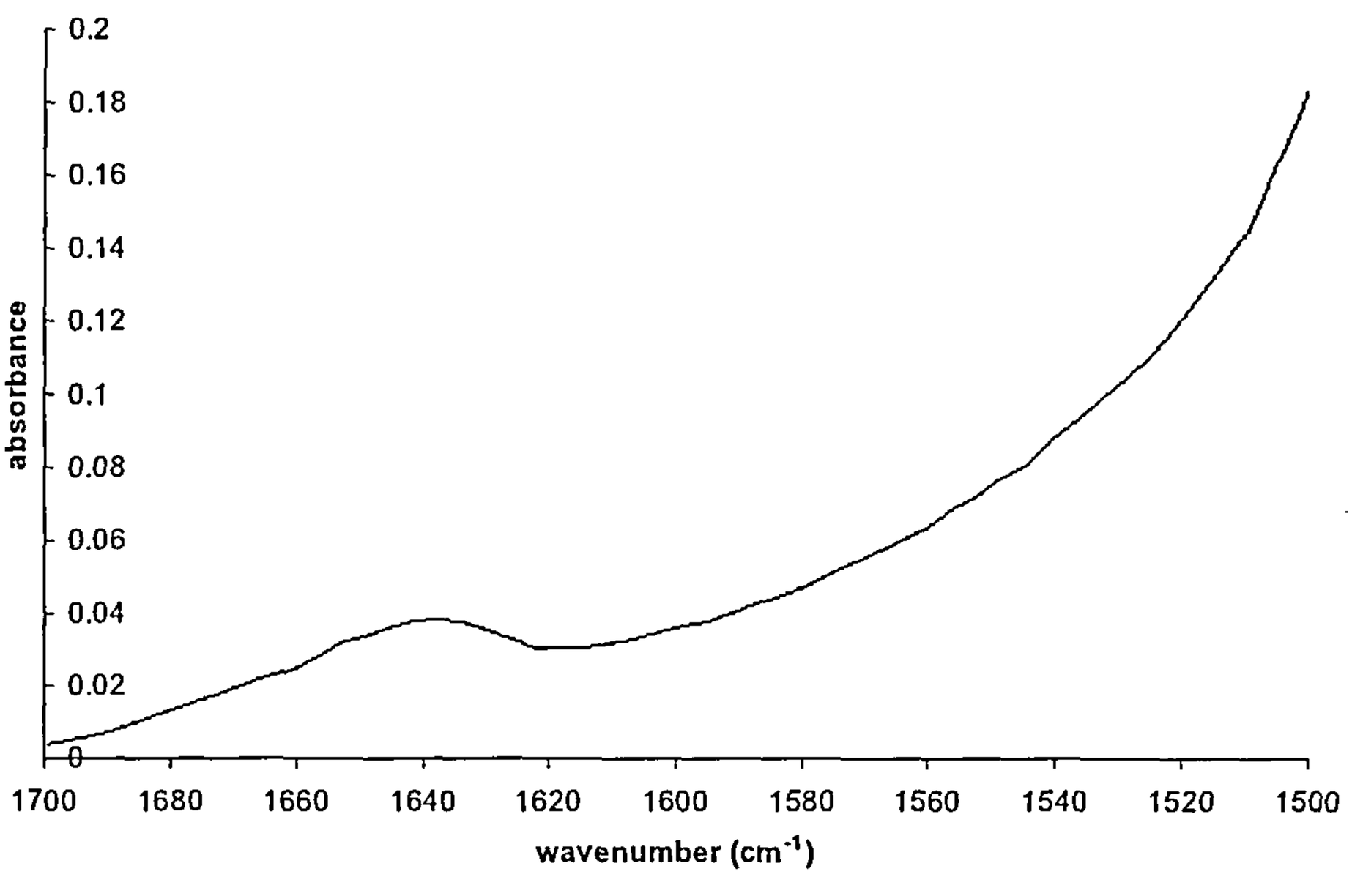

Figure 4.42: IR spectrum of methanol contacted with Davisil (150 Å pore size)-TBD

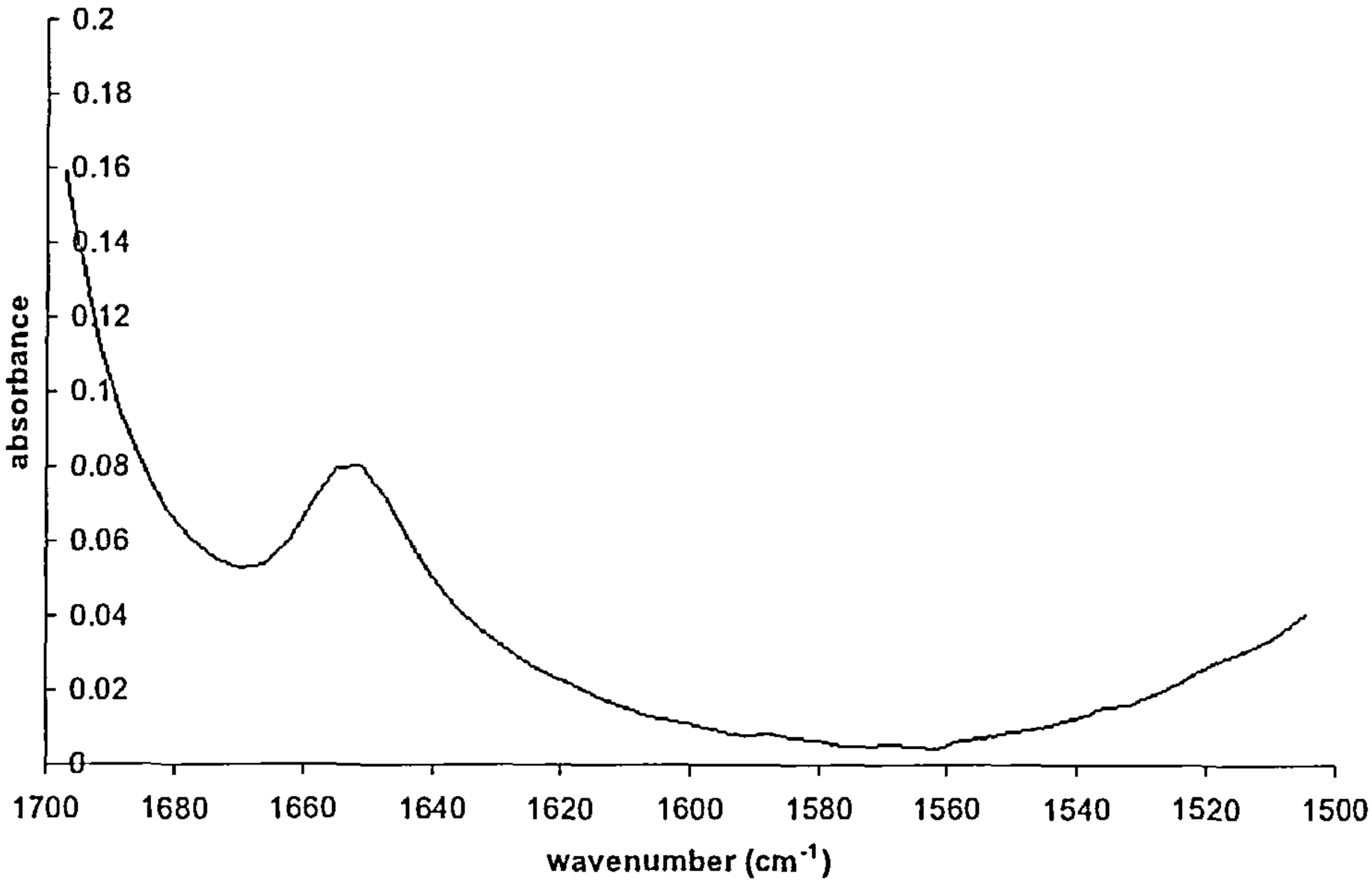

Figure 4.43: IR spectrum of final reaction product (triglyceride/biodiesel/methanol mixture) catalysed by Davisil (150 Å pore size)-TBD

Known concentrations of TBD in methanol and in biodiesel were used to quantify the concentration of TBD in the samples of interest by comparing the peak heights. This result is shown in Table 4.23 . There is no correlation between the activity of the solid catalyst and the amount of TBD lost into methanol, as HMS-TBD, the most active, loses the least amount of TBD into methanol. However, as it has a smaller particle size, the external surface area of the particles is greater, so there could be a greater heterogeneous contribution.

Table 4.23: % TBD lost into methanol after contact at 60 °C for 3 hours

Sample	% TBD lost
HMS-TBD in methanol	28
Davisil (60 Å pore size)-TBD in methanol	89
Davisil (150 Å pore size)-TBD in methanol	91

There is a large amount of leaching into the triglyceride/biodiesel. As most of the TBD has leached into the reaction mixture, few TBD groups remain on the silica surface to catalyse the next reaction when the catalyst is recovered, and so the reuse of the catalysts will be poor. When the catalysts were reused, the conversions reached were very small, as shown in Table 4.22.

Leaching of the TBD into methanol and biodiesel/triglyceride from the silica-TBD is unexpected, as silica-TBD, when prepared by the method of surface glycidylation has been described as a stable catalyst (Subba Rao *et al.*, 1997; Srivastava, 2007; Kantam and Sreekanth, 2001, Carloni *et al.*, 2002, Kharchafi *et al.*, 2005). In particular, the paper by Kantam and Sreekanth states that 'no leaching was observed'. This is in contrast to polystyrene supported TBD, where the alkoxide ions formed can attack the benzylic CH_2 groups causing leaching, but by using silica supported TBD with an alkyl spacer arm this was avoided.

Although it has been reported that silica-TBD is a stable catalyst in these conditions, it appears that this is not the case. When silica-TBD is contacted with methanol, the TBD leaches into solution.

Silica-supported TBD and polystyrene-supported TBD were found to leach slowly when these catalysts were reused in the transesterification of soya oil (Sercheli *et al.*, 1999). Polystyrene supported guanidines were found to leach from the support due to the attack by the methoxide ion on the benzylic CH_2 group. This was shown through a decrease in activity and in base capacity (Schuchardt *et al.*, 1996). Polystyrene-supported biguanides performed better in terms of initial activity, and also in reusability, but the activity began to fall after the 10^{th} cycle of use, and at this point the amount of N on the catalysts began to drop. This drop in N content was attributed to the cleavage of the biguanide units by methanolysis (Gelbard and Vielfaure-Joly, 2001). It then appears that the methoxide ion formed from the interaction of methanol with the TBD group may be responsible for attacking the immobilization method of the TBD to its support.

Figure 4.45 shows the IR spectra of Davisil (60 Å pore size)-TBD catalyst before and after use. The spectra of glymo-functionalized silica was subtracted from these spectra to show only the functional species. The main changes after use are the decrease in peak height of the peak at 1600 cm^{-1}, which is a loss of C=N (TBD) functionality (Fessenden and Fessenden, 1982), and a new peak at 1700 cm^{-1} corresponding to a carbonyl group being formed (Fessenden and Fessenden, 1982). There is also an increase in the C-H stretch absorption, at 2800 cm^{-1} (Fessenden and Fessenden, 1982). From this, it can be concluded that a glyceride or methyl ester is adsorbed on the surface. This matches with the mass spectrometry of the gel coating on the catalyst, which showed peaks corresponding to tri-, di- and monoglycerides.

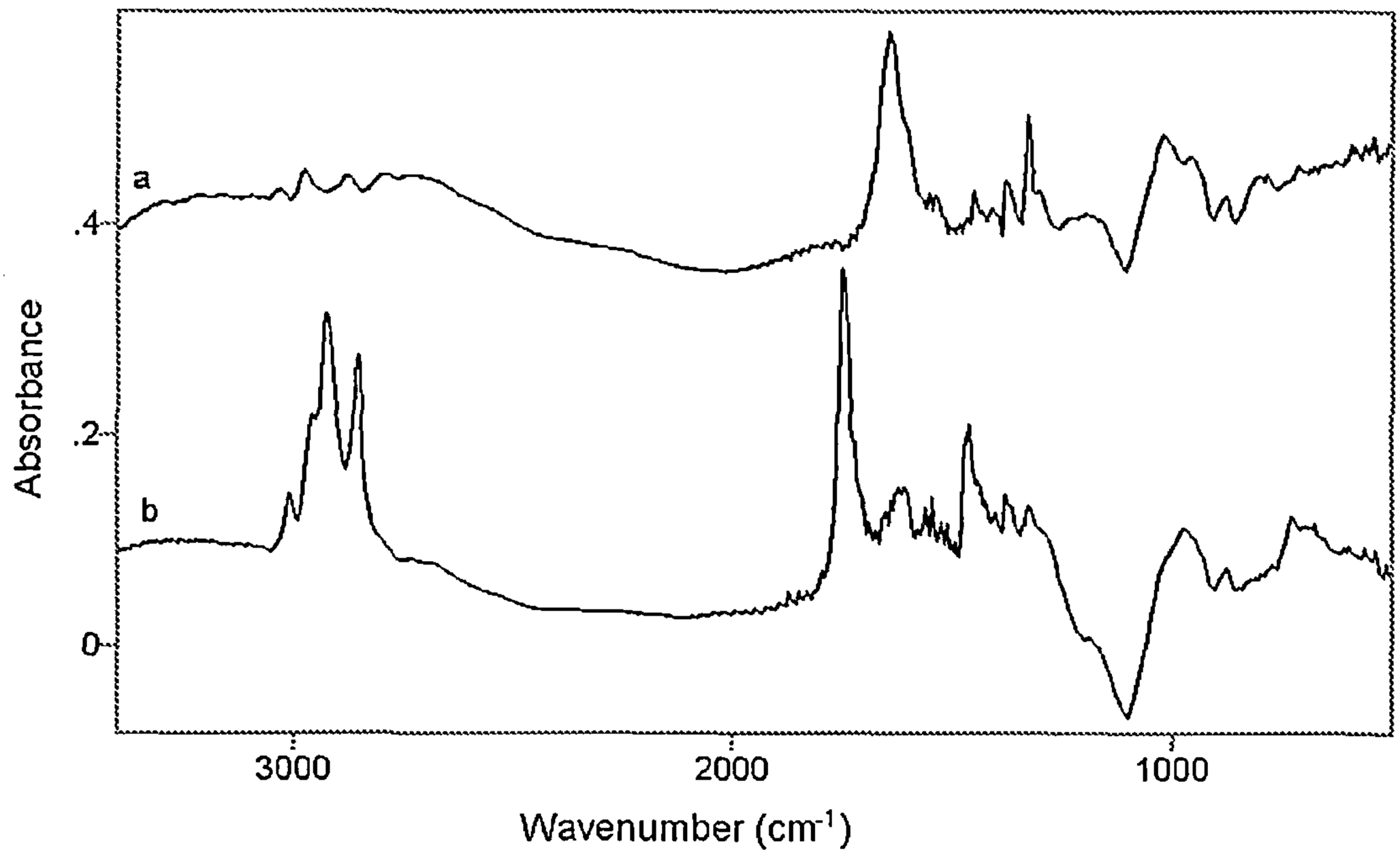

Figure 4.44: IR spectra of D-60 before (a) and after (b) use in transesterification reaction

4.5 Basic ion exchange resin

Amberlyst A46 is a quaternary ammonium (QN^+OH^-) functionalized polymeric resin that was found to be active and stable for the transesterification of triacetin with methanol (Liu *et al.*, 2007). Figure 4.45 shows the mass % biodiesel formed when Amberlyst 26 was used as the catalyst for the transesterification of vegetable oil with methanol. The conversion achieved is substantially less than the conversion with triacetin as reactant, where after 4 hours a conversion of 65% was reached. The catalyst loading used for the transesterification of triacetin was 0.88 wt% whereas for the transesterification of vegetable oil the catalyst loading was 2.5 wt%. It was found that when using the smaller reagent of triacetin, only 30-40 % of the active sites were accessible to the triacetin (Lopez *et al.*, 2007), so with vegetable oil, a bigger molecule with a lower diffusivity, this number will be further reduced, thus reducing the conversion attained with the catalyst.

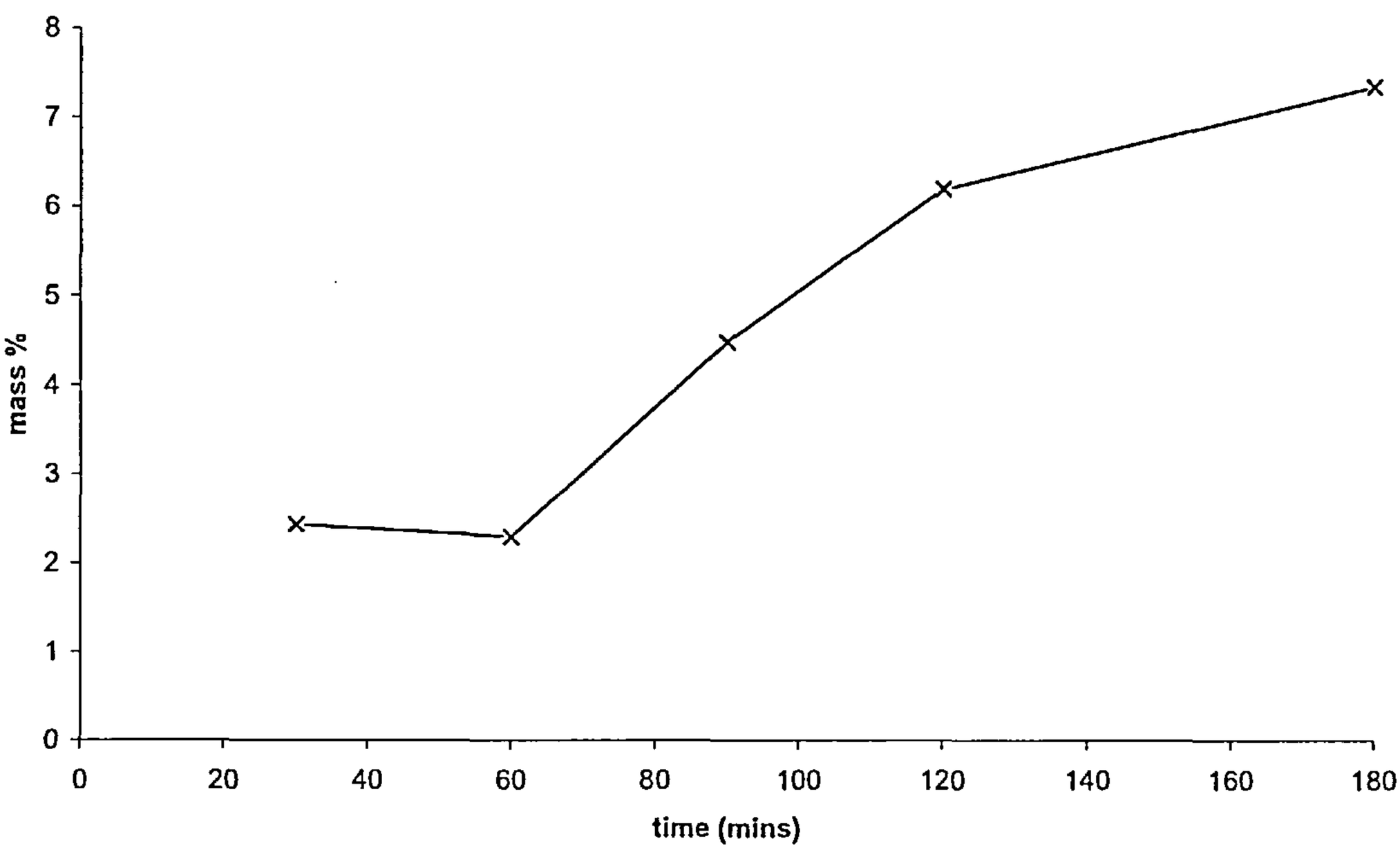

Figure 4.45: mass % biodiesel with Amberlyst 26 as catalyst. 5g Amberlyst 26, 6:1 molar ratio methanol to oil, 60 °C.

The Amberlyst 26 was reused in the batch reactor, and after 3 hours a conversion to biodiesel of 1% was obtained. The leachate activity test was also applied and there was no detectable conversion to biodiesel, so the catalyst is stable. There is some deactivation but it is not due to leaching of active species. Amberlyst 26 was reused 4 times for the transesterification of triacetin and there exhibited no drop in activity, and the leachate had negligible activity (Liu *et al.*, 2007)

It appears that Amberlyst 26 is a stable catalyst, but the conversion achieved using it is not high. One possibility would be to increase the loading of this catalyst. Only the base sites on the external surface of the catalyst are accessible to the large triglyceride molecule, and this contributes to the low activity of the catalyst.

4.6 Magnetic catalysts

Table 4.25 contains a summary of the catalytic activity of the magnetic catalysts investigated. Only $SnFe_2O_4$ and Fe_3O_4 with $SnCO_3$ precipitated onto the surface and subsequently decomposed to SnO showed any activity. The conversion to biodiesel in the other cases was less than 3% after 4 hours at methanol reflux temperature. Therefore magnetite is not in itself active, so other known catalysts must be supported on the magnetite in order to make an active catalyst.

Table 4.24: Summary of activity of magnetic catalysts

Catalyst	Coversion to biodiesel at 65°C after 4 hours of reaction with 6:1 molar ratio triglyceride to methanol and 1% wt catalyst
Fe_3O_4	3 %
$CoFe_2O_4$	3 %
$SnFe_2O_4$	13 %
Fe_3O_4 surface functionalized with soya fatty acid	2 %
Fe_3O_4 core with SnO shell formed by $SnCO_3$ precipitation	27 %
Fe_3O_4 core with shell formed by $Sn(acac)_2$ adsorption	3 %

The activity of tin compounds in transesterification and esterification is known (Macedo *et al.*, 2006). For this reason we also expect that the shell-and-core magnetic particles functionalized with tin or tin-doped magnetite will be active. $SnFe_2O_4$ was found to be slightly active, reaching a conversion to biodiesel of 13 % after 6 hours, as shown in figure 4.46.

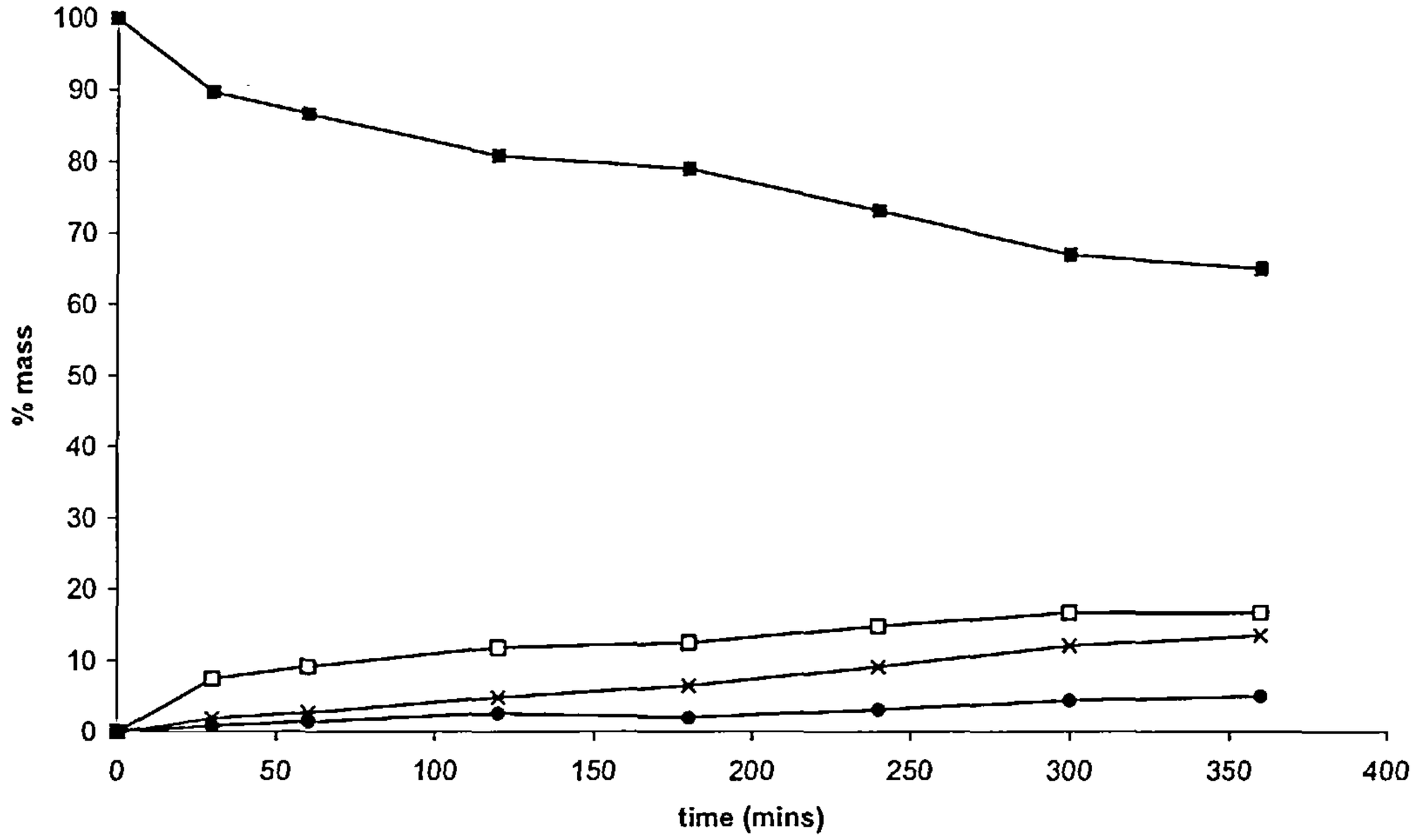

Figure 4.46: $SnFe_2O_4$ catalysed reaction, methanol reflux temperature, 6:1 molar ratio oil to methanol, 1% weight catalyst. Triglycerides ■, diglycerides □, monoglycerides ●, biodiesel x.

Although the tin was added to the magnetite precursor solution as tin (II), the tin will have been oxidized to tin (IV) and the iron (III) reduced to iron (II). The structure becomes a reverse spinel phase, where the Sn(IV) sits in the octrahedral sites and Fe (II) and Fe(III) in the tetrahedral sites (Yanwu *et al.*, 2006). Sn (IV) is less catalytically active than Sn(II) (Ferreira *et al.*, 2006), so it is not surprising that the activity of this catalyst is small.

The lack of activity of the $Sn(acac)_2$ adsorbed magnetite could be because the $Sn(acac)_2$ was only sparingly soluble in the acetylacetone, and the $Sn(acac)_2$ could have adsorbed on to the glass surface of the flask when the acetylacetone was evaporated off. The shell-and-core type catalyst formed by precipitation of $SnCO_3$ onto magnetite was found to be more active. The reaction profile is shown in figure 4.47. A conversion of 26% was reached in 3 hours. This catalyst was found to be able to be reused with no loss in activity. Only the magnetic solid was collected after the first reaction (there was a small amount of non-magnetic solid also present after preparation of the catalyst). A comparison of the 1st and 2nd use of the catalyst is shown in figure 4.48, and all of the catalyst activity is preserved. However, when the leachate activity test was performed, biodiesel was formed, so the

catalyst is not stable. However, as other tin oxide catalysts are stable (Macedo *et al.*, 2006), the stability could be improved by using a different method to attach the tin oxide to the core magnetite particle [1].

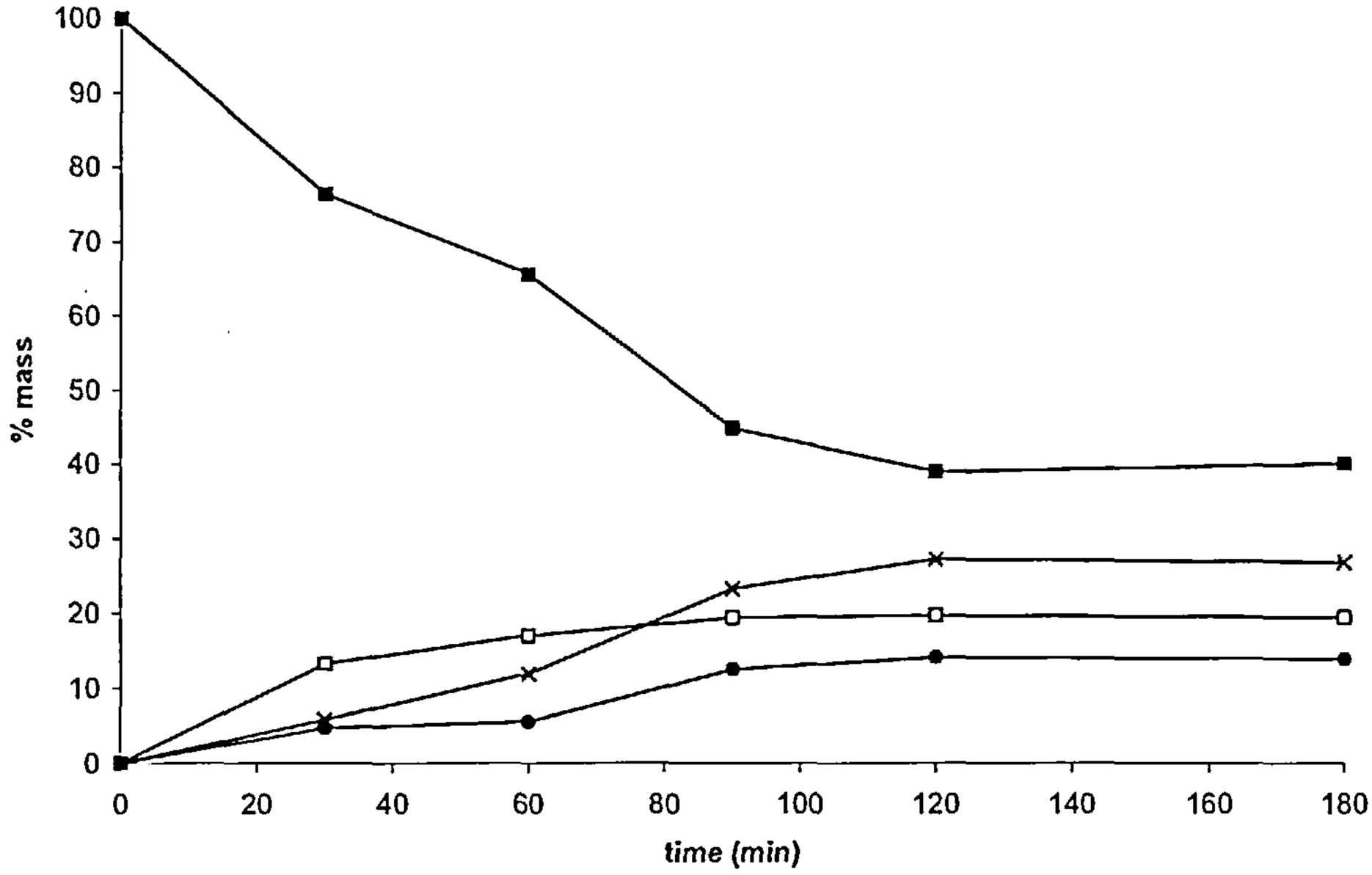

Figure 4.47: Fe_3O_4 plus shell formed by precipitation by $SnCO_3$ precipitation catalysed reaction, methanol reflux temperature, 6:1 molar ratio oil to methanol, 1% weight catalyst. Triglycerides ■, diglycerides □, monoglycerides •, biodiesel x.

[1] The work on magnetic catalysts was carried out during an exchange to the University of Brasilia. The time constraints of the exchange visit meant that work on magnetic catalysts could not be completed.

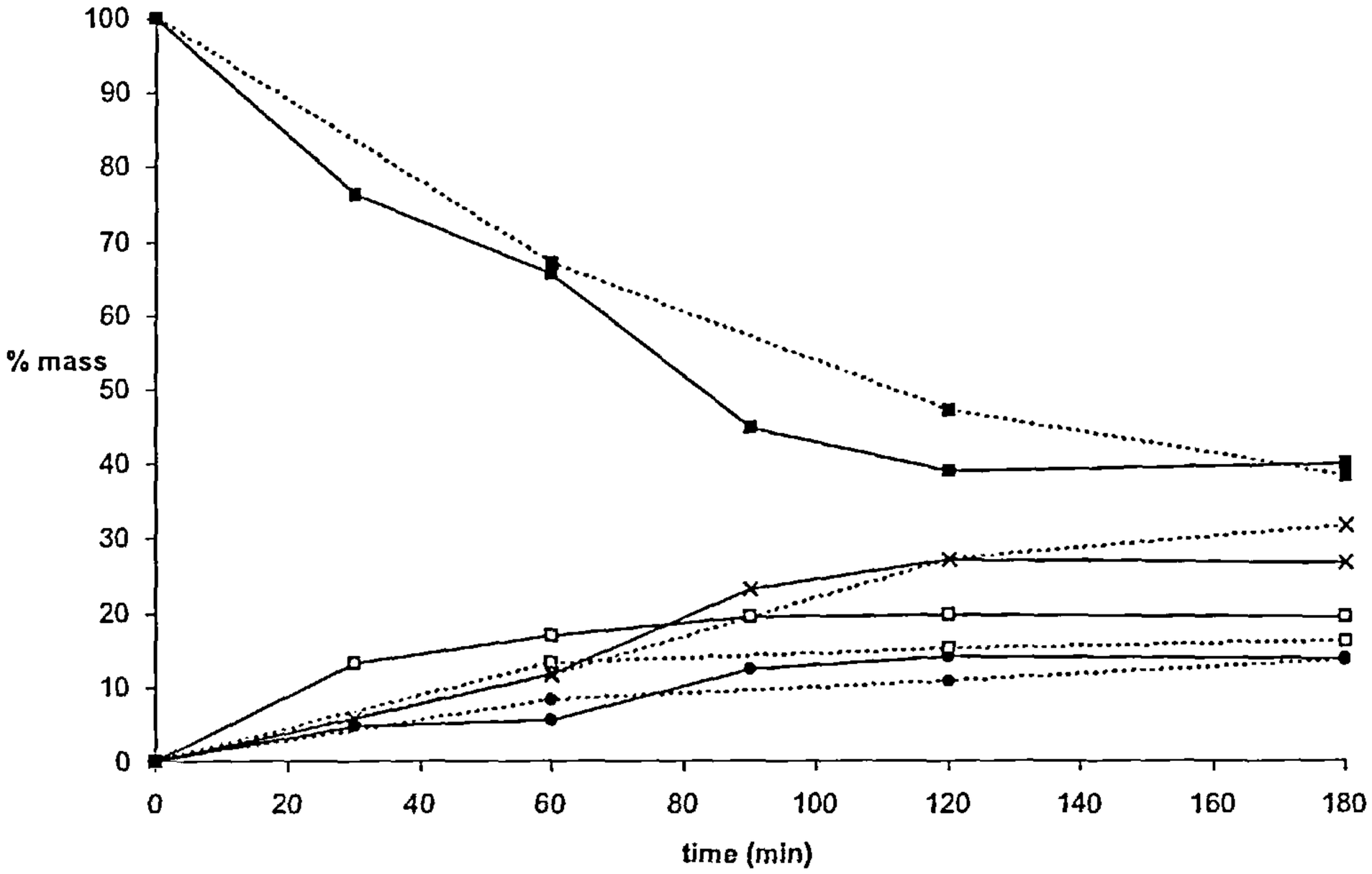

Figure 4.48: Fe_3O_4 plus shell formed by precipitation by $SnCO_3$ precipitation catalysed reaction, methanol reflux temperature, initial use and reuse, 6:1 molar ratio oil to methanol, 1 % weight catalyst. Triglycerides ■, diglycerides □, monoglycerides •, biodiesel x. Initial use solid lines, reuse dotted lines.

4.7 Modelling catalytic performance

4.7.1 Fitting kinetics to alkali-doped metal oxide catalysed reactions

Second order rate constants were fitted to the batch reaction profiles of the alkali-doped metal oxide catalysed reactions. The reaction scheme (figure 4.49) and rate expressions (figure 4.50) are shown below

$$TG + A \underset{k_2}{\overset{k_1}{\longleftrightarrow}} DG + BD$$

$$DG + A \underset{k_4}{\overset{k_3}{\longleftrightarrow}} MG + BD$$

$$MG + A \underset{k_6}{\overset{k_5}{\longleftrightarrow}} G + BD$$

Figure 4.49: Reaction scheme for sequential transesterification of triglycerides to methyl esters

$$\frac{d[TG]}{dt} = -k_1[TG][A] + k_2[DG][BD]$$

$$\frac{d[DG]}{dt} = k_1[TG][A] - k_2[DG][BD] - k_3[DG][A] + k_4[MG][BD]$$

$$\frac{d[MG]}{dt} = k_3[DG][A] - k_4[MG][BD] - k_5[MG][A] + k_6[G][BD]$$

$$\frac{d[BD]}{dt} = k_1[TG][A] + k_3[DG][A] + k_5[MG][A] - k_2[DG][BD] - k_4[MG][BD] - k_6[G][BD]$$

Figure 4.50: rate expressions for 2nd order kinetics for transesterification of triglycerides to methyl esters

The modelled and real data are shown in figures 4.51 to 4.57. Second order kinetics were found for the homogeneously-catalysed reaction (Noureddini and Zhu ,1997; Vicente *et al.*, 2005), so this type of kinetics was viewed as the best starting point for modelling the

reaction. The oscillations observed in some of the profiles are due to the numerical differentiation used to create the modelled profile. The real and modelled data often do not coincide to within experimental error. This is partly due to lack of information at intermediate conversions in the experimental data, so it is possible that more information at intermediate conversions could improve the model. The fit between modelled and actual data is often weakest for the MG and DG for the alkali-doped oxide catalysed reactions. The compounds have different profiles to the homogeneous case, as discussed in section 4.3.3, so it is likely that 2nd order homogeneous kinetics do not adequately describe MG and DG formation and reaction in alkali-doped metal oxide catalysed reactions.

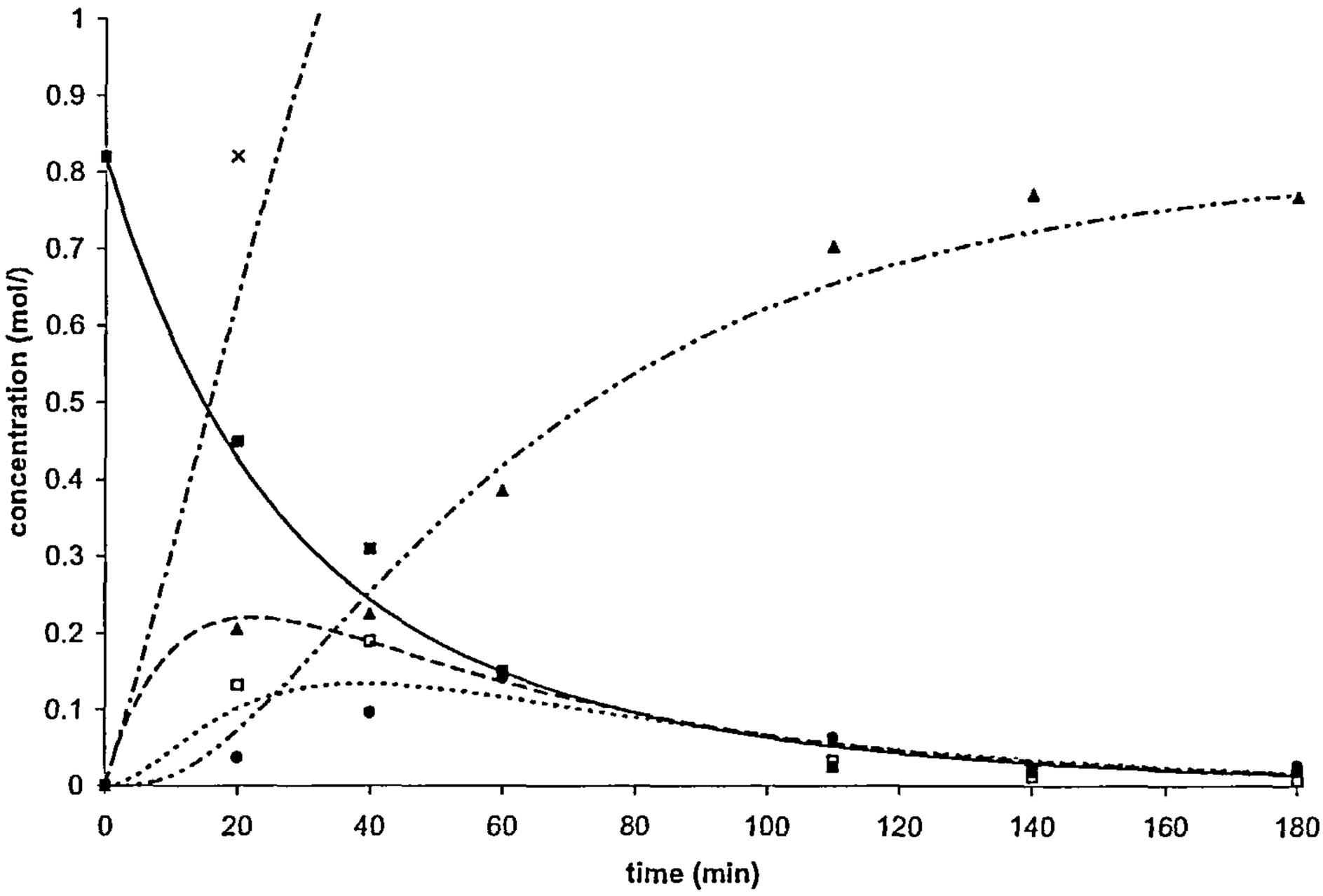

Figure 4.51: 2nd order model fitted to Li-CaO catalysed reaction. Experimental data: Triglycerides ■, diglycerides □, monoglycerides ●, biodiesel x, glycerol ▲. Modelled data: TG —, DG - - -, MG ···, Biodiesel-·-·- (scale only shows initial data), glycerol -··-··

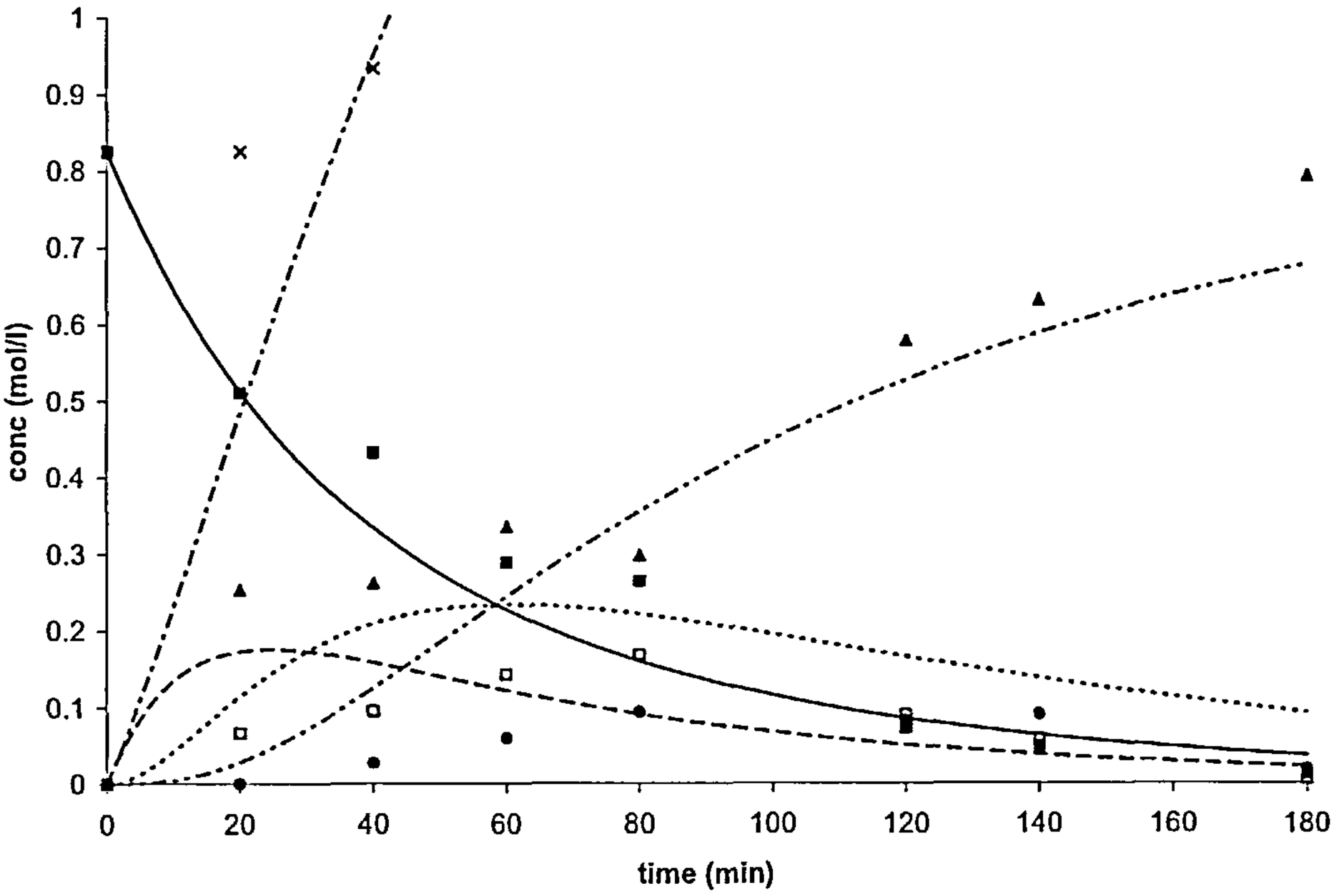

Figure 4.52: 2nd order model fitted to Na-CaO reaction. Experimental data: Triglycerides ■, diglycerides □, monoglycerides ●, biodiesel x, glycerol ▲. Modelled data: TG —, DG - - -, MG ····, Biodiesel-·-·-(scale only shows initial data), glycerol -··-··

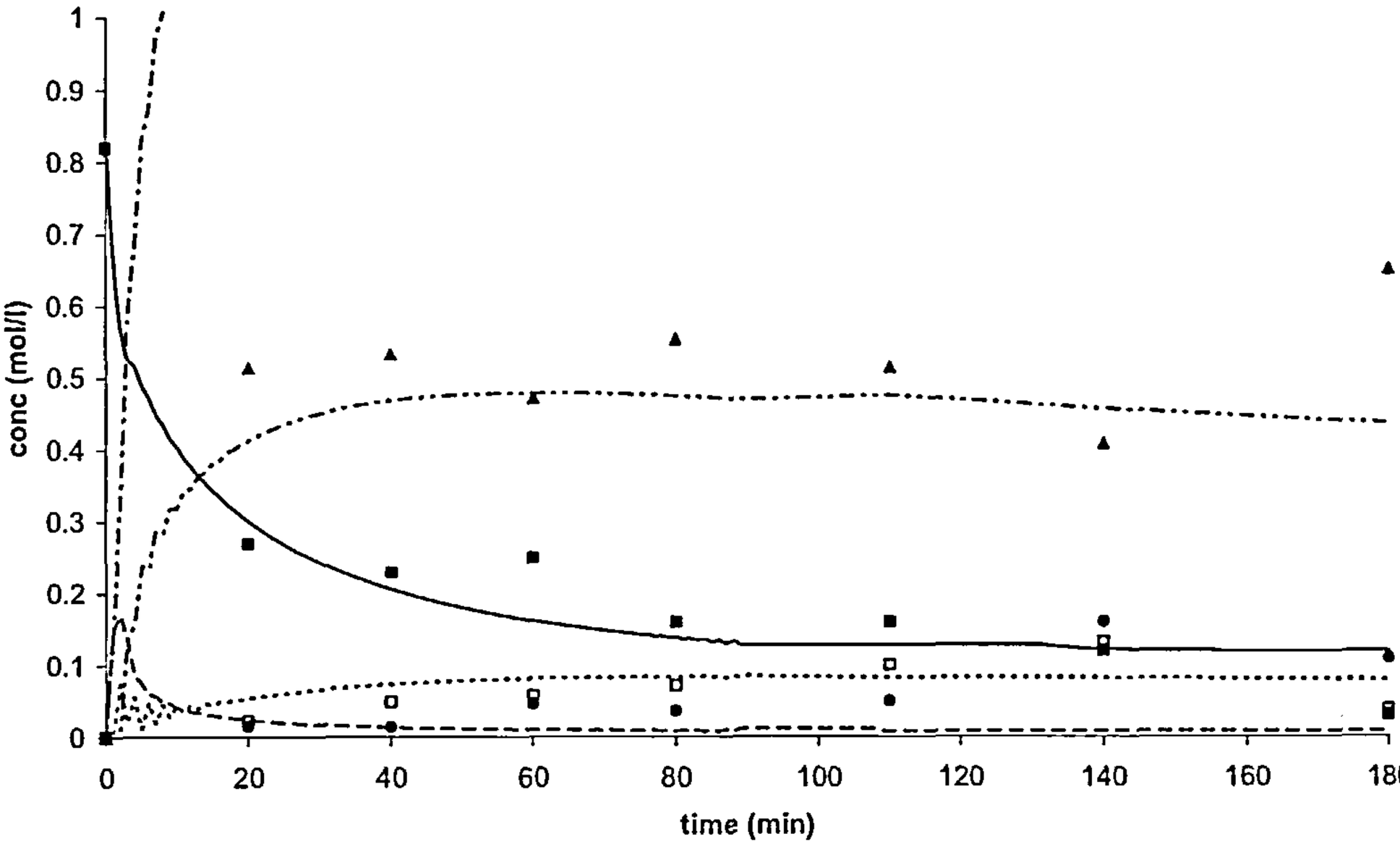

Figure 4.53: 2nd order model fitted to K-CaO reaction. Experimental data: Triglycerides ■, diglycerides □, monoglycerides ●, biodiesel x, glycerol ▲. Modelled data: TG —, DG - - -, MG ····, Biodiesel-·-·-(scale only shows initial data), glycerol -··-··

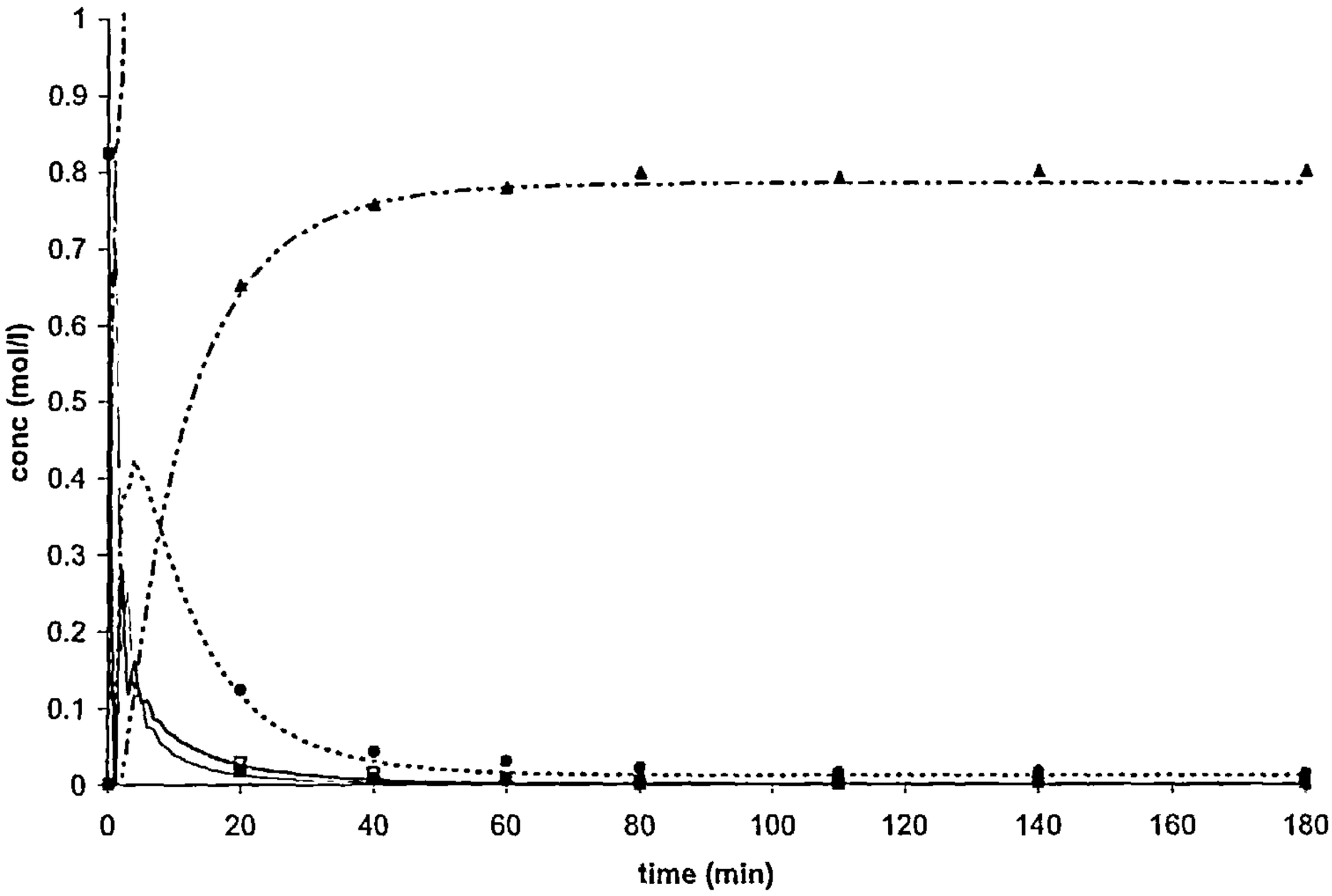

Figure 4.54: 2nd order model fitted to Li-CaO cal reaction. Experimental data: Triglycerides ■, diglycerides □, monoglycerides •, biodiesel x, glycerol ▲. Modelled data: TG —, DG - - -, MG ····, Biodiesel-·-·- (scale only shows initial data), glycerol _··_··_··

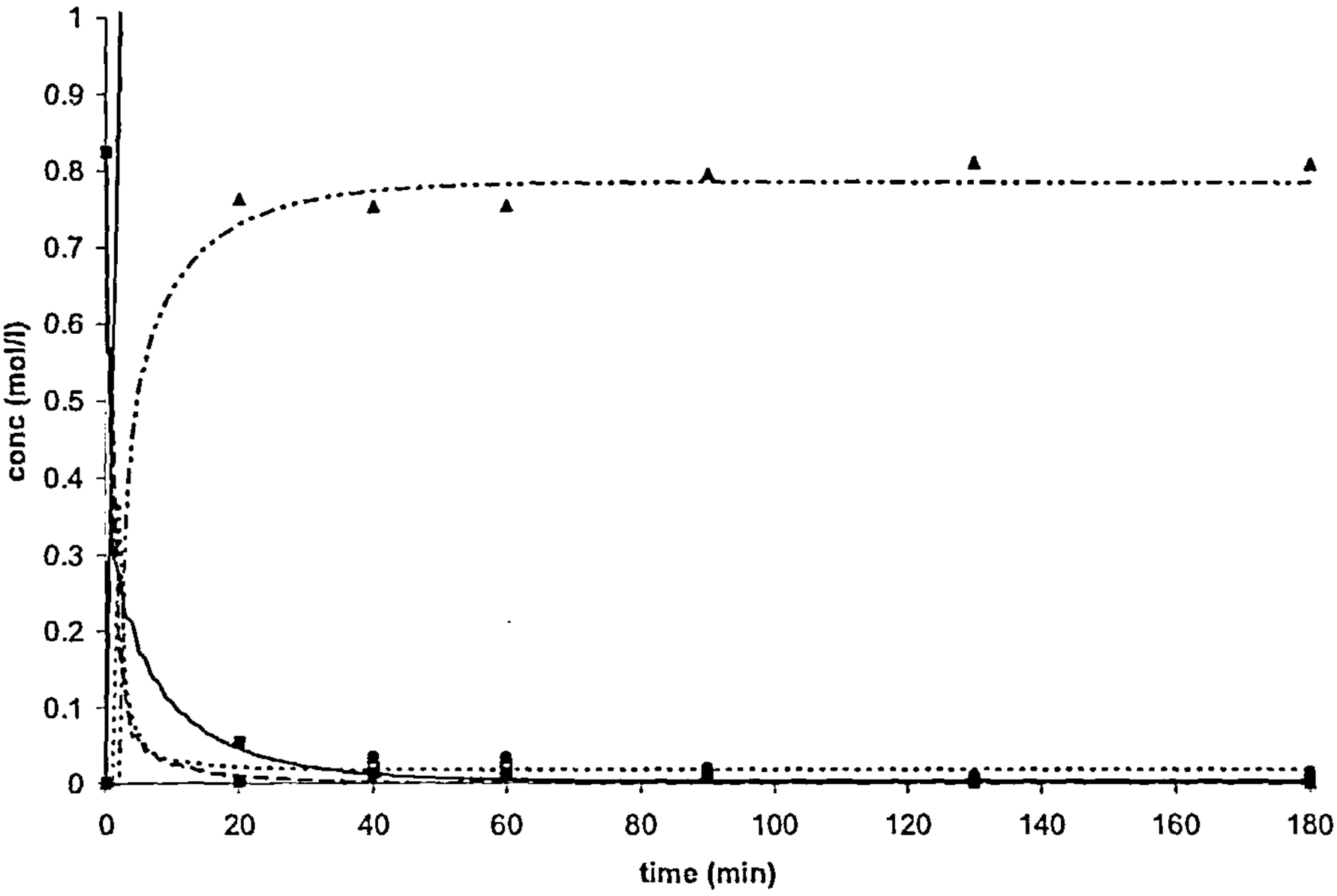

Figure 4.55: 2nd order model fitted toNa-CaO cal reaction. Experimental data: Triglycerides ■, diglycerides □, monoglycerides •, biodiesel x, glycerol ▲. Modelled data: TG —, DG - - -, MG ····, Biodiesel-·-·- (scale only shows initial data), glycerol -··-··

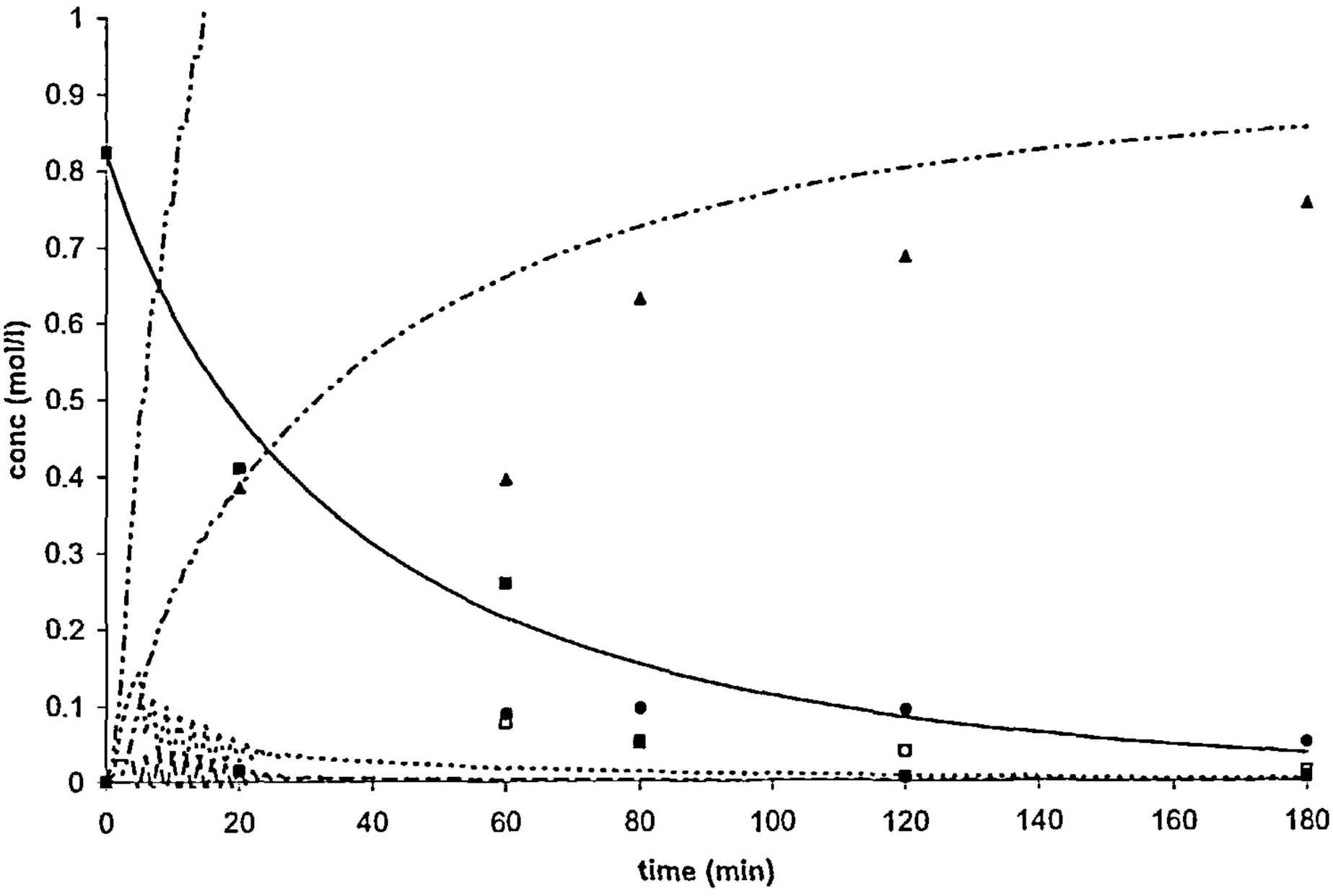

Figure 4.56: 2nd order model fitted to K-CaO cal reaction. Experimental data: Triglycerides ■, diglycerides □, monoglycerides ●, biodiesel x, glycerol ▲. Modelled data: TG —, DG - - -, MG ····, Biodiesel-·-·- (scale only shows initial data), glycerol -··-··

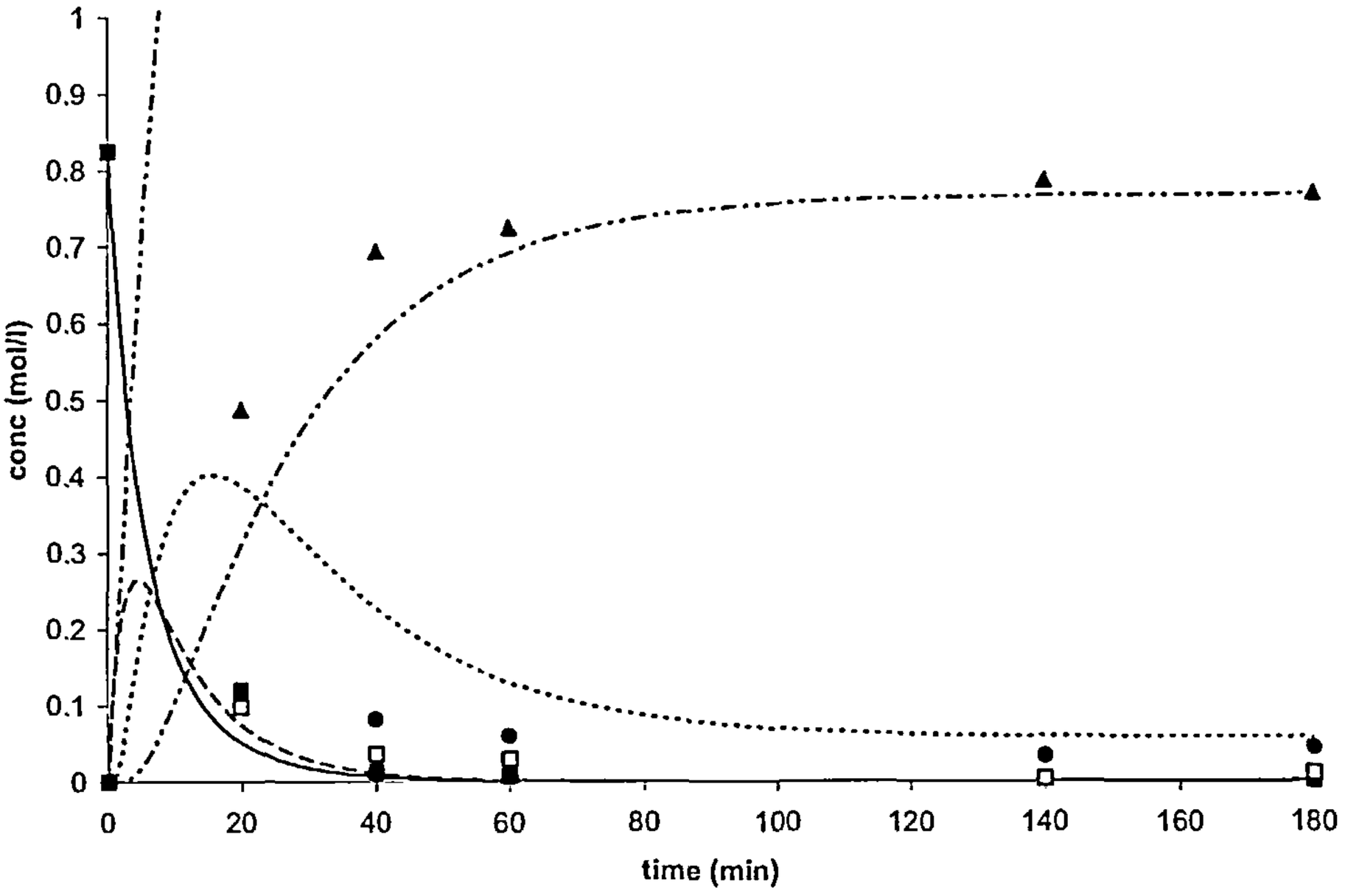

Figure 4.57: 2nd order model fitted to Li-MgO cal reaction. Experimental data: Triglycerides ■, diglycerides □, monoglycerides ●, biodiesel x, glycerol ▲. Modelled data: TG —, DG - - -, MG ····, Biodiesel-·-·- (scale only shows intial data), glycerol -··-··

The fitted second order reaction rate constants are shown in table 4.26, and the sum of squared errors between the model and experimental data in table 4.27. There is some variation in the form of the rate constants. In the TG to DG reaction, some catalysts have no back reaction (Li-CaO, Na-CaO and Li-MgO calcined), some (Li-CaO calcined and Na-CaO calcined) have ratios of rate constants comparable to those for 2nd order homogeneous kinetics, shown Table 4.27 and Table 4.28. K-CaO and calcined K-CaO catalysts have much stronger back reaction for the TG to DG stage than the homogeneous equivalents. The similar-to-homogeneous character for the rate constants for Li-CaO calcined and Na-CaO calcined catalysts could indicate that a homogeneously catalysed reaction is occurring.

Table 4.25: 2nd order rate constants fitted to batch data

Catalyst	k_1 (l mol^{-1} min^{-1})	k_2 (l mol^{-1} min^{-1})	k_3 (l mol^{-1} min^{-1})	k_4 (l mol^{-1} min^{-1})	k_5 (l mol^{-1} min^{-1})	k_6 (l mol^{-1} min^{-1})
LiCaO	0.007	0	0.013	0	0.018	0
LiCaO calcined	0.20	0.42	0.11	0.003	0.04	0.001
NaCaO	0.005	0	0.014	0	0.07	0
NaCaO calcined	0.13	0.52	0.16	0.008	0.24	0.005
KCaO	0.04	0.90	0.10	0.01	0.39	0.12
KCaO calcined	0.006	0.06	0.46	0.01	0.07	0
LiMgO calcined	0.03	0	0.05	0	0.02	0.001

Table 4.26: Sum of squared error for fitting to 2nd order batch data

Catalyst	Error Squared sum
LiCaO	0.21
LiCaO cal	0.02
NaCaO	1.36
NaCaO cal	0.04
KCaO	0.62
KCaO cal	0.85
LiMgO	0.47

Table 4.27: 2nd order homogeneous, with 0.2 % wt NaOH, =0.045 mol/l, 50 ° C, Noureddini and Zhu (1997)

Rate constant	Value k=k'cat (l/mol/min)	k' (l/mol/min/mol_{cat})
k1	0.05	1.1
k2	0.11	2.4
k3	0.215	4.8
k4	1.228	27.3
k5	0.242	5.4
k6	0.007	0.15

Table 4.28: 2nd order homogeneous, 1% KOH = 0.16 mol/l, 65 °C, Vicente *et al.*, (2002)

Rate constant	Value k=k'cat (l/mol/min)	k' (l/mol/min/mol_{cat})
k1	3.06	19
k2	23.9	149
k3	32.5	203
k4	57.5	359
k5	0.54	3.3
k6	0.0009	0.006

Particularly in the case of Na-CaO calcined, there is not enough data in the initial stages of the reaction, as most of the change occurs before the first data point was measured.There is not enough information to determine how well the model represents the experimental data. The validity of the fitted model increases as the reactions become slower because there are more significant data points to fit the reaction to. This is not reflected in the sum of squared error because the higher concentrations of components lead to a larger squared error.

Other reasons for the poor fit could be inhibition of access of triglycerides to the catalyst surface, or containment of the leached metals from the catalyst in glycerol particles. The inhibitory layer of glycerol on catalyst surfaces has been found for supported enzymes and ion-exchange resins (Dossat *et al.*, 1999; Bondioli,, 2004). The distribution coefficient, K_{dis} (K_{dis} = wt% solute in glycerine phase/wt % solute in biodiesel phase) of KOH between glycerol and biodiesel was found to be 45 at 75 °C and 95 at 25 °C. So, the vast majority of the dissolved catalyst will be in the glycerol phase, and therefore not easily accessible to the majority of the reactants.

4.7.2 Eley-Rideal and Langmuir-Hinshelwood kinetics

The kinetic models for Eley-Rideal kinetics and Langmuir-Hinshelwood kinetics were fitted to the batch reaction data for Li-CaO. The batch reaction profile for Li-CaO was chosen because the reaction was sufficiently slow to give a number of data points at intermediate conversions. The Eley-Rideal fitted kinetics are shown in figure 4.58. The reaction profile is very similar to that of the 2nd order homogeneous catalysed reaction, with the initial rise in partial glyceride concentrations, which decay as the reaction proceeds. The Langmuir-Hinshelwood fitted kinetics are shown in figure 4.59. Again the reaction profile is similar to that of the second order homogeneous case and Eley-Rideal kinetics. The fitted rate constants are presented in Table 4.29. The units of the rate constant are not equal because of the differences in the models, and this means the values are not directly comparable. However the ratios between k_1, k_3 and k_5 are approximately equal for each kinetic model: k_3 is approximately double k_1 and k_5 slightly larger than k_3 in all cases. This

should be expected because the models are fitted to the same data. The fit, as quantified by the sum of squared errors is slightly better for Eley-Rideal kinetics than Langmuir-Hinshelwood, and both heterogeneous models have a better fit than the 2nd order homogeneous case. Therefore, Eley-Rideal kinetics may be considered as the most applicable model to use to describe the Li-CaO catalysed reaction.

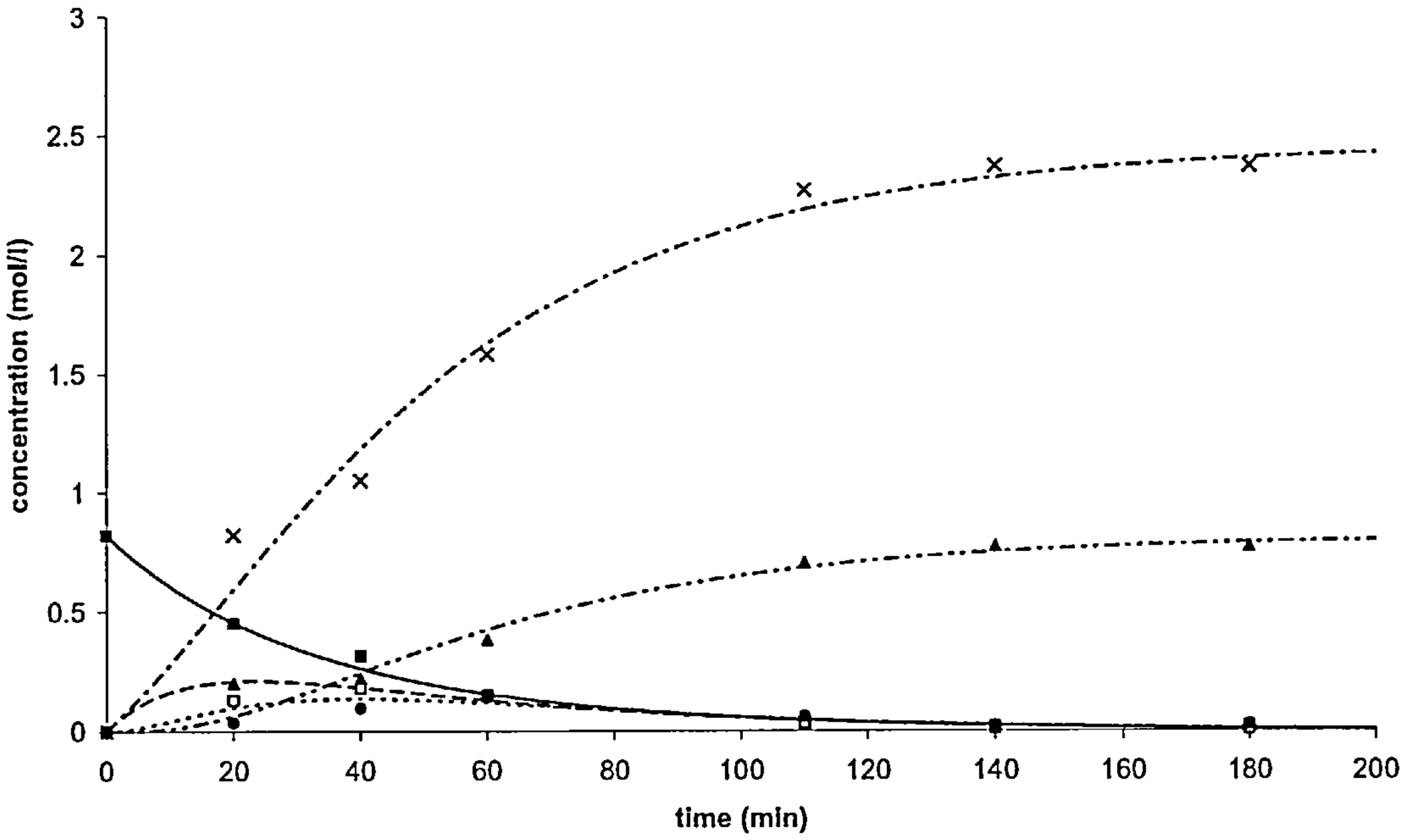

Figure 4.58: Li-CaO catalysed reaction fitted to Eley-Rideal kientics, K = 3 l/mol for involved species, TG —, DG – – –, MG ····, Biodiesel-·-·-, glycerol -··-··

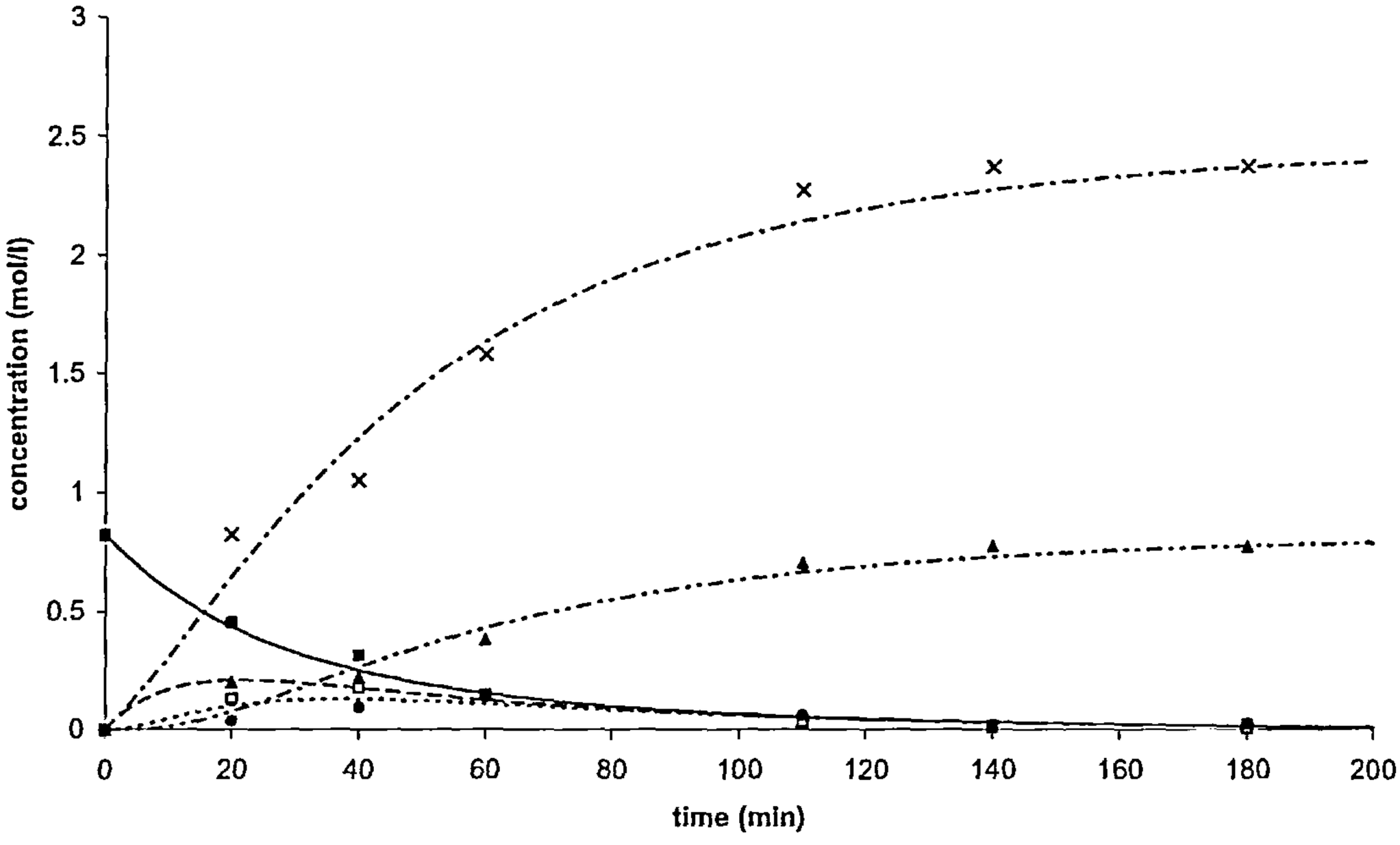

Figure 4.59: Li-CaO catalysed reaction fitted to Langmuir Hinshelwood kinetics, K =3 l/mol for all species, TG —, DG - - -, MG ····, Biodiesel-·-·-, glycerol -··-

Table 4.29: rate constants from fitting kinetic models to batch reaction data for LiCaO and sum of squared error in each case

Rate constant	2nd order homogeneous (l/mol/min)	Eley-Rideal (1/min)	Langmuir-Hinshelwood (mol/l/min)
k1	0.007	0.033	0.25
k2	0	0	0
k3	0.013	0.065	0.5
k4	0	0.0001	0
k5	0.018	0.08	0.71
k6	0	0	0
Squared error	0.21	0.12	0.14

The assumptions present in these kinetic models may not necessarily be correct for the biodiesel reaction. Both models assume that all adsorbed species can adsorb with equal

probability, which will not be the case when the molecule have widely varying sizes. Additionally, adsorption of the large triglyceride molecules could cover more than one active site, and this size effect has not been taken into account. It was also assumed that surface reaction was the rate-limiting step, but it could be possible that the rate limiting step is actually adsorption or desorption of the formed species.

4.7.3 Effect of Adsorption coefficient on Eley-Rideal Kinetics

It is possible that the strongly polar glycerol could adsorb more strongly than methanol onto the catalyst particle and so the adsorption coefficient for glycerol could be larger. The effect of changing adsorption coefficient on the Eley-Rideal kinetic model for the Li-CaO catalysed reaction was investigated. Figure 4.60 shows the batch reaction profile for Eley-Rideal kinetics with the adsorption coefficient of glycerol increased from 3 l/mol to 30 l/mol.

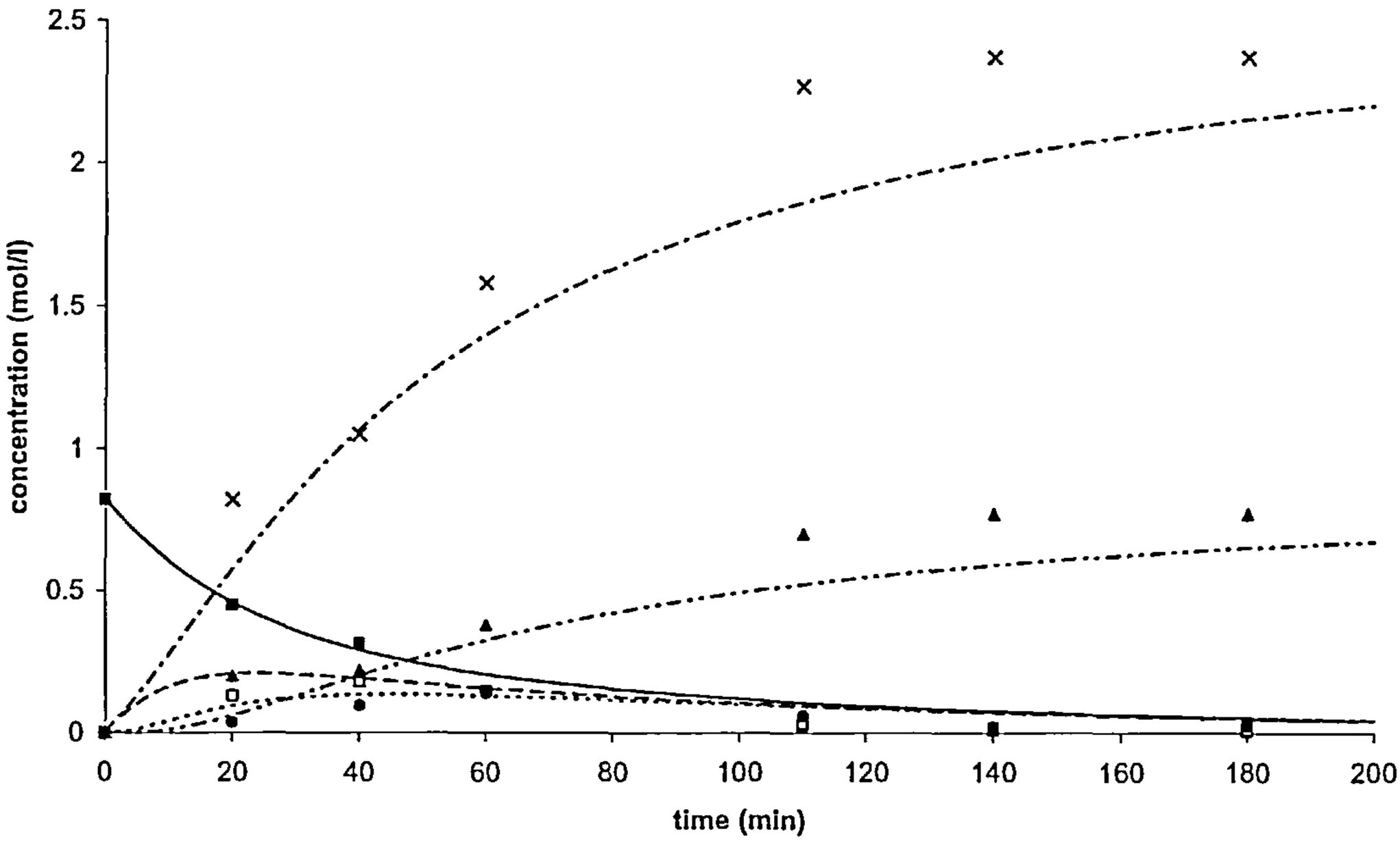

Figure 4.60: Eley-Rideal kinetics for Li-CaO catalysed reaction, K=30 l/mol for glycerol, 3 l/mol for other species, TG —, DG – – –, MG ····, Biodiesel–·–·–, glycerol –··–··

Comparison of figure 4.60 with figure 4.59 shows that increasing the adsorption coefficient of glycerol decreases the conversion to biodiesel and glycerol and increases the final content of glycerides. Figure 4.61 shows the reaction profile when the adsorption coefficient of partial glyceride is increased to 30 l/mol, and again the conversion to biodiesel and glycerol is decreased. When the adsorption coefficients of glycerol and partial glycerides are increased to 30 l/mol (Figure 4.62), the conversion is significantly decreased: after 200 minutes 5 wt% triglycerides remain compared with 0.5 wt% triglycerides for Eley-Rideal kinetics with K=3 l/mol for all species. If, in the heterogeneously catalysed transesterification reaction, the adsorption coefficients of glycerol or partial glycerides onto the catalyst are found to be high, it will be difficult to reach the glyceride contents specified in EN14214 because increased adsorption of these species increases the rate of the reverse reaction and so the equilibrium composition is slightly closer to the reactant side. This could be a potential difficulty in using a heterogeneous catalyst, but couold be potentially mitigated by increasing the excess of methanol present.

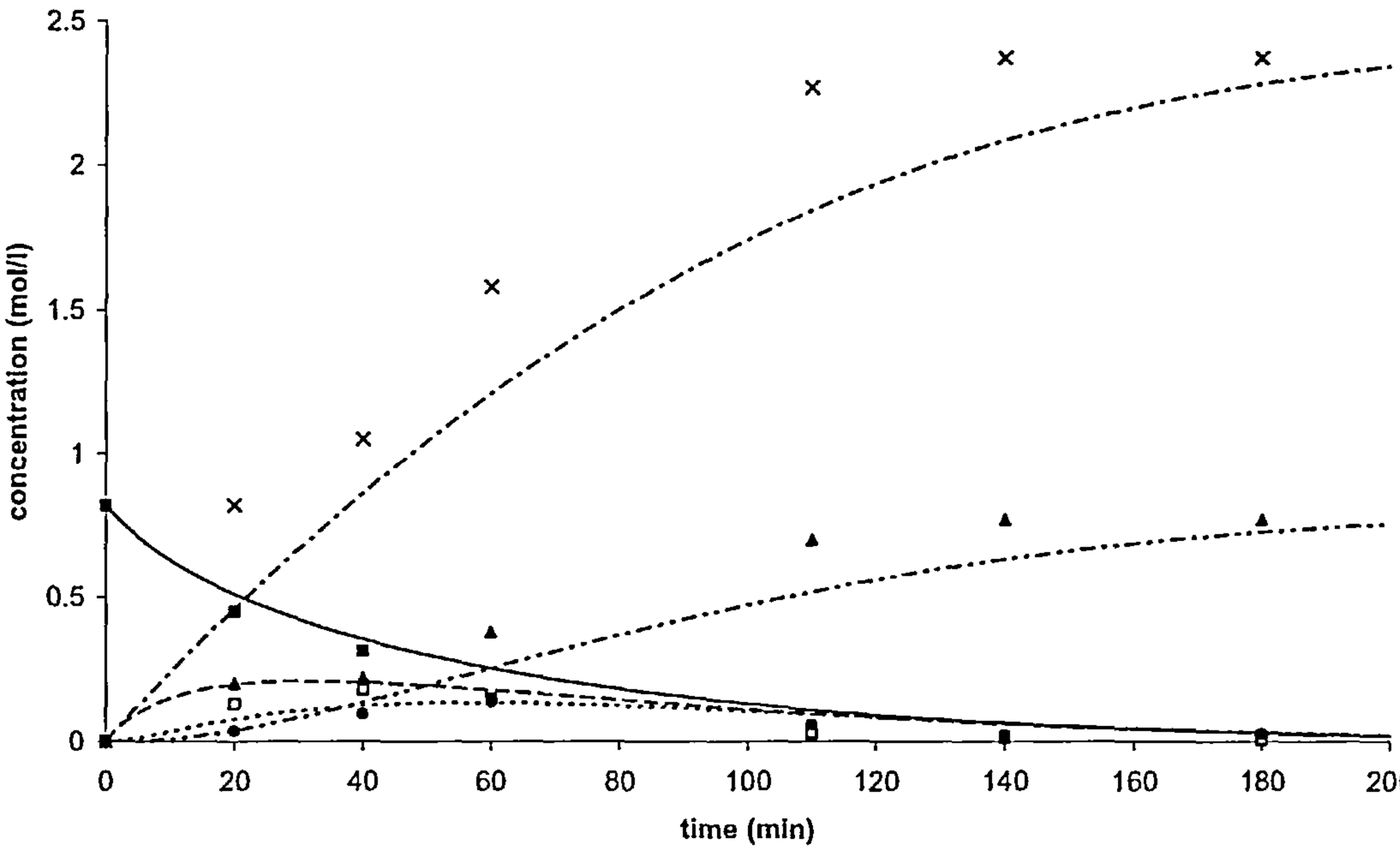

Figure 4.61: Eley-Rideal kinetics for Li-CaO catalysed reaction, K=30 l/mol for partial glycerides, 3 l/mol for other species, TG —, DG – – –, MG ····, Biodiesel-·-·-, glycerol -··-··

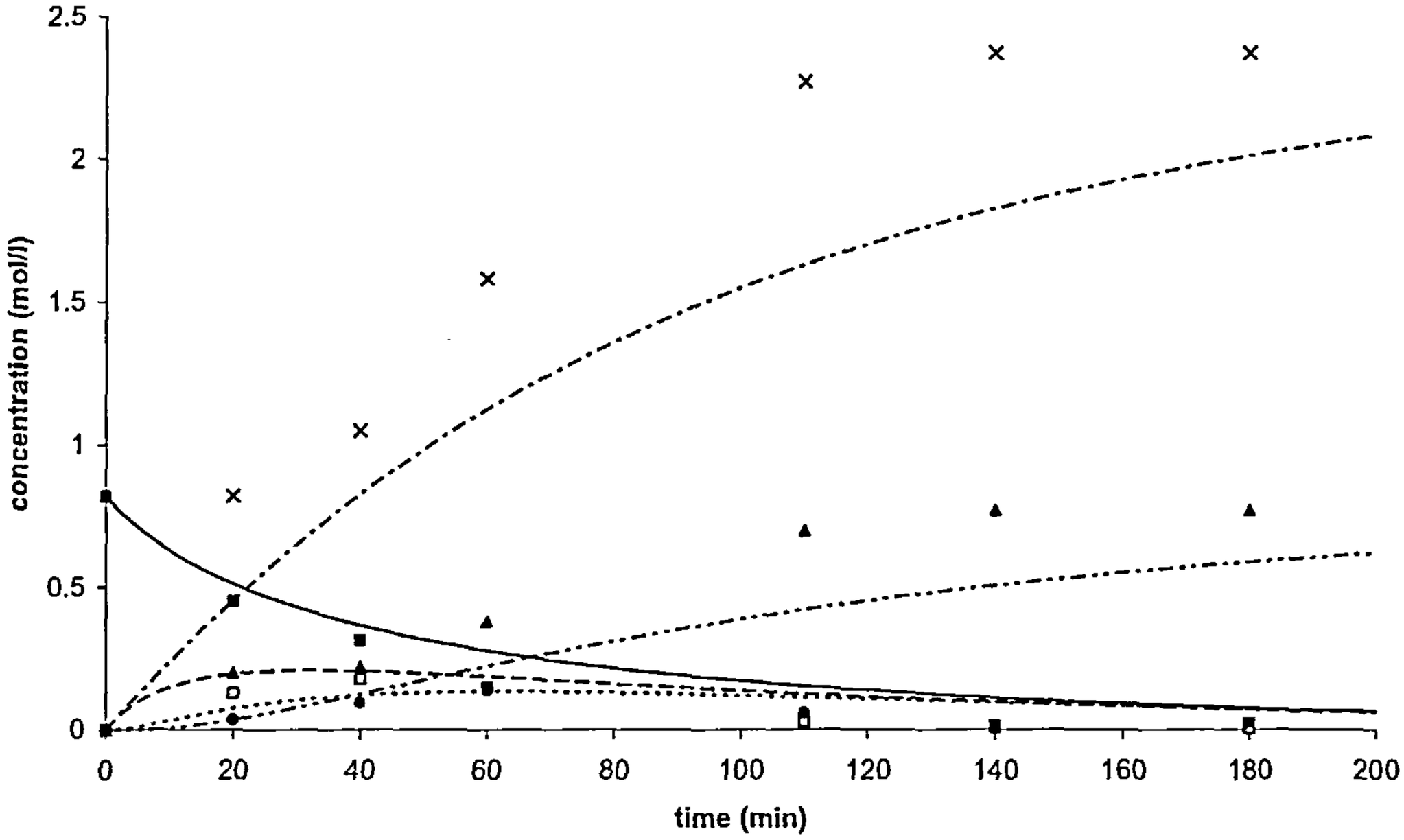

Figure 4.62: Eley-Rideal kinetics for Li-CaO catalysed reaction, K=0.03 for glycerol and partial glycerides, 0.003 for methanol, TG —, DG - - -, MG ···, Biodiesel-·-·-, glycerol -··-

4.7.4 External mass transfer

The rates of reaction using the rate constants for the Li-CaO catalysed reaction at conversions of 0%, 50% and 90% were compared to the rate of mass transfer to the particle surface. The rate of mass transfer was calculated with different diffusivities representing different scenarios for transport of triglycerides to the particle surface:

- Triglyceride in methanol, D=5x10^{-10} m^2/s
- Triglyceride in biodiesel, D=3x10^{-11} m^2/s
- Triglyceride in glycerol, D=3x10^{-13} m^2/s

Mass transfer rates were calculated by assuming that the Sherwood number was 2, as was previously used to calculate mass transfer rates in a solid catalysed slurry-type reactor (Kumbhar and Yadav, 1989). As a Sherwood number of 2 represents a stagnant environment, it is likely that the mass transfer coefficient has been significantly under-estimated at 0% conversion and 50% conversion. At 90% conversion, however, it is likely

that the glycerol coating can form a pseudo-stagnant environment (Moo-Young and Blanch, 1989), and the assumption of Sh=2 is correct.

A comparison between rates of reaction and external mass transport is presented in Table 4.30. If we assume that initially the triglyceride diffuses through methanol to reach the catalyst surface, the rate of mass transfer is greater than the rate of reaction so the reaction is reaction controlled. However as the reaction progresses it is more likely that the triglyceride diffuses through biodiesel, and this rate of mass transfer is in the same order of magnitude as the rate of reaction. Allowing for the increase in mass transfer coefficient due to the agitation of the system, the initial and mid stages of the reaction are not limited by external mass transfer. As the reaction nears completion, the triglyceride may have to diffuse through glycerol to reach the catalyst, and this rate of mass transfer is slow, approximately one order of magnitude slower than the rate of reaction at 90 % conversion. The impedance of the reaction by a glycerol layer has already been noted (Dossat *et al.*, 1999; Bondioli,, 2004). This transport limitation through glycerol could prevent a conversion of >95% being reached, and this conversion is required to reach the glyceride content specified in EN14214, without subsequent removal of glycerides.

Table 4.30: comparison of rates of reaction and rate of external mass transport to catalyst surface

External mass transfer		Rate of reaction	
Scenario	Rate (mol/l/s)	Scenario	Rate (mol/l/s)
Triglyceride in methanol	1.0×10^{-3}	0% conversion	4.6×10^{-4}
Triglyceride in biodiesel	3.6×10^{-4}	50% conversion	1.2×10^{-4}
Triglyceride in glycerol	7.2×10^{-7}	90% conversion	4.6×10^{-6}

4.7.5 Effectiveness factor

The effectiveness factor compares the rate of reaction in the absence of intra-particle mass transfer limitation to the rate of reaction observed. The effectiveness factor η is calculated from the Thiele modulus ø as described in equations 4.2 and 4.3.

$$\eta = \frac{\tanh \phi}{\phi} \qquad [4.2]$$

$$\phi = \frac{1}{3}\sqrt{\frac{(n+1)k_v C_s^{n-1}}{2D_e}} \qquad [4.3]$$

The effective diffusivity D_e can be calculated from the relation with pore size as described in equation 4.4, where ε is the voidage of the catalyst, τ is the tortuosity, α is the radius of the molecule and β is the radius of the pore (Jonker *et al.*, 1998).

$$D_e = D \times \frac{\varepsilon}{\tau} \times 10^{\frac{-\alpha}{\beta}} \qquad [4.4]$$

Figure 4.64 shows the effect of particle diameter on effectiveness factor when the diffusivity considered is oil in methanol. In this case the effectiveness factor is near 1 for particle sizes up to 1 mm. Figure 4.64 shows the effect of particle diameter on effectiveness factor when the diffusivity considered is oil in biodiesel. In this case the effectiveness factor is close to 1 for particle sizes up to 100 μm. Finally, Figure 4.65 shows the effect of particle diameter on effectiveness factor when the diffusivity considered in oil in oil. In this case the effectiveness factor starts to decrease at particle sizes above 10 μm.

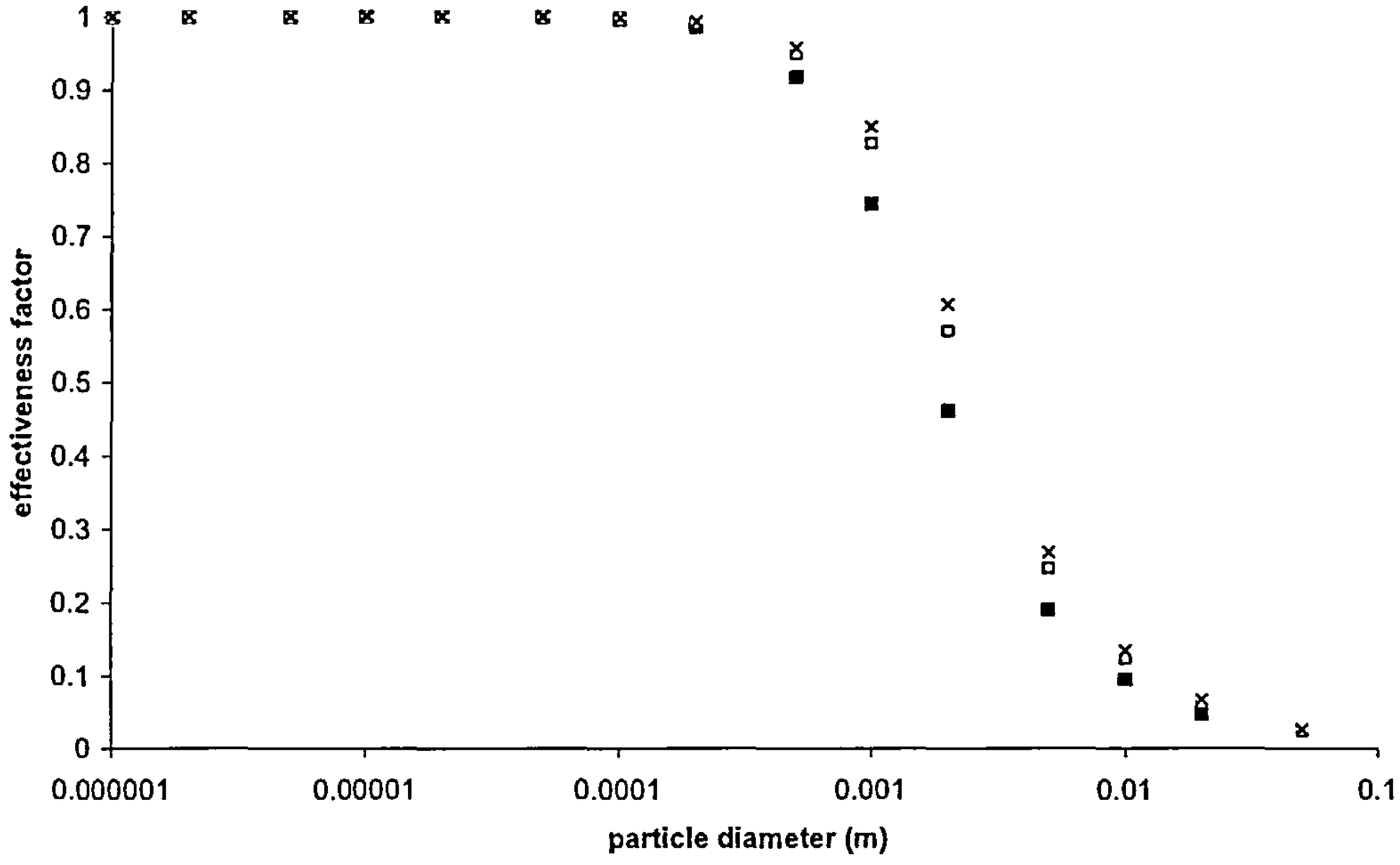

Figure 4.63: Effectiveness factor versus particle diameter at different pore sizes. D=$5x10^{-10}$ representative of oil in methanolize/pore size), x - pore size 150 Å, □ - pore size 60 Å, ■ - pore size 20 Å

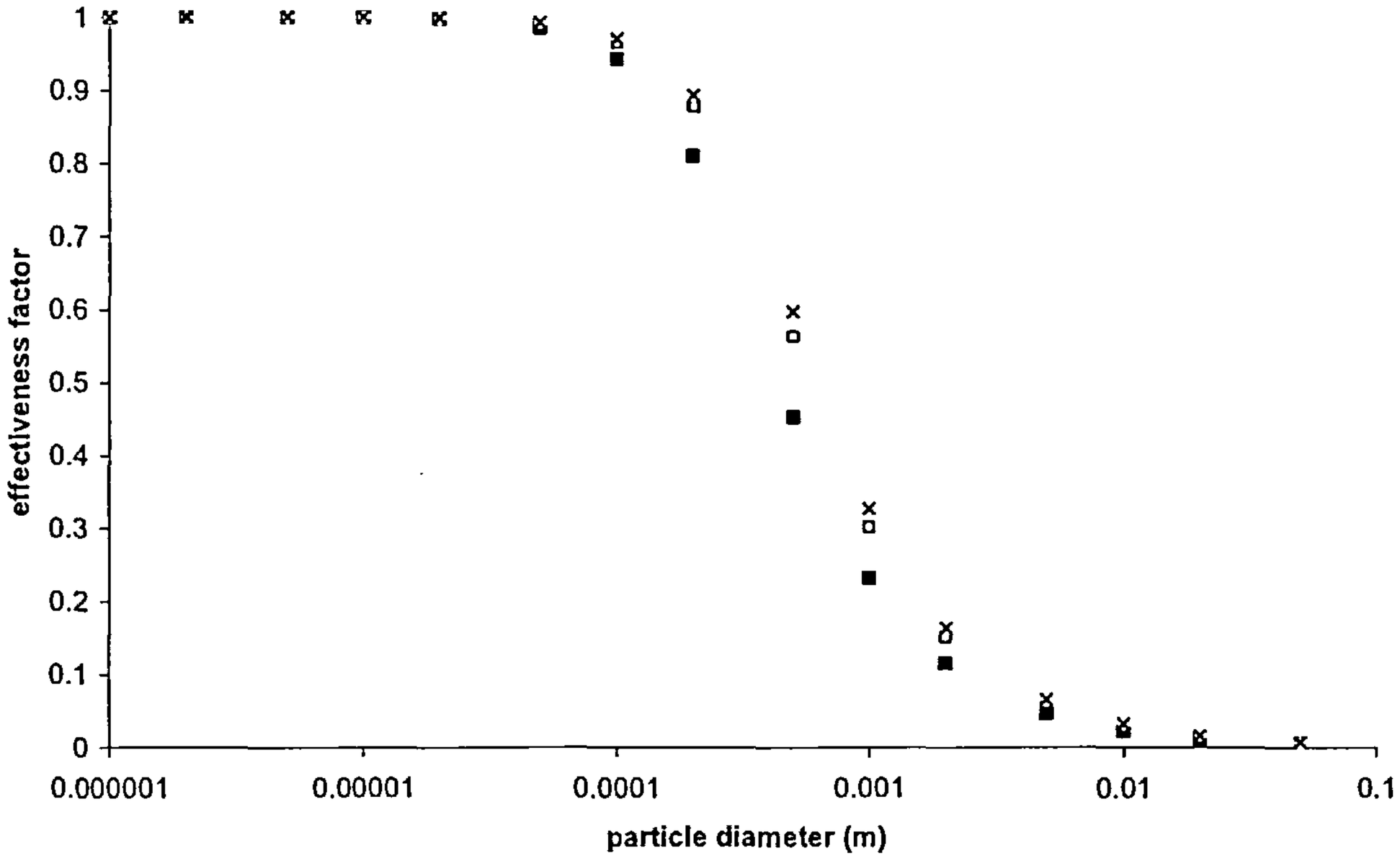

Figure 4.64: Effectiveness factor versus particle diameter at different pore sizes. D=$3x10^{-11}$ representative of oil in biodiesel, x - pore size 150 Å, □ - pore size 60 Å, ■ - pore size 20 Å

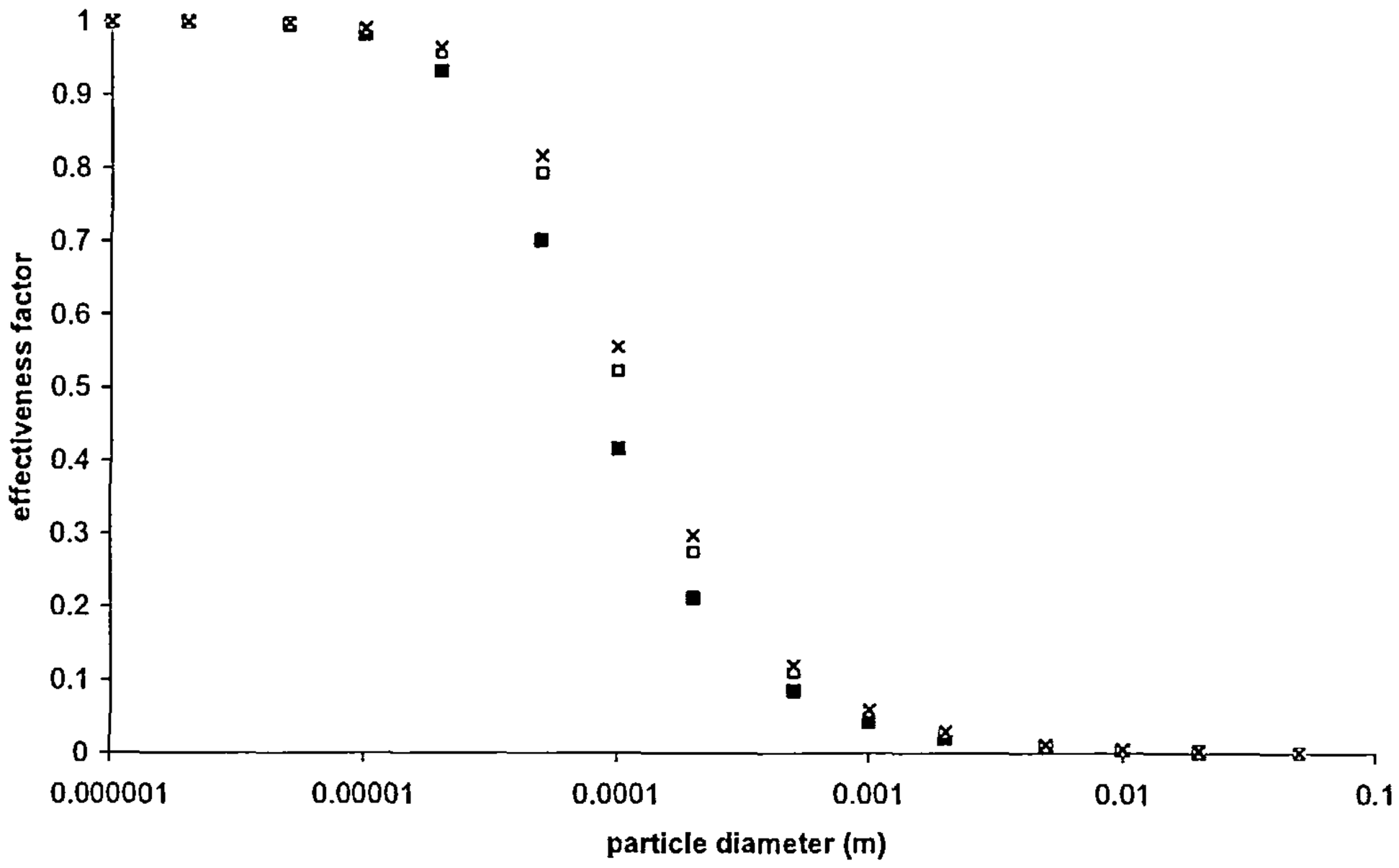

Figure 4.65: Effectiveness factor versus particle diameter at different pore sizes. D=1x10^{-12} representative of oil in oil, x - pore size 150 Å, □ - pore size 60 Å, ■ - pore size 20 Å

The effective diffusivity used for these effectiveness factor calculations may be rather large, as the voidage and tortuosity have not been taken into consideration. This means effectiveness factors will be smaller than those presented. An intraparticle diffusion coefficient of D_e=4x10^{-12} m^2/s was calculated from observation of intraparticle diffusion in trioleate hydrogenation in medium pore catalysts (Jonker *et al.*, 1998). This is of the same order of magnitude as the diffusivity value used in figure 4.65. Thus we can expect that the effectiveness factor to be in the region of that predicted by figure 4.65. This means that catalyst particles with diameters less than 50 μm should be used, if intraparticle diffusion limitations are to be avoided. Working with this size of catalyst will cause difficulties with separating the catalyst particles from the reaction mixture, as pressure drop on the filter increases with decreasing particle size (Sioutas *et al.*, 1999). In fact, materials with particle diameters < 50 μm become difficult to handle (Sherrington, 1980 a). Catalysts with dimaters significantly larger than 10 μm can be expected to have significant intraparticle mass transfer limitations. This is seen in the transesterification of vegetable oil using

Amberlyst 26 as catalyst, where only a small conversion was obtained (section 4.5), but using triacetin, which will have a higher diffusivity, the conversion is larger (Liu *et al.*, 2007).

The effect of pore size on effectiveness factor is as expected, the rate of reaction will increase with increasing pore size. However, the model cannot show when the triglyceride molecule cannot physically fit inside the pores. This may be the case for the 20 Å pore size material, because the diameter of the triglyceride molecule itself is 16 Å. To maximize the rate of reaction it is necessary to use a large pore material with a small particle diameter.

4.7.6 Summary of findings from modelled data

The batch reaction profiles for the alkali-doped oxides can be described by second order homogeneous kinetics, as would be expected because it has been shown that these catalysts also have a significant homogeneous contribution to their activity. However, the fit between modelled and real data is not within experimental error, so the 2nd order model may not be the best representation of the kinetics. The sum of squares error was found to be lowest for Eley-Rideal kinetics for the Li-CaO catalysed reaction. The Eley-Rideal model has several limitations for describing the alkali-doped metal oxide catalysed reaction, the first being that the reaction is not fully heterogeneous. Secondly the adsorption coefficient was estimated using a literature value and taken as constant for the various adsorbing species with widely varying sizes. The effect of the different sizes of the components on surface coverage was also not taken into account.

The adsorption coefficients of glycerol and partial glycerides were increased to evaluate the effect on the reaction profile. Increasing the adsorption coefficient of these species increased the rate of the back reaction and so decreased the conversion.

Mass transport will be a limiting factor in this heterogeneously catalysed reaction. It has been shown that as the reaction reaches high conversion, the reaction goes from being reaction rate limited to mass transfer limited. When the reaction nears completion the rate of mass transfer to the surface of the catalyst particle is very slow, because the catalyst is coated in glycerol which has a high viscosity. Intra-particle diffusion is also slow and this

will necessitate the use of particles with small diameters. For example, the effectiveness factor at a diameter of 0.5 mm, the typical diameter of an ion exchange resin bead is 0.1.

This means in designing a heterogeneous catalyst for biodiesel production, the catalyst particles must be small, and this would make magnetic supported catalysts suitable for this reaction. Functionalization of the surface to make it hydrophobic would also be desirable to stop the glycerol layer being formed. If an active heterogeneous catalyst is found, the challenge may be achieving >95% conversion.

4.8 Costings

4.8.1.1 Capital cost

Using the process model to estimate biodiesel production costs by Haas *et al.* (2006) it was possible to estimate the capital cost of biodiesel production for 5 different catalyst scenarios:

1 ideal heterogeneous catalyst. The catalyst does not leach, does not lose activity and requires the same residence time for full conversion as NaOMe (1 h)
2 heterogeneous catalyst, with increased reaction time. The catalyst does not leach, does not lose activity but requires a residence time three times larger than that for NaOMe (3 h)
3 heterogeneous catalyst, but higher reaction temperature required. Similar to Esterfip-H process. The catalyst does not leach and does not lose activity.
4 LiCaO calcined type heterogeneous catalyst. The catalyst leaches, and can only catalyse 3 cycles in batch operation. Dissolved metals must be removed from biodiesel.
5 NaOMe catalysed reaction – standard process.

Significant changes can be made to a biodiesel production flowsheet when an ideal heterogeneous catalyst is used, as shown in figure 1.5. The catalyst remains in the reactor, so no neutralization and washing steps are required. Further, as the catalyst has been completely removed, the back reaction cannot occur, so the biodiesel and glycerol do not need to be separated before the excess methanol removed, so only one unit operation is required to recycle all of the excess methanol. This means that for the heterogeneous catalysts the steps dealing with neutralization and washing can be eliminated. The glycerol distillation steps are also removed because there is no neutralization and washing, and also because the methanol is removed from the combined glycerol/biodiesel stream before the settling tank.

No allowance for the costs of solids handling equipment has been made in this analysis and for the case of an ideal heterogeneous catalyst it has been assumed that the lifetime is infinite.

As expected, the greatest saving achieved is for the ideal heterogeneous catalyst. Increasing the residence time required only increases the capital costs by a small amount. A heterogeneously catalysed process requiring high temperatures also offers a significant saving on capital costs compared to the conventional process. Unfortunately, the capital costs saving on using a Li-CaO calcined catalysed process is negligible, and this is because the catalyst leaches so the washing stages are still required, so the number of unit operations required is not reduced.

Table 4.31 Capital Costs in 1000 US$ for process equipment based on a 37.8 kte/year plant. Data taken from Haas *et al.*, 2006.

Item	Cost – NaOMe catalysed	Cost – ideal heterogeneous catalyst	Cost – heterogeneous catalyst, 3x residence time	Cost – heterogeneous catalyst, high temperature	Cost – LiCaO (cal) catalysed process
Storage (oil, biodiesel, methanol)	1047	1047	1047	1047	1047
Methanol storage tank	24	24	24	24	24
Sodium methoxide tank	25				
Methanol catalyst mixer	7				
Reactor 1 preheater	3	3	3	3	3
Reactor 1	70	70	105	140	70
Glycerol biodiesel separator 1	311	311	311	311	311
Reactor 2 preheater	9	9	9	9	9
Reactor 2	61	61	95	122	61
Glycerol biodiesel separator 2	315	315	315	315	315
Biodiesel HCl mixer	7				7
Biodiesel wash tank	35				35
Biodiesel wash water separator	328				328

	Cost – NaOMe catalysed	Cost – ideal heterogeneous catalyst	Cost – heterogeneous catalyst, 3x residence time	Cost – heterogeneous catalyst, high temperature	Cost – LiCaO (calcined) catalysed process
Biodiesel final water removal preheater	9				9
Biodiesel final water removal heater	2				2
Biodiesel final water removal flash tank	15				15
Biodiesel final water removal vacuum system	75				75
Glycerol methanol tank	6	6	6	6	6
Methanol distillation tower preheater	4				4
Methanol distillation tower	95				95
Distillation reboiler	5				5
Distillation condensor	13				13
Glycerol fatty acid separator	174				174
Fattyacid storage tank	10				10
NaOHmix feeder	5				5
Glycerol NaOH mix tank	6				6
Glycerol distillation tower	16				16

	Cost – NaOMe catalysed	Cost – ideal heterogeneous catalyst	Cost – heterogeneous catalyst, 3x residence time	Cost – heterogeneous catalyst, high temperature	Cost – LiCaO (calcined) catalysed process
Glycerol distillation reboiler	26				26
Glycerol distillation condensor	2				2
Glycerol distillation postcondensor	13				13
Pumps	62	62	62	62	62
Additonal process equipment	433	433	433	433	433
Cooling tower systen	174	174	174	348	174
Steam generation system	104	104	104	210	104
Instrument air system	25	25	25	25	25
Electrical distribution system	100	100	100	100	100
Total equipment	3616	2744	2813	3093	3584
installation	7232	5488	5626	6186	7168
rail siding	500	500	500	500	500
Total	**11348**	**8732**	**8939**	**9779**	**11252**
Saving %	**0**	**23**	**21**	**14**	**1**

4.8.1.2 Operating costs

Tables 4.33 to 4.36 are comparisons of the raw material and operating costs per kg of biodiesel produced for different catalysts. This includes: disposal costs for spent solid catalyst, soap and waste water; steam costs and losses due to saponification. The lifetime of heterogeneous catalyst has been assumed to be infinite.

Table: 4.32 Operating costs for NaOMe catalysed

Item	Price £/kg	require kg / kg biodiesel	Price £/ kg biodiesel
methanol (a)	-0.27	0.097	-0.026
oil (b)	-0.26	1	-0.26
NaOMe (c)	-0.693	0.016	-0.011
CaO (d)	-3.68		
$LiNO_3$ (d)	-25		
soap (e)	-0.021	0.0015 (k)	-0.00003
wash water (f)	-0.06	0.1 (l)	-0.006
spent catalyst (e)	-0.021		
biodiesel (g)	0.45	0.985	0.443
glycerol (h)	0.3	0.1	
crude glycerol (i)	0.06	0.1	0.006
steam (j)	-0.007		
process water (j)	-0.0006	0.1	-0.00006
balance/ kg biodiesel			0.145

Table 4.33: Operating costs for ideal heterogeneous process

Item	Price £/kg	require kg / kg biodiesel	Price £/ kg biodiesel
methanol	-0.27	0.108	-0.029
oil	-0.26	1	-0.26
NaOMe	-0.693		
CaO	-3.68		
$LiNO_3$	-25		
soap	-0.021		
wash water	-0.06		
spent catalyst	-0.021		
biodiesel	0.45	1	0.45
glycerol	0.3	0.1	0.03
crude glycerol	0.06		
steam	-0.007		
process water	-0.0006		
balance/ kg biodiesel			0.191

Table 4.34 Operating costs for high temperature

Item	Cost £/kg	require kg / kg biodiesel	Cost £/ kg biodiesel
methanol	-0.27	0.108	-0.029
oil	-0.26	1	-0.26
NaOMe	-0.693		
CaO	-3.68		
$LiNO_3$	-25		
soap	-0.021		
wash water	-0.06		
spent catalyst	-0.021		
biodiesel	0.45	1	0.45
glycerol	0.3	0.1	0.03
crude glycerol	0.06		
steam	-0.007	0.5	-0.004
process water	-0.0006	0.5	-0.0003
balance/ kg biodiesel			0.187

Table 4.35 Operating costs for LiCaO calcined (3 cycles of use)

Item	Cost £/kg	require kg / kg biodiesel	Cost £/ kg biodiesel
methanol	-0.27	0.108	-0.029
oil	-0.26	1	-0.26
NaOMe	-0.693		
CaO	-3.68	0.07	-0.025
$LiNO_3$	-25	0.0003	-0.008
soap	-0.021	0.0015	-0.00003
wash water	-0.06	0.1	-0.003
spent catalyst	-0.021	0.007	-0.00014
biodiesel	0.45	0.985	0.443
glycerol	0.3		
crude glycerol	0.06	0.1	0.006
steam	-0.007		
process water	-0.0006	0.1	-0.00006
balance/ kg biodiesel			0.124

(a) Methanex, 2007

(b) Haas *et al.*, 2006

(c) Lawrence, P., (Degussa), Personal communication, January 2007

(d) Spectrum Chemicals, 2007

(e) Landfill tax, HM Revenue and Customs, 2007

(f) Trade effluent standard rate, Southwest Water, 2007

(g) Fuel retail price (95.9 p/l as of January 2007 less VAT and Fuel Excise duty (28.35 p/l as of January 2007) HM Revenue and Customs, 2007

(h) ICIS pricing,2007

(i) Dorado *et al.*, 2006

(j) Sinnott, 1999

(k) Vicente *et al.*, 2005

(l) Dorado *et al.*, 2004

According to this analysis, it is less economic to use Li-CaO calcined catalyst than NaOMe. If the catalyst had a longer lifetime then Li-CaO calcined may become viable. Figure 4.66 shows the effect of number of cycles of reuse on the profit/loss per kg of biodiesel (excluding capital costs). At 9 cycles of reuse the catalyst becomes equally economically viable with NaOMe, and above that number of cycles, it is more economically viable to use a Li-CaO calcined type catalyst. The dominant cost is the cost of the feedstock oil, and the profit per kg biodiesel is sensitive to the cost of the oil and also to the yield of biodiesel obtained. The heterogeneous catalysts achieve a higher profit per kg of biodiesel, firstly because the glycerol is sold at a higher grade, and secondly it is assumed there is a 100% yield of biodiesel, because no saponification occurs.

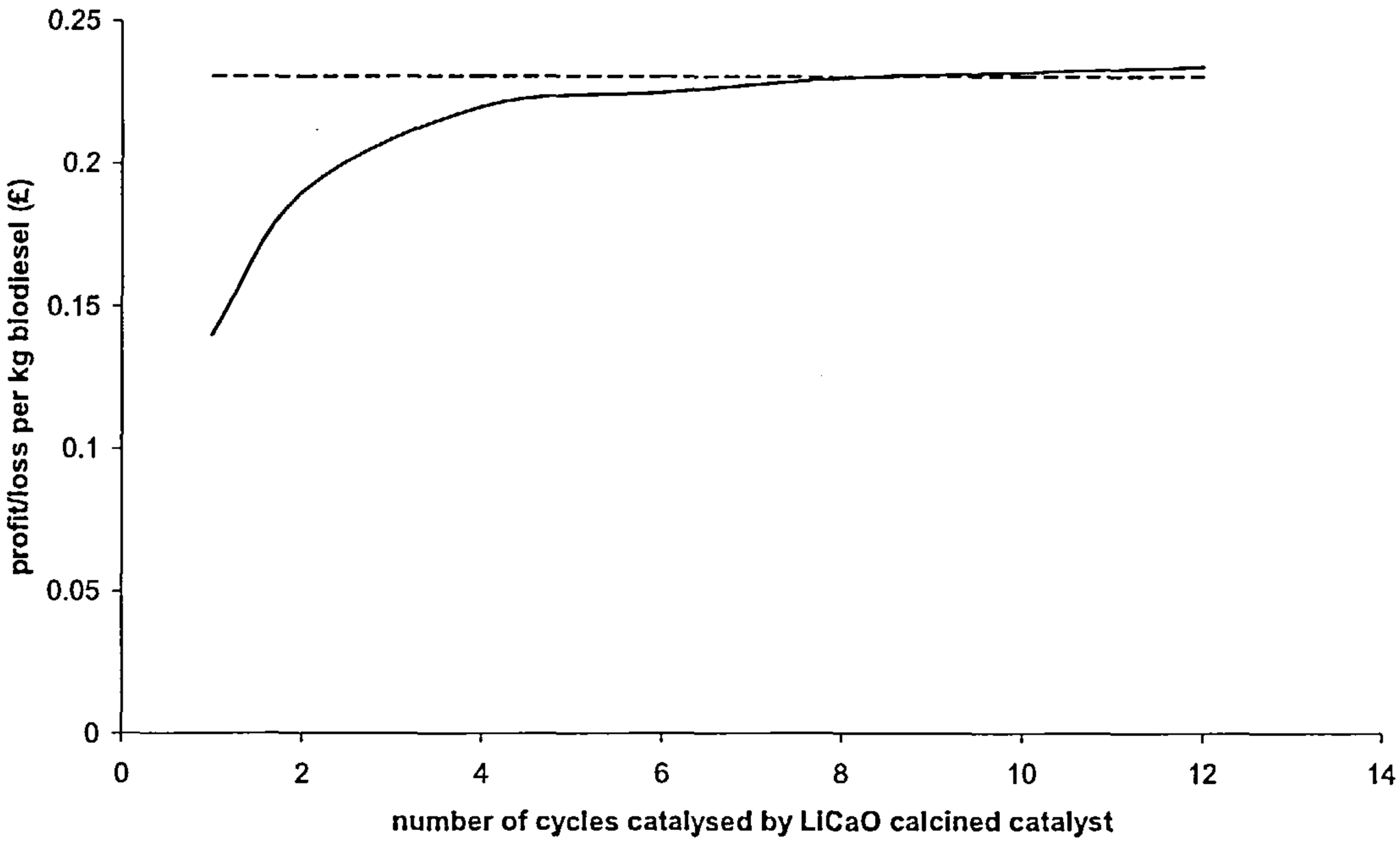

Figure 4.66: Effect of number of cycle for which Li-CaO catalyst can be reused on balance of operating costs and sale prices

5 Conclusions and Further Work

Design of a biodiesel production process is relatively easy, but design of a heterogeneous catalyst for biodiesel production is not. The catalyst must be active, stable and relatively easy to procure on a large scale. The transesterification reaction between methanol and vegetable oils is difficult to design a catalyst for because:

- triglycerides are bulky molecules, so internal diffusion limitations are significant
- the reactants are initially in 2 phases and have very different polarities
- the polar character of the undesired co-product, glycerol, could limit conversion
- real feedstocks contain acid and water which may deactivate catalysts

The stability to leaching of the catalyst is difficult to achieve because methanol is a polar reagent and will dissolve many species. This means that leaching of catalytic species is likely from catalysts. It has been shown that alkali-doped metal oxides, supported guanidines and sulfonated polystyrenes leach into methanol, precluding their use as heterogeneous catalysts. These catalysts were found to be active, but because they leach, the advantages of using a heterogeneous catalyst are lost. An economic analysis showed that use of an ideal heterogeneous catalyst would reduce capital cost by 24 % and operating costs by 32 %. However, use of a catalyst which leaches does not reduce the capital costs and the operating costs only break even with operating costs of an NaOMe catalysed process if the catalyst can be recycled 9 times.

5.1 Acidic Catalysts

Acidic catalysts were tested for their activity for the transesterification of vegetable oil and esterification of free fatty acid. None of the catalysts were active for transesterification, but all 3 showed activity for the esterification of free fatty acid. Sulfonated polyHIPE and montmorillonite were found to leach into methanol, but Amberlyst 46, a sulfonic acid ion-exchange resin, was stable to leaching. Using Amberlyst 46 a conversion of 72 % could be achieved in 5 hours at 80 °C with a 9-fold excess of methanol.

5.2 Alkali-doped metal oxides

Alkali-doped metal oxides were found to be very active for the transesterification of vegetable oils at 60 °C, and the timescale required to reach >90% conversion was practical for use at an industrial level (~ 3 hours). There was a strong correlation between base strength and activity, as in previous studies (Kim *et al.*, 2004, Suppes *et al.*, 2004). Only catalysts with base strength $pK_{BH+}>11$ were active, namely Li-CaO, Na-CaO, K-CaO, calcined Li-CaO, calcined Na-CaO, calcined K-CaO and calcined Li-MgO. The calcined catalysts were found to be more active than non-calcined, which was attributed to the decomposition of $CaCO_3$ to CaO and the higher temperature increasing the mobility of the alkali-metal atoms to increase the number of defect sites formed in the CaO lattice. The origin of the catalytic activity of Li-MgO calcined was from the decomposition of $LiNO_3$ to LiOH and Li_2O.

However, these catalysts were found to leach active species into methanol. Significant concentrations of alkali metal and support metal were found in the final reaction mixture. It was shown that part of the activity of these catalysts is due to the activity of these homogeneous species, because:

- The leachate from the catalysts into methanol was found to be catalytically active
- There was a correlation between soluble basicity and catalytic activity of the catalysts
- Concentrations of dissolved LiOH equivalent to the concentration of Li found in the final reaction mixture were catalytically active

As previously discussed, the advantages of using a heterogeneous catalyst are severely reduced if it leaches and therefore, these catalysts would not be suitable for biodiesel production.

5.3 Other transesterification catalysts

Other catalysts tested for transesterification were silica supported TBD, an anionic ion exchange resin and magnetic supported catalysts:

- TBD, an organic base was covalently anchored to mesoporous silica. Conversions in excess of 80% were achieved in 3 hours, but with a relatively high loading of catalyst (5 mol%) . The high loading of catalyst and relative difficulty and therefore high cost of making this catalyst meant that it was vital that the lifetime of this catalyst was long. Unfortunately, the catalytically active TBD species were found to leach into methanol and the reaction mixture so the catalyst could not be reused.

- Amberlyst 26, a quaternary ammonium functionalized ion exchange resin was found to be stable to leaching into methanol. However, the activity of Amberlyst 26 for the transesterification of triglyceride is very low: after 3 hours a conversion of 8% was reached. This is due to internal diffusion limitations, because the effectiveness factor for this reaction is low for ion-exchange resin beads.

- Magnetic catalysts were evaluated because they can be easily separated from the reaction mixture even at small particle diameters. This means the internal diffusion limitation can be minimised. Tin-doped magnetite reached a conversion of 13% in 6 hours, and a shell-and-core magnetic supported catalyst with a SnO shell reached a conversion of 26 % in 3 hours.

5.4 Modelling catalytic performance

2^{nd} order kinetic models were fitted to the batch reaction data for the alkali-doped metal oxides with a reasonable fit. The batch reaction profile for the Li-CaO catalysed reaction was also fitted to Eley-Rideal and Langmuir-Hinshelwood kinetics. The sum of squared errors was lowest for the Eley-Rideal model, so this was the best model to describe the kinetics of the reaction. The value of the adsorption coefficient was taken from a literature value for a similar reaction, so there is some degree of uncertainty in its value, especially because the adsorbed species have very different sizes and polarities. The effect of increasing the value of the adsorption coefficient for glycerol and partial glycerides was to decrease the conversion to biodiesel.

The rate of mass transfer to the catalyst surface was compared with the rate of reaction, and at high conversions the reaction was shown to be mass transfer controlled. Transport through a glycerol layer will be very slow, so it would be desirable to minimise formation of this glycerol layer by functionalizing the catalyst surface with hydrophobic species. Internal diffusion was also found to be limiting when the particle diameter was greater than 50 μm. This means a small particle diameter material with large pores should be used as a catalyst support.

5.5 Further Work

There are few examples in the literature of successful heterogeneous catalysts for biodiesel production. The zinc aluminate catalyst used in the Esterfip-H process is one example. However, the relatively slow take-up of this process by the biodiesel industry may indicate that the benefits of the high-temperature heterogeneous process are not sufficient for producers to consider it.

A catalyst which may be suitable for a lower temperature process is Zn-arginate. Peter *et al.* (2002) showed that Zn-arginate was stable to leaching into methanol and reached a conversion of 70% in 3 hours at 75 °C. The activity of Zn-arginate is sufficient that the reaction times are not prohibitively long and therefore its stability and performance in different reactors should be investigated further.

Magnetic supported catalysts are an interesting class of catalyst for biodiesel production because small particles can be used without encountering difficulties in separation. Many different species can be supported on the magnetic core including:

- Magnetic core plus quaternary ammonium functionalized polymer shell
- Magnetic core plus SnO shell attached via deposition of Sn salt on silica

Supporting a quaternary ammonium functionalized polymer on a magnetic support allows a very small particle size to be used, and therefore the internal diffusion will not limit the rate of reaction as it did when the resin beads were used.

The future of the biodiesel industry is not certain, because it is an industry that relies on government subsidies, and if opinion turns against biodiesel then the subsidies might

disappear. Research into alternative processes including ligno-cellulosic ethanol production or gasification of whole-plant biomass may take priority in future.

One niche application where biodiesel will always have a future is conversion of waste oils to biodiesel. In this case an acid catalyst is required, and there exists in the literature some examples of catalysts active for both transesterification and esterification that are stable, namely double metal cyanide complexes and supported heteropoly acids. The reaction times of these catalysts are long, but further investigation of the optimum reaction conditions could reduce the reaction time. Future research should focus on the application of solid acid catalysts to the production of biodiesel from waste oils.

6 References

Abreu, F., Hamu E.H., Einloft, S., Rubim, J.C. and Suarez P.A.Z. (2003), 'New metal catalysts for soybean oil transesterification', *Journal of the American Oil Chemists' Society*, vol 80, pp 601-604

Akay, G., Birch, M., Bokhari, M., 2004, 'Microcellular polyHIPE polymer supports osteoblast growth and bone formation in vitro' *Biomaterials,* vol 25, pp 3991-4000.

Aramandia, M., Borau, V., Jimenez, V., Marinas, A., Marinas, J., Ruiz, J., Urbano, F. (2004), 'Magnesium containing mixed oxides as basic catalysts: base characterization by carbon dioxide TPD-MS and test reactions', *Journal of Molecular Catalysis A: Chemical,* vol 218, pp 81-90

Augustine, R. (1996) *Heterogeneous Catalysts for the Synthetic Chemist*, Marcel Dekker, New York

Bailer, J., de Heuber, K. (1991), 'Determination of saponifiable glycerol in biodiesel', *Fresenius Journal of Analytical Chemistry*, vol 340, pp186-187

Baronetti, G., Padro, C., Scelza, O., Castro, A. (1993), 'Structure and Reactivity of alkali doped calcium oxide catalysts for oxidative coupling of methane', *Applied Catalysis A: General,* vol 101, pp 167-183

Binitha, N, Sugunan, S, (2006) 'Preparation, characterization and and catalytic activity of titania pillared montmorillonite clays, *Microporous and mesoporous materials,* vol 93, pp82-89

Bondioli, P. (2004), 'The preparation of fatty acid esters by means of catalytic reactions', *Topics in catalysis,* vol 27, pp 77-82

Bournay, L., Hillion, G., Boucot, P., Chodorge, J., Bronner, C., Forestiere, A. (2005). Process for producing alkyl esters from a vegetable or animal oil and an aliphatic monoalcohol. US 6878837 B2. United States.

Brunel, D., Blanc, A., Galarneau, A., Fajula, F. (2002), 'New trends in the design of supported catalysts on mesoporous silicas and their application in fine chemicals', *Catalysis Today,* vol 73, pp 139-152

BSi, 2003, 'Fat and oil derivatives. Fatty acid methyl esters (FAME). Determination of free and total glycerol and mono-, di-, triglyceride contents', BS EN 14105

Cameron, N., Sherrington, D., Ando, I., Kurosou, H., 1996, 'Chemical modification of monolithic poly(styrene-divinylbenzene) polyHIPE materials' *Journal of Materials Chemistry,* vol 6 pp 719-726

Cameron, N. (2005), 'High internal phase emulsion templating as a route to well-defined porous polymers', *Polymer*, vol 46, pp 1439-1449

Cantrell, D., Gillie, L., Lee, A., Wilson, K. (2005), 'Structure-reactivity correlations in MgAl hydrotalcite catalysts for biodiesel synthesis', *Applied Catalysis A: General,* vol 287, pp 183-190

Carloni, S., De Vos, D., Jacobs, P., Maggi, R., Sartori, G., Sartorio, R., (2002), 'Catalytic activity of MCM-41-TBD in the selective preparation of carbamates and unsymmetrical alkyl carbonates from diethyl carbonate', *Journal of catalysis,* vol 205, pp199-204

Chai, F., Cao, F., Zhai, F., Chen, Y., Wang, X., Su, Z. (2007), 'Transesterification of vegetable oil to biodiesel using a heteropolyacid solid catalyst', *Advanced synthesis and Catalysis,* vol 349, pp1057-1065

Chang, C., Wang, C., Kumta, P., (2001), 'Chemical Synthesis and characterization of lithium orthosilicate', *Materials and Design*, vol 22, pp 617-623

Christie, W 1990, *Gas Chromatography and Lipids,* The Oily Press, Ayr

Clacens, J., Genuit, D., Veldurthy, B., Bergeret, G., Delmotte, L., Garcia-Ruiz, A., Figueras, F. (2004), 'CsF supported by α-alumina: an efficient basic catalyst', *Applied Catalysis B: Environmental*, vol 53, pp 95-100

Corma, A., Iborra, S., Miquel, S., Primo, J. (1998), 'Catalysts for the production of fine chemicals', *Journal of catalysis,* vol 173, pp 315-321.

Corma, A., Hamid, S., Iborra, S., Velty, A. (2005), 'Lewis and Bronsted basic active sites on solid catalysts and their role in the synthesis of monoglycerides', *Journal of catalysis*, vol 234, pp 340-347.

Corma, A., Garcia, H., (2006), 'Silica-bound homogeneous catalysts as recoverable and reusable catalysts in organic synthesis', *Advanced Synthesis and Catalysis,* vol 348, pp1391-1412.

Darnako, D., Cheryan, M. (2000), 'Kinetics of Palm oil Transesterification in a batch reactor', *Journal of the American Oil Chemists' Society*, vol 77, pp 1263-1267

Demirbas, A. (2003), 'Biodiesel fuels from vegetable oils via catalytic and non-catalytic supercritical alcohol transesterifications and other methods: a survey', *Energy Conversion and Management,* vol 44, pp 2093-2109

DFT (2007) Department for Transport, 'Biofuels: risks and opportunities', accessed from www.dft.gov.uk, October 2007

Di Serio, M., Tesser, R., Dimiccoli, M., Cammarota, F., Nastasi, M., Santacesaria, E. (2005), 'Synthesis of biodiesel via homogeneous Lewis acid catalyst', *Journal of Molecular Catalysis A:Chemical,* vol 239, pp111-115

Di Serio, M., Cozzolino, M., Minutillo, G., Tesser, R., Santacesaria, E. (2006), 'Transesterification of soybean oil to biodiesel by using heterogeneous basic catalysts', *Industrial and Engineering Chemistry Research,* vol 45, pp 3009-3014.

Di Serio, M., Cozzolino, M., Tesser, R., Patrono, P., Pinzari, F., Bonelli, B., Santacesaria, E. (2007), 'Vanadyl phosphate catalysts in biodiesel production', *Applied Catalysis A: General* , vol 320, pp 1-7.

Diez, V., Apesteguia, C., Di Cosimo, J (2000), 'Acid-base properties and active site requirements for elimination reactions on alkali-promoted MgO catalysts', *Catalysis Today,* vol 63, pp 53-62

Diez, V., Apesteguia, C., Di Cosimo, J., (2006), 'Aldol condenation of citral with acetone on MgO and alkali-promoted MgO catalysts', *Journal of Catalysis*, vol 240, pp235-244.

Dittmar, T., Dimmig, T., Ondruschka B., Heyn, B., Haupt, J. and Lauterbach, M (2003), 'Herstellung von Fettsaeuremethylestern aus Rapsoel und Altfetten im diskontinuierlichen Betrieb', *Chemie Ingenieur Technik,* vol 75, pp 595-601

Dorado, M., Ballesteros, E., Mittelbach, M., Lopez, F. (2004), 'Kinetic parameters affecting the alkali-catalyzed transesterification of used olive oil', *Energy and Fuels,* vol 18, pp1457-1462

Dorado, M., Cruz, F., Palomar, J., Lopez, F. (2006), 'An approach to the economics of two vegetable oil base biofuels in Spain', *Renewable Energy,* vol 31, pp1231-1237

Dossat, V., Combes, D. and Marty, A., (1999), 'Continuous enzymatic transesterification of high oleic sunflower oil in a packed bed reactor: influence of the glycerol production', *Enzyme and microbial technology,* vol 25, pp 194-200

Dossin, T., Reyniers, M., Marin, G. (2005), 'Kinetics of heterogeneously-MgO catalysed transesterification', *Applied catalysis B: Environmental,* vol62, pp35-45

EBB(2007) European Biodiesel Board Statistics, accessed from www.ebb.eu.org, October 2007

Ebiura, T., Echizen, T., Ishikiwa, A., Murai, K., Toshide, B. (2005), 'Selective transesterification of triolein with methanol to methyl oleate and glycerol using alumina loaded with alkali metal salt as a solid-base catalyst', *Applied Catalysis A: General,* vol 283, pp111-116

Ferreira, D., Meneghetti, M., Meneghetti, S., Wolf, C. (2007), 'Methanolysis of soybean oil in the presence of tin(IV) complexes', *Applied Catalysis A: General,* vol 317, pp 58-61

Fessenden, R. and Fessenden, J. (1982) *Organic Chemistry*. Brookes Cole Publishing, Monterey.

Freedman, B., Butterfield, R.O. and Pryde E.H. (1986), 'Transesterification kinetics of soybean oil', *Journal of the American Oil Chemists' Society,* vol 63, pp 1375-1380

Freeman, E., (1956), 'The kinetics of the thermal decomposition of sodium nitrate and the of the reaction between sodium nitrite and oxygen', *Journal of the American Chemical Society,* vol 60, pp1487-1493

Freeman, E.,(1957), 'The kinetics of the thermal decomposition of potassium nitrate and the reaction between potassium nitrite and oxygen' *Journal of the American Chemical Society,* vol 79, pp 838-842

Frondel, M., Peters, J., 'Biodiesel: A new Oildorado', *Energy Policy,* vol 35, pp 1675-1684

Furuta, S., Matsuhashi, H., Arata, K. (2004). "Biodiesel fuel production with solid superacid catalysis in fixed bed reactor under atmospheric pressure." Catalysis Communications 5: 721-723

Gelbard, G., Vielfaure-Joly, F. (2001), 'Polynitrogen strong bases as immobilized catalysts' *Reactive and Functional polymers,* vol 48, pp65-74

Gryglewicz, S. (1999), 'Rapeseed oil methyl esters preparation using heterogeneous catalysts', *Bioresource Technology,* vol 70, pp 249-253

Gryglewicz, S. (2000), 'Alkaline-earth metal compounds as alcoholysis catalysts for ester oil synthesis', *Applied Catalysis A: General,* vol 192, pp 23-28

Guin, D., Baruwati, B., Manorama, S. (2005), 'A simple chemical synthesis of nano-crystalline AFe_2O_4 (A=Fe, Ni, Zn). An efficient catalyst for the selective oxidation of styrene', *Journal of Molecular Catalysis A:Chemical,* vol 242, pp26-31

Haas, M. (2004), 'The interplay between feedstock quality and esterification technology in biodiesel production', *Lipid Technology* , vol 16, pp 7-11

Haas, M., McAloon, A., Yee, W., Foglia, T. (2006), 'A Process model to estimate biodiesel production costs', *Bioreosurce Technology,* vol 97, pp 671-678.

Hagen, J. (1999), *Industrial Catalysis,* Wiley-VCH, Weinheim

Hartman, L. (1956), 'Methanolysis of triglycerides' *Journal of the American Oil Chemists' Society*, vol 33, pp129–132 .

Hattori, H. (1995), 'Heterogeneous basic catalysts' *Chemical Reviews*, vol 95, pp537-558.

HM Revenue and Customs (2007). Accessed from www.customs.hmrc.gov.uk, January 2007.

Hoydonckx, H. E., De Vos, D.E., Chavan, S.A. and Jacobs P.A. (2004), 'Esterification and transesterification of renewable chemicals', *Topics in catalysis* , vol 27, pp 83-96

ICIS Pricing (2007). Accessed from www.icispricing.com, January 2007.

Ito, T., Wang, J., Lin, C., Lunsford, J. (1985), 'Oxidative dimerization of methane over a lithium promoted magnesium oxide catalyst', *Journal of the American Chemcial Society,* vol 107, pp 5062-5068

Jerome, F., Karchafi, G., Adam , I., Barrault, J (2004), '"One pot" and selective synthesis of monoglycerides over homogeneous and heterogeneous guanidine catalysts', *Green Chemistry*, vol 6, pp 72-74.

Jitputti, J., Kitiyanan, B., Rangsunvigit, P., Bunyakiat, K., Attanatho, L., Jenvanitpajakul, P. (2006), 'Transesterification of crude palm kernel oil and crude coconut oil by different solid catalysts', *Chemical Engineering Journal*, vol 116, pp 61-66

Jonker, G., Veldsink, J., Beenackers, A., 1998, 'Intraparticle diffusion limitation in the hydrogenation of monounsaturated oils and their fatty acid methyl esters', *Industrial and Chemical Engineering Research*, vol 36, pp4646-4656

Juan, J., Zhang, J., Yarmo, M., (2007), '12 Tungstophosphoric acid supported on MCM-41 for esterification of fatty acid under solvent free conditions', *Journal of Molecular Catalysis A: Chemical*, vol 267, pp 265-271

Kantam, M., Sreekanth, P., (2001), 'Transesterification of β-keto esters catalysed by basic porous materials', *Catalysis Letters,* vol 77, pp241-243

Khumbar, P., Yadav, G., (1989), 'Catalysis by sulfur-promoted superacidic zirconia: condensation reactions of hydroquinone with aniline and substituted anilines', *Chemical Engineering Science*, vol 44, pp 2535-2544

Kim, H., Kang, B., Kim, M., Park, Y.M., Kim, D., Lee, J. and Lee, K. (2004), 'Transesterification of vegetable oil to biodiesel using heterogeneous base catalyst', *Catalysis today,* vol 93-95, pp 315-320

Kharchafi, G., Jerome, F., Adam, I, Pouilloux, Y., Barrault, J. (2005), 'Design of well balanced hydrophilic-lipophilic catalystic surfaces for the direct and selective monoesterification of various polyols', *New Journal of Chemistry,* vol 29,pp 928-934

Kiss, A., Dimian, A. and Rothenburg, G. (2006), 'Solid acid catalysts for biodiesel production – towards sustainable energy', *Advances in Synthesis and Catalysis,* vol 348, pp 75-81

Kiss, A., Omata, F., Dimian, A., Rothenberg, G. (2006), 'The heterogeneous advantage: biodiesel by catalytic reactive distillation', *Topics in Catalysis*, vol 40, pp 141-150

Koh, L.(2007), 'Potential Habitat and Biodiversity Losses from Intensified Biodiesel Feedstock Production', *Conservation Biology,* vol 21, pp 1373–1375

Kulkarni, M. and Dalai, A. (2006), 'Waste cooking oil- an economical source for biodiesel: a review', *Industrial and Engineering Chemistry Research,* vol 45, pp 2901-2913

Kulkarni, M., Gopinath, R., Meher, L., Dalai, A. (2006), 'Solid acid catalyzed biodiesel production by simultaneous esterification and transesterification', *Green Chemistry,* vol 8, pp 1056-1062

Linssen, T., Cassiers, K., Cool, P., and Vansant, E., 2003, 'Mesoporous templated silicates: an overview of their synthesis, catalytic activation and evaluation of the stability', *Advances in Colloid and Interface Science,* vol 103, pp 121-147.

Liu, Y., Lotero, E., Goodwin, J., Changqing, L., 2007 'Transesterification of triacetin using solid Bronsted bases' *Journal of catalysis,* vol 246, pp 428-433.

Lopez, D., Goodwin, J., Bruce, D., Lotero, E. (2005), 'Transesterification of triacetin with methanol on solid acid and base catalysts', *Applied Catalysis A: General,* vol 295, pp 97-105

Lopez, D., Suwwannakarn, K., Bruce, D., Goodwin, J. (2007), 'Esterification and transesterification on tungstated zirconia: Effect of calcination temperature', *Journal of catalysis,* vol 247, pp 43-50

Lopez Granados, M., Zafra Poves, M., MArtin Alonso, D., Mariscal, R., Cabello Galisteo, F., Moreno-Tost, R., Santamaria, J., Fierro, J. (2007), 'Biodiesel form sunflower oil by using activated calcium oxide', *Applied catalysis B: Environmental*, vol 73, pp 317-326.

Lotero, E., Liu, Y., Lopez, D., Suwannkarn, K., Bruce, D., Goodwin, J. (2005), 'Synthesis of biodiesel via acid catalysis', *Industrial and Engineering Chemical Research,* vol 44, pp 5353-5363

Ma, F., Hanna, M.A. (1999), 'Biodiesel Production: a review', *Bioresource Technology,* vol 70, pp 1-15

Macedo, C., Abreu, F., Tavares, A., Alves, M., Zara, L., Rubin, J., Suarez, P. (2006), 'New heterogeneous metal-oxides based catalyst for vegetable oil transesterification' Journal of the Brazilian Chemical Society, vol 17, pp 1291-1296

MacQuarrie, D. (1999), 'Organically modified hexagonal mesoporous silicas', *Green Chemistry,* vol 1, pp195-198

Martinez-Mera, I., Espinosa-Pesquiera, M., Perez-Hernandez, R., Arena-Alatorre, J. (2007), 'Synthesis of magnetite (Fe_3O_4) nanoparticles without surfactants at room temperature', *Materials Letters*, vol 61, pp 4447-4451

Matsuhashi, H., Oikawa, M., Arata, K., (2000), 'Formation of superbase sites on alkaline earth metal oxides by doping alkali metals', *Langmuir,* vol 16, pp8201-8205

Mazzochia, C., Modica, G., Kaddouri, A.,Nannicini, R. (2004), 'Fatty acid methyl esters synthesis over heterogeneous catalysts in the presence of microwaves', *Comptes Rendus Chimie*, vol 7, pp 601-605.

Mbaraka, I. K., Radu, D.R., Lin, V. and Shanks, B.H. (2003), 'Organosulfonic acid-functionalized mesoporous silicas for the esterification of fatty acid' *Journal of Catalysis,* vol 219, pp 329-336

Mbaraka, I., McGuire, K., Shanks, B. (2006), 'Acidic mesoporous silica for the catalytic conversion of fatty acids in beef tallow', *Industrial and Engineering Chemsitry Research,* vol 45, pp 3022-3028

Mdoe, J., Clark, J., Macquarrie, D. (1998), 'Michael additions catalysed by N,N-dimethyl-3-aminopropyl-derivatised amorphous silica and hexagonal mesoporous silica (HMS), *Synlett,* vol 6, pp 625-627

Meher, L., Kulkarni, M., Dalai, A., Naik, S. (2006), 'Transesterification of karanja (Pongamia pinnata) oil by solid basic catalysts', *European Journal of Lipid Science and Technology*, vol 108, pp 389-397

Methanex (2007). Accessed from www.methanex.com, January, 2007.

MME (2007) Brazilian Ministry of Mines and Environment, 'Biodiesel the new fuel from Brasil

Moo-Young, M., Blanch, H. (1981), 'Design of biochemical reactors: mass transfer criteria for simple and complex systems', *Advances in Biochemical Engineering/ Biotechnology,* vol 19, pp 1-61

Narasimharao, K., Brown, D., Lee, A., Newman, A., Siril, P., Taverner, S., Wilson, K. (2007), 'Structure-activity relations in Cs-doped heteropoly acid catalysts for biodiesel production', *Journal of catalysis,* vol 248, pp 226-234

NBB(2007) National Biodiesel Board 'Biodiesel Production Estimate Graph', accessed from www.nbb.org

Noureddini, H., Zhu, D. (1997), 'Kinetics of transesterification of soybean oil', *Journal of the American Oil Chemists' Society*, vol 74, pp 1457-1463

Ono, Y. (2003), 'Solid base catalysts for the synthesis of fine chemicals', *Journal of Catalysis,* vol 216, pp406-415

Otera, J. (1993), 'Transesterification', *Chemical Reviews,* vol 93, pp 1449-1470

Ottens, M., Leene, G., Beenackers, A., Cameron, N., Sherrington, D. (2000), 'PolyHIPE: A new polymeric support for heterogeneous catalytic reactions: Kinetics of hydration of cyclohexene in two- and three- phase systems over a strongly acidic sulfonated polyhipe', *Industrial and Engineering Chemistry Research,* vol 39, pp 259-266

Peter, S., Ganswindt, R., Neuner, H., Weidner, E. (2002), 'Alcoholysis of triacylglycerols by heterogeneous catalysis', *European Journal of Lipid Science and Technology,* vol 104, pp 324-330.

Peters, T., Benes, N., Holmen, A., Keurentjes, J. (2006), 'Comparison of commerical solid acid catalysts for the esterification of acetic acid with butanol', *Applied Catalysis A-General,* vol 297, pp 182-186

Phan, N, Jones, C. (2007), 'Highly accessible catalytic sites on recyclable organosilane-functionalized magnetic nano particles: An alternative to functionalized mesoporous silica catalysts', *Journal of Molecular Catalysis A: Chemical,* vol 253, pp 123-131

Quantochrome (1998), 'Quantochrome NOVA 2000 Instruction Manual'

Ramu, S., Lingaiah, N., Prabhavathi Devi, B., Prasad, R., Suryanarayana, I., Sai Prasad, P. (2004), 'Esterification of palmitic acid with methanol over tungsten oxide supported on zirconia solid acid catalysts:effect of method of preparation of the catalyst on its structural stability and reactivity', *Applied Catalysis A-General,* vol 276, pp 163-168

Rao, B., Caltun, O., Cho, W, Kim, C.O., Kim, C, (2007), 'Synthesis and characterization of mixed ferrite nano-particles', *Journal of magnetism and magnetic particles,* vol 310, pp812-814

Reddy, C., Oshel, R., Verkade, J. (2006), 'Room-temperature cpnversion of soybean oil and poultry fat to biodiesel catalyzed by nanocrystalline calcium oxides', *Energy and Fuels,* vol 20, pp1310-1314

Santacesaria, E, Tesser, R., Di Serio, M., Guida, M., Gaetano, D., Agreda, A. (2007), 'Kinetics and mass transfer of free fatty acids esterification with methanol in a tubular packed bed reactor: a key pre-treatment in biodiesel production' *Industrial and Engienering Chemsitry Research,* vol 46, pp 5113-5121

Schuchardt, U., Vargas, R.M. and Gelbard G. (1996), 'Transesterification of soybean oil catalyzed by alkylguanidines heterogenized on different sustituted polystyrenes', *Journal of Molecular Catalysis A: Chemical,* vol 109, pp 37-44

Schuchardt, U., Sercheli, R. and Vargas R.M. (1997), 'Transesterification of vegetable oils: a review', *Journal of the Brazilian Chemical Society,* vol 9, pp 199-210

Sercheli, R., Vargas,R., Schuchardt, U. (1999), 'Alkylguanidine-catalyzed heterogeneous transesterification of soybean oil', *Journal of the American Oil Chemists' Association,* vol 76, pp1207-1210

Sheldon, R., Wallau, R., Arends, I., Schuchardt, U., 1998, 'Heterogeneous catalysts for liquid–phase oxidations: Philosophers' stones or Trojan horses?' *Accounts of Chemical Research,* vol 31, pp485-493

Sherrington, D. (1980 a), 'Preparation, Functionalization and Characteristics of polymer supports', in P Hodge and D Sherrington (eds.), *Polymer-supported reactions in organic synthesis,* John Wiley and Sons, Chichester

Sherrington, D. (1980 b), 'Catalysis by ion-exchange resins and related materials', in P Hodge and D Sherrington (eds.), *Polymer-supported reactions in organic synthesis,* John Wiley and Sons, Chichester

Shibasaki-Kitakawa, N., Honda, H., Kuribayashi, H., Toda, T., Fukumura, T., Yonemoto, T. (2007), 'Biodiesel production using anionic ion-exchange resin as heterogeneous catalyst', *Bioresource Technology*, vol 98, pp 416-421

Schuhmacher, L., Clark, N., Lyons, D., Marshall, W. (2001a), 'Diesel engine exhausts emissions evaluation of biodiesel blends using a Cummins L10E engine', *Transactions of the American Society of Agricultural Engineers',* vol 44, pp 1461-1464

Schuhmacher, L., Marshall, W., Krahl, J., Wetherell, W., Grabowski, M. (2001b), 'Biodiesel Emissions data from series 60 DDC engines', *Transactions of the American Society of Agricultural Engineers,* vol44, pp1465-1468

Shumaker, J., Crofcheck, C, Tackett, S., Santillan-Jimenez, E., Crocker, M. (2007), 'Biodiesel production from soybean oil using calcined Li-Al layered double hydroxide catalysts', *Catalysis Letters*, vol 115, pp 56-61

Sinnott, R.K. (1999).*Coulson and Richardson's Chemical Engineering Volume 6,* Butterworth Heinemann, London.

Sioutas, C., Joutrakis, P., Wang, P., Babich, P., Wolfson, J., 1999, 'Experimental investigation of pressure drop with particle loading in nuclepore filters, *Aerosol Science and Technology,* vol 30, pp71-83. 264, pp146-152

Southwest Water (2007). Accessed from www.southwestwater.co.uk, January 2007.

Spectrum Chemicals (2007). Accessed from www.spectrumchemicals.co.uk. January, 2007.

Sreepasanth, P., Srivastava, R., Srinivas, D., Ratnasamy, P. (2006), 'Hydrophobic, solid acid catalysts for production of biofuels and lubricants', *Applied Catalysis A: General,* vol 314, pp 148-159.

Srivastava, R., (2007), 'An efficient, eco-friendly process for aldol and Michael reactions of trimethylsilyl enolate over organic base functionalized SBA-15 catalysts, *Journal of Molecular Catalysis A: Chemical,* vol 264, pp146-152

Stevens, P., Li, G., Fan, J., Yen, M., Gao, Y. (2005), 'Recycling of homogeneous Pd catalysts using superparamagnetic nanoparticles as novel soluble supports for Suzuki, Heck, and Sonogashira cross-coupling reactions', *Chemcial Communications,* vol 35, pp4435-4437

Subba Rao, Y., De Vos, D., and Jacobs, P., 1997, '1,5,7-Triazabicyclo[4.4.0] dec-5-ene immobolized in MCM-41: A strongly basic porous catalyst', *Angewandte Chemie International Edition,* vol 36, pp 2661-2663

Suppes, G. J., Dasari, M.A., Doskocil, E.J., Mankidy, P.J. and Goff M.J. (2004), 'Transesterification of soybean oil with zeolite and metal catalysts', *Applied Catalysis A: General,* vol 257, pp 213-223

Tesser, R., Di Serio, M., Guida, M., Nastasi, M., Santacesaria, E. (2005), 'Kinetics of oleic acid esterification with methanol in the presence of triglycerides', *Industrial and Engineering Chemistry Research,* vol 44, pp 7978-7982

Thaler, W. (1983), 'Hydrocarbon soluble sulfonating reagents. Sulfonation of aromatic polymers in hydrocarbon solution using soluble acyl sulfates', *Macromolecules,* vol 16, pp 623-628

UN (2007), 'Sustainable Bioenergy: A Framework for Decision makers', *UN-Energy*

Van Gerpen, J., 2005, 'Biodiesel processing and Production', *Fuel Processing Technology*, vol 86, pp 1097-1107

Vicente, G., Coteron, A., Martinez, M., Aracil, J., (1998), 'Application of the factorial design of experiments and response surface methodology to optimize biodiesel production', *Industrial Crops and Products,* vol 8, pp29-35

Vicente, G., Martinez M. and Aracil, J., (2004) 'Integrated biodiesel production: a comparison of different homogeneous catalyst systems', *Bioresource Technology,* vol 92 pp 297-305

Vicente, G., Martinez, M., Aracil J., Esteban, A. (2005), 'Kinetics of sunflower oil methanolysis', *Industrial and Engineering Chemistry Research,* vol 44, pp 5447-5454

Wang, W., Lyons, D., Clark, N., Gautam, M. (2000), 'Emissions from nine heavy trucks fuelled by diesel and biodiesel belnd without engine modification', *Environmental Science and Technology,* vol 34, 933-939

Watkins R., Lee, A., and Wilson, K., 2004, 'Li-CaO catalysed tri-glyceride transesterification for biodiesel applications', *Green Chemistry,* vol 6, pp335-340.

Williams, J., Gray, A.J., Wilkerson, M. (1990), 'Emulsion Stability and Rigid foams from styrene or divinylbenzene water-in-oil emulsions', *Langmuir*, vol 6, pp 437-444

Wilson, K., Clark, J. (2000), 'Solid acids and their use as environmentally friendly catalysts in organic synthesis', *Pure and Applied Chemistry,* vol 72, pp 1313-1319

Wrzyszcz, J., Zawadzki, M., Trawczyński, J., Grabowska, H., Miśta, J. (2001), 'Some catalytic properties of hydrothermally synthesised zinc aluminate spinel', *Applied Catalysis A: General*, vol 210 pp263-267

Xie, W., Peng, H, Chen, L. (2006a), 'Transesterification of soybean oil catalzed by potassium loaded on alumina as a solid base catalyst', *Applied Catalysis A: General,* vol 300, pp 67-74

Xie, W., Li, H. (2006), 'Alumina supported potassium iodidie as a hetrogeneous catalyst for biodeisel production from soybean oil', *Journal of molecular catalysis A: Chemical,* vol 255, pp 1-9.

Xie, W. and X. M. Huang (2006), 'Synthesis of biodiesel from soybean oil using heterogeneous KF/ZnO catalyst', *Catalysis Letters,* vol 107, pp 53-59.

Xie, W., Peng, H., Chen, L. (2006b) 'Calcined Mg-Al hydrotalcites as solid base catalysts for methanolysi of sunflower oil', *Journal of molecular catalysis A: Chemical,* vol 246, pp 24-32.

Xie, W., Huang, X., Li, H. (2007), 'Soybean methyl esters preparation using NaX zeolites loaded with KOH as a heterogeneous catalyst', *Bioresource Technology,* vol 98, pp 936-939.

Yamaguchi, T., Wang, Y., Komatsu, M., Ookawa, M. (2002), 'Preparation of new solid bases derived from supported metal nitrates and carbonates', *Catalysis Surveys from Japan,* vol 5, pp 81-89

Yang, Z., Xie, W. (2007), 'Soybean oil transesterification over zinc oxide modified with alkali earth metals', *Fuel processing technology*, vol 88, pp 631-638.

Yanwu, L., Yiya, O., Fangxin, L. (2006), 'Magnetic properties of tin doped ferrite nanoparticles $Sn_xFe_{3-x}O_4$, *Rare Metals*, vol 25, pp 493-495

ounts

10000

5000

0

5-100.CAF

* MgO
□ $Mg(OH)_2$.
Others peaks Li_2CO_3.

Appendix 1A : Li-MgO uncalcined XRD

20 30 40 50 60 70 80

Position [°2Theta]

Li-MgO series.

Peak List

08-0466; Li N O3; Lithium Nitrate

12-0254; Li2 O; lithia

22-1141; Li2 C O3; Zabuyelite, syn

32-0564; Li O H; Lithium Hydroxide

44-1482; Mg (O H)2; Brucite, syn

76-1074; Li O H H2 O; Lithium Hydroxide Hydrate

10 20 30 40 50 60 70 80

Position [°2Theta]

Appendix 1B: Li-MgO uncalcined assignments.

Appendix 1C: LiMgO calcined XRD & assignments.

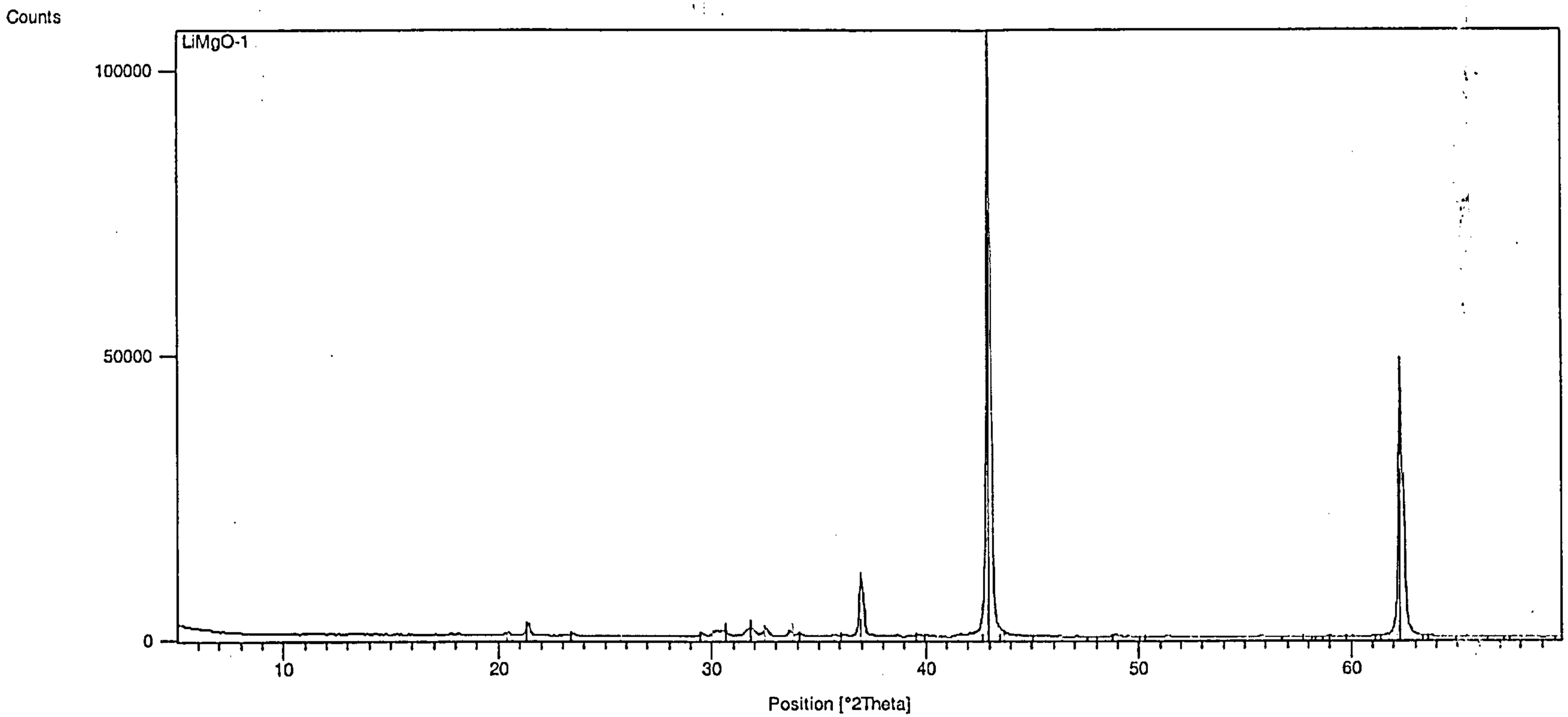

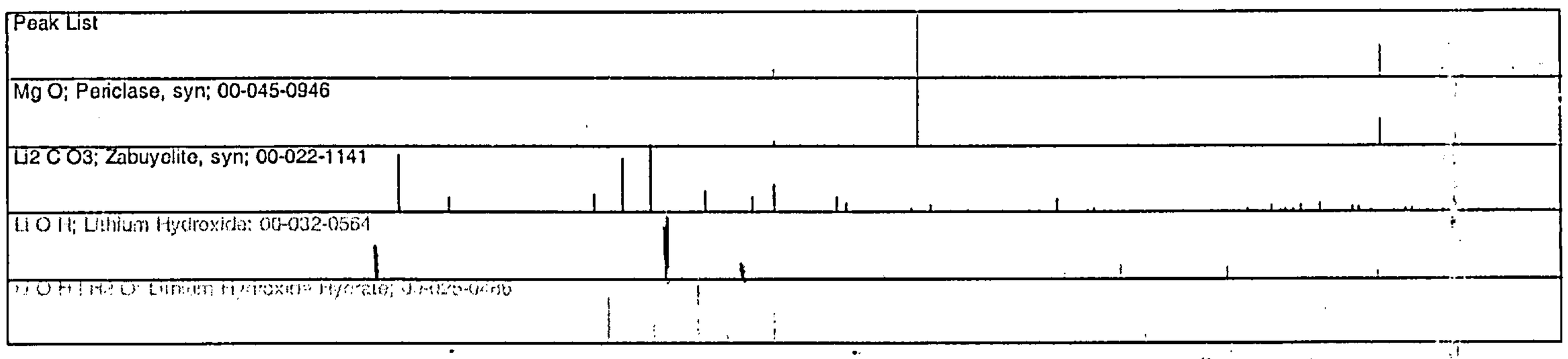

Appendix ID: Li-CaO uncalcined XRD & assignments

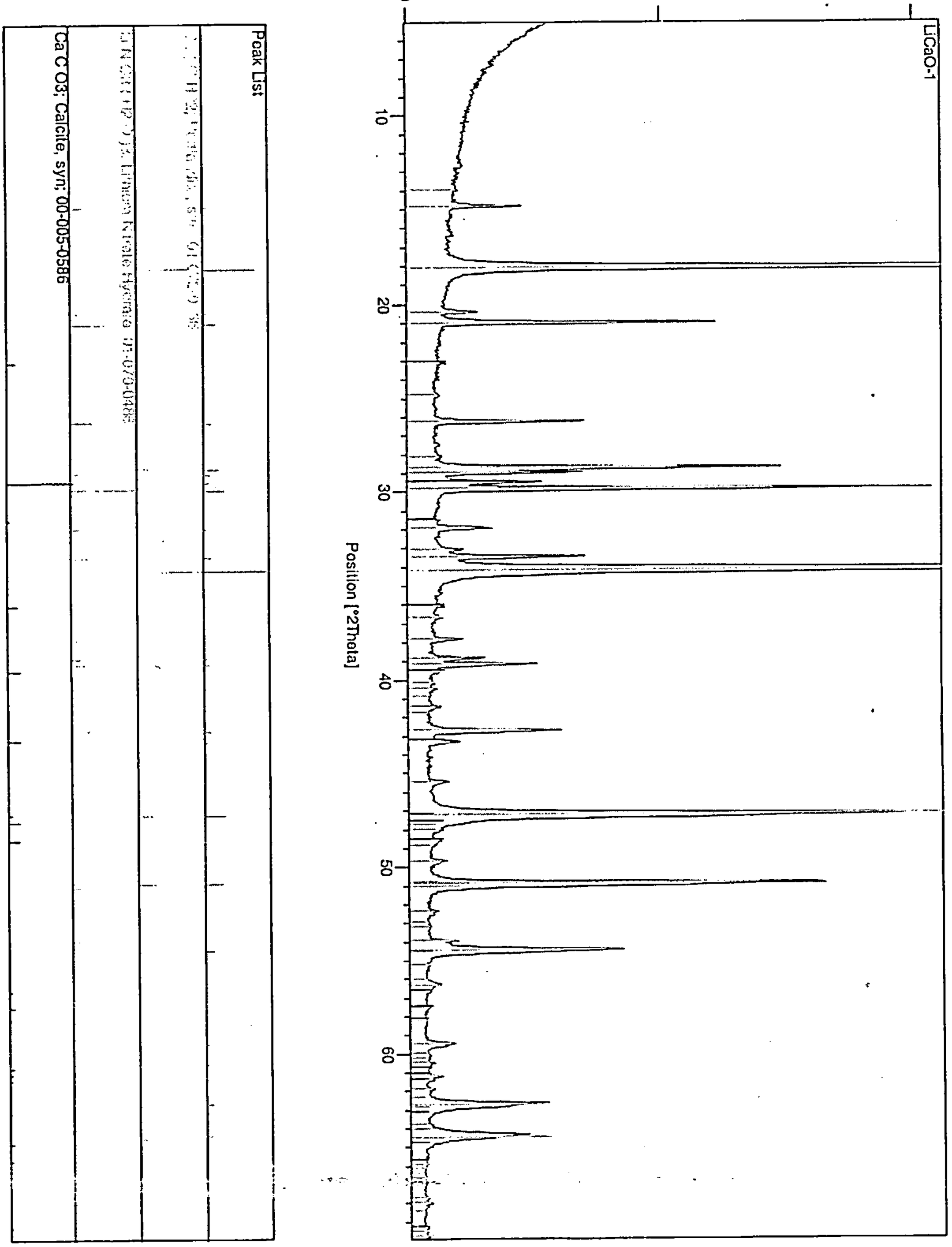

Appendix 1E : Li-CaO calcined XRD & assignments.

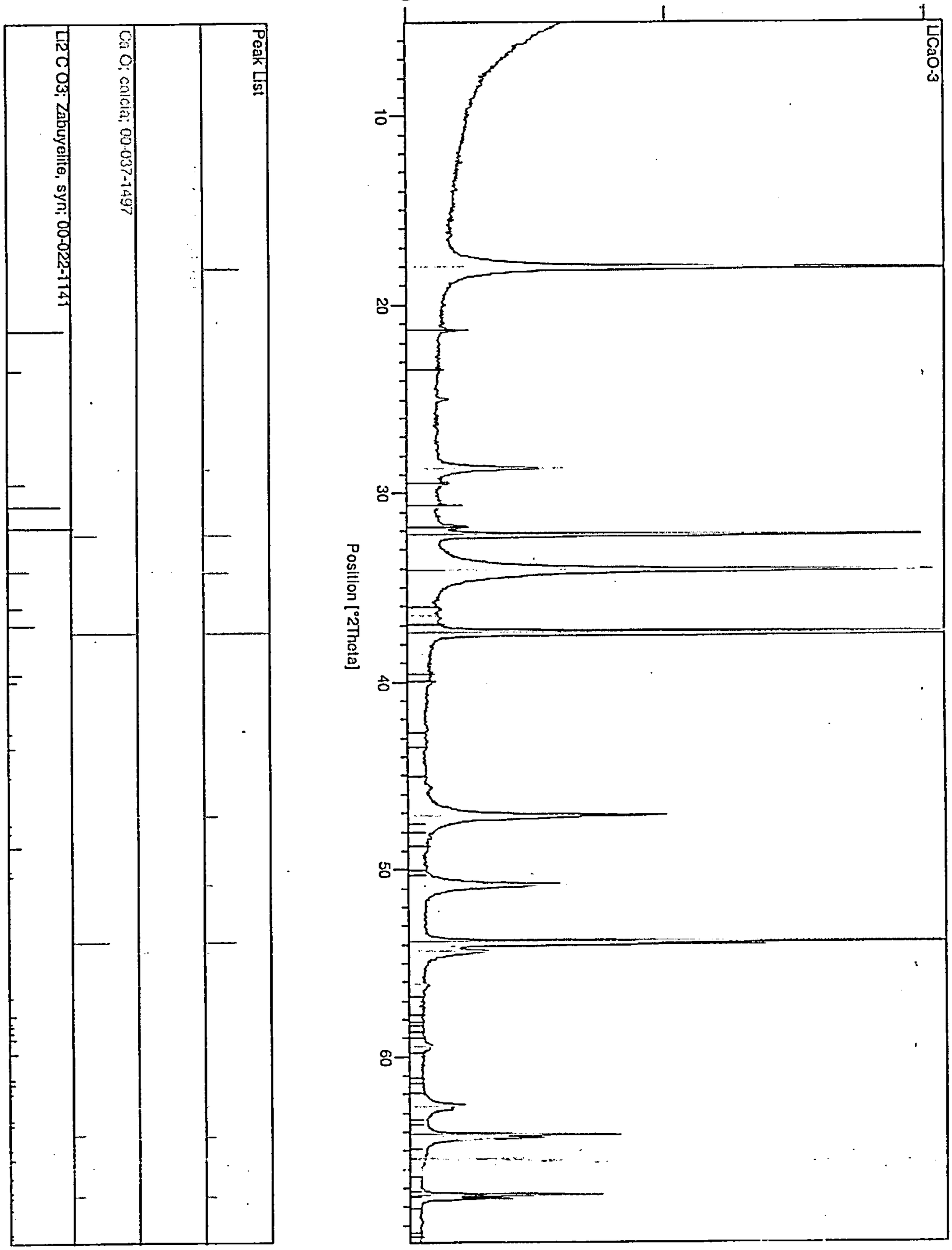

Counts

LiMgO-2

100000

50000

0

10

20

30

40

50

60

Position [°2Theta]

Peak List

Mg O; Periclase, syn; 00-045-0946

Li2 C O3; Zabuyelite, syn; 00-022-1141

Figure 1: LiF: Li-MgO calcined, used XRD and assignments

Appendix 16: Li-CaO uncalcined, used XRD and assignments

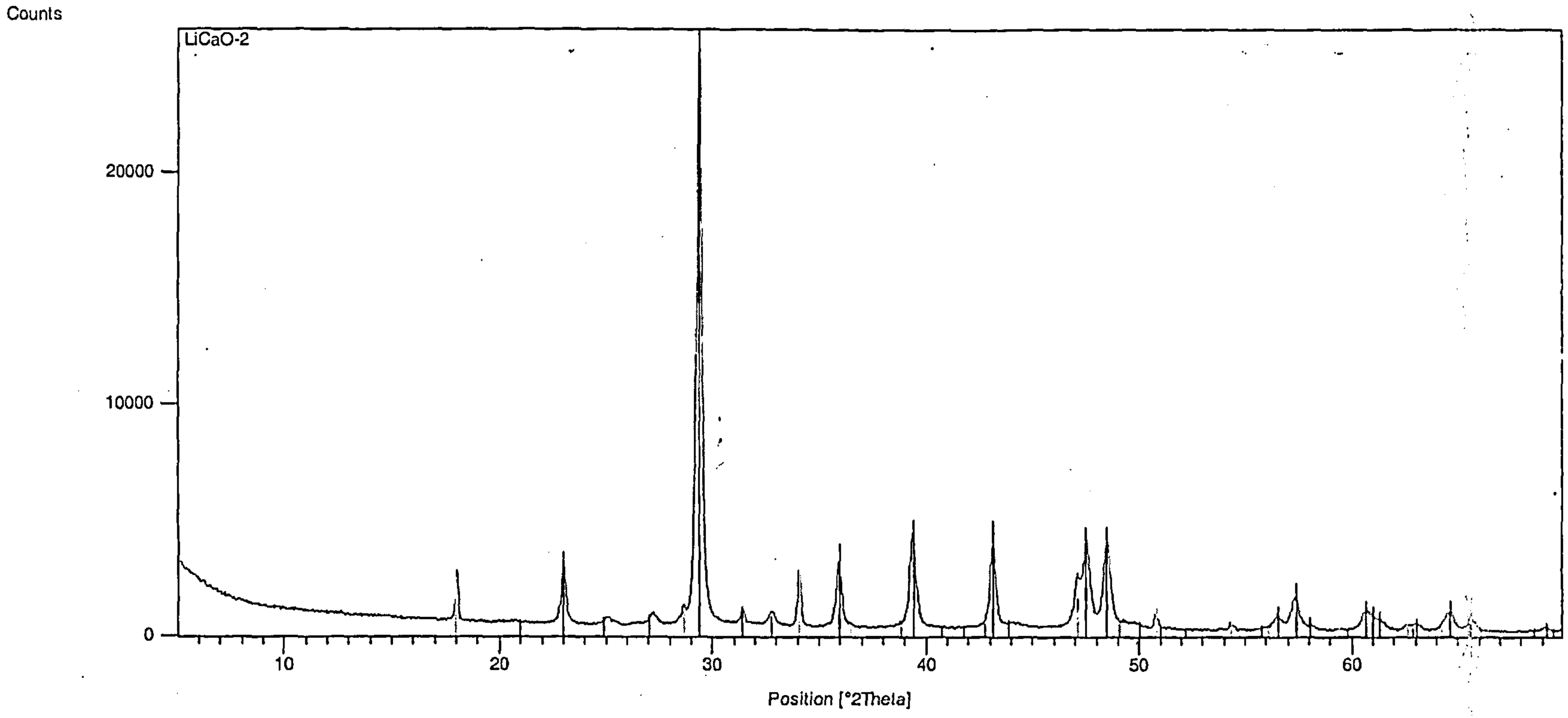

Appendix 1H: Li-CaO calcined, used & XRD & assignments.

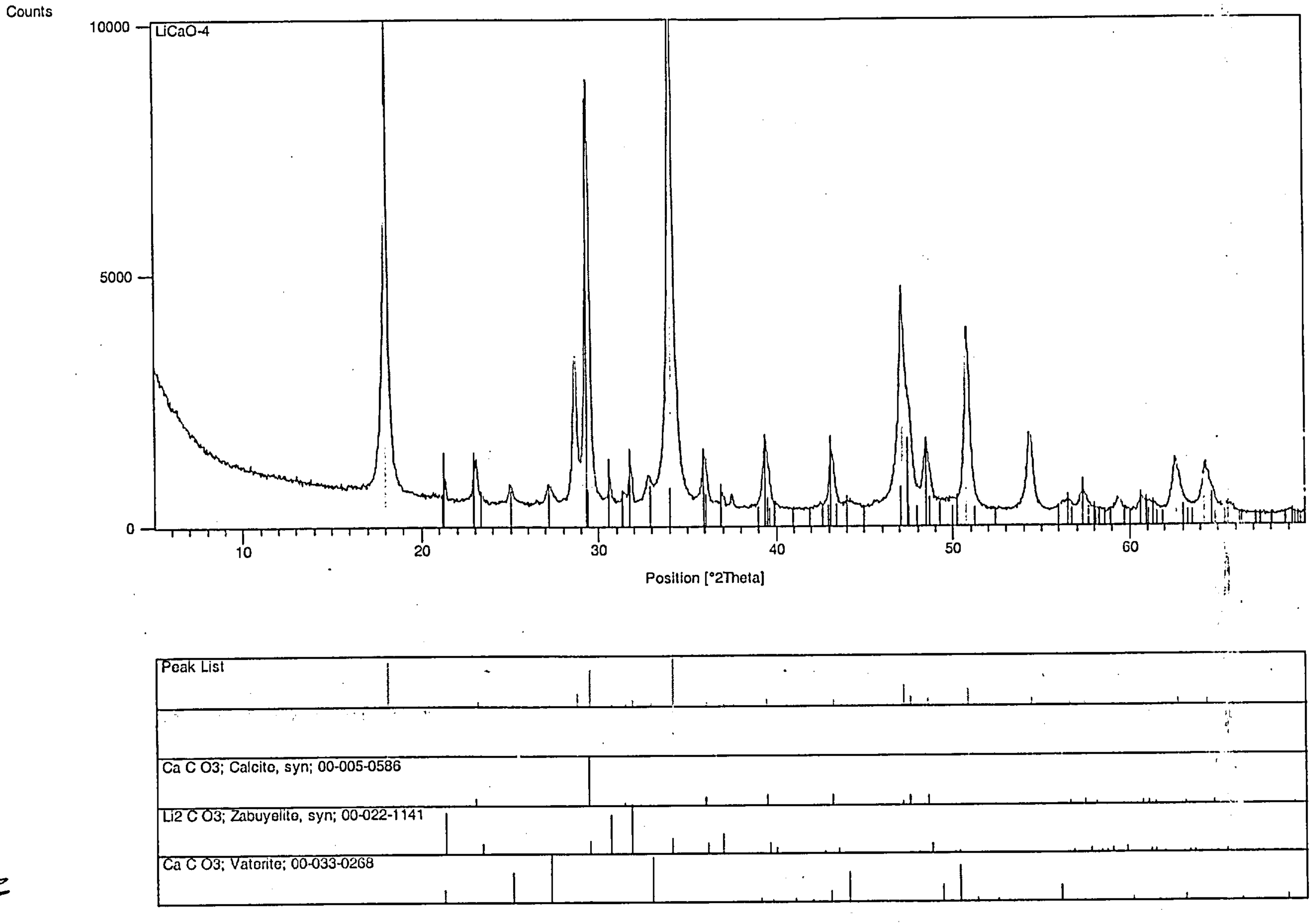

Appendix 2

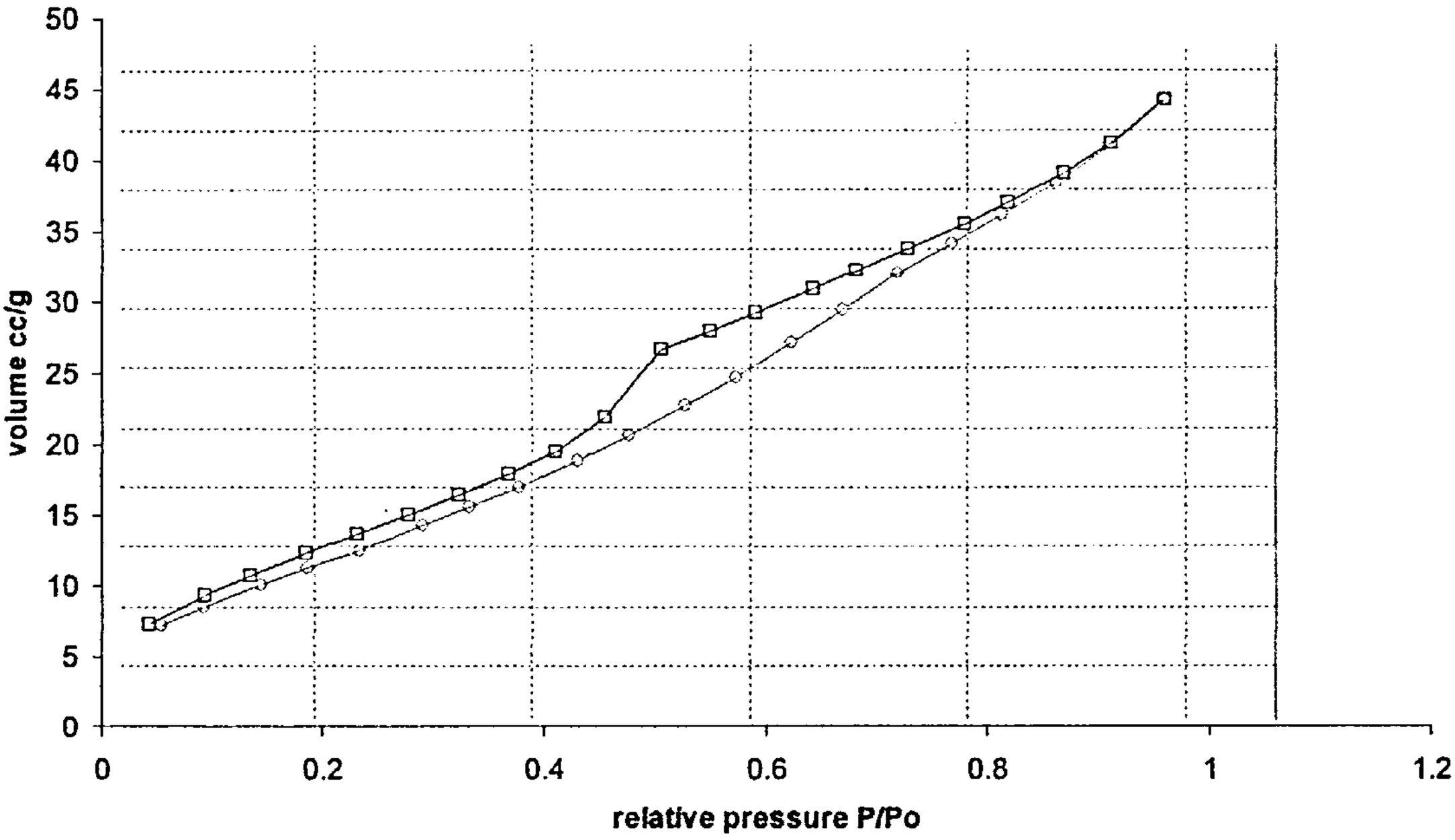

Nitrogen isotherm for HMS supported TBD, adsorption ○, desorption □

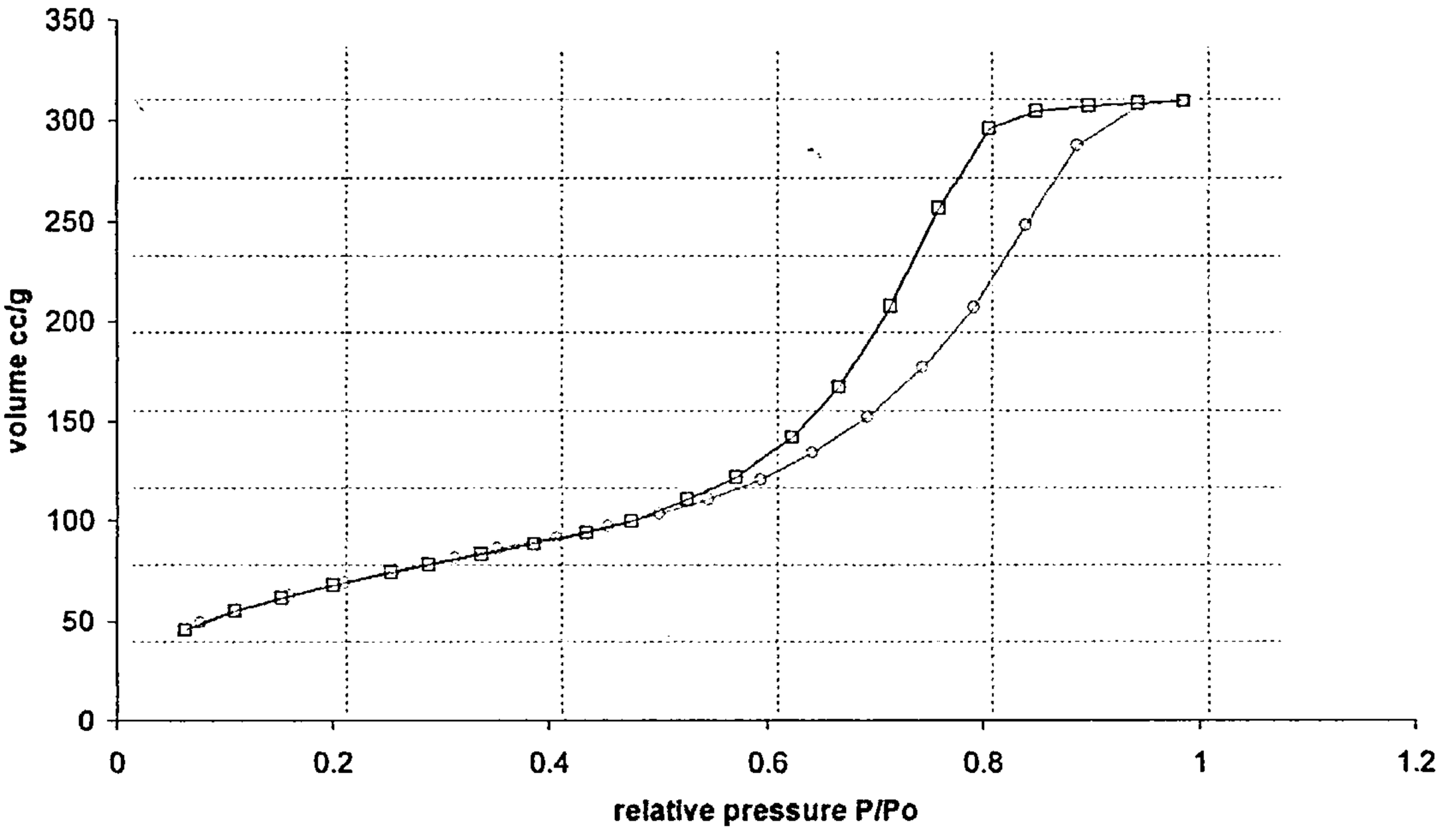

Nitrogen isotherm for Davisil (60Å) supported TBD, adsorption ○, desorption □

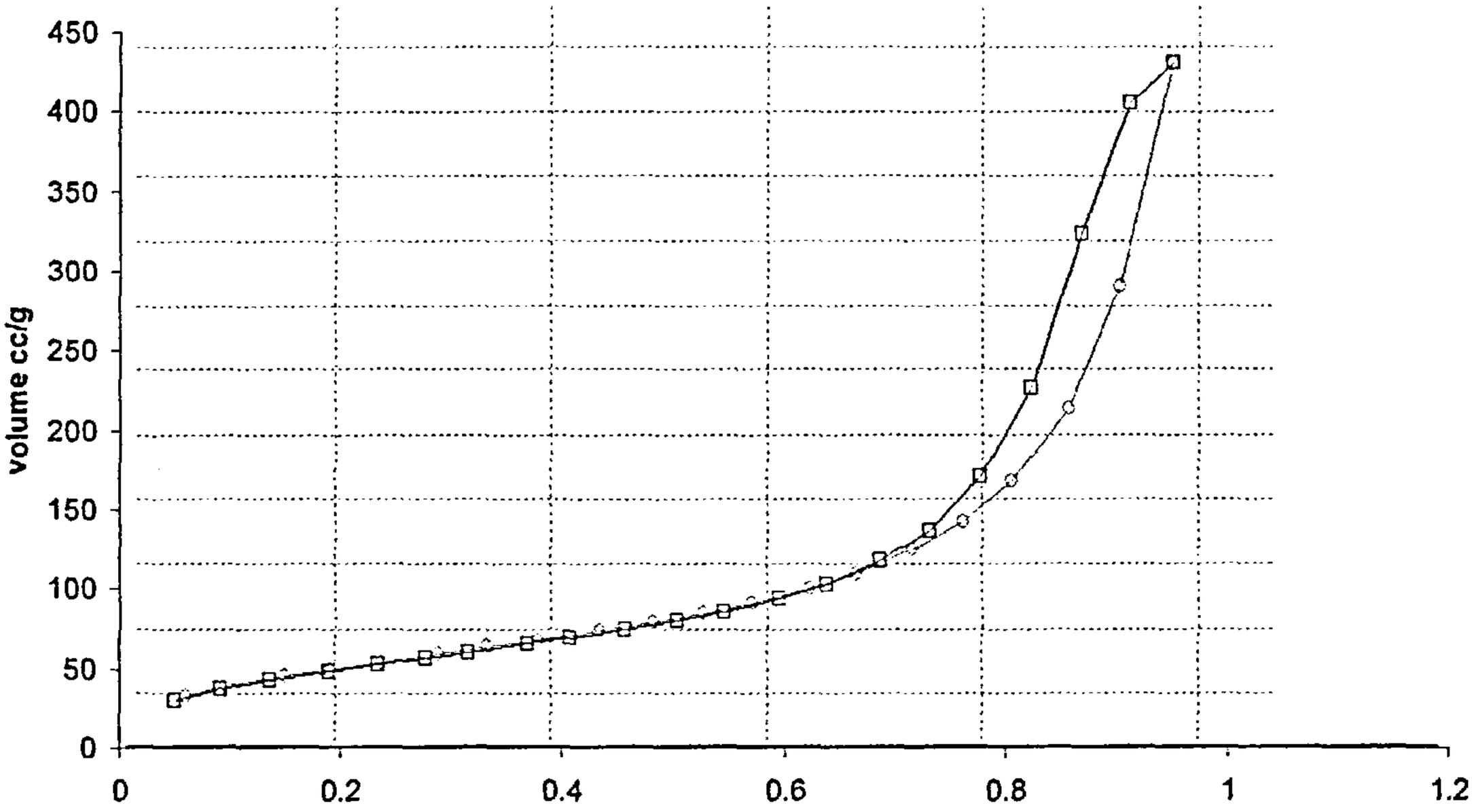

Nitrogen isotherm for Davisil 150 Å supported TBD, adsorption ○, desorption □

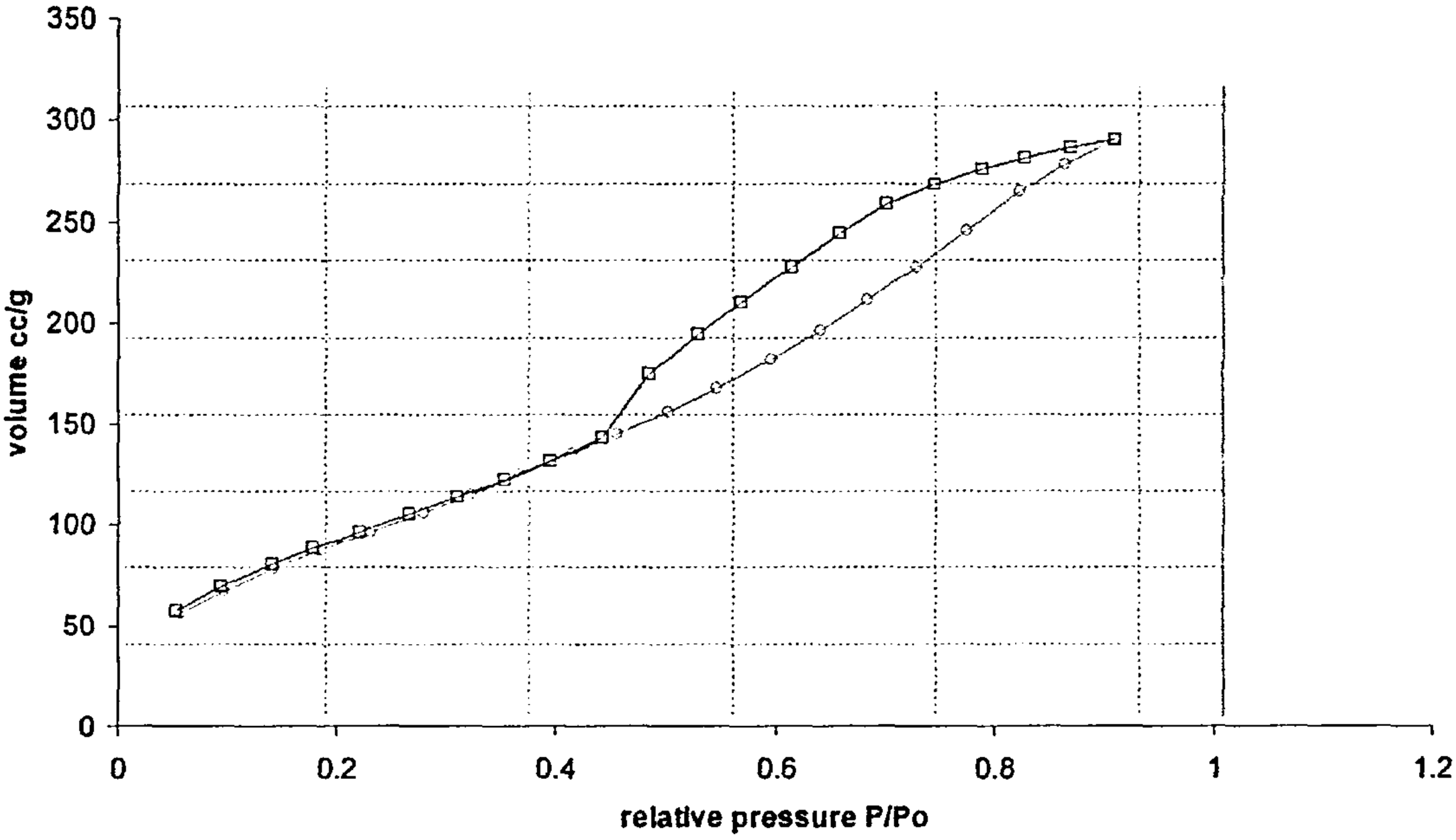

Nitrogen isotherm for HMS supported tertiary amine, adsorption ○, desorption □

Appendix 3: Calculation for 2nd order homogeneous case

Triglyceride $[TG]_t=[TG]_{t-1}- k_1[TG]_{t-1}[A]_{t-1}+ k_2[DG]_{t-1}[BD]_{t-1}$

Diglyceride $[DG]_t=[DG]_{t-1}+ k_1[TG]_{t-1}[A]_{t-1}- k_2[DG]_{t-1}[BD]_{t-1}- k_3[DG]_{t-1}[A]_{t-1}+ k_4[MG]_{t-1}[BD]_{t-1}$

Monoglyceride $[MG]_t=[MG]_{t-1}+k_3[DG]_{t-1}[A]_{t-1}-k_4[MG]_{t-1}[BD]_{t-1}-k_5[MG]_{t-1}[A]_{t-1}+k_6[G]_{t-1}[BD]_{t-1}$

Biodiesel $[BD]_t=[BD]_{t-1}+ k_1[TG]_{t-1}[A]_{t-1}-k_2[DG]_{t-1}[BD]_{t-1}+ k_3[DG]_{t-1}[A]_{t-1}- k_4[MG]_{t-1}[BD]_{t-1}+ k_5[MG]_{t-1}[A]_{t-1}- k_6[G]_{t-1}[BD]_{t-1}$

Methanol $[A]_t=[A]_{t-1}- k_1[TG]_{t-1}[A]_{t-1}+k_2[DG]_{t-1}[BD]_{t-1}-k_3[DG]_{t-1}[A]_{t-1}+ k_4[MG]_{t-1}[BD]_{t-1} -k_5[MG]_{t-1}[A]_{t-1}+k_6[G]_{t-1}[BD]_{t-1}$

Glycerol $[G]_t=[G]_{t-1}+k_5[MG]_{t-1}[A]_{t-1}-k_6[G]_{t-1}[BD]_{t-1}$

time	triglyceride	diglyceride	monoglyceride	biodiesel	glycerol	methanol
0	0.820	0.000	0.000	0.000	0.000	4.950
1	0.792	0.028	0.000	0.028	0.000	4.922
2	0.765	0.053	0.002	0.056	0.000	4.894
3	0.739	0.075	0.005	0.086	0.000	4.864
4	0.715	0.096	0.009	0.116	0.001	4.834
5	0.691	0.114	0.014	0.146	0.001	4.804
6	0.668	0.129	0.020	0.177	0.003	4.773
7	0.646	0.144	0.026	0.208	0.004	4.742
8	0.625	0.156	0.032	0.240	0.007	4.710
9	0.605	0.167	0.039	0.273	0.009	4.677
10	0.585	0.177	0.045	0.305	0.013	4.645
11	0.567	0.185	0.052	0.338	0.017	4.612
12	0.549	0.192	0.058	0.371	0.021	4.579
13	0.531	0.198	0.065	0.405	0.026	4.545
14	0.515	0.203	0.071	0.438	0.031	4.512
15	0.499	0.208	0.076	0.472	0.037	4.478

Appendix 4: Eley-Rideal kinetics

Triglyceride $[TG]_t=[TG]_{t-1}- k_1[TG]_{t-1}\theta_{A,t-1}+ k_2\theta_{DG,t-1}[BD]_{t-1}$

Diglyceride $[DG]_t=[DG]_{t-1}+k_1[TG]_{t-1}\theta_{A,t-1}-k_2\theta_{DG,t-1}[BD]_{t-1}-k_3[DG]_{t-1}\ \theta_{A,t-1}+k_4\theta_{MG,t-1}[BD]_{t-1}$

Monoglyceride $[MG]_t=[MG]_{t-1}+k_3[DG]_{t-1}\theta_{A,t-1}-k_4\theta_{MG,t-1}[BD]_{t-1}-k_5[MG]_{t-1}\theta_{A,t-1}+k_6\theta_{G,t-1}[BD]_{t-1}$

Biodiesel $[BD]_t=[BD]_{t-1}+ k_1[TG]_{t-1}\ \theta_{A,t-1}-k_2\ \theta_{DG,t-1}[BD]_{t-1}+k_3[DG]_{t-1}\ \theta_{A,t-1}-k_4\theta_{MG,t-1}[BD]_{t-1}+k_5[MG]_{t-1}\theta_{A,t-1}-k_6\theta_{G,t-1}[BD]_{t-1}$

Methanol $[A]_t=[A]_{t-1}- k_1[TG]_{t-1}\theta_{A,t-1}+k_2\ \theta_{DG,t-1}[BD]_{t-1}-k_3[DG]_{t-1}\theta_{A,t-1}+ k_4\theta_{MG,t-1}[BD]_{t-1}-k_5[MG]_{t-1}\theta_{A,t-1}+k_6\theta_{G,t-1}[BD]_{t-1}$

Glycerol $[G]_t=[G]_{t-1}+k_5[MG]_{t-1}\theta_{A,t-1}-k_6\theta_{G,t-1}[BD]_{t-1}$

time	triglyceride	diglyceride	monoglyceride	biodiesel	methanol	glycerol	()A	()G	()DG	(MG)
0	0.820	0.000	0.000	0.000	4.950	0.000	0.937	0.000	0.000	0.000
1	0.795	0.025	0.000	0.025	4.925	0.000	0.932	0.000	0.004	0.000
2	0.771	0.048	0.002	0.051	4.899	0.000	0.928	0.000	0.008	0.000
3	0.747	0.068	0.004	0.077	4.873	0.000	0.923	0.000	0.011	0.001
4	0.725	0.087	0.008	0.104	4.846	0.000	0.919	0.000	0.014	0.001
5	0.703	0.103	0.013	0.132	4.818	0.001	0.915	0.000	0.017	0.002
6	0.682	0.118	0.018	0.160	4.790	0.002	0.910	0.000	0.019	0.003
7	0.662	0.131	0.023	0.189	4.761	0.004	0.906	0.001	0.022	0.004
8	0.642	0.143	0.029	0.218	4.732	0.005	0.903	0.001	0.023	0.005
9	0.623	0.154	0.035	0.247	4.703	0.008	0.899	0.001	0.025	0.006
10	0.605	0.163	0.041	0.277	4.673	0.011	0.895	0.002	0.027	0.007
11	0.587	0.171	0.048	0.308	4.642	0.014	0.891	0.003	0.028	0.008
12	0.570	0.178	0.054	0.339	4.611	0.018	0.888	0.003	0.029	0.009
13	0.554	0.185	0.060	0.370	4.580	0.022	0.884	0.004	0.030	0.010
14	0.538	0.190	0.066	0.401	4.549	0.026	0.881	0.005	0.031	0.011

Appendix 5: Langmuir-Hinshelwood kinetics

$[TG]_t=[TG]_{t-1}-k_1\ \theta_{TG,t-1}\theta_{A,t-1}+k_2\theta_{DG,t-1}\theta_{BD,t-1}$

$[DG]_t=[DG]_{t-1}+k_1\theta_{BD,t-1}\theta_{A,t-1}-k_2\theta_{DG,t-1}\theta_{BD,t-1}-k_3\theta_{DG,t-1}\theta_{A,t-1}+k_4\theta_{MG,t-1}\theta_{BD,t-1}$

$[MG]_t=[MG]_{t-1}+k_3\theta_{DG,t-1}\theta_{A,t-1}-k_4\theta_{MG,t-1}\theta_{BD,t-1}-k_5\theta_{MG,t-1}\theta_{A,t-1}+k_6\theta_{G,t-1}\theta_{BD,t-1}$

$[BD]_t=[BD]_{t-1}+k_1\theta_{TG,t-1}\theta_{A,t-1}-k_2\ \theta_{DG,t-1}\theta_{BD,t-1}+k_3\theta_{DG,t-1}\theta_{A,t-1}-k_4\theta_{MG,t-1}\theta_{BD,t-1}+k_5\theta_{MG,t-1}\theta_{A,t-1}-k_6\theta_{G,t-1}\theta_{BD,t-1}$

$[A]_t=[A]_{t-1}-k_1\theta_{TG,t-1}\theta_{A,t-1}+k_2\ \theta_{DG,t-1}\theta_{BD,t-1}-k_3\theta_{DG,t-1}\theta_{A,t-1}+k_4\theta_{MG,t-1}\theta_{BD,t-1}-k_5\theta_{MG,t-1}\theta_{A,t-1}+k_6\theta_{G,t-1}\theta_{BD,t-1}$

$[G]_t=[G]_{t-1}+k_5\ \theta_{MG,t-1}\theta_{A,t-1}-k_6\theta_{G,t-1}\theta_{BD,t-1}$

$$\theta_i=\frac{K_i[i]}{1+K_A[A]+K_{DG}[DG]+K_{MG}[MG]+K_G[G]+K_{TG}[TG]+K_{BD}[BD]}$$

time	triglyceride	diglyceride	monoglyceride	biodiesel	methanol	glycerol	()A	()G	()DG	()MG	()TG	()BD
0	0.820	0.000	0.000	0.000	4.950	0.000	0.811	0.000	0.000	0.000	0.134	0.000
1	0.793	0.027	0.000	0.027	4.923	0.000	0.807	0.000	0.004	0.000	0.130	0.004
2	0.766	0.052	0.002	0.056	4.894	0.000	0.802	0.000	0.009	0.000	0.126	0.009
3	0.741	0.074	0.005	0.085	4.865	0.000	0.797	0.000	0.012	0.001	0.121	0.014
4	0.717	0.093	0.009	0.114	4.836	0.001	0.792	0.000	0.015	0.002	0.117	0.019
5	0.693	0.111	0.015	0.145	4.805	0.002	0.787	0.000	0.018	0.002	0.114	0.024
6	0.671	0.126	0.021	0.176	4.774	0.003	0.782	0.000	0.021	0.003	0.110	0.029
7	0.649	0.139	0.027	0.207	4.743	0.005	0.777	0.001	0.023	0.004	0.106	0.034
8	0.628	0.151	0.033	0.239	4.711	0.007	0.772	0.001	0.025	0.005	0.103	0.039
9	0.608	0.162	0.040	0.272	4.678	0.010	0.766	0.002	0.026	0.007	0.100	0.045
10	0.589	0.171	0.047	0.305	4.645	0.014	0.761	0.002	0.028	0.008	0.097	0.050